2010

Thermodynamic and structural determinants of calcium-independent interactions of Calmodulin

Michael Dennis Feldkamp
University of Iowa

THERMODYNAMIC AND STRUCTURAL DETERMINANTS OF CALCIUM-INDEPENDENT INTERACTIONS OF CALMODULIN

by

Michael Dennis Feldkamp

An Abstract

Of a thesis submitted in partial fulfillment
of the requirements for the Doctor of
Philosophy degree in Biochemistry
in the Graduate College of
The University of Iowa

July 2010

Thesis Supervisor: Professor Madeline A. Shea

ABSTRACT

Calmodulin (CaM) is an essential protein found in all eukaryotes ranging from vertebrates to unicellular organisms such as *Paramecia*. CaM is a calcium sensor protein composed of two domains (N and C) responsible for the regulation of numerous calcium-mediated signaling pathways. Four calcium ions bind to CaM, changing its conformation and determining how it recognizes and regulates its cellular targets. Since the discovery of CaM, most studies have focused on the role of its calcium-saturated form.

However, an increasing number of target proteins have been discovered that preferentially bind apo (calcium-depleted) CaM. My study focused on understanding how apo CaM recognizes drugs and protein sequences, and how those interactions differ from those of calcium-saturated CaM. I have used spectroscopic methods to explore CaM binding the drug Trifluoperazine (TFP) and the IQ-motif of the type 2 Voltage-Dependent Sodium Channel ($Na_v1.2_{IQp}$). These studies have shown that both TFP and $Na_v1.2_{IQp}$ preferentially bind to the "semi-open" conformation of apo CaM.

TFP was shown to be an unusual allosteric effector of calcium binding to CaM. Using ^{15}N-HSQC NMR spectroscopy, I determined the stoichiometry of TFP binding to apo Cam to be 2:1 and to $(Ca^{2+})_4$-CaM to be 4:1 TFP:CaM. That difference in stoichiometry determined whether TFP decreased or increased the affinity of CaM for calcium. Analysis of residue-specific chemical shift differences indicated that TFP binding to apo and $(Ca^{2+})_4$-CaM perturbed the C-domain more than the N-domain, prompting high-resolution structural studies of the isolated C-domain of CaM.

Crystallographic studies of TFP bound to a calcium-saturated C-domain fragment of CaM (CaM_{76-148}) revealed that CaM adopted an "open" tertiary conformation. The unit cell contained two protein and 4 drug molecules. The orientation of TFP revealed that its trifluoromethyl group was found in two alternative positions (one in each protein in the unit cell), and that Met 144 acted as a gatekeeper to select the orientation of TFP.

In contrast to TFP binding to the "open" conformation of calcium-saturated $CaM_{76\text{-}148}$, my NMR studies showed that TFP bound the "semi-open" conformation of apo $CaM_{76\text{-}148}$. TFP interacted with CaM residues near the perimeter of the hydrophobic pocket, but did not contact residues that are solvent-accessible only in the "open" form. Allosteric effects due to TFP binding were observed in the calcium-binding loops of apo $CaM_{76\text{-}148}$. These properties suggest that TFP may antagonize interactions between apo CaM and target proteins such as ion channels that preferentially bind apo CaM.

$Na_v1.2$, is responsible for the passage of Na^+ ion across cellular membranes. Apo binding of CaM to $Na_v1.2$ poises it for action upon calcium release in the cell. My NMR studies of CaM binding to the $Na_v1.2$ IQ-motif sequence ($Na_v1.2_{IQp}$) showed that the C-domain of apo CaM was necessary and sufficient for binding. My high-resolution structure of the isolated C-domain of CaM bound to $Na_v1.2_{IQp}$ revealed that the domain adopted a "semi-open" conformation. At the interface between the IQ-motif and CaM, the highly conserved I and two Y residues of $Na_v1.2_{IQp}$ interacted with hydrophobic residues of CaM, while the invariant Q residue interacted with residues in the loop between helices F and G of CaM. This is the first CaM-IQ complex to be determined by NMR; the only other available structure of apo CaM bound to an IQ-motif was determined crystallographically.

To accomplish its regulatory roles in response to cellular Ca^{2+} fluxes, CaM has evolved multiple binding interfaces that are allosterically linked to its Ca^{2+}-ligation state. My studies of CaM binding to TFP and $Na_V1.2$ demonstrate the versatility of CaM functioning as a regulatory protein comprised of domains having separable functions.

Abstract Approved: _____
Thesis Supervisor

_____
Title and Department

_____
Date

THERMODYNAMIC AND STRUCTURAL DETERMINANTS OF CALCIUM-INDEPENDENT INTERACTIONS OF CALMODULIN

by

Michael Dennis Feldkamp

A thesis submitted in partial fulfillment
of the requirements for the Doctor of
Philosophy degree in Biochemistry
in the Graduate College of
The University of Iowa

July 2010

Thesis Supervisor: Professor Madeline A. Shea

Graduate College
The University of Iowa
Iowa City, Iowa

CERTIFICATE OF APPROVAL

_____

PH.D. THESIS

_____

This is to certify that the Ph.D. thesis of

Michael Dennis Feldkamp

has been approved by the Examining Committee
for the thesis requirement for the Doctor of Philosophy
degree in Biochemistry at the July 2010 graduation.

Thesis Committee: _____
Adrian Elcock, Thesis Chair

_____
Ernesto Fuentes

_____
Lei Geng

_____
Shahram Khademi

_____
Daniel Weeks

For those who value truth more than dogma

To laugh often and much; to win the respect of intelligent people and the affection of children; to earn the appreciation of honest critics and endure the betrayal of false friends; to appreciate beauty; to find the best in others; to leave the world a bit better, whether by a healthy child, a garden patch or a redeemed social condition; to know even one life has breathed easier because you have lived. This is to have succeeded.

-Ralph Waldo Emerson

ACKNOWLEDGMENTS

I have often heard the saying that "science is done by standing on top of the shoulders of giants". The further I have progressed in my Ph.D. studies, I have found a deeper and deeper appreciation for this phrase. Science is truly a team sport and there are many people I would like to thank for their personal or professional support over the course of obtaining my Ph.D.

I would like to first and foremost thank my advisor Madeline Shea, whose support and guidance has shaped me as a scientist. She provided me the opportunity to pursue studies in x-ray crystallography and NMR, and allowed me to attend multiple local and national conferences to present my work. She has always kept my best interests at heart and made numerous sacrifices to ensure that my training in her lab was second to none. Above all I thank her for her compassion and understanding, the door to her office was always open to discuss problems I had science related or not. I would like to thank the past and present members of the Shea lab, all of whom made coming to work everyday an enjoyable and positive experience. I would especially like to thank Susan O'Donnell, I am glad to have had the benefit of progressing through graduate school with someone as energetic and skilled as her. I would like to thank my thesis committee Adrian Elcock, Ernie Fuentes, Lei Geng, Sharham Khademi, and Dan Weeks. I can honestly say that each of you has individually taken the time to help me outside the committee meeting environment. Your input, and encouragement throughout this process is greatly appreciated. To my unofficial 6th committee member, Liping Yu. I'm grateful for your help and guidance in my NMR based studies as well as encouragement over the course of what seemed like a never ending onslaught of peak assignments to be made. Your dedication to helping others succeed using NMR is unmatched. I would like to thank Rams and Lokesh Gakhar for their help in collection and processing of x-ray diffraction data.

I'm honored to have met the many friends that I've made in Iowa, you have helped make my time here so much more enjoyable. Our conversations about science initially brought us together, but it is the non-science conversations that I will miss most dearly when I leave.

My family has always been a never-ending source of strength and support, without you, all of this would not have been possible. I am forever indebted to my grandparents whose lives have been a testament to me that the rewards of hard work and honesty are worth the sacrifices that they require. I am extremely grateful to my nieces Raeba, and Natalie; and nephews Ravi and Michael, who were always able to bring a much needed smile to my face and brighten my day with a phone call or visit. Света, Вилен, Саша и Марагрет - спасибо, что приняли меня в Вашу семью. Спасибо за Ваше постоянное доброжелание и гостепреимство. Ваша поддержка для Лены и меня во время нашего пребывания в Айове никогда не будет забыта. To my sisters Sara, Julie, Anne, Rachel and brother-in-law Raj, you are awesome, I'm so lucky to have each of you in my life. You are my best friends and have been with me since the beginning. To my parents, Mom and Dad you have sacrificed so much to allow me to follow my dreams, I hope that someday I can do the same. You have both taught me more than any institution ever could. I have never been more proud to be your son and count myself lucky to have grown up on a dairy farm in Wisconsin, I wouldn't have had it any other way.

Finally to my fiancé Helen, your unwavering love and support has and continues to mean the world to me. Thank you for everything you do and the sacrifices you have made. Я люблю тебя всем сердцем и душой. Из за тебя, я стал лучшим человеком и всегда буду тебе за это благодарен. Пожалуйста знай, что всё это было зделано для тебя и для нашей семьи.

TABLE OF CONTENTS

LIST OF TABLES x

LIST OF FIGURES xii

LIST OF ABBREVIATIONS xiv

CHAPTER I INTRODUCTION 1

CaM Background 1
Interaction of $(Ca^{2+})_4$-CaM with Protein Targets 2
Interaction of apo CaM with Protein Targets 3
The Voltage-Dependent Sodium Channel$_v$1.2 4
Interaction of CaM with Drugs 6
TFP 7
Electrostatic Interactions of CaM with Targets 8
Description of Thesis Content 8

CHAPTER II ALLOSTERIC EFFECTS OF THE ANTI-PSYCHOTIC DRUG TRIFLUOPERAZINE ON THE ENERGETICS OF CA^{2+} BINDING BY CAM 21

Introduction 21
Materials and Methods 25
Protein over-expression and purification 25
Equilibrium calcium titrations monitored by intrinsic protein fluorescence 25
NMR Spectra 28
TFP titration of CaM Monitored by NMR 28
Computational Modeling of TFP Binding 29
Results 30
TFP Titration of apo ^{15}N-PCaM 30
TFP Titration of $(Ca^{2+})_4$-^{15}N-PCaM 31
Equilibrium Calcium Titration of CaM_{1-148} 32
Effect of TFP on Calcium Binding to CaM_{1-148} 32
Effect of TFP on Calcium Binding to CaM_{1-80} 34
Effect of TFP on Calcium Binding to CaM_{76-148} 35
Piecewise Analysis of Biphasic Calcium Titrations of CaM_{76-148} 36
Discussion 38
Two TFP molecules bind to apo CaM 38
Four TFP bind to $(Ca^{2+})_4$-CaM 42
Interdomain Interactions 43
Effects of TFP on the Calcium Affinity of CaM 45
Summary 49

CHAPTER III BINDING OF TRIFLUOPERAZINE TO THE C-DOMAIN OF CAM 64

Introduction 64

Materials and Methods 65
Protein Overexpression 65
Crystallography Materials and Methods 66
Overexpression and Purification of Isotope Enriched CaM 66
Assignment of Backbone and Sidechain Resonances 67
Quantification of ^{15}N-apo CaM_{76-148} Chemical Shifts due to TFP Addition 67
Results 68
Structure of TFP Bound $(Ca^{2+})_2$-CaM_{76-148} 68
TFP-Induced Changes of apo CaM_{76-148} as Monitored by ^{15}N-HSQC Spectroscopy 79
Dynamics of TFP Bound apo CaM_{76-148} Monitored with T_2 Relaxation Spectroscopy 70
Discussion 71
Protein Crystallography of $(Ca^{2+})_2$-CaM_{76-148}-TFP Complex 71
TFP-Induced Changes of apo CaM_{76-148} as Monitored by ^{15}N-HSCQ Spectroscopy 74
TFP-Induced Changes of apo CaM_{76-148} as Monitored by T_2 Relaxation 75

CHAPTER IV BINDING OF $NA_V1.2_{IQP}$ TO THE C-DOMAIN OF APO CAM 90

Introduction 90
Materials and Methods 93
Overexpression and Purification of Calmodulin 93
Prepared $Na_v1.2_{IQp}$ 93
^{15}N-HSQC Monitored $Na_v1.2_{IQp}$ and Ca^{2+} Titration of CaM_{1-148} 94
Preparation of ^{13}C/^{15}N-CaM76-148:$Na_v1.2_{IQp}$ Complex 94
^{15}N-HSQC Monitored Amide Exchange of ^{15}N-CaM76-148:$Na_v1.2_{IQp}$ Complex 95
NMR Spectroscopy for Structure Determination 95
Apo CaM_{76-148} :$Na_v1.2_{IQp}$ Structure Calculations 96
Quantification of chemical shifts due to $Na_v1.2_{IQp}$ or Ca^{2+} addition 97
NaCl Titration of apo CaM-$Na_v1.2_{IQp}$ Complex 97
Results 98
The C-domain of apo CaM_{1-148} is Necessary and Sufficient to Bind $Na_v1.2_{IQp}$ 98
Hydrogen/Deuterium Backbone Amide Exchange 99
Determination of apo CaM_{76-148}:$Na_v1.2_{IQp}$ Structure 100
Interaction Interface of $Na_v1.2_{IQp}$ with apo CaM_{76-148} 101
Effect of Ca^{2+} upon apo CaM_{1-148}:$Na_v1.2_{IQp}$ Complex 102
Effect of Ca^{2+} upon Molecular Size of CaM_{1-148}:$Na_v1.2_{IQp}$ Complex 103
Effect of Na^+ upon $Na_v1.2_{IQp}$ Binding to CaM 104
Discussion 104
A “Semi-open” apo C-domain Binds $Na_v1.2_{IQp}$. 104
A “Semi-open” apo C-domain is used to Bind a Non IQ-motif Containing Target 105
Canonical IQ-motifs Bind to apo CaM using Similar Orientations 107
Role of the N-domain of CaM_{1-148} in $Na_v1.2$ Regulation 108

CHAPTER V INFLUENCE OF ELECTROSTATIC INTERACTIONS ON CA^{2+} AND TARGET BINDING BY CAM 122

Introduction....122
Poisson-Boltzmann Equation....123
Materials and Methods....125
Poisson-Boltzmann calculations....125
Fluorescence Anisotropy Monitored Titrations of CaM Binding to Either $CaMKII_p$ or $Na_v1.2_{IQp}$ at Varied [NaCl or KCl]....126
Analysis of K_d for CaM Binding to $Na_v1.2_{IQp}$ or $CaMKII_p$....127
Results....129
Fluorescence Anisotropy Monitored CaM Titrations of $Na_v1.2_{IQp}$....129
Fluorescence Anisotropy Monitored CaM Titrations of $CaMKII_p$....130
Electrostatic Binding Energy of CaMKII for $(Ca^{2+})_4$-CaM_{1-148} Calculated via APBS....130
Discussion....131
Salt Dependence of $Na_v1.2_{IQp}$ Binding to apo and (Ca^{2+})-CaM....132

CHAPTER VI SUMMARY AND FUTURE DIRECTIONS....147

Thesis Summary....147
TFP Binding Induces a Biphasic Response in the Ca^{2+}-Binding Affinity of CaM....147
CaM uses Distinct Interfaces to Bind TFP under apo and Ca^{2+}-Saturating Conditions....148
Conservation of Carboxamide-Containing Sidechains in apo CaM Binding Motifs....150
Changes in the Electrostatic Environment of CaM Alters its Interaction with Targets....151
Future Studies....152
Changes in Met 144 Dynamics upon Binding $(Ca^{2+})_2$-CaM_{76-148}....152
Determination of Binding Site for N-domain of $(Ca^{2+})_4$-CaM on $Na_v1.2$....153
Circular Permutation of Charge Residues in $Na_v1.2_{IQp}$....153
In Vitro Evolution of apo CaM Binding IQ-motifs....154
Examination of Naturally Occurring $Na_v1.2_{IQp}$ R1902C Mutation on CaM....155
Structure Determination of Larger Intracellular Fragments of $Na_v1.2$ in Complex with CaM....155

APPENDIX A FORTRAN FUNCTION FOR FITTING FLUORESCENCE ANISOTROPY DATA TO A SIMPLE LANGMUIR BINDING ISOTHERM....161

APPENDIX B FORTRAN FUNCTION FOR ANALYSIS OF CALCIUM-DEPENDENT CHANGES IN FLUORESCENCE THAT DESCRIBE FILLING OF ONLY TWO SITES....164

APPENDIX C NMR ASSIGNMENTS OF APO $PCAM_{76-148}$....167

Amide Assignments of Apo $PCaM_{76-148}$....167
Carbonyl Assignments of apo $PCaM_{76-148}$....168
Methine, Methylene, and Methyl Assignments of apo $PCaM_{76-148}$....169

APPENDIX D NMR ASSIGNMENTS OF APO $PCAM_{76\_148}$ WHEN BOUND TO TFP....173

Amide Assignments of Apo $PCaM_{76-148}$ When Bound to TFP.....173
Carbonyl Assignments of apo $PCaM_{76-148}$ when Bound to TFP.....174
Methine, Methylene, and Methyl Assignments of apo $PCaM_{76-148}$ When Bound to TFP.....175

APPENDIX E NMR ASSIGNMENTS OF APO $PCAM_{76-148}$ WHEN BOUND TO $NA_V1.2_{IQP}$ 179

Amide Assignments of apo $PCaM_{76-148}$ When Bound to $Na_v1.2_{IQp}$ 179
Carbonyl Assignments of apo CaM_{76-148} When Bound to $Na_v1.2_{IQp}$.....180
Methine, Methyline, and Methyl Assignments of apo $PCaM_{76-148}$ When Bound to $Na_v1.2_{IQp}$ 181
Intramolecular NOE Assignments of $Na_v1.2_{IQp}$ 184

APPENDIX F RESTRAINT FILES USED FOR APO CAM_{76-148}:$NA_V1.2_{IQP}$ STRUCTURE CALCULATION.....191

Carbon NOE Restraint File.....191
Nitrogen NOE Restraint File 212
Hydrogen Bonding Restraint File.....225
$Na_v1.2_{IQp}$ Intramolecular Restraint File.....227
TALOS Dihedral Angle Restraint File.....233

BIBLIOGRAPHY.....248

LIST OF TABLES

Table 2.1 TFP Effects on Calcium Binding to CaM.....51

Table 3.1: Data collection and refinement statistis of $(Ca^{2+})_2$-CaM_{76-148}:TFP complex.....76

Table 4.1:Apparent amide exchange rates of apo CaM_{76-148} when bound to $Na_v1.2_{IQp}$ 110

Table 4.2:Structural statistics and root-mean-square deviation for 20 structures of apo CaM_{76-148}:$Na_v1.2_{IQp}$ complex 111

Table 5.1: Calculated effect of salt on $CaMKII_p$ binding to $(Ca^{2+})_4$-CaM_{1-148} 135

Table 5.2: Effect of salt on $Na_v1.2_{IQp}$ binding to apo and (Ca^{2+})-CaM 136

Table 5.3: Calculated effect of salt on $CaMKII_P$ binding to $(Ca^{2+})_4$-CaM_{1-148} 137

LIST OF FIGURES

Figure 1.1: Structure of $(Ca^{2+})_4$-CaM. 11

Figure 1.2: Ribbon diagram of an EF-hand motif....12

Figure 1.3: Sequence comparison of *Paramecium* (PCaM and Mammalian (mCaM) sequences....13

Figure 1.4: Superposition of experimentally observed conformations of CaM....14

Figure 1.5: Structures of apo CaM or partially Ca^{2+}-ligated CaM interacting with a target. 15

Figure 1.6: IQ-motif amino acid sequence conservation from 208 sequences derived from 108 human proteins, where Q at position 1 is almost invariant. 16

Figure 1.7: Domain structure of $Na_v1.2$. 17

Figure 1.8: Sequence alignment of all ten human Na^+ channel isoforms. 18

Figure 1.9: Chemical structures of CaM-binding drugs whose binding interface with CaM has been determined structurally. 19

Figure 1.10: Structures of $(Ca^{2+})_4$-CaM bound to drugs. 20

Figure 2.1: Structures of apo CaM, $(Ca^{2+})_4$-CaM, and Trifluoperazine. 52

Figure 2.2: Superposition of 3 Tertiary structures of the C-domain of CaM. 53

Figure 2.3: Structures of $(Ca^{2+})_4$-CaM bound to TFP. 54

Figure 2.4: ^{15}N-HSQC-monitored TFP titration of uniformly ^{15}N-labeled apo PCaM 55

Figure 2.5: ^{15}N-HSQC-monitored TFP titration of uniformly ^{15}N-labeled $(Ca^{2+})_4$-CaM. 56

Figure 2.6: Multiple chemical environments observed upon TFP titration of $(Ca^{2+})_4$-CaM....57

Figure 2.7: Effect of TFP on calcium binding to CaM_{1-148}....58

Figure 2.8: Effect of TFP on the calcium binding affinity of CaM_{1-80} and CaM_{76-148}....59

Figure 2.9: Biphasic fluorescence response to calcium binding at intermediate TFP....60

Figure 2.10: Comparison of TFP-saturated apo CaN $(Ca^{2+})_4$-CaM_{1-148} 61

Figure 2.11: Docking and models of TFP binding to the C-domain of CaM 62

Figure 2.12: Interdomain interactions mediated by TFP 63

Figure 3.1: Superposition of TFP:$(Ca^{2+})_4$-CaM_{1-148} structures 77

Figure 3.2: Sidechain Orientations of $(Ca^{2+})_4$-$CaM_{1-148}$when binding TFP at site A 78

Figure 3.3: Crystal structure of TFP bound $(Ca^{2+})_2$-CaM_{76-148} 79

Figure 3.4: Comparison of common TFP binding sites within $(Ca^{2+})_2$-CaM_{76-148} 80

Figure 3.5: Met 144 gating determines TFP orientation 81

Figure 3.6: Contacts made by TFP molecules with $(Ca^{2+})_2$-CaM_{76-148} 82

Figure 3.7: ^{15}N-HSQC spectrum of apo CaM_{76-148} showing the effect of TFP binding 83

Figure 3.8: Change in amide chemical shift of apo CaM_{76-148} upon TFP addition 84

Figure 3.9: T_2 Values for apo CaM_{76-148} in the absence and presence of TFP 85

Figure 3.10: Change in T_2 values of apo CaM_{76-148} upon TFP addition mapped upon the structure of apo CaM_{76-148} 86

Figure 3.11: Electron density of TFP binding sites in $(Ca^{2+})_2$-CaM_{76-148} 87

Figure 3.12: Superposition of common TFP binding sites in $(Ca^{2+})_2$-CaM_{76-148} and $(Ca^{2+})_4$-CaM_{1-148} 88

Figure 3.13: Structural morph between chain A and B or TFP-bound $(Ca^{2+})_2$-CaM_{76-148} 89

Figure 4.1: CaM and target interaction background 112

Figure 4.2: ^{15}N-HSQC Spectra of apo CaM_{76-148} and apo CaM_{1-148} bound to $Na_v1.2_{IQp}$ 113

Figure 4.3: $Na_v1.2_{IQp}$ binding to apo CaM_{76-148} quantified by ^{15}N-HSQC spectroscopy 114

Figure 4.4: ^{15}N-HSQC-monitored amide exchange of apo CaM_{76-148}:$Na_v1.2_{IQp}$ complex 115

Figure 4.5: Solution structure of apo CaM_{76-148} bound to $Na_v1.2_{IQp}$ 116

Figure 4.6: Binding interfaces of apo CaM_{76-148} and $Na_v1.2_{IQp}$ 117

Figure 4.7: Effect of Ca^{2+} upon apo CaM_{76-148} when bound to $Na_v1.2_{IQp}$ 118

Figure 4.8: Fluorescence anisotropy monitored titration of apo CaM bound to $Na_v1.2_{IQp}$ 119

Figure 4.9: Superposition of target bound apo CaM and CaM-like protein C-domains 120

Figure 4.10: Directionality of IQ-motif binding to the C-domain of CaM 121

Figure 5.1: CaM-binding domains classified by residues used to interact with the N- and C-domain of CaM 138

Figure 5.2: Helical Wheel Diagrams of CaM-Binding Domains 139

Figure 5.3: Intracellular and extracellular ion concentrations of a resting cell 140

Figure 5.4: Apo or $(Ca^{2+})_4$-CaM_{1-148} titration of $Na_v1.2_{IQp}$ at varied [KCl] 141

Figure 5.5: Simulated fitting curves used to determine $Na_v1.2_{IQp}$ binding affinity for CaM 142

Figure 5.6: Apo or $(Ca^{2+})_2$-CaM_{76-148} titration of $Na_v1.2_{IQp}$ at varied [KCl] 143

Figure 5.7: $(Ca^{2+})_4$-CaM_{1-148} titration of $CaMKII_p$ at varied [NaCl] and [KCl] 144

Figure 5.8: Calculated electrostatic binding energies of $CaMKII_p$ for $(Ca^{2+})_4$-CaM_{1-148} 145

Figure 5.9: Comparison of calculated and observed changes in $CaMKII_p$ binding to $(Ca^{2+})_4$-CaM_{1-148} as a function of salt 146

Figure 6.1: Model of apo and $(Ca^{2+})_4$-CaM C-domain conformations used when binding targets 157

Figure 6.2: ^{15}N-HSQC Spectrum and diffraction image of PCaM Mutants 158

Figure 6.3: Sequence alignment of $Na_v1.2$ and $Na_v1.5$ IQ-motifs 159

Figure 6.4: Schematic of phage display selection procedure 160

LIST OF ABBREVIATIONS

APBS	Adaptive Poisson-Boltzmann Solver
BAA	Basic Amphipathic Alpha-helix
CaMBD	Calmodulin binding domain
CaMKII	CaM Kinase II (CaMKII)
DPD	N-(3,3,-Diphenylpropyl-N'-[1-R-(2 3,4-Bis-Butoxyphenyl)-Ethyl]-Propylenediamine
EGTA	Ethylene Glycol bis2 (aminoethylether)=N,N,N',N' Tetraacetic Acid
FRET	Fluorescence Resonance Energy Transfer
HPLC	High Pressure Liquid Chromotography
KAR-2	3"-(Beta-Chloroethyl)-2",4"-Dioxo-3, 5"-Spiro-Oxazolidino-4-Deacetoxy-Vinblastine
LPBE	Linearized Poisson-Boltzmann Equation
mCaM	Mammalian Calmodulin
MLCK	Myosin Light Chain Kinase
$Na_v1.2$	Voltage-Dependent Sodium Channel type 2
$Nav1.2_{BAA}$	BAA-motif of Nav1.2
$Nav1.2_v1.2_{IQp}$	Voltage-Dependent Sodium Channel type 2 IQ-motif
NOE	Nuclear Overhauser Effect
NOESY	Nuclear Overhauser Effect Spectroscopy
PCaM	*Paramecium* Calmodulin
RMSD	Root Mean Standard Deviation
SAXS	Small Angle x-ray Scattering
SPAN	Value determined by subtracting minimum data value from maximum data value, for use in normalization of data

T2	Transverse Relaxation
TFP	10-[3-(4-Methyl-Piperazin-1-yl)-Propyl]-2-Trifluoromethyl-10H-Phenothiazine
TFP	Trifluoperazine
TOCSY	Total Correlation Spectroscopy
W-7	N-(6-Aminohexyl)-5-Chloro-1-Naphthalenesulfonamide

CHAPTER I

INTRODUCTION

The Ca^{2+} ion plays a vital role as a secondary messenger where its spatial and temporal location can be tightly regulated to perform a myriad of regulatory functions. Upon signaling, Ca^{2+} can be released into the cytosol from both intracellular and extracellular stores where it is then sensed by a variety of Ca^{2+}-binding proteins. The most prominent of these Ca^{2+}-binding proteins is Calmodulin, which regulates over 300 target proteins in a Ca^{2+}-dependent manner (Yap et al., 2000). To accomplish its regulatory functions, CaM interacts with its protein targets using a variety of Ca^{2+} ligation states. The first CaM-dependent proteins identified were Ca^{2+}-dependent, and the conclusion was drawn (prematurely) that Ca^{2+} was required for target binding by CaM. Targets have since been identified that interact with either apo or partially Ca^{2+}-saturated CaM, representing new classes of proteins whose interaction with one or both domains of CaM is Ca^{2+}-independent. This thesis seeks to examine the structural and thermodynamic properties of apo CaM when interacting with the anti-psychotic drug Trifluoperazine (TFP) as well as a peptide that represents the CaM binding domain of the voltage dependent sodium channel 1.2 isoform ($Na_v1.2$).

CaM Background

CaM is a Ca^{2+} sensor protein that is essential to many eukaryotic signal transduction pathways. The CaM sequence (148 a.a.) is highly acidic (pI of 4) and divided between two homologous domains which are connected by a flexible 5-residue linker (**Figure 1.1**). Each domain binds two Ca^{2+} ions cooperatively in neighboring EF-Hand motifs, giving rise to a total of 4 bound Ca^{2+} ions per molecule of CaM (Chattopadhyaya et al., 1992; Crouch and Klee, 1980; Pedigo and Shea, 1995; Rao et al., 1993). Sequence comparison of EF-hand Ca^{2+}-binding sites reveals a high level of sequence conservation among residues that coordinate the Ca^{2+} ion via pentagonal

bipyramidal geometry (Strynadka and James, 1989; Wilson and Brunger, 2000; Yang et al., 2002) (**Figure 1.2**). The primary sequence of CaM is highly conserved among eukaryotes. *Paramecium* CaM (PCaM) is 88% identical to all mammalian CaM (mCaM) sequences, with only four differences in the N-domain (residues 1-80, sites I and II) and 13 differences in the C-domain (residues 76-148, sites III and IV) (Kung et al., 1992; VanScyoc et al., 2006) (**Figure 1.3**). Although the two domains are similar in sequence and structure, the N-domain binds $Ca^{2+}$with a 10-fold lower affinity than the C-domain (Linse and Chazin, 1995; VanScyoc et al., 2002).

CaM has been observed to adopt multiple conformations (closed, semi-open, and open) dependent upon its ligation state (**Figure 1.4**) (Ataman et al., 2007; Chattopadhyaya et al., 1992; Houdusse et al., 2006; Kuboniwa et al., 1995; Meador et al., 1992). These conformations are defined by the inter-helical angles adopted by the EF-hand motifs within each domain. The "open" domain conformation of CaM is adopted by the N- and C-domains of CaM when Ca^{2+} binds to them either in the absence or presence of a target (Ataman et al., 2007; Swindells and Ikura, 1996; Wilson and Brunger, 2000). The "semi-open" domain conformation of CaM, which has only been observed in the C-domain of CaM, is adopted when binding to targets in the absence of Ca^{2+} (Houdusse et al., 2006; Swindells and Ikura, 1996). More commonly the absence of Ca^{2+} results in a "closed" conformation for both the N- and C-domains (Kuboniwa et al., 1995).

Interaction of $(Ca^{2+})_4$-CaM with Protein Targets

Changes in intracellular Ca^{2+} levels are linked to cellular events by the effect of Ca^{2+} on CaM: it triggers conformational changes that expose hydrophobic surfaces in both domains, altering its binding affinity for many target proteins (Bayley et al., 1996; Colbran, 1992; Klee, 1980). The Ca^{2+} binding affinity of CaM is "tuned" dependent upon which target it is bound to, allowing CaM to regulate numerous cellular processes

dependent upon [intra-cellular Ca^{2+}] (Evans and Shea, 2006; Peersen et al., 1997). The canonical mode of interaction of $(Ca^{2+})_4$-CaM with intra-cellular protein targets such as metabolic enzymes, cyclases, kinases, phosphatases, and ion channels is a compact ellipsoidal conformation (Hoeflich and Ikura, 2002; Meador et al., 1993; Mori et al., 2000) . The protein target sequence recognized by CaM is often a Basic Amphipathic Alpha-helix (BAA) motif where CaM typically binds in a Ca^{2+}-saturated manner (O'Neil and DeGrado, 1990). When bound to Ca^{2+}-dependent targets such as CaM Kinase II (CaMKII), or myosin light chain kinase (MLCK), the domains of CaM adopt an "open" conformation that exposes hydrophobic patches used for target binding resulting in Ca^{2+}-dependent regulation as shown previously in **Figure 1.4** (O'Neil et al., 1987).

Interaction of apo CaM with Protein Targets

Historically, activation of target proteins by CaM was thought to occur in a strictly Ca^{2+}-dependent manner where target binding always increased the Ca^{2+} affinity of CaM (Prozialeck and Weiss, 1982; Roberts and Harmon, 1992; Wang and Sharma, 1980; Weiss and Wallace, 1980). An emerging class of Ca^{2+}-independent CaM targets, typically found with ion channels and myosin motor proteins, interact more favorably with apo CaM instead of $(Ca^{2+})_4$-CaM. These targets typically contain IQ-motifs, although other non IQ-motif apo CaM Binding Domains (apo CaMBD's) have been observed (Fanger et al., 1999; Gerendasy et al., 1994; Liu and Storm, 1990; Martin and Bayley, 2004; Swindells and Ikura, 1996). Compared to structural studies of $(Ca^{2+})_4$-CaM, structural studies of apo-CaM interacting with targets are much less common. The disparity in representation of targets bound to $(Ca^{2+})_4$-CaM compared to apo-CaM is likely due to the mobility of the N-domain relative to the C-domain in the absence of Ca^{2+}, as well as the lack of an ordered structure within the Ca^{2+} binding loops of CaM in the absence of Ca^{2+}. The two high-resolution structures available of an apo C-domain

CaM interacting with peptides derived from either Myosin V (IQ-motif) or the SK-channel (non IQ-motif), depict CaM in an extended conformation where its C-domain interacts with each target through a "semi-open" conformation (**Figure 1.5**) (Houdusse et al., 2006; Schumacher et al., 2001).

The IQ-motif was first discovered and characterized from neuromodulin, a neurospecific apo CaM binding protein (Chapman et al., 1991; Liu and Storm, 1990). The IQ-motif is approximately 11 amino acids in length and distributed across multiple protein families ranging from myosins and ion channels, to Ras exchange and neuronal growth proteins (Bähler and Rhoads, 2002). The consensus sequence of this motif is (IQxxxBGxxxB, B=Lys or Arg), which forms an amphiphilic α-helix characterized as capable of binding to calmodulin in a Ca^{2+}-independent manner (**Figure 1.6**) (Swindells and Ikura, 1996). Analysis of genomic sequencing results indicate that there are at least 208 IQ-motifs in 108 proteins within the human genome (Venter et al., 2001). Examination of IQ-motifs across all eukaryotes reveals that of the IQ-motif defining residue Gln at position 1 is invariant, while IQ-motif position 6 (Gly) is the most variable (**Figure 1.6**). As indicated by the higher number of IQ-motifs than number of proteins which contain them (208 IQ-motifs per 108 proteins), several proteins contain multiple IQ-motifs (Houdusse et al., 2006; Martin and Bayley, 2004; Trybus et al., 2007). These proteins are mainly found in the myosin family, which depending upon the myosin variant, possess between 1 and 7 IQ-motifs typically separated by 9-16 residues (Koide et al., 2006).

The Voltage-Dependent Sodium Channel$_v$1.2

The voltage-dependent sodium channel$_v$1.2 ($Na_v1.2$) is an integral membrane protein comprised of one pore-forming α–subunit (2005 aa, 260 kDa), and one or more β–subunits (215 aa, 33–36 kDa each) which control the kinetics and gating of the channel as shown in (**Figure 1.7**) (Yu and Catterall, 2003). The physiological role of this channel

is to selectively regulate the flow of Na^+ ions across the cell membrane of central and peripheral neurons, allowing for the creation of action potentials (Catterall, 2000b). The IQ–motif containing CaM binding region of $Na_V1.2$ is located near its C-terminus and has a high degree of sequence identity to corresponding regions of all 10 known human sodium channel isoforms (**Figure 1.8**) (Mori et al., 2003; Theoharis et al., 2008; Yu and Catterall, 2003).

The α–subunit is comprised of four domains formed from six transmembrane helices, where the fourth helix contains a voltage sensor, responsible for activation of the $Na_v1.2$ upon depolarization of the cell membrane (Cormier et al., 2002; Mantegazza et al., 2001). Inactivation of $Na_V1.2$ is achieved via an intracellular loop between domains III and IV which contains the inactivation gate and the C–terminal tail of the α–subunit (**Figure 1.7**) (Chin and Means, 2000; Herzog et al., 2003; Mantegazza et al., 2001; Yu and Catterall, 2003). The mechanism of inactivation is hypothesized to occur when the inactivation gate physically blocks the channel pore via a CaM mediated interaction with C-terminal tail of $Na_v1.2$ (Chin and Means, 2000; Herzog et al., 2003; Mantegazza et al., 2001; Yu and Catterall, 2003). Among the ten known sodium channel isoforms the C–terminal tail is responsible for the different rates of inactivation of the α–subunit (Deschênes et al., 2001; Mantegazza et al., 2001). The membrane proximal half of the intracellular C–terminal tail has been modeled to contain six α–helices, where deletion of the putative sixth α–helix region slows recovery from inactivation, maintaining $Na_V1.2$ in a closed inactivated state (Cormier et al., 2002). In this proposed sixth α–helix of the C–terminal region, between residues 1901–1927 of the $Na_V1.2$, is located a CaM binding IQ-motif (Mori et al., 2000; Theoharis et al., 2008). Studies of $Na_V1.2$, as well as other sodium channel isoforms have shown that CaM binding is necessary for functional sodium currents, indicating a regulatory role for CaM on the sodium channel (Mori et al., 2003; Yu and Catterall, 2003).

The two CaM domains (N and C) may have distinct regulatory roles in sodium channel modulation. Separable roles for the CaM domains were first shown physiologically with *in vivo* studies by Kung and associates (Gustin et al., 1986). A genetic screen of mutagenized but viable *Paramecium* identified two classes of mutants that under– or over–reacted to chemical stimuli (Preston et al., 1992). These mutants were found to have defective regulation of their Ca^{2+}–dependent sodium and potassium channel currents, and the mutations were located in CaM. Under–reacting mutations that occurred between sites I and II and in site II of the N–domain of CaM were shown to affect only sodium conductance. In contrast, over–reacting mutations occurred within sites III and IV and the fourth helix of the C–domain and only affected potassium conductance.

Interaction of CaM with Drugs

In addition to interacting with naturally occurring protein targets, $(Ca^{2+})_4$-CaM has also been shown to interact with small molecule compounds such as N-(6-Aminohexyl)-5-Chloro-1-Naphthalenesulfonamide (W-7), N-(3,3,-Diphenylpropyl-N'-[1-R-(2 3,4-Bis-Butoxyphenyl)-Ethyl]-Propylenediamine (DPD), 3"-(Beta-Chloroethyl)-2",4"-Dioxo-3, 5"-Spiro-Oxazolidino-4-Deacetoxy-Vinblastine (KAR-2), and 10-[3-(4-Methyl-Piperazin-1-yl)-Propyl]-2-Trifluoromethyl-10H-Phenothiazine (Trifluoperazine, TFP) (**Figure 1.9**) (Cook et al., 1994; Harmat et al., 2000a; Hennessey and Kung, 1984; Horvath et al., 2005; Matsushima et al., 2007; Osawa et al., 1998; Tang et al., 2006; Vandonselaar et al., 1994a; Vertessy et al., 1998b). The compounds W-7 and DPD have primarily been used *in vitro* as CaM antagonists, while KAR-2 (a potent anti-microtubular agent), and TFP (antipsychotic agent) have been used in the clinical setting (Cook et al., 1994; Harmat et al., 2000a; Hennessey and Kung, 1984; Horvath et al., 2005; Matsushima et al., 2007; Osawa et al., 1998; Tang et al., 2006; Vandonselaar et al., 1994a; Vertessy et al., 1998b). In structures of these drugs bound to $(Ca^{2+})_4$-CaM, their

aromatic moieties insert into the hydrophobic pockets of CaM, mimicking CaM-peptide interactions which employ similar interactions to insert aromatic groups into CaM. In all of these structures the drug bound to the "open" conformation and like peptide targets all crystallographically determined structures of these drugs bound to $(Ca^{2+})_4$-CaM (with the exception of W-7 determined via NMR) depict CaM in a collapsed conformation as seen with peptides (**Figure 1.10**) (Cook et al., 1994; Harmat et al., 2000b; Horvath et al., 2005; Osawa et al., 1998; Vandonselaar et al., 1994a; Vertessy et al., 1998a). Although CaM has been observed to bind drugs *in vitro*, it is not the intended primary *in vivo* target of the previously mentioned compounds making *in vivo* CaM interactions with these drugs a secondary or off target effect (Sheets et al., 2006).

TFP

Trifluoperazine (TFP) is a phenothiazine class antipsychotic drug primarily used in the treatment of schizophrenia and related mental disorders (Abuzzahab, 1977; Oybir, 1962). Its first clinical trial for use in human patients with mental disorders was in 1958; more recently TFP has been indicated to reduce levels of opioid addiction (Tang et al., 2006; Wallis, 1958). Its primary function is that of a dopamine antagonist where it binds to, but does not activate, the dopamine receptor, thus blocking the action of dopamine or exogenous agonists (Clow et al., 1980; Kerwin et al., 1984; Roudebush et al., 1991). Clinically, TFP can be administered orally in solid pill form, as a liquid, or as an intramuscular injection where the daily amount administered is typically 15-20 mg per day (Carscallen et al., 1968; Gauron and Rowley, 1970; Hodes, 1960). The clinical use of TFP as an anti-psychotic has been discontinued in favor of newer formulations that do not carry the often irreversible side-effect of tardive dyskinesia typical of TFP and other first generation anti-psychotics like it (Lahti et al., 1993).

TFP has been shown *in vitro* to be a potent CaM antagonist, where it is often added to cell cultures to disrupt CaM interactions with its protein targets (Lydan and

O'Day, 1988; Pelech et al., 1983). The interaction of TFP with CaM is the most studied of small molecule CaM antagonists. However, the results of many of these studies which focused on the stoichiometry of TFP binding, its effect on Ca^{2+}-binding affinity, as well as how it alters the structure of CaM have been inconclusive (Cook et al., 1994; Massom et al., 1990b; Matsushima et al., 2000; Matsushima et al., 2007; Vogel et al., 1984; Yamaotsu et al., 2001). An example of this can be found in the stoichiometry of TFP bound to $(Ca^{2+})_4$-CaM in the three structures of that have been determined, where depending upon the structure examined, either 1, 2, or 4 TFP are bound to $(Ca^{2+})_4$-CaM as shown previously in (**Figure 1.10**).

Electrostatic Interactions of CaM with Targets

In addition to hydrophobic interactions, electrostatic interactions between CaM and its protein targets have a significant role in recognition and binding (Linse et al., 1991; Noguchi et al., 2004; Ogawa and Tanokura, 1984). At pH 7.4, CaM is highly acidic (pI = 4) and carries a net charge of -24 (apo) or -16 (Ca^{2+}-saturated), while the CaMBD's of target proteins contain basic residues arginine or lysine, resulting in electrostatic attraction between the two molecules. The opening and closing of ion channels necessary for cell signaling results in a constant flux of Ca^{2+}, K^+, and Na^+ ions, altering the strength of electrostatic interactions between CaM and its targets. K^+ and Na^+ also reduce the Ca^{2+}-binding affinity of CaM, making it intriguing to learn the functional consequences of how they affect CaM-protein interactions.

Description of Thesis Content

Chapter II describes studies conducted to explore how the Ca^{2+}-binding properties of CaM are altered upon binding TFP, as well as the binding stoichiometry of TFP to apo and $(Ca^{2+})_4$-CaM. In this chapter fluorescence-monitored Ca^{2+} titrations demonstrate that dependent upon the [TFP] examined that the Ca^{2+}-binding affinity of CaM can either increase or decrease relative to values observed in the absence of TFP.

Additionally using ^{15}N-HSQC NMR spectroscopy the stoichiometry of TFP binding was dependent upon the Ca^{2+} ligation state of CaM where 2 and 4 TFP were found to bind to apo and $(Ca^{2+})_4$-CaM respectively. The major finding of experiments conducted in **Chapter II** were reported in a manuscript titled *"Allosteric Effects of the Anti-Psychotic Drug Trifluoperazine on the Energetics of Calcium Binding by Calmodulin"* that has been published in Proteins: Structure, Function, and Bioinformatics.

Chapter III addresses how TFP alters the structures of apo and $(Ca^{2+})_4$-CaM at the atomic level. In this chapter I show, using x-ray crystallography, that TFP binds $(Ca^{2+})_2$-$CaM_{76\text{-}148}$ in two different orientations, unifying what were otherwise conflicting observations within the field. I will also show, using NMR spectroscopy, that the chemical environment of specific atoms of apo $CaM_{76\text{-}148}$ are perturbed upon TFP addition. The major findings of experiments conducted in **Chapter III** will be reported in a manuscript that is in preparation for submission

Chapter IV discusses how binding of $Na_v1.2_{IQp}$ alters the structure of apo $CaM_{76\text{-}148}$. In this chapter I will show using NMR spectroscopy how apo $CaM_{76\text{-}148}$ adopts a "semi-open" conformation upon binding $Na_v1.2_{IQp}$. I will also demonstrate, using NMR spectroscopy, that when $Na_v1.2_{IQp}$ binds to apo $CaM_{1\text{-}148}$, the N- and C-domains adopt "closed" and "semi-open" domain conformations respectively. The major findings of experiments conducted in **Chapter IV** will be reported in a manuscript that is in preparation for submission.

Chapter V presents preliminary studies of how changing the solution ionic strength via KCl or NaCl alters the strength of electrostatic interaction between CaM and peptides (melittin, CaMKII, and $Na_v1.2_{IQp}$). In this chapter I show using fluorescence anisotropy the effect that varied [NaCl] and [KCl] salts have on the binding affinity of CaM for the peptides Melittin, CaMKII, and $Na_v1.2_{IQp}$. Poisson-Boltzman calculations were performed to theoretically examine how varying [NaCl] or [KCl] altered the electrostatic attraction between $(Ca^{2+})_4$-CaM and CaMKII. These studies indicated that

increasing [salt] lowered the electrostatic attraction of CaM for all peptides tested. Significant differences were observed though between experimental and theoretical studies involving $(Ca^{2+})_4$-CaM and CaMKII suggesting that another factor, possibly conformational change by CaM and/or CaMKII influence the electrostatic interaction between these two molecules.

Chapter VI discusses the results of the prior chapters and their contribution to our understanding of the role of target interactions with CaM under apo conditions. While the work described in this thesis presents a high-resolution structure of apo CaM bound to $Na_v1.2_{IQp}$, the structural basis of how $(Ca^{2+})_4$-CaM interacts with $Na_v1.2_{IQp}$ or another proposed Ca^{2+}-dependent CaM binding site ($Na_v1.2_{BAA}$) is not clear. Future experiments well determine how $(Ca^{2+})_4$-CaM interacts with its binding domains ($Na_v1.2_{IQp}$ and $Na_v1.2_{BAA}$) of $Na_v1.2$. Experiments are proposed to resolve the role of the N-domain in $Na_v1.2$ regulation under Ca^{2+}-saturating conditions where it has been implicated in interacting with the $Na_v1.2_{BAA}$ region of $Na_v1.2$.

Appendices provide Fortran functions used in nonlinear squares analysis, and chemical shift assignments of apo CaM_{76}, apo $CaM_{76\text{-}148}$ when bound to TFP, and apo $CaM_{76\text{-}148}$ when bound to $Na_v1.2_{IQp}$.

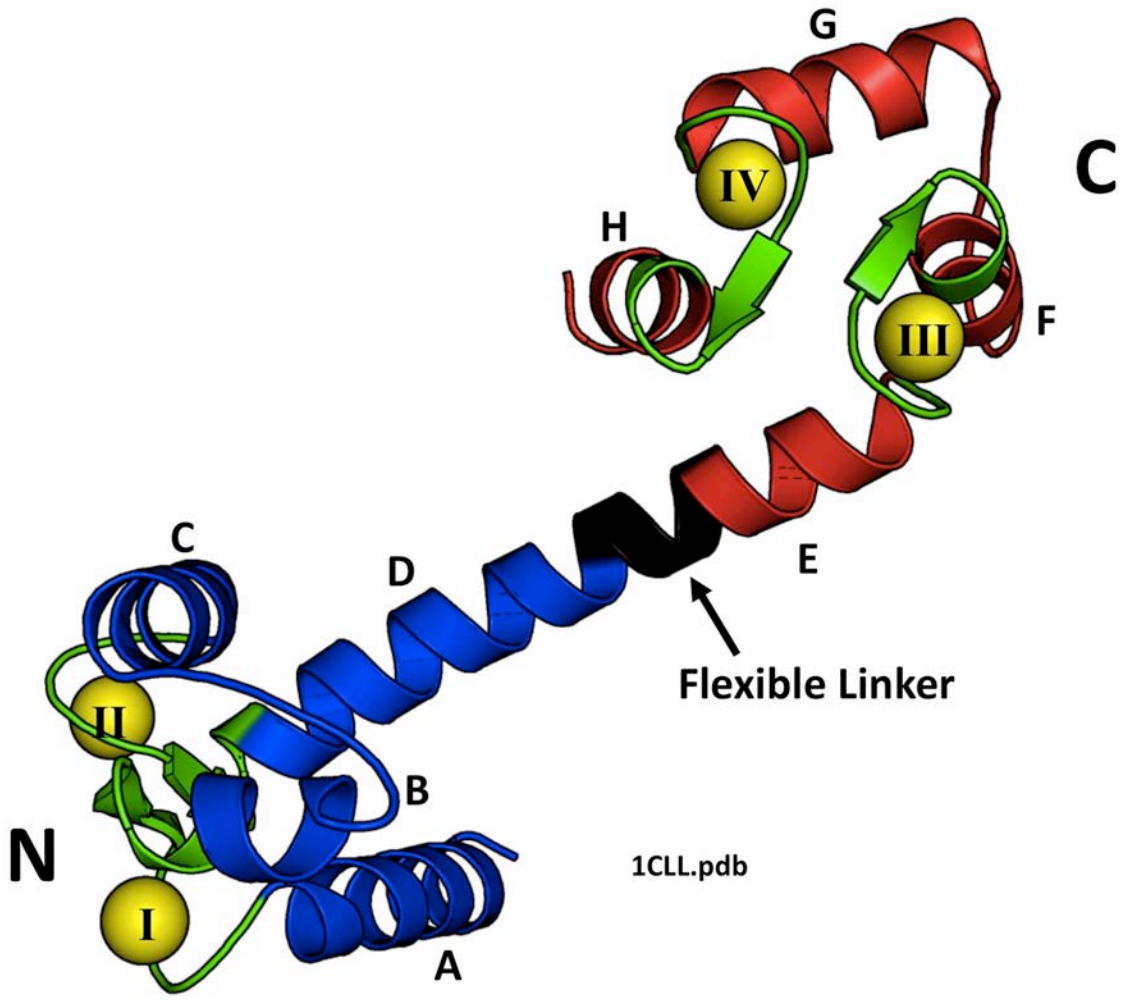

Figure 1.1: Structure of $(Ca^{2+})_4$-CaM.
Ca^{2+}-binding sites (green) I and II are located in the N-domain (blue, helices A-D), while Ca^{2+}-binding sites III and IV and located in the C-domain (red, helices E-H), allowing CaM to bind 4 Ca^{+} ions (yellow spheres). The N- and C- domains of CaM are connected by a 5 residue linker (black).
Users/nmr_mike/Thesis/Chapter_I/Figure1_1.jpg

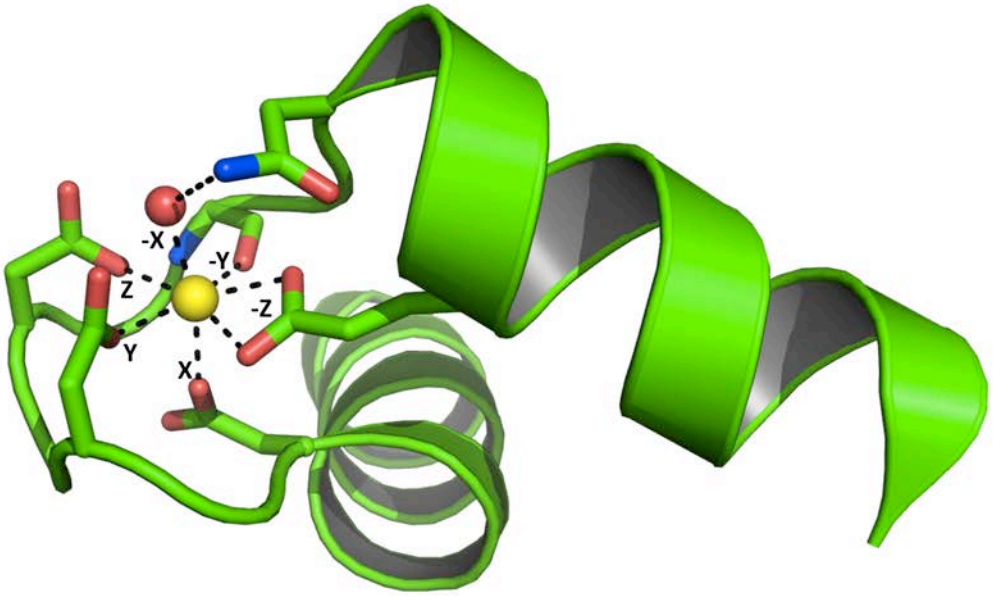

	X		Y		Z		-Y		-X			-Z
PCaM	D	K	D	G	D	G	T	I	T	T	K	E
mCaM	D	K	D	G	D	G	T	I	T	T	K	E
	20	21	22	23	24	25	26	27	28	29	30	31
PCaM	D	A	D	G	N	G	T	I	D	F	P	E
mCaM	D	A	D	G	N	G	T	I	D	F	P	E
	56	57	58	59	60	61	62	63	64	65	66	67
PCaM	D	R	D	G	N	G	L	I	S	A	A	E
mCaM	D	K	D	G	N	G	Y	I	S	A	A	E
	93	94	95	96	97	98	99	100	101	102	103	104
PCaM	D	I	D	G	D	G	H	I	N	Y	E	E
mCaM	D	I	D	G	D	G	Q	V	N	Y	E	E
	129	130	131	132	133	134	135	136	137	138	139	140

Figure 1.2: Ribbon diagram of an EF-hand motif.
The EF-hand consists of two α-helices connected by a 12-residue loop. Residues 1, 3, 5, 7, 9 and 12 (sticks) of the loop contribute a side chain or backbone oxygen (red) atom necessary for Ca^{2+} (yellow sphere) binding. Residue 12, which is a Glu, contributes both oxygens from its side chain carboxylic acid group. Residue 9 of the Ca^{2+}-binding loop does not directly bind the Ca^{2+} ion but instead coordinates a water (red sphere) at position -X. Below are aligned *Paramecium* and mammalian CaM sequences where the identity of X, Y, Z, -X, -Y, and –Z are in each of the 4 Ca^{2+}-bidning loops are boxed. Differences in primary sequence of the Ca^{2+}-binding loops are highlighted in gray.
Users/nmr_mike/Thesis/Chapter_I/Figure1_2.jpg

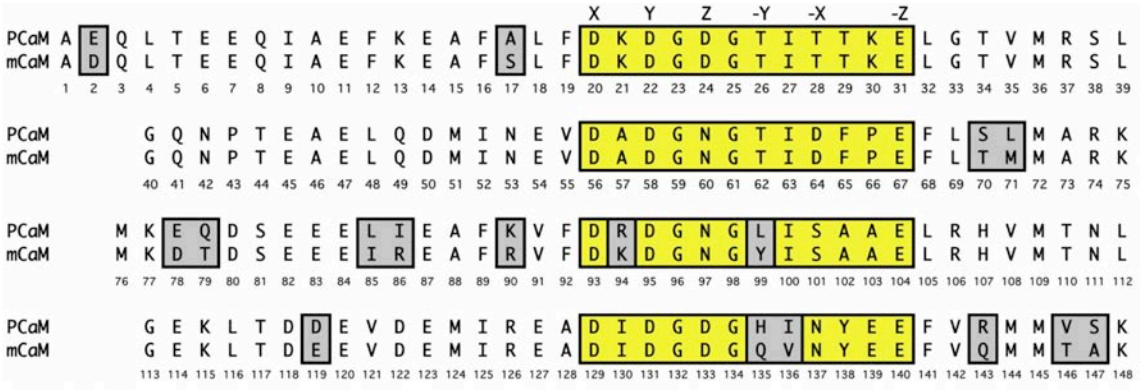

Figure 1.3: Comparison of *Paramecium* (PCaM) and Mammalian (mCaM) sequences. Differences are highlighted in gray, while Ca^{2+}-binding sites are highlighted in yellow. Users/nmr_mike/Thesis/Chapter_I/Figure1_3.jpg

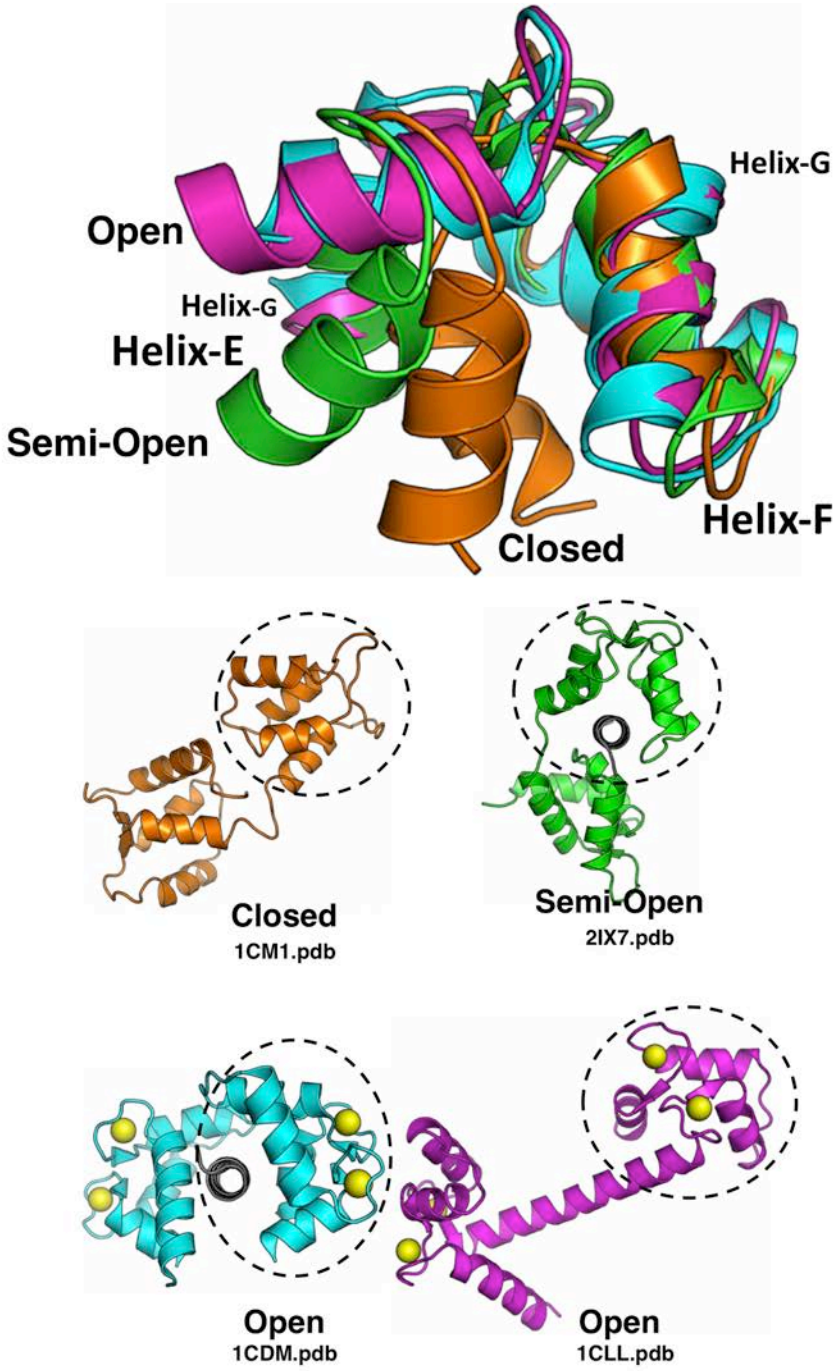

Figure 1.4: Superposition of experimentally observed conformations of CaM. Examples of the "closed" (1CFC.pdb orange), "semi-open" (2IX7.pdb green) and "open" (1CDM.pdb aqua and 1CLL.pdb magenta) conformations of the C-domain are aligned according to the positions of the F and G (first and fourth) helices of the domain. Users/nmr_mike/Thesis/Chapter_I/Figure1_4.jpg

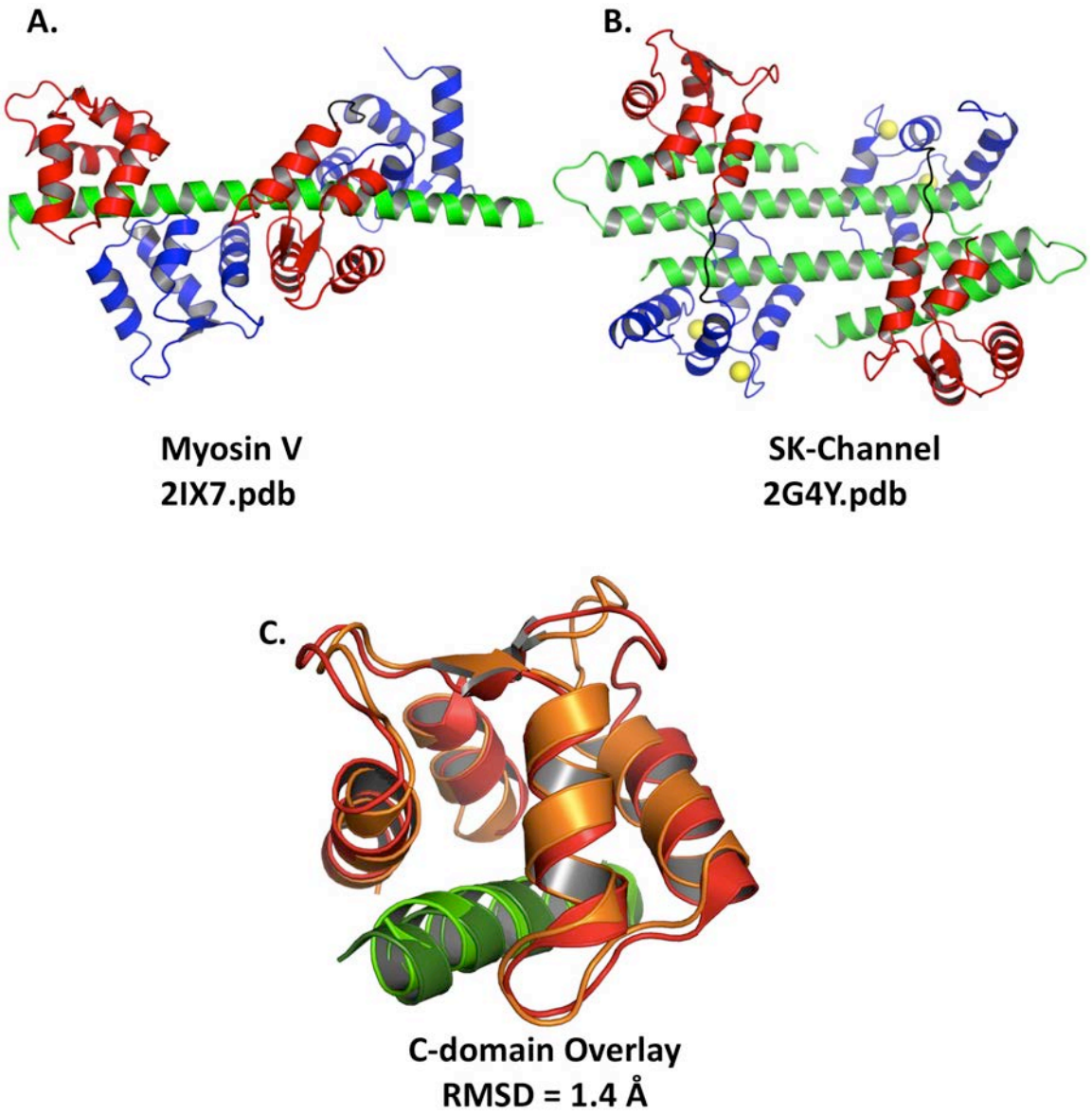

Figure 1.5: Structures of apo CaM or partially Ca^{2+}-ligated CaM interacting with a target.
A. Apo CaM ("closed" N-domain blue, "semi-open" C-domain red) bound to a peptide containing tandem IQ-motifs derived from Myosin V (green). B. Partially Ca^{2+}-ligated CaM ("open" N-domain blue, "semi-open" C-domain red) where its N-domain is Ca^{2+}-saturated (Ca^{2+} yellow sphere), and apo C-domain are bound to peptide derived from the small-conductance Ca^{2+}-activated K^{+} channels (SK-channel) in green. C. Superposition of apo C-domains of CaM from myosin V (red and green) and SK-channel (orange and dark green).
Users/nmr_mike/Thesis/Chapter_I/Figure1_5.jpg

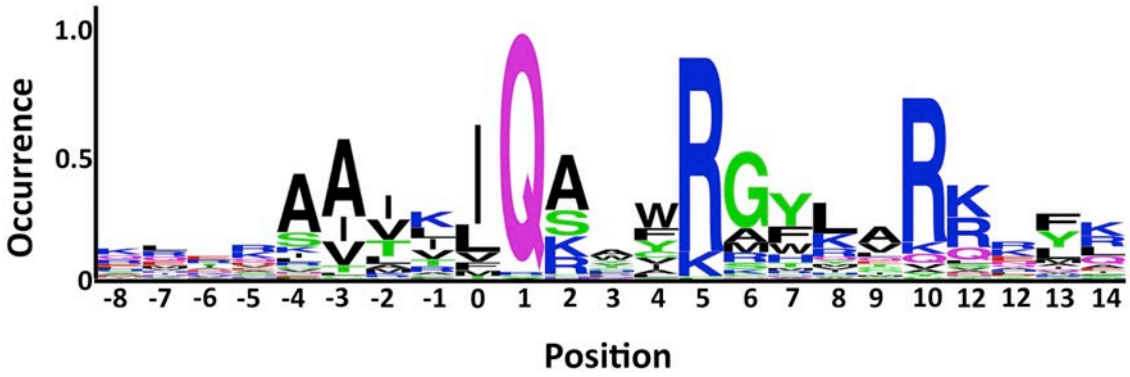

Figure 1.6: IQ-motif amino acid sequence conservation from 208 sequences derived from 108 human proteins, where Q at position 1 is almost invariant. Users/nmr_mike/Thesis/Chapter_I/Figure1_6.jpg

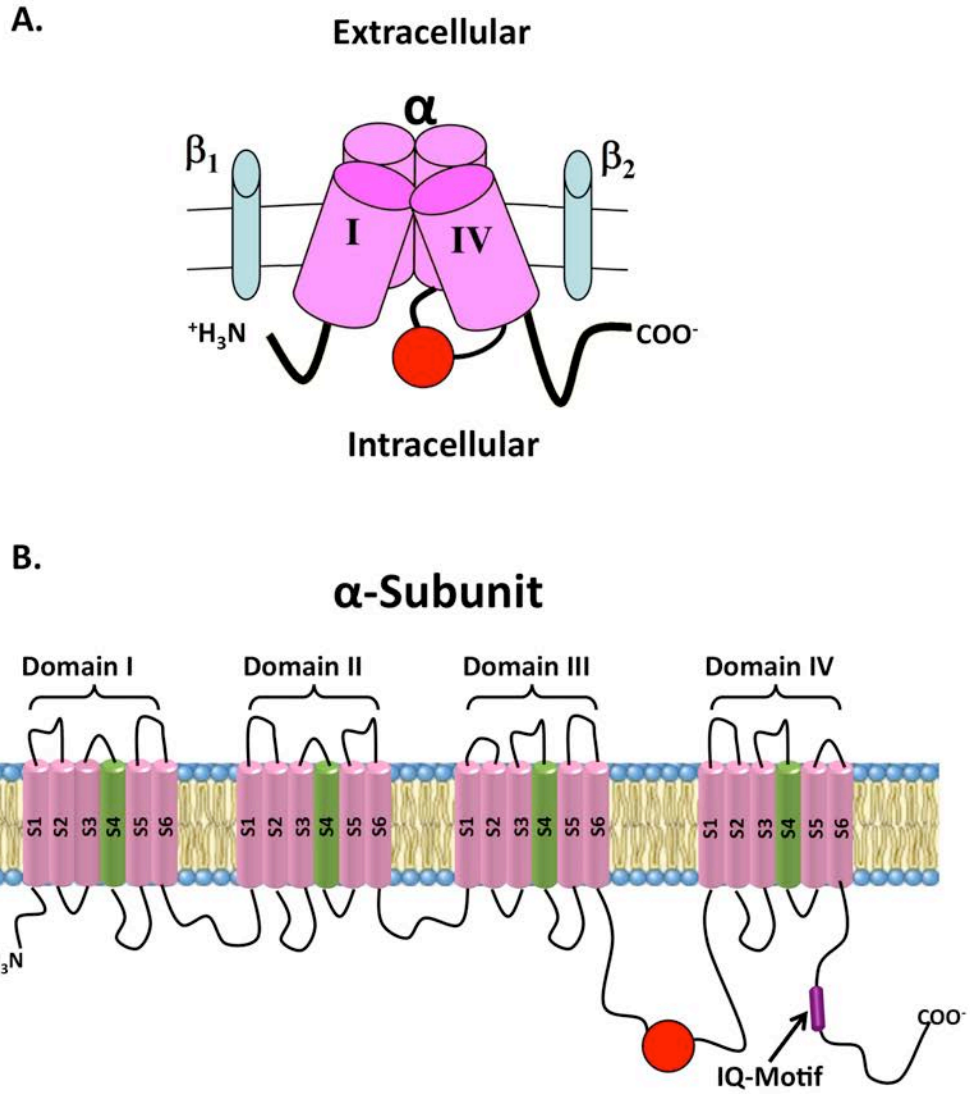

Figure 1.7: Domain structure of $Na_v1.2$.
A. $Na_v1.2$ is composed of a single 4-domain α-subunit, and multiple noncovalently attached β-subunits.
B. The α-subunit of $Na_v1.2$ is composed of 4 domains, each of which is made up of 6 helices, where the 4^{th} helix (green) is part of the Na^+ channel pore. The loop between domains III and IV, contains the inactivation gate (red sphere) which is responsible for blocking the inside of the channel shortly after it has been activated. The CaM-binding IQ-motif (purple cylinder) is located near the C-terminus of the channel.
Users/nmr_mike/Thesis/Chapter_I/Figure1_7.jpg

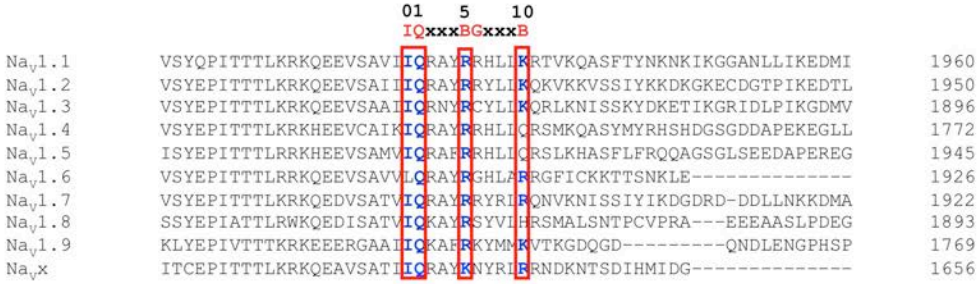

Figure 1.8: Sequence alignment of all ten human Na^+ channel isoforms. The locations of IQ-motif defining residues have been highlighted in red. Users/nmr_mike/Thesis/Chapter_I/Figure1_8.jpg

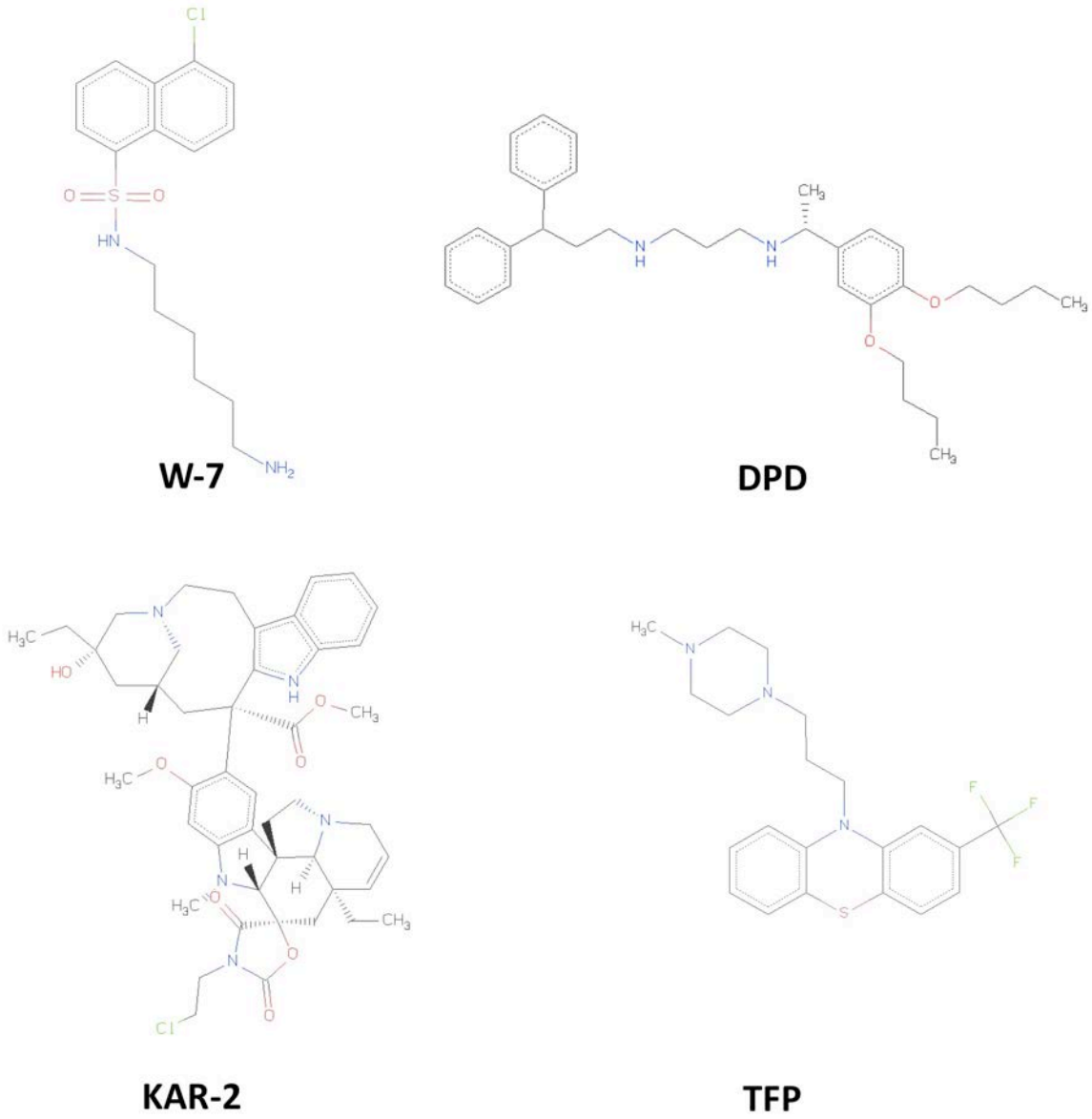

Figure 1.9: Chemical structures of CaM-binding drugs whose binding interface with CaM has been determined structurally.
Users/nmr_mike/Thesis/Chapter_I/Figure1_9.jpg

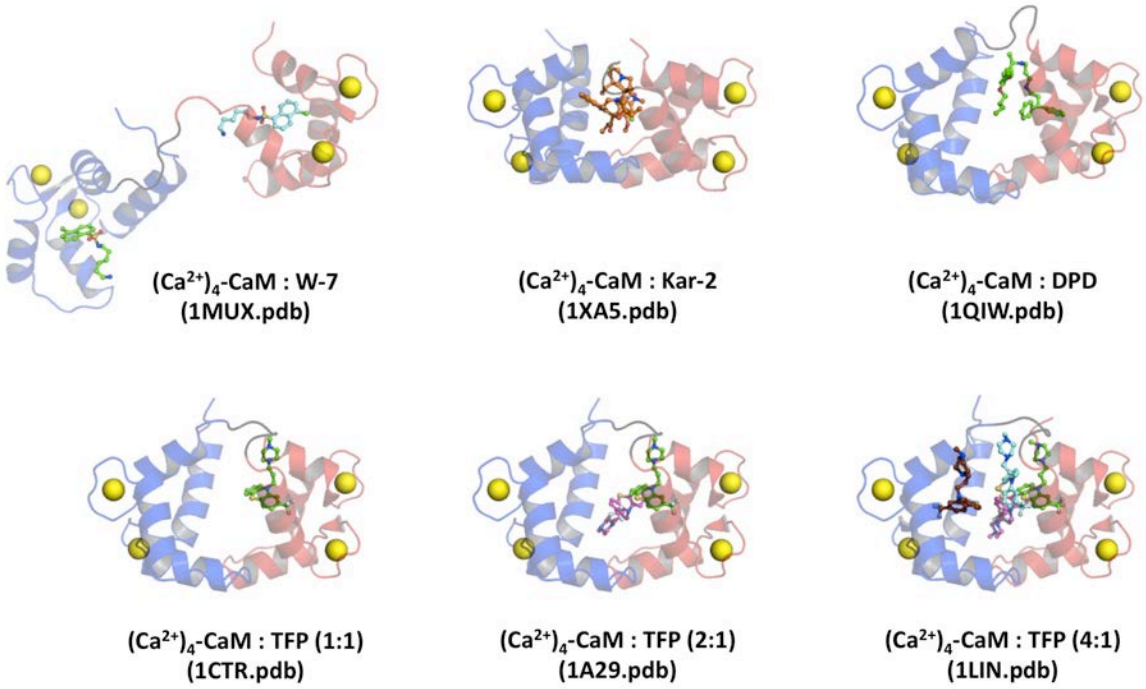

Figure 1.10: Structures of $(Ca^{2+})_4$-CaM bound to drugs.
X-ray (Kar-2, DPD, TFP) or NMR (W-7) determined structures of $(Ca^{2+})_4$-CaM bound to drugs where the N- and C-domain of $(Ca^{2+})_4$-CaM are colored blue and red respectively, drug molecules are shown in sticks, while Ca^{2+} ions are represented by yellow spheres.
Users/nmr_mike/Thesis/Chapter_I/Figure1_10.jpg

CHAPTER II

ALLOSTERIC EFFECTS OF THE ANTI-PSYCHOTIC DRUG TRIFLUOPERAZINE ON THE ENERGETICS OF CA^{2+} BINDING BY CAM

Introduction

Calmodulin (CaM) is a small (148 a.a.), essential, and highly conserved eukaryotic protein that is required for many calcium-sensitive signal transduction pathways (Hidaka and Ishikawa, 1992; Newman, 2008). It is composed of two homologous domains (N and C). Each domain consists of a pair of EF-hands (a helix-loop-helix motif) that forms a 4-helix bundle, and binds two calcium ions cooperatively. The domains are connected by a linker that plays a regulatory role in determining calcium affinity, and permits the domains to adopt multiple relative orientations to optimize interactions with target proteins (**Figure 2.1a**) (Sorensen et al., 2002b; Sorensen and Shea, 1998; Zhang et al., 1995).

Although the two domains are similar in sequence and structure, the affinity of the N-domain for calcium is an order of magnitude lower than that of the C-domain (Seamon, 1980; VanScyoc et al., 2002). As the concentration of intracellular calcium increases, calcium binding to 12-residue sites in CaM triggers conformational changes, causing the pairs of helices in each 4-helix bundle to separate. This structural change associated with the transition from apo (calcium-depleted) to $(Ca^{2+})_4$-CaM exposes hydrophobic residues that alter the affinity of CaM for target proteins (Chattopadhyaya et al., 1992; Kuboniwa et al., 1995; Meador et al., 1992; Wilson and Brunger, 2000). $(Ca^{2+})_4$-CaM (4 bound calcium ions) is shown in **Figure 2.1b**.

In a CaM-target complex, the protein-protein interface is determined by the number and location of occupied calcium-binding sites of CaM, conformational change propagated from those binding sites, and the surface of the target protein. Based

on the interhelical angles adopted by the paired helices of each domain, the CaM C-domain has been categorized as adopting three distinct conformations: "closed", "semi-open", and "open" (Chattopadhyaya et al., 1992; Kuboniwa et al., 1995; Meador et al., 1992; Wilson and Brunger, 2000). Any of these may be adopted by free CaM (**Figure 2.2**), consistent with the hypothesis that changes in the distribution of pre-existing conformational states occur upon binding to Ca^{2+} or a target protein (Yap et al., 1999). In high-resolution structures, only apo CaM has been observed to adopt the "closed" (**Figure 2.2B**) and "semi-open" forms (**Figure 2.2C**), while only $(Ca^{2+})_4$-CaM has been observed in the "open" form (**Figure 2.2D-E**). Binding of a target protein stabilizes the "semi-open" or "open" conformation of CaM by burying hydrophobic surface area that would otherwise be exposed to solvent. For example, a CaMKII peptide bound to calcium-saturated "open" CaM (1CM1.pdb) buries 1226 $Å^2$ of the surface area of CaM; of that, 990 $Å^2$ (81%) is hydrophobic (Wall et al., 1997).

For many years, activation of CaM-regulated target proteins such as metabolic enzymes, kinases, and phosphatases was thought to occur in a strictly calcium-dependent manner, such that the extent of binding of a target protein to apo CaM was negligible, and binding to $(Ca^{2+})_4$-CaM always increased its calcium affinity (Cox, 1988). However, there are subclasses of CaM-regulated target proteins, including some ion channels, that contain IQ-motifs that reduce the calcium affinity of CaM (Martin and Bayley, 2004; Theoharis et al., 2008). These targets interact preferentially with apo CaM. The only high resolution structure of apo CaM interacting with an IQ-motif (2IX7.pdb) is the crystallographic observation of two apo CaM molecules bound to a peptide containing two adjacent IQ-motifs derived from Myosin V (Houdusse et al., 2006) (see **Figure 2.2c**). In this complex, both N-domains were "closed" whereas the C-domains were "semi-open". Analysis of the CaM-peptide interface showed that hydrophobic residues of CaM accounted for most (71% and 75%) of the buried surface of the two CaM C-domains.

Drugs with aromatic moieties bind to CaM in a manner similar to protein targets that bury a phenylalanine or tryptophan residue in the hydrophobic pockets of CaM (Cook et al., 1994; Vandonselaar et al., 1994b; Vertessy et al., 1998b). Trifluoperazine (TFP) (**Figure 2.1c**) is a CaM antagonist historically used in the treatment of mental illness because of its interaction with the dopamine receptor; recently, it was implicated in the disruption of opioid tolerance (Tang et al., 2006). TFP is membrane-permeable and is commonly added to cell culture media to disrupt CaM-mediated processes (Barrington and Majewski, 1994; Chen et al., 2008; Frankfurt et al., 1995). Structures of three TFP-CaM complexes (Cook et al., 1994; Vandonselaar et al., 1994b; Vertessy et al., 1998b) have been determined crystallographically. In these, 1, 2, or 4 molecules of TFP are bound to $(Ca^{2+})_4$-CaM; all of them share a TFP-binding site in the C-domain but only one structure (1LIN.pdb) has a TFP-binding site in the N-domain. Superposition of these structures showed that the backbone of CaM adopts indistinguishable conformations in all of them, despite differences in the number and location of TFP molecules bound (**Figure 2.3D**). The relative abundance of these three ligation states of TFP bound to CaM in solution is not known. In all three complexes, the tertiary structure of CaM mimics that of $(Ca^{2+})_4$-CaM when bound to CaMKII, and other kinases that increase its calcium affinity (Clapperton et al., 2002; Heidorn et al., 1989; Ikura et al., 1992). The CaM-binding domain in those enzymes is a BAA (basic amphipathic alpha helical) motif.

The conflicting structural evidence regarding a preferred binding stoichiometry for TFP binding to CaM, as well as disagreement on the effects of TFP on the calcium-binding properties of CaM (Cook et al., 1994; Craven et al., 1996; Massom et al., 1990c; Tanokura and Yamada, 1985; Vandonselaar et al., 1994b; Vertessy et al., 1998b), motivated this study of the thermodynamic and structural properties of intermediate ligation states. These are critical for understanding how the highly homologous N- and C-domains of CaM exert different physiological effects on target proteins, and exploring

whether exogenous, pharmaceutical applications of TFP and related drugs truly target only the calcium-saturated form of CaM, as has been assumed.

TFP titrations of CaM monitored by ^{15}N-HSQC spectroscopy showed that TFP saturated apo CaM at a ratio of 2:1, but saturated $(Ca^{2+})_4$-CaM at a ratio of 4:1. Equilibrium calcium titrations monitored by steady-state fluorescence spectroscopy demonstrated that, unlike the majority of effectors (e.g., peptides and proteins) whose binding to CaM has been examined in detail, TFP reduced the calcium affinity of CaM at low stoichiometries. Thus, thermodynamic linkage requires that TFP have a higher affinity for apo CaM than for $(Ca^{2+})_4$-CaM; this is similar to the preferential binding of most IQ-motifs to apo CaM.

However, the multiplicity of binding stoichiometries allows for reversal of this effect. At higher ratios (8:1) of TFP:CaM, the calcium affinity of CaM reversed, and was more favorable than that in the absence of TFP. These effects were found to be similar, but not identical, in each domain (N and C) of CaM and were compared to the effects of TFP on isolated domain fragments. On this basis, a model is proposed in which the "semi-open" conformation offers a "pocket" for binding of aromatic moieties that is unlike the FLMM pocket (Ataman et al., 2007) of the "open" conformation where aromatic side chains of many peptides are known to bind to CaM. TFP recognizes this site on the "semi-open" conformation of an apo domain that is not available when CaM adopts the "open" conformation.

The binding preference of a single TFP molecule for apo CaM is significant because, to the best of our knowledge, it is the only drug identified to reduce calcium affinity. This motivates a review of studies in which TFP antagonizes CaM-dependent cellular phenomena. The interference observed in those studies has been interpreted as arising from the effects of the drug on $(Ca^{2+})_4$-CaM and its regulation of enzymes or channels. However, the findings presented here show that TFP can act as an antagonist

of apo CaM, which is critical for regulating pathways that are distinct from those modulated by $(Ca^{2+})_4$-CaM.

Materials and Methods

Protein over-expression and purification

IPTG-induced over-expression of CaM was performed using transformed in the *E. coli* strains BL21 DE3 or BL21 DE3-pLysS cells containing the recombinant pT7-7 vector of interest: full-length mammalian CaM_{1-148}, CaM_{1-80}, and CaM_{76-148} (Pedigo et al., 1992). For ^{15}N-labeled proteins used in the NMR studies, *Paramecium* CaM_{1-148} (PCaM) was over-expressed in minimal medium with ^{15}N-NH_4Cl (Cambridge Isotopes) as the sole nitrogen source. The proteins were then purified as described by Putkey (Putkey et al., 1985). The recombinant proteins were 97-99% pure as judged by silver-stained SDS-PAGE and reversed-phase HPLC. Protein concentrations were calculated from UV absorbance in 0.1 N NaOH, using the extinction coefficients for Phe and Tyr reported by Beaven and Holiday (Beaven and Holiday, 1952)

Equilibrium calcium titrations monitored by intrinsic protein fluorescence

Calcium titrations were monitored at 22 °C with a PTI-QM4 Fluorimeter (Photon Technology International, Birmingham, NJ) using bandpasses of 4 nm (for excitation) and 6 nm (for emission). CaM (CaM_{1-148}, CaM_{1-80}, or CaM_{76-148} at 6 μM) solutions, containing 0, 6, 12, 18, 24, or 48 μM TFP (Sigma-Aldrich, St. Louis, MO), were prepared in 50 mM HEPES, 100 mM KCl, 5 mM NTA, 0.05 mM EGTA, 1 mM $MgCl_2$, and 5.75 nM Oregon Green (pH 7.4). The concentration of TFP was determined using an $\varepsilon_{305.5}$ of 3540 M^{-1} cm^{-1} (Hart et al., 1983). CaM was titrated using a microburet (Micro-Metric Instrument Co., Cleveland, OH) fitted with a 250 μL Hamilton syringe (Hamilton Co., Reno, NV) containing a concentrated $CaCl_2$ solution prepared in a matching buffer.

Binding of calcium to sites I and II in the N-domain was monitored with λ_{ex} of 250 nm, and λ_{em} of 280 nm, based on the intrinsic phenylalanine fluorescence. Binding to sites III and IV in the C-domain was monitored with λ_{ex} of 277 nm, and λ_{em} of 320 nm, based on the intrinsic tyrosine fluorescence as previously described (VanScyoc et al., 2002). The fluorescent calcium indicator dye Oregon Green 488 BAPTA-5N (Oregon Green, 5.75 nM) (Molecular Probes, Eugene, OR) whose increase in fluorescence intensity was linearly proportional the $[Calcium]_{free}$ was used to determine the free calcium concentration at each point in the titration according to **Equation 2.1**, described previously by (VanScyoc et al., 2002)

$$[calcium]_{free} = K_d \frac{f_{[x]} - f_{low}}{f_{high} - f_{[x]}} \qquad (2.1)$$

where f_{high} and f_{low} are the highest and lowest observed fluorescence intensity signals, respectively, observed for Oregon Green during the titration. The K_d of calcium binding to Oregon Green was determined previously to be 34.24 μM in 50 mM HEPES, 100 mM KCl, and 1 mM $MgCl_2$ (pH 7.4) at 22 C (λ_{ex} of 494 nm, λ_{em} of 521 nm) (VanScyoc et al., 2002). Each titration was repeated at least three times.

Free energies of calcium binding to the pair of sites in each domain were determined by fitting the titrations to a model-independent two-site (Adair) function (**Equation 2.2**), as described previously (VanScyoc et al., 2002),

$$\bar{Y} = \frac{K_1[X] + 2K_2[X]^2}{2(1 + K_1[X] + K_2[X]^2)} \qquad (2.2)$$

where $[X]$ is free calcium, and the macroscopic association constant K_1 is the sum of intrinsic microscopic equilibrium constants ($k_1 + k_2$) for two sites: either sites I and II in the N-domain, or sites III and IV in the C-domain. This formulation allows the microscopic binding constants (k_1 and k_2) to be nonequivalent. The second macroscopic equilibrium constant K_2 ($k_1k_2k_c$) is the product of the intrinsic microscopic equilibrium

constants (k_1, k_2) and the cooperativity constant (k_c). The parameters ΔG_1 and ΔG_2 are macroscopic binding free energies, with $\Delta G_i = -RT \ln K_i$. The parameter ΔG_2 is thus the total free energy of saturating both calcium-binding sites in a domain.

Changes in fluorescence intensity for the calcium titrations were normalized to the highest and lowest experimentally determined signals. To account for experimental variations in the asymptotes of replicate titrations, we performed nonlinear least-squares analysis of the fluorescence intensity signal using the function *f(X)*, as given by **Equation 2.3**, as described previously (VanScyoc et al., 2002).

$$f(X) = Y_{[X]low} + \bar{Y} \bullet Span \qquad (2.3)$$

where $\bar{Y}$ refers to the average fractional saturation as described by **Equation 2.2**, and $Y_{[X]low}$ corresponds to the value of the fluorescence intensity in the absence of calcium. *Span* refers the normalized range (0-1, or -1-0) of the data signal. The parameter *Span* was negative in the case of a decreasing signal and positive in the case of an increasing signal. For monotonic titrations with well defined asymptotes, values for all parameters (ΔG_1, ΔG_2, $Y_{[X]low}$ and *Span*) were fit simultaneously using NONLIN (Johnson et al., 1981; Johnson and Frasier, 1985).

Note that a ratio of N:1 TFP:CaM does not indicate that all CaM molecules in the solution have N TFP molecules bound. Because it was not possible to determine the population distribution of TFP:CaM species in solution from an independent, experimentally observable property, the values of ΔG_2 determined in the presence of TFP are apparent values (i.e., ΔG_2^{app}).

NONLIN provides several measures of the goodness-of-fit for the parameters that minimize the variance of each fit. These error statistics include (a) the value of the square root of variance, (b) the values of asymmetric 65% confidence intervals, (c) the systematic trends in the distribution of residuals, (d) the magnitude of the span of residuals, and (e) the absolute value of elements of the correlation matrix. From these,

best-fit values were selected after testing multiple sets of initial guesses for parameters to probe for the presence of local minima. Free energies determined from at least three replicate titrations were averaged; those values and standard deviations are reported in **Table 2.1**.

In some titrations, the value determined for ΔG_1 was sensitive to starting guesses; in those cases, a manual grid search was conducted to obtain the lowest square root of variance. For titrations (**Figure 2.9)** that exhibited alternating increasing and decreasing calcium-dependent changes in fluorescence intensity, it was necessary to fix the values of both ΔG_1, and Span, as described in the *Results* section. Estimates of the apparent total free energy corresponding to each transition are reported separately in **Table 2.1**.

NMR Spectra

^{15}N-HSQC spectra were acquired at 25 °C on a Bruker Avance II 800 MHz US^2 spectrometer with a 5 mm TXI ^{1}H (^{15}N/^{13}C/D) probe featuring XYZ gradients. All spectra were processed in NMRPipe/NMRDraw (Delaglio et al., 1995b), while peak-picking and analysis were performed using SPARKY(Goddard and Kneller). TFP titrations of ^{15}N-PCaM$_{1\text{-}148}$ under apo conditions were carried out in 10% D_2O, 10 mM imidazole, 100 mM KCl, 50 μM EDTA, pH 6.5 at 22°C; in the case of $(Ca^{2+})_4$-PCaM$_{1\text{-}148}$ TFP titration studies, 10 mM $CaCl_2$ was included. Starting volumes were 500 μL.

TFP titration of CaM Monitored by NMR

^{15}N-HSQC spectra of apo ^{15}N-PCaM$_{1\text{-}148}$ were acquired at incrementally increasing concentrations of TFP. The initial concentration of both apo- and $(Ca^{2+})_4$-^{15}N-PCaM$_{1\text{-}148}$ was 617 μM. In the TFP titration series performed under apo conditions, the $[TFP]_{total}$ was 0, 0.15, 0.29, 0.44, 0.61, 0.75, 0.90, 1.04, 1.21, 1.35, 1.49, 1.63, 1.79, 1.93, 2.07, and 2.37 mM (16 spectra). In the $(Ca^{2+})_4$-^{15}N-PCaM$_{1\text{-}148}$ TFP titration series, the $[TFP]_{total}$ was 0, 0.14, 0.28, 0.41, 0.58, 0.71, 0.85, 0.99, 1.15, 1.28, 1.41, 1.55, 1.70, 1.83, 1.96, 2.25, and 2.75 mM (17 spectra). The amide assignments for apo and $(Ca^{2+})_4$-^{15}N-

$PCaM_{1\text{-}148}$ in the absence of TFP were reported previously (Jaren et al., 2002). To determine the change in chemical shift upon TFP binding to apo and $(Ca^{2+})_4$-$PCaM_{1\text{-}148}$, chemical-shift changes in both the ^{1}H and ^{15}N dimensions were quantified using the modified Pythagorean theorem shown in **Equation 2.4**, described previously (Jaren et al., 2002).

$$\Delta ppm = \sqrt{(\Delta^{1}Hppm)^2 + (0.10134 \bullet \Delta^{15}Nppm)^2} \qquad (2.4)$$

In this equation, Δppm refers to the linear change of a specific resonance peak from its initial starting position as TFP is titrated into solution, as done previously (Jaren et al., 2002).

Computational Modeling of TFP Binding

AutoDock Vina 1.0.3 (Trott and Olson, 2009) was used to simulate the binding of a single molecule of TFP to a fragment of CaM corresponding to the apo C-domain in three different tertiary conformations: "closed", "semi-open" and "open". Coordinates for residues 82-146 were extracted from these structures: 1DMO.pdb (apo, "closed"), 2IX7.pdb (apo, "semi-open"), 2HQW.pdb (calcium-saturated, "open", bound to NR1C1 peptide), and 1LIN.pdb (calcium-saturated, "open", 4 TFP molecules bound). To approximate an apo "open" structure (which has not been observed experimentally), calcium ions were removed from 2HQW and 1LIN. Each of the four protein fragments were placed in a cubic (45 $Å^3$) search space with implicit water. The exhaustiveness parameter (number of times calculation was re-run) was 128. In **Figure 2.11A,** the 20 models that had the most favorable (lowest) free energies are depicted by PyMol™ v.1.2r2 (DeLano Scientific), using a gradient of green (most favorable) to white (least favorable) for the position of the unique sulfur atom in TFP. The remainder of each drug molecule is shown in light gray sticks. For each of the four CaM structures, CaM-TFP complexes calculated to have identical free energies are shown in the same color.

Results

The major aims of this study were to understand the allosteric effects of TFP on the domains of CaM by comparing the stoichiometry of TFP binding to apo and calcium-saturated domains of CaM, and determining thermodynamic effects of TFP on calcium-binding affinity.

TFP Titration of apo ^{15}N-PCaM

The stoichiometry of TFP binding to apo PCaM was determined using ^{15}N-HSQC spectra to examine changes in the local chemical environment of individual amide resonances as TFP was titrated into a solution of uniformly ^{15}N-labeled PCaM . The sample had been depleted of calcium via extensive dialysis against metal chelators.

In the absence of TFP, 126 resonances were identified for $PCaM_{1-148}$. TFP addition resulted in residue-specific perturbations of almost all of these resonances. Individual peaks found to be in fast exchange were tracked over the course of the TFP titration (a subset are shown in **Figure 2.4a-c**). This analysis revealed that TFP saturated apo PCaM at a stoichiometry of 2:1. At saturation by TFP, resonances corresponding to the C-domain of PCaM showed a greater average degree of chemical shift perturbation (Δppm of 0.044) than those of the N-domain (Δppm of 0.030) (**Figure 2.4c**). As shown in **Figure 2.4d**, residues having significant backbone amide chemical shifts (Δppm ≥ 0.05 a value used previously by Jaren et al., 2002 (Jaren et al., 2002)) are mapped onto corresponding residues of a high resolution solution structure of apo CaM in its extended form (Kuboniwa et al., 1995; Zhang et al., 1995).

The drug was observed to bind sequentially to the two domains of apo PCaM. The largest change in most resonances of the C-domain occurred in the range of 0 to 1 molar equivalents of TFP, whereas the largest change in most resonances of the N-domain occurred in the range between 1 and 2 molar equivalents of TFP. This indicated that TFP bound preferentially to the C-domain, despite the extensive similarity of the N-

and C-domains in sequence and structure. A distinct subset of residues (~30%) responded continuously over the range of zero to 2 molar equivalents of TFP. That group included Phe16, Ile86, Thr110, and Gly113; their response is shown in **Figure 2.4b**.

TFP Titration of $(Ca^{2+})_4$-^{15}N-PCaM

For calcium-saturated PCaM, 133 resonances were resolved. Saturation with TFP was reached at a ratio of 4:1 TFP:PCaM (**Figure 2.5**). Over the course of the titration, 17 resonances experienced slow or intermediate exchange, with the majority (13) of these located in the C-domain of $(Ca^{2+})_4$-PCaM. Final chemical shift values due to TFP addition for these residues were unable to be determined, because only ^{15}N-HSQC spectra were collected for this study. Therefore, it was not possible to determine Δppm. Their positions are represented by the absence of a bar in **Figure 2.5c**.

Of the 116 resonances that were observed to be in fast exchange upon TFP addition, 98 were classified as being perturbed significantly (Δppm ≥ 0.05). They correlated closely with the location of TFP-binding sites observed in the crystallographic structure (1LIN.pdb) that showed 4 TFP bound to $(Ca^{2+})_4$-CaM (**Figure 2.5d)**. Although the calcium-binding sites of CaM are distant from the TFP-binding sites observed in all three of the crystal structures shown in **Figure 2.1**, some of their resonances were perturbed also.

Part of each ^{15}N-HSQC spectrum collected for the first and last point of the titration is shown overlapped in **Figure 2.5a;** representative titrations of individual residues are shown in **Figure 2.5b**. Of the 98 peaks that could be tracked throughout the titration, there were 74 that shifted monotonically; approximately half of those were in each domain of CaM (35 in the N-domain *vs*. 39 in the C-domain). The remaining 24 resonances exhibited a biphasic response to TFP addition. Some examples are shown in **Figure 2.6a-c.** Many of these residues were located at the interface between the N- and C-domains of CaM (**Figure 2.6d**).

This analysis of TFP-induced chemical shifts in $(Ca^{2+})_4$-^{15}N-PCaM indicated that the TFP-binding sites were non-equivalent, and that some residues responded to TFP binding at more than one of its sites. Notably, some residues in the N-domain (e.g., Glu11 and Glu14) were among this group, even though the N-domain of calcium-saturated CaM has only been observed to have a single TFP-binding site.

Equilibrium Calcium Titration of CaM_{1-148}

To determine the effect of TFP on the affinity of calcium for CaM, equilibrium calcium titrations of CaM_{1-148} were conducted in the presence of discrete molar ratios of TFP:CaM ranging from zero to eight. In the absence of TFP, calcium binding to sites I and II in the N-domain of CaM_{1-148} was monitored by observing a decrease in intrinsic phenylalanine fluorescence intensity (**Figure 2.7a**, blue) as described in *Materials and Methods*. Nonlinear least squares analysis according to a model-independent two-site (Adair) function (Eq 2) established a reference total free energy (ΔG_2) of -13.05 ± 0.06 kcal/mol (**Table 2.1**). An increase in intrinsic tyrosine fluorescence intensity was used to monitor calcium binding to sites III and IV in the C-domain of CaM_{1-148} (**Figure 2. b**, blue). In the absence of TFP, the total free energy was -15.00 ± 0.06 kcal/mol (**Table 2.1**).

Effect of TFP on Calcium Binding to CaM_{1-148}

Calcium titrations of CaM_{1-148} were conducted at molar ratios of 1:1 (green), 2:1 (red), 3:1 (black), 4:1 (cyan), and 8:1 (purple) TFP:CaM_{1-148} (**Figure 2.7, 2.8)**. In these titrations, there is no experimental signal that reports directly on the number of TFP molecules bound to CaM or the fractional population of the possible ligation states of TFP bound to apo and calcium-saturated CaM. Therefore, each set of titrations will be referred to by the known independent variable: the ratio of the final mols of TFP to mols of CaM.

The calcium affinity of sites I and II of CaM_{1-148} decreased or increased depending upon the concentration of TFP (**Figure 2.7a**). Of the TFP:CaM_{1-148} ratios examined, a 1:1 ratio caused the largest decrease (2.08 kcal/mol) in calcium affinity at sites I and II (apparent free energy of -10.97 kcal/mol; green bar in inset). Calcium affinity was diminished at ratios of 2:1 (red) and 3:1 (black), but the effects were less severe than the ratio of 1:1. The smallest decrease (0.58 kcal/mol) in apparent free energy of binding at sites I and II occurred at a ratio of 4:1 TFP:CaM_{1-148} (-12.47 kcal/mol, turquoise). In contrast, an 8:1 ratio reversed the effect and made calcium binding to sites I and II more favorable by -0.54 kcal/mol (relative to the binding affinity observed in the absence of TFP). This effect is represented by the bar graph inset in **Figure 2.7a** showing values of $\Delta\Delta G_2$. Although small in absolute magnitude, this reversal is considered significant because the standard deviation of replicate measurements for all of these titrations ranged from 0.04 to 0.16 kcal/mol, and was much smaller than 0.54 kcal/mol.

The effects of TFP on calcium sites III and IV of CaM_{1-148} shared several features of its effects on sites in the N-domain. At all levels tested, TFP made calcium binding to sites III and IV of CaM_{1-148} less favorable. The pattern of effects (**Figure 2.7b**) in response to an increasing ratio of TFP:CaM_{1-148} was similar to that observed for sites I and II (**Figure 2.7a**). The bar graph inset shows that the free energy of -12.39 kcal/mol at a 1:1 TFP:CaM_{1-148} ratio represented the maximum change in ΔG_2 of 2.61 kcal/mol. At a ratio of 2:1, the effect was slightly smaller; ratios of 3:1 and 4:1 both caused a decrease of ~1.8 kcal/mol in the calcium affinity of sites III and IV. A TFP:CaM_{1-148} ratio of 8:1 had the smallest effect; the apparent ΔG_2 was -13.99 kcal/mol, representing a change of only 1 kcal/mol relative to the absence of TFP. In this set of titrations, the *Span* was positive for ratios of 0, 1:1, 2:1 TFP:CaM. At ratios above 2:1, the fluorescence intensity decreased in response to an increase in calcium. For ease of comparison of medians and

slopes of the titration, the signal for the titrations conducted at ratios of 3:1, 4:1 and 8:1 TFP:CaM are shown inverted.

The inversion of the C-domain Tyr signal may be attributed to multiple factors linked to TFP binding to CaM. One possible scenario that may alter the fluorescence properties of the C-domain Tyr signal may be TFP increasing the exposure of Tyr residues to the solvent in a Ca^{2+}-dependent manner resulting in quenching of the Tyr signal. Another possibility may be that dipole-dipole interactions are occur between TFP and Tyr as well as between neighboring TFP that result in quenching of the Tyr signal upon Ca^{2+} addition. These possibilities are complicated due the stoichiometry of TFP binding to CaM, as each ratio of TFP:CaM carries the potential to exhibit a unique fluorescence signal. Even further complicating the nature of the Tyr signal is the heterogeneous mix of CaM bound to TFP at varied ratios at the intermediate [TFP] examined. In these cases the fluorescent signal of CaM likely is the result of an ensemble of CaM in complex with TFP at various ratios based on the 6 μM [CaM] and 1-5 μM K_d of TFP previously reported (Massom et al., 1990b).

The domain-specific effects of TFP on calcium binding to CaM_{1-148} were complex, and suggested that the domains had intrinsic differences in affinity for TFP, and possibly stoichiometry of TFP binding. The NMR-monitored TFP titrations of CaM_{1-148} suggested that TFP might bind to an interface between domains, as well as a hydrophobic cleft in each domain. To attempt to simplify these linked binding processes, each half-CaM domain fragment (CaM_{1-80} and CaM_{76-148}) was studied independently. Each one contains a pair of EF-hands that retain (a) cooperative calcium binding energetics, and (b) secondary and tertiary structure nearly identical to that of full-length CaM.

Effect of TFP on Calcium Binding to CaM_{1-80}

Equilibrium calcium titrations of the CaM_{1-80} fragment (N-domain) were performed to examine the effect that TFP has on the calcium affinity of sites I and II in

the absence of the C-domain. Analysis of a calcium titration in the absence of TFP (**Figure 2.8a,** blue) showed that the total free energy of ΔG_2 of calcium binding to sites I and II was -12.91 kcal/mol (**Table 2.1**)

As was observed for CaM_{1-148}, the effect of TFP on the apparent free energy of calcium binding to sites I and II changed in magnitude in a nonlinear manner between ratios of 1:1 and 8:1 TFP:CaM (**Figure 2.8a**). At a ratio of 1:1, the apparent ΔG_2 was -11.12 kcal/mol, almost 2 kcal/mol less favorable than for CaM alone. This ratio of TFP: CaM_{1-80} induced a smaller change than had been observed for calcium binding to sites I and II of CaM_{1-148}. A TFP:CaM_{1-80} ratio of 2:1 reduced the calcium affinity further, such that ΔG_2 was -10.70 kcal/mol; this was the largest effect that TFP was observed to have on CaM_{1-80}, as shown in the bar graph inset of $\Delta\Delta G_2$ values in **Figure 2.8a**. A TFP:CaM_{1-80} ratio of 3:1 had a slightly greater, but nearly identical effect, to a ratio of 4:1,, consistent with its effect on sites I and II in CaM_{1-148} at these ratios. The most striking difference was observed at the ratio of 8:1 TFP:CaM. Calcium binding to sites I and II remained less favorable by 0.63 kcal/mol for $CaM_{1-80.}$ This indicated that the C-domain was necessary for the favorable effect (-0.54 kcal/mol) of TFP on sites I and II in CaM_{1-148} that had been observed at an 8:1 TFP:CaM ratio.

Effect of TFP on Calcium Binding to CaM_{76-148}

To examine the effect that TFP had on the calcium affinity of sites III and IV in the absence of the N-domain, the free energy of calcium binding to the pair of sites in CaM_{76-148} was determined. In the absence of TFP, ΔG_2 was determined to be -14.47 kcal/mol (Table 2. 1) (**Figure 2.8b**). A ratio of 1:1 TFP:CaM_{76-148} led to a decrease in affinity (the apparent ΔG_2 was less favorable by 1.67 kcal/mol). This was smaller than the change (2.56 kcal/mol) observed for calcium binding to the same sites in CaM_{1-148}. The difference of almost 1 kcal/mol is greater than the largest standard deviation (0.26 kcal/mol) observed for a single condition. The calcium-dependent change in

fluorescence intensity was positive, as it was in the absence of TFP. However, the absolute magnitude of the intensity was lower (data not shown).

At ratios of 2:1 (red) and 3:1 (black) TFP:$CaM_{76\text{-}148}$, non-monotonic calcium-dependent changes in fluorescence intensity signals were observed. The first inflection was an increase in intensity, like that observed for calcium titrations conducted at a ratio of 1:1 TFP:CaM. Representative normalized data sets are shown in **Figure 2.8b.** The second inflection was a decrease in intensity; both the first and second transitions are shown in **Figure 2.9** for the ratios of 2:1 and 3:1. Apparent free energies were estimated using piece-wise analysis of the two transitions, as described below.

As shown in **Figure 2.8b,** at ratios of 4:1 and 8:1 TFP:$CaM_{76\text{-}148}$, a greater decrease in the calcium affinity of sites III and IV was observed than had been seen at the same ratio of TFP:CaM for these sites in $CaM_{1\text{-}148}$. Presumably this relates to the absence of the N-domain and interdomain sites as locations for TFP binding. Also, as had been observed for $CaM_{1\text{-}148}$, the *Span* observed for the calcium-dependent change in fluorescence intensity was negative. For ease of comparing medians and slopes of the titrations, the normalized titrations at these two conditions were inverted in **Figure 2.8b.** The slope of the calcium titration at a ratio of 8:1 TFP:CaM was notably more shallow than those at other molar ratios of TFP:CaM. This may arise from a change in cooperativity and/or may represent a mixed population of ligation states: $CaM_{76\text{-}148}$ saturated with varying numbers of TFP.

Piecewise Analysis of Biphasic Calcium Titrations of $CaM_{76\text{-}148}$

The calcium titrations conducted at ratios of 2:1 and 3:1 TFP:CaM (**Figure 2.9**) are comprised of two phases with a sharp transition between them. Because the asymptotes for each phase were not well defined, it was not possible to determine an

independent maximum for the upward-trending signal, or minimum for the downward-trending signal by fitting the data to **Equation 2.3**.

Instead, to estimate the apparent free energy of calcium binding, the fluorescence signal was normalized to the maximal observed intensity, and the value of *Span* was set equal to 1.0. Using that approach, the apparent free energies of Ca^{2+} binding were -12.78 kcal/mol (at ratio of 2:1) and -13.02 kcal/mol at a ratio of 3:1. The corresponding estimates of $\Delta\Delta G_2$ for calcium binding to sites III and IV are shown in the solid bars in the inset of **Figure 2.8b**. These values were similar to what had been observed at 1:1 TFP:CaM. (The maximal fluorescence intensity for the increasing phase must be at least as high the value observed, but could be higher. If it were under-estimated, this approach would also under-estimate the effect of TFP by estimating a median calcium concentration lower than the actual value and therefore closer to the value in the absence of TFP.)

A similar approach was applied to analysis of the decreasing signal recorded at ratios of 2:1 (red) and 3:1 (black) TFP:$CaM_{76\text{-}148}$. The net downward deflection was fixed to be as large as that for the increasing phase. Using this approach, the apparent free energies were -9.55 (a ratio of 2:1) and -10.65 kcal/mol (at 3:1). The dashed bars shown in the inset of **Figure 2.8b** represent the value of $\Delta\Delta G_2$ values obtained assuming that the net change in affinity is equal to the effect represented by the decreasing fluorescent intensity. If the value of the *Span* of this transition were not as large as the increasing phase, this assumption would err on the side of reporting a weaker calcium-binding affinity (i.e., a median concentration for the titration that would be higher than the actual one).

The presence of multi-phasic fluorescence signals, changes in direction of calcium-depending response of steady-state fluorescence, and differing free energies of Ca^{2+} binding as a function of [TFP] provide strong evidence for the existence of populated intermediates that have different fluorescence signals. All estimates of calcium

binding affinity in the presence of TFP are denoted as apparent free energies to draw attention to the complexity of analysis of multiple, partial ligation states.

Discussion

The studies presented here address the nature of TFP binding to apo and calcium-saturated CaM, and the allosteric effects of TFP on calcium binding to the non-equivalent domains of CaM. Their combined effects on conformational switching of this essential regulatory protein are of interest because of the ubiquitous practice of applying drugs to cell cultures to disrupt CaM-mediated pathways of calcium-dependent signal transduction.

Two TFP molecules bind to apo CaM

Although some reports have suggested that TFP binds to apo CaM (Matsushima et al., 2000) (Matsushima et al., 2007) most have not supported this premise (Massom et al., 1990a; Massom et al., 1991; Tanokura and Yamada, 1985). However, stoichiometric TFP titrations of apo $CaM_{1\text{-}148}$ (460 μM) monitored by NMR showed it to be saturated by two TFP molecules, with preferential binding to the C-domain; studies of calcium binding to TFP-saturated apo CaM demonstrated that TFP reduced calcium affinity. This was similar to the effect of peptides derived from individual protein targets, such as those containing IQ-motifs, that bind preferentially to apo CaM (Martin and Bayley, 2004; Theoharis et al., 2008). They also have the thermodynamic property of decreasing the calcium-binding affinity of the EF-hand sites of CaM. However, to our knowledge, this is the first time such behavior has been reported for a drug binding to CaM.

In a unique high resolution study of apo CaM bound to a peptide representing an IQ-motif (from myosin V (Houdusse et al., 2006)), the C-domain of CaM adopted the "semi-open" tertiary conformation (**Figure 2.2**). The interface between the peptide and the C-domain buries more surface area than does the peptide interaction with N-domain which is in the "closed" conformation. In other structures of CaM:peptide complexes,

the C-domain has been observed to adopt multiple conformations, depending on the nature and number of ligand(s) (calcium and/or protein) bound (**Figure 2.2**). Solution studies of apo CaM alone have shown that the C-domain has a lower fraction of ordered secondary structure and is less thermodynamically stable than the N-domain (Masino et al., 2000; Sorensen and Shea, 1998). These findings indicate that, under apo conditions, fluctuation between a "closed" and "semi-open" conformation is more energetically favorable for the C-domain than for the N-domain, consistent with TFP binding preferentially to the C-domain. It is also possible for either apo N- or C-domain to sample the "open" conformation. However, favorable tertiary constraints within each domain provide an energetic barrier for this transition. Thus, the population of this conformation of apo CaM will be low.

Small-angle x-ray scattering (SAXS) data indicate that TFP binds to both apo and $(Ca^{2+})_4$-CaM. However, the radius of gyration of each ensemble is different ($(Ca^{2+})_4$-CaM:TFP = 20.5 ± 0.3 Å, versus apo CaM 20.5 ± 0.3 Å) (Matsushima et al., 2000; Matsushima et al., 2007), suggesting that the dominant tertiary structure and stoichiometry of TFP binding are not identical for both apo and $(Ca^{2+})_4$-CaM. Because both of these differ from apo CaM alone (radius of gyration = 21.5 ± 0.3 Å)which preferentially samples the "closed" conformation, we hypothesize that TFP binds preferentially to the "semi-open" conformation of the 4-helix bundle domains of apo CaM. At any specific level of TFP, the fraction of apo CaM having TFP bound to a "semi-open" domain will be determined by the energy of isomerization reactions needed for conformational rearrangements, the energy of TFP binding to CaM and concentration of TFP.

Additional evidence that TFP recognizes different sites within apo and $(Ca^{2+})_4$-CaM comes from comparing ^{15}N-HSQC spectra of TFP-saturated apo and $(Ca^{2+})_4$-CaM (**Figure 2. 10**). The spectra differ at most positions, meaning that the local chemical environments of most amide bonds in the CaM backbone are dissimilar. Note that the

changes observed in this study appear to be considerably larger than those observed by Matsushima et al. (Matsushima et al., 2007); although a direct comparison cannot be made because chemical shifts due to TFP binding were not quantified in that study.

It would be attractive to determine a high-resolution structural model of TFP bound to apo CaM. This would allow us to determine residues participating in the drug-protein interfaces and interhelical angles of each 4-helix bundle domain. However, it is beyond the scope of this study. Instead, a computational approach (*AutoDock Vina*) (Trott and Olson, 2010) was used to identify an ensemble of preferred binding sites for TFP on the apo C-domain of CaM in a "closed", "semi-open" and "open" conformation (**Figure 2. 11a**).

For each tertiary structure, an overlay of the 20 models that were most favorable energetically are shown. The single sulfur atom in each computationally docked TFP molecule is shown as an enlarged sphere. The color of that sphere corresponds to the predicted free energy of binding (darkest green corresponds to most favorable positions); the range of predicted energies of the models is shown in the bar below. The docking results of *AutoDock Vina* have been validated in control experiments in which a ligand was extracted from a known complex and then successfully re-docked in a similar orientation by *AutoDock Vina* as was observed experimentally (Trott and Olson, 2010). *AutoDock Vina* was also validated for use in TFP binding to CaM, by extracting TFP from the x-ray structure of $(Ca^{2+})_4$-CaM bound to 1 TFP and then allowing *AutoDock Vina* to determine where the extracted TFP molecule would bind. Upon completion of docking simulation, it was observed that the predicted TFP binding site was less than Å away from the experimentally determined TFP binding site (**Figure 2.11a**).

For the "closed" C-domain (based on 1DMO), the preferred binding locations of TFP were on the exterior surface near the first and second helix of the domain, and near the highly acidic calcium-binding sites III and IV; predicted free energies for this set of models ranged from -6 to -5.1 kcal/mol. For the "semi-open" C-domain (based on 2IX7),

there were two preferred binding locations: one was in the shallow cleft between the pairs of helices in the 4-helix bundle and the other was near site III. Free energies of TFP binding to the "semi-open" domain ranged from -6.8 to -6.0 kcal/mol.

The "open" C-domain has only been observed in structures of calcium-saturated CaM. However, it may be sampled at a very low frequency by apo CaM. Therefore, TFP binding to an apo "open" C-domain was modeled by removing the calcium ions from two "open" tertiary structures of calcium-saturated CaM that differed in their side chain orientations. One set of coordinates was taken from a structure of $(Ca^{2+})_4$-CaM bound to a peptide (2HQW) and another was from a structure of $(Ca^{2+})_4$-CaM bound to 4 TFP (1LIN). In both cases, the most favorable binding site for TFP was located deep in the hydrophobic pocket between the pairs of helices.

The "open" conformation is the only one for which there are high resolution structures showing the location(s) of TFP bound to the C-domain. The position of TFP at site A of 1LIN.pdb (see **Figure 2.3**) is shown in magenta for comparison to the models. This is the site that is occupied in all three of the crystallographic structures of TFP bound to $(Ca^{2+})_4$-CaM. For the 20 models having the lowest energy, the sulfur atom in each computationally docked TFP molecule was within 1 Å of the location where it had been observed experimentally in 1LIN, suggesting that the interhelical angles and surface residues are necessary and sufficient to provide a binding site for TFP in the absence of calcium.

This prediction of sites of TFP binding to the "closed" and "semi-open" conformations of a single domain does not explore additional possible sites that might exist in full-length CaM in pockets created by the juxtaposition of the two domains. However, the models suggest that TFP binding to the "semi-open" form has the potential of interfering with calcium binding. Note that all of these calculations have CaM account only for TFP binding, and not for the energy required for conformational isomerization. That barrier exists, in part, because the "open" form of each 4-helix bundle domain of

$(Ca^{2+})_4$-CaM exposes more hydrophobic surface to solvent than the "closed" or "semi-open" conformations (Houdusse et al., 2006; Kuboniwa et al., 1995).

Four TFP bind to $(Ca^{2+})_4$-CaM

Residue-specific titrations monitored by NMR (**Figure 2.5)** showed the stoichiometry of TFP binding to $(Ca^{2+})_4$-CaM was 4:1 in agreement with a SAXS study (Matsushima et al., 2000), an HPLC study (Massom et al., 1991), (Massom et al., 1990c), and one of the three crystallographic structures 1LIN.pdb (Vandonselaar et al., 1994a). The stoichiometry of 4 contrasts with two other crystallographic structures of CaM:TFP (1CTR.pdb, 1A29.pdb, see **Figure 2.3**), and a recent computational study that concluded that TFP binds only to the C-domain of $(Ca^{2+})_4$-CaM (Kovesi et al., 2008). Although NMR is a powerful method for precisely determining the stoichiometry of binding, the observed spectral changes report on changes in chemical environment that may arise from local binding, or a global conformational change. Thus, it is challenging to determine the location of individual binding sites when multiple ligands bind. It was evident that TFP binding perturbed amide resonances in both domains of $(Ca^{2+})_4$-CaM, consistent with TFP binding to each, as depicted in the superposition shown in **Figure 2.3d** (sites A, B, C, and D). The majority of residues in slow exchange mapped to the C-domain, indicating that this domain of $(Ca^{2+})_4$-CaM contained the site with highest affinity for TFP. This observation, coupled with the locations of residues in both domains that undergo fast exchange, indicates that a hierarchy of 4 TFP-binding sites is present in $(Ca^{2+})_4$-CaM. Interpreted according to the positions of TFP in 1LIN.pdb, it appeared that two TFP binding sites with different affinities exist in the C-domain, that a third low-affinity site is present in the N-domain, and that a fourth site (also of low affinity) bridges the two domains (**Figure 2.3**). Although a hierarchy of TFP binding sites was identified in this work, it was not possible to distinguish a preferential order of binding order to the low-affinity sites.

Interdomain Interactions

For any protein binding 4 ligands, there are 5 macroscopic ligation states (0, 1, 2, 3, 4 ligand:protein). Thus, in principle, it might be possible to titrate $(Ca^{2+})_4$-CaM with TFP and monitor 4 independent transitions corresponding to individual TFP-binding sites as has been done for calcium binding to 4 sites in CaM (Jaren et al., 2002), *(Martin et al., 1986; Starovasnik et al., 1992)***.** For residues of CaM affected by a single TFP molecule, a monotonic transition between a "free" and "bound" state might be observed. For each residue that experienced only those two chemical environments, a stoichiometric titration would show (a) a linear transition, if in fast exchange, or (b) reciprocal changes in intensity for pairs of peaks (one diminishing, one increasing), if in slow exchange. Similarly, if there were 4 sites with identical affinity, all residues affected by TFP binding would titrate identically over the range of 0 to 4 equivalents of TFP added.

However, it is also possible that intermediate ligation states adopt distinct conformers with unique biophysical properties. A residue that responds to TFP binding at multiple sites has the potential to experience a different environment in each, and therefore show a nonlinear response to TFP binding as monitored by NMR or fluorescence. In HSQC spectra, this was observed for a subset of residues (**Figure 2.6b**) that experienced at least three chemical environments and sampled at least one intermediate conformation. These residues responding to multiple TFP-binding sites are most likely located at the interface between the N- and C-domains, or between TFP binding sites within a single domain (**Figure 2.6d**). The crystallographic structure of 4 TFP molecules bound to $(Ca^{2+})_4$-CaM shows that, at their closest approach, TFP binding sites A, B, and C are in close proximity (~4 Å) to each other, while the TFP molecule bound at site D is ~9 Å away from site C (**Figure 2.3d**). This constellation would allow for unique chemical environments to be sampled as TFP sequentially fills its 4 binding sites, and would lead to changes in the chemical environment of adjacent TFP binding sites.

This type of biphasic response of CaM resonances was observed previously in calcium titrations monitored by ^{15}N-HSQC that showed that several residues within the linker region between domains of CaM experienced three distinct chemical environments (Jaren et al., 2002). These residues were in slow exchange between 0 and 2 equivalents of calcium (i.e., during saturation of the C-domain), and were in fast exchange between 2 and 4 (i.e, during saturation of the N-domain). Similar biphasic responses were observed in drug titrations of cardiac Troponin C (a related calcium-binding EF-hand protein) (Kleerekoper et al., 1998). Nonlinear peak shifts due to the significant population of an intermediate state have also been observed for other proteins such as the phosphorylated kinase-inducible activation domain (pKID) of the transcription factor camp response element-binding protein (CREB) binding to subdomain of CREB Binding Protien (CBP) termed KIX (Sugase et al., 2007).

Further evidence for domain interactions was provided by the behavior of residues Glu11 and Glu 14, located in the first helix of the N-domain of $(Ca^{2+})_4$-CaM. It was expected that these residues would respond to TFP binding to the N-domain itself based on their location and proximity to a target peptide or drug observed in 17 $(Ca^{2+})_4$-CaM-peptide or drug complexes (Ataman et al., 2007). In those, both Glu11 and Glu14 were within 4.5 Å of the peptide or drug interacting with $(Ca^{2+})_4$-CaM. Over the full range of 0 to 4 TFP molecules binding to $(Ca^{2+})_4$-CaM, these residues exhibited a biphasic response to TFP binding (**Figure 2.6d**), initially increasing with a maximum at 2 TFP:CaM. As observed in TFP-CaM structures shown in **Figure 2. 2**, these residues are located between TFP-binding sites in the N- and C-domain of $(Ca^{2+})_4$-CaM which positions them to respond to saturation of all TFP binding sites. The highest affinity TFP-binding site in $(Ca^{2+})_4$-CaM is in the C-domain, assumed to be TFP-site A **(Figure 2.3d, Figure 2. 1a**). Glu11 and Glu14 are also < 4 Å from TFP-site B which is comprised primarily of C-domain residues. This hints at the possibility that the response of Glu11 and Glu14 from 0 to 2 relates to occupancy of sites A and B, and the response

from 2 to 4 indicates occupancy of sites C and D. But, other models of hierarchical binding are also consistent with the titrations.

Effects of TFP on the Calcium Affinity of CaM

Most proteins known to be regulated by CaM contain a BAA motif (basic amphipathic alpha-helix) that binds to CaM, and causes an increase in the calcium affinity of CaM. Thermodynamic linkage requires that the BAA motif bind to $(Ca^{2+})_4$-CaM with higher affinity than it binds to apo CaM in order to increase the Ca^{2+}-binding affinity of CaM. A subset of CaM-target interactions—typically those between CaM and targets bearing IQ-motifs—lead to a reduction in the calcium affinity of CaM, due to the higher affinity of these targets for apo CaM (Bahler and Rhoads, 2002; Cui et al., 2003; Martin and Bayley, 2004; Mori et al., 2003; Putkey et al., 2003). A peptide ($Na_v1.2$ IQp) representing the IQ-motif from the Voltage-Dependent Sodium Channel $Na_V1.2$ has been shown to have a negligible effect on calcium binding to the N-domain of CaM, while significantly lowering calcium-binding affinity of the C-domain (Theoharis et al., 2008). To satisfy thermodynamic constraints, an IQ-motif with this property has a higher affinity for the apo C-domain than the $(Ca^{2+})_2$-C-domain.

Like an IQ-motif, at most concentrations studied in this study, TFP diminished the calcium-binding affinity of both domains of CaM. TFP binds with lower absolute affinity to apo CaM (Massom et al., 1990a) than does $Na_v1.2$ IQp (Theoharis et al., 2008). However, like $Na_v1.2$ IQp, it has a higher relative affinity for the C-domain of apo CaM (**Figure 2.5**) than for the N-domain. This is consistent with the observation that the C-domain exhibited a larger TFP-induced decrease in calcium affinity than the N-domain (**Figure 2. b**).

If $(Ca^{2+})_4$-CaM had not bound TFP at all, or bound TFP more weakly than apo CaM but at the same sites, then the major allosteric effect of TFP would be to decrease calcium affinity by binding preferentially to apo CaM. The magnitude of the TFP effect

would increase monotonically until CaM was saturated with TFP. In this way, its effect on CaM would be analogous to that of 2,3-BPG reducing oxygen binding affinity by binding preferentially to deoxy hemoglobin (Ackers, 1979; Arnone, 1972; Benesch and Benesch, 1967). Mammalian adaptation to high altitudes depends on this mechanism of promoting oxygen release from hemoglobin under the low-oxygen conditions of human tissues (Martin et al., 1975). However, this mechanism of negative allosteric regulation would not explain how the effect of TFP on calcium binding reversed direction (**Figures 2.7** and **2.8**) when the ratio of TFP:CaM increased from 1 to 8. Several possible explanations were considered.

The reversal of the initially negative allosteric effect of TFP on calcium binding by CaM might be explained if higher levels of total added TFP did not actually represent higher soluble concentrations. For example, the effective concentration of TFP might drop if it formed micelles that would compete with CaM as a sink for additional TFP. However, that micelle-sink model contradicts several observations in this study (Caetano et al., 2003; Caetano and Tabak, 2000). For example, a prediction of that model is that increasing TFP would ameliorate the initially negative effect until all of it was drawn into micelles and the calcium-binding affinity of CaM returned to that observed in the absence of TFP. Instead, an increase in TFP ultimately increased the calcium-binding affinity of N-domain of CaM, rather than returning it to the values in the absence of TFP. An additional contrary observation was that the direction of calcium-dependent changes in fluorescence signal changed over the course of the TFP titration: monotonically increasing in the absence of TFP, and monotonically decreasing at the 8:1 ratio, showing that TFP was still associated with CaM at the 8:1 ratio. Finally, in all CaM-TFP samples (including the millimolar CaM samples used in NMR studies), there was no visual evidence of turbidity that would indicate the formation of a significant population of micelles.

Another possibility is that the mechanism of allosteric reversal depends on TFP changing the relative populations of "closed", "semi-open", and "open" tertiary structures of apo CaM. Given that both calcium and TFP have micromolar affinity for CaM, and that two calcium ions are needed to drive each domain to adopt the "open" state in the absence of TFP, it may be that 2 TFP molecules are needed to drive the conformational change of opening each domain. The NMR-monitored TFP titrations showed only two TFP bound to apo $CaM_{1\text{-}148}$, but they did so sequentially with higher affinity for the C-domain. In contrast, multiple TFP may bind cooperatively to "open" calcium-saturated domains. Thus, as the level of TFP increases above 1:1, there is a chance for more than 1 to bind to a single domain. TFP may promote the "open" conformation of apo CaM in a manner similar to that of BAA-motif peptides that bind with high affinity to the hydrophobic surfaces exposed upon Ca^{2+}binding (Ataman et al., 2007; Meador et al., 1993). That would then increase calcium-binding affinity. This biphasic binding shares some features with that observed for an IQ-motif from neuromodulin studied by Persechini and colleagues (Black et al., 2006).

Comparison of the calcium-binding free energies for sites I and II in $CaM_{1\text{-}148}$ and $CaM_{1\text{-}80}$ at a ratio of 8:1 TFP:CaM revealed that the calcium affinity does not become more favorable than that in the absence of TFP. This difference may result from the loss of a TFP-binding site that bridges the N- and C-domains of $CaM_{1\text{-}148}$ with contributions from both (**Figure 2.12**). Calcium titrations of $CaM_{76\text{-}148}$ at ratios of 2:1 and 3:1 TFP:$CaM_{76\text{-}148}$ resulted in multiphasic fluorescence signals attributed to a mix of different TFP-bound $CaM_{76\text{-}148}$, complexes that each have unique properties. This is consistent with kinetic studies of calcium release from $(Ca^{2+})_4$-CaM mixed with TFP (Martin et al., 1985). The different species in solution are sufficiently populated at ratios of 2:1 and 3:1 TFP:$CaM_{76\text{-}148}$ to exhibit multiple signals, but are not abundant at the ratios of 1:1, 4:1, and 8:1. For the ratios of 2:1 and 3:1, the maximum value of raw fluorescent intensity was approximately a third of that observed for the calcium titrations conducted at 1:1 and

4:1 ratios of TFP:$CaM_{76\text{-}148}$. All of these observations are consistent with a mechanism of drug action that specifies that the apo C-domain has a higher affinity for TFP than does the apo N-domain, and that TFP binding interferes with calcium binding by inhibiting the conformational switch from "semi-open" to "open" conformation.

Unlike Ca^{2+}-titration curves at 1, 2, 3, or 4:1 TFP:$CaM_{76\text{-}148}$, a significant decrease in cooperativity of Ca^{2+} binding to $CaM_{76\text{-}148}$ was observed at a ratio of 8:1 (**Figure 2.8**). This decrease in cooperativity may be a result of multiple factors such as TFP uncoupling Ca^{2+}-binding sites III and IV such that one site has a more favorable Ca^{2+}-binding affinity than the other and/or a heterogeneous mix of TFP bound $CaM_{76\text{-}148}$ species in solution.

These interpretations are summarized in a simplified isomerization and binding model shown in **Figure 2.11b.** Distinct tertiary conformations of CaM provide unique TFP binding interfaces with different relative affinities for TFP. A "closed" domain of apo CaM is depicted as having no interaction with TFP. A "semi-open" apo domain has hydrophobic residues located sufficiently near the perimeter of the canonical target binding pocket (blue patches) to interact with TFP. With TFP bound at these positions, the domain responds as it does when interacting with the Ile-Gln dipeptide found in a canonical IQ-motif of ion channels. Calcium binding is sufficient to switch the tertiary structure from the "semi-open" to "open" conformation, exposing hydrophobic residues (indicated by blue patches) located deep in the hydrophobic cleft. The "open" conformation may also be sampled by apo CaM, allowing TFP at high concentrations to bind there. In either case, TFP bound at the blue sites may have an allosteric effect on calcium affinity more like that of a BAA motif peptide which consistently buries an aromatic group in the FLMM pocket of the C-domain (Ataman et al., 2007; Yamniuk and Vogel, 2004).

Summary

This study of the allosteric regulation of calcium binding to CaM by TFP demonstrates that there is considerable complexity in the interactions between these two ligands of CaM. TFP interacts with distinct interfaces available in the dominant tertiary conformations of apo and $(Ca^{2+})_4$-CaM. These are likely to be primarily a "semi-open" state in the ensemble of conformations that are energetically sampled by apo CaM, and the "open" conformation for $(Ca^{2+})_4$-CaM. TFP lowered the calcium binding affinity of sites III and IV in the C-domain of $CaM_{1\text{-}148}$ more than sites I and II in the N-domain, indicating that the apo C-domain has a higher affinity for TFP. TFP titrations monitored by NMR showed differences in the stoichiometry and location of binding of TFP to apo and $(Ca^{2+})_4$-CaM; this is the driving force behind the non-monotonic allosteric effect of TFP on the calcium affinity of CaM.

This analysis suggests that despite the significant number of calcium-dependent processes regulated by $(Ca^{2+})_4$-CaM, it is equally important to consider interactions of target proteins with apo CaM when testing drugs similar to TFP. This broadens the interpretation of a widely used approach of bathing cells *in vitro* in a TFP-containing solution with the goal of disrupting pathways that are regulated by $(Ca^{2+})_4$-CaM.

Like other anti-psychotic drugs, TFP can cause the debilitating side-effect of tardive dyskinesia (Lahti et al., 1993). The etiology of this is not completely understood, but believed to originate from hypersensitive dopamine receptors, which have been shown to be regulated by CaM under both apo and calcium-saturating conditions (Liu et al., 2007; Woods et al., 2008). Apo and $(Ca^{2+})_4$-CaM have also been shown to regulate numerous ion channels responsible for the propagation of nerve impulses (Ataman et al., 2007; Schumacher et al., 2004; Shah et al., 2006; van Petegem et al., 2005). It is possible that TFP alters physiological processes by disrupting interactions of apo CaM with these receptors.

Given the large number of signaling pathways that CaM regulates, CaM itself is not a promising target for drug design. However, an interface between CaM and a particular target may offer more selectivity. This study of allosteric interactions between calcium and TFP suggests that interactions between channels and the "semi-open" form of CaM may be an especially attractive target for future drug testing.

Table 2.1 TFP Effects on Calcium Binding to CaM

		Sites I and II of CaM_{1-148}			Sites III and IV of CaM_{1-148}	
[TFP]	**Ratio**	**ΔG_2[a]**	**$\Delta\Delta G_2$[b]**		**ΔG_2[a]**	**$\Delta\Delta G_2$[b]**
-		-13.05 ± 0.06	-		-15.00 ± 0.06	-
6 μM	1:1	-10.97 ± 0.11	2.08		-12.39 ± 0.07	2.61
12 μM	2:1	-11.57 ± 0.11	1.48		-12.76 ± 0.18	2.24
18 μM	3:1	-11.60 ± 0.16	1.45		-13.23 ± 0.20	1.77
24 μM	4:1	-12.47 ± 0.04	0.58		-13.07 ± 0.09	1.83
48 μM	8:1	-13.59 ± 0.08	-0.54		-13.99 ± 0.06	0.99

		Sites I and II of CaM_{1-80}			Sites III and IV of CaM_{76-148}	
[TFP]	**Ratio**	**ΔG_2[a]**	**$\Delta\Delta G_2$[b]**		**ΔG_2[a]**	**$\Delta\Delta G_2$[b]**
-		-12.91 ± 0.09	-		-14.47 ± 0.12	-
6 μM	1:1	-11.12 ± 0.03	1.79		-12.80 ± 0.08	1.67
12 μM	2:1	-10.70 ± 0.17	2.21		-12.78 ± 0.20[c] -9.55 ± 0.31[d]	1.69 4.92
18 μM	3:1	-11.37 ± 0.05	1.54		-13.02 ± 0.18[c] -10.65 ± 0.27[d]	1.45 3.82
24 μM	4:1	-11.56 ± 0.05	1.35		-11.56 ± 0.05	2.91
48 μM	8:1	-12.28 ± 0.18	0.63		-12.71 ± 0.21	1.76

[a] **ΔG_2** (kcal/mol) represents apparent total free energy indicated $TFP]_{total}/[CaM]_{total}$ ratio

[b] $\Delta\Delta G_2 = \Delta G_2^{app}$ (TFP Added) - ΔG_2 (TFP Absent)

[c] Values determined from initial phase of increasing fluorescent signal.

[d] Values determined from decreasing fluorescent signal at higher [calcium].

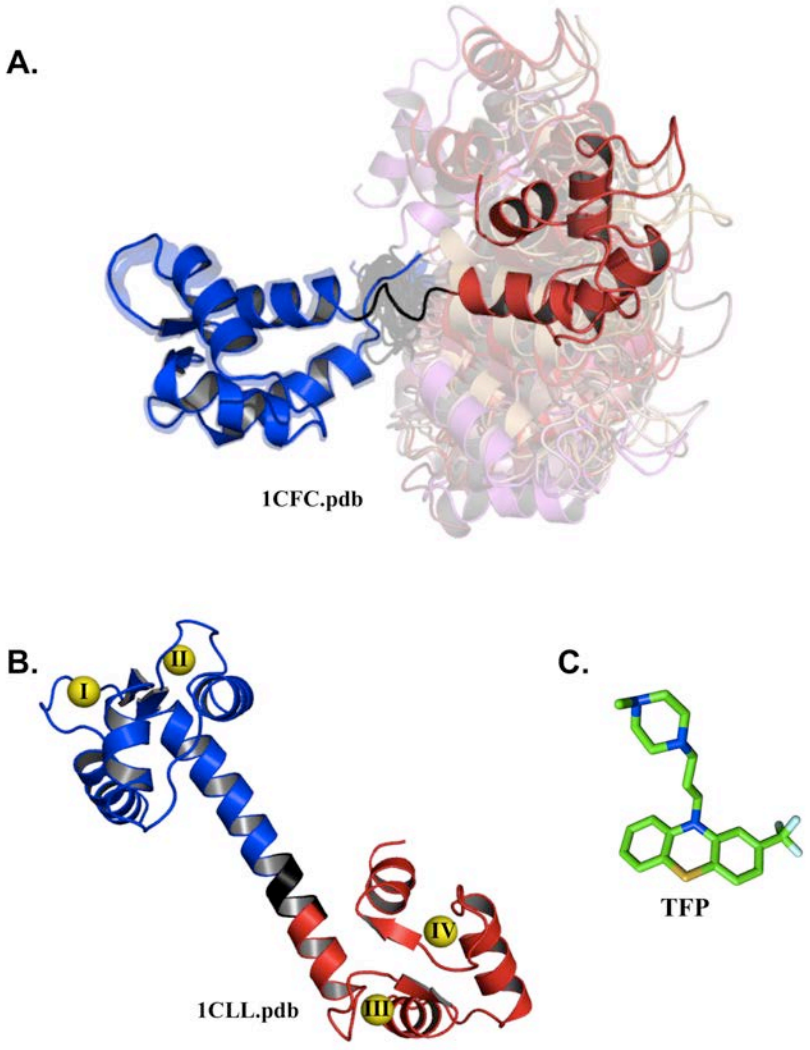

Figure 2.1: Structures of apo CaM, $(Ca^{2+})_4$-CaM, and Trifluoperazine.
A: Superposition of solution structure models of CaM (1CFC.pdb) determined by NMR. Alignment minimized the difference between models with respect to the N-domain (residues 1-75 in blue), illustrating flexibility of interdomain linker (resides 76-80 in black) and range of positions adopted by C-domain (residues 81-148 in red). A single model is highlighted to reveal the tertiary structures of the apo N- and C-domains B: $(Ca^{2+})_4$-CaM structure determined crystallographically (1CLL.PDB); backbone colored as in panel A. Ca^{2+} ions (yellow) are bound at sites I and II in the N-domain, and at sites III and IV in the C-domain. C: Chemical structure of the antipsychotic drug Trifluoperazine (TFP; green), with sulfur atom in yellow and fluorine atoms in light blue.
Users/nmr_mike/Thesis/Chapter_II/Figure2_1.jpg

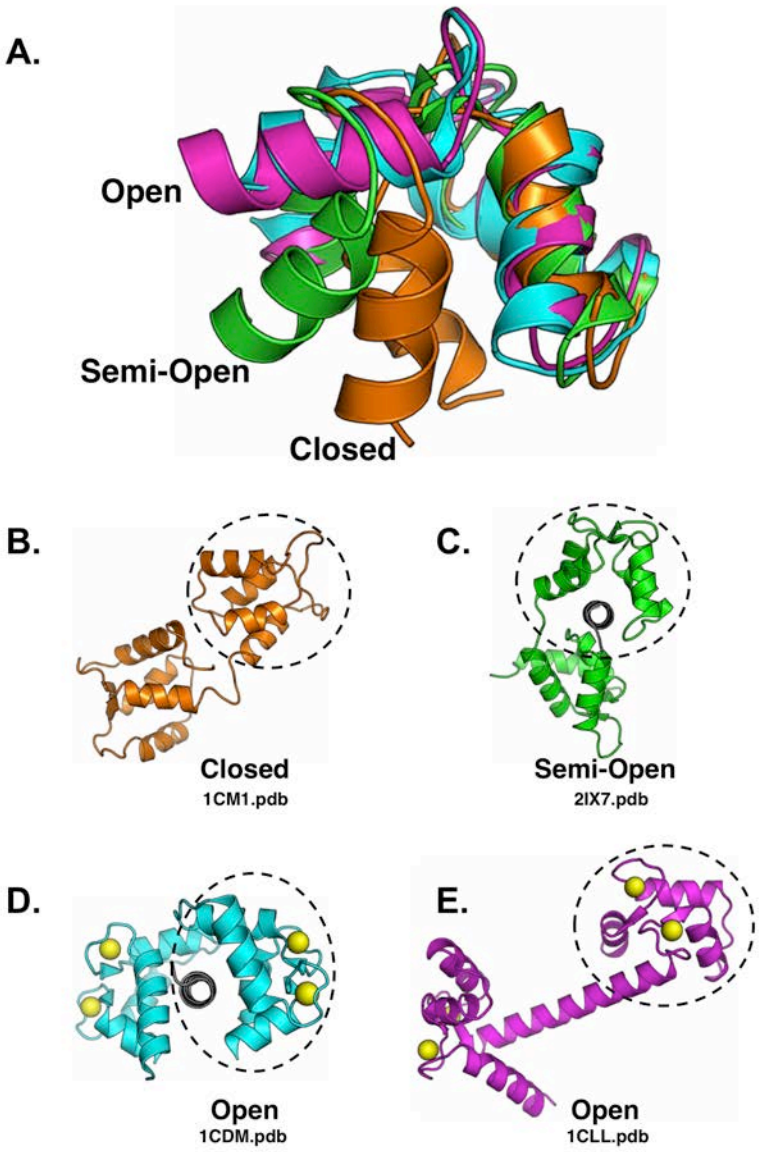

Figure 2.2: Superposition of 3 Tertiary structures of the C-domain of CaM. Examples of the "closed" (1CFC.pdb–orange), "semi-open" (2IX7.pdb–green) and "open" (1CDM.pdb–aqua and 1CLL.pdb–magenta) conformations of the C-domain of CaM are aligned according to the positions of the F and G (second and third) helices of the domain. Structures of the corresponding full-length CaM is shown below. Users/nmr_mike/Thesis/Chapter_II/Figure2_2.jpg

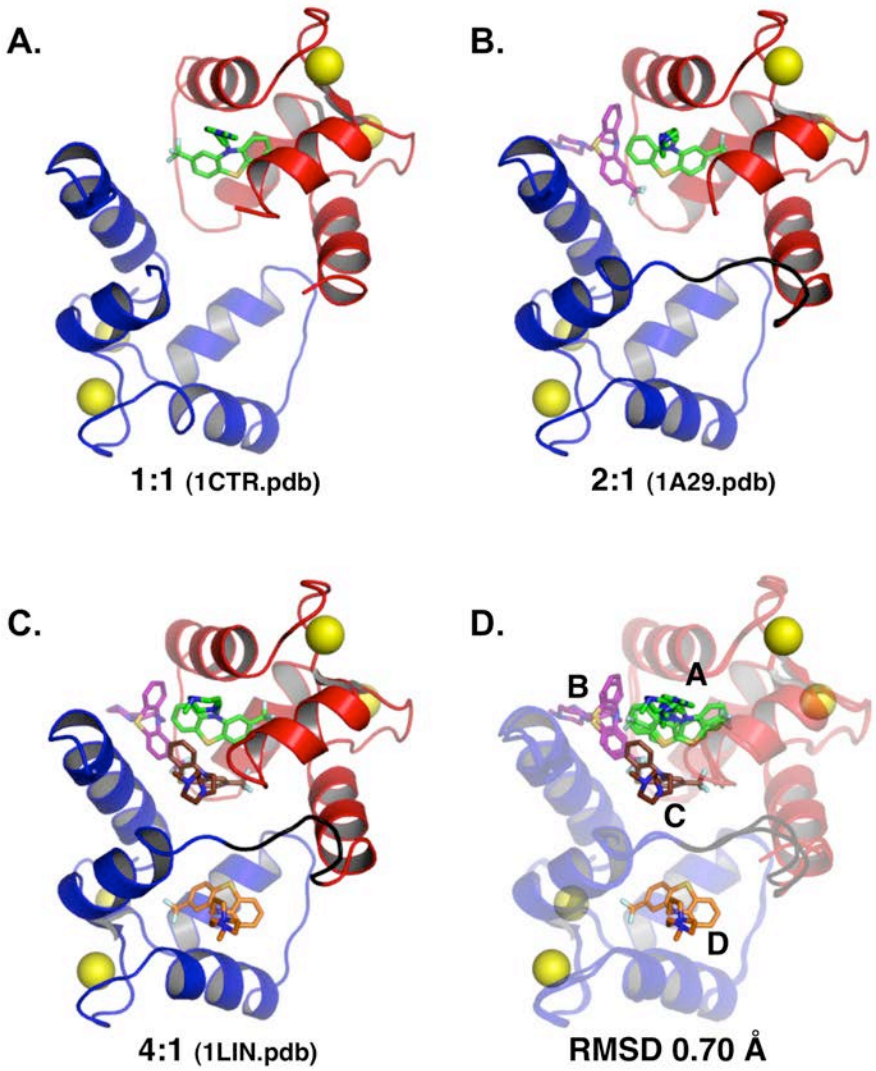

Figure 2.3: Structures of $(Ca^{2+})_4$-CaM bound to TFP.
Individual panels show crystallographically derived structures of TFP:$(Ca^{2+})_4$-CaM complexes, with drug:protein ratios of 1:1 (1CTR.pdb), 2:1 (1A29.pdf), and 4:1 (1LIN.pdb), as well as a structural superposition of these three structures, with the TFP-binding sites labeled A (green), B (magenta), C (brown) and D (orange). TFP-binding sites A and B are located in the C-domain (backbone red), site C bridges the two domains, and site D is located in the N-domain (backbone blue).
Users/nmr_mike/Thesis/Chapter_II/Figure2_3.jpg

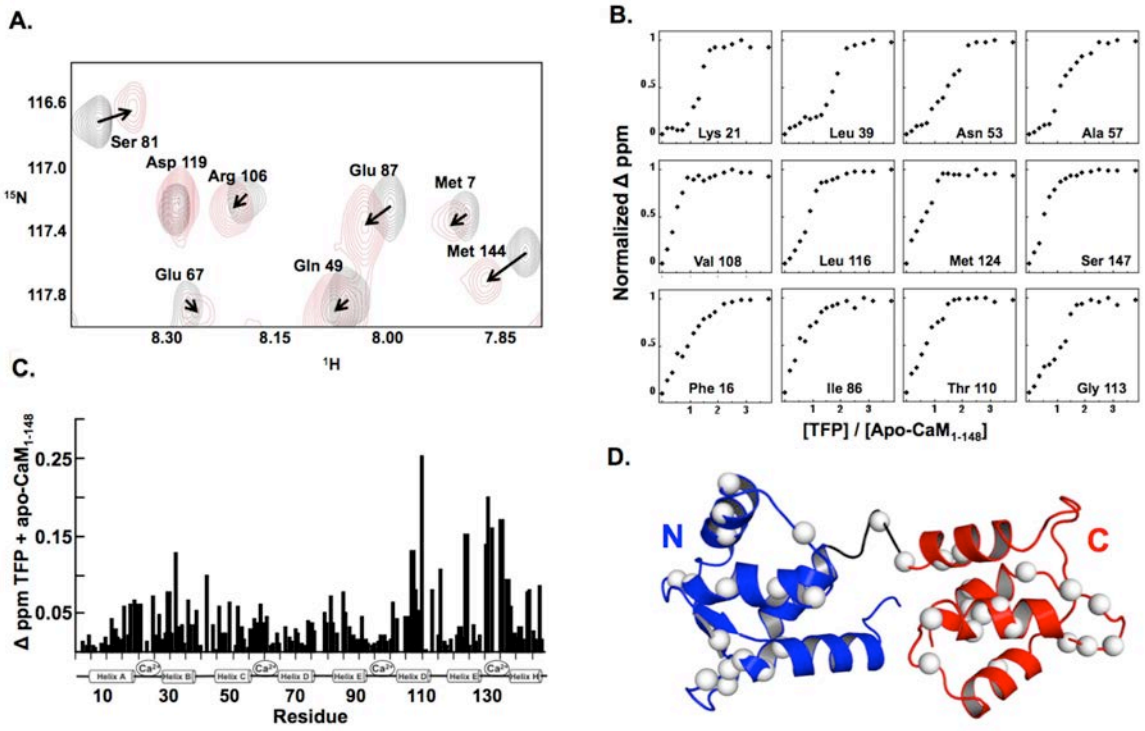

Figure 2.4: ^{15}N-HSQC-monitored TFP titration of uniformly ^{15}N-labeled apo PCaM A: Comparison of subset of ^{15}N-HSQC spectra for apo PCaM (black) and TFP-saturated apo PCaM (red); arrows indicate change in resonance positions over the course of the TFP titration. B: Normalized TFP-induced chemical shifts of individual representative residues of apo CaM. C: Bar graph of net chemical shift per residue caused by TFP saturation of CaM. D: Location of each apo CaM residue whose chemical shift was perturbed > 0.05 ppm by TFP saturation (white spheres); backbone modeled as that of apo CaM (1DMO.pdb). Solution conditions: 10% D_2O, 10 mM imidazole, 100 mM KCl, 50 µM EDTA, 5mM, pH 6.5 at 22°C.
Users/nmr_mike/Thesis/Chapter_II/Figure2_4.jpg

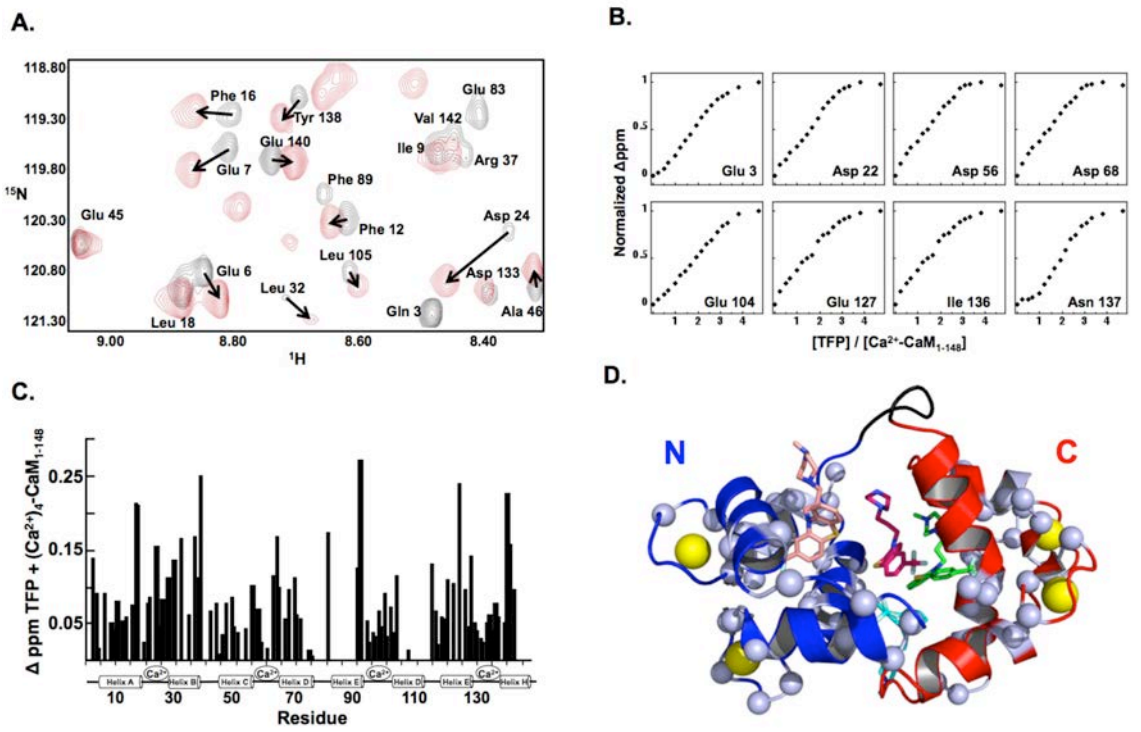

Figure 2.5: ^{15}N-HSQC-monitored TFP titration of uniformly ^{15}N-labeled $(Ca^{2+})_4$-CaM. A: Comparison of $(Ca^{2+})_4$-CaM (black) and TFP-saturated $(Ca^{2+})_4$-CaM (red) ^{15}N-HSQC spectra, arrows indicate change in resonance positions over the course of the TFP titration. B: Normalized TFP-induced chemical shifts of individual representative residues of $(Ca^{2+})_4$-CaM. C: Bar graph of net chemical shift per residue caused by TFP saturation of CaM. D: Location of each $(Ca^{2+})_4$-CaM residue whose chemical shift was perturbed > 0.05 ppm by TFP saturation (white spheres); backbone modeled according to the structure of TFP bound to $(Ca^{2+})_4$-CaM at a 4:1 ratio (1LIN.pdb). Solution conditions: 10% D_2O, 10 mM imidazole, 100 mM KCl, 50 µM EDTA, 5mM $CaCl_2$, pH 6.5 at 22°C. Users/nmr_mike/Thesis/Chapter_II/Figure2_5.jpg

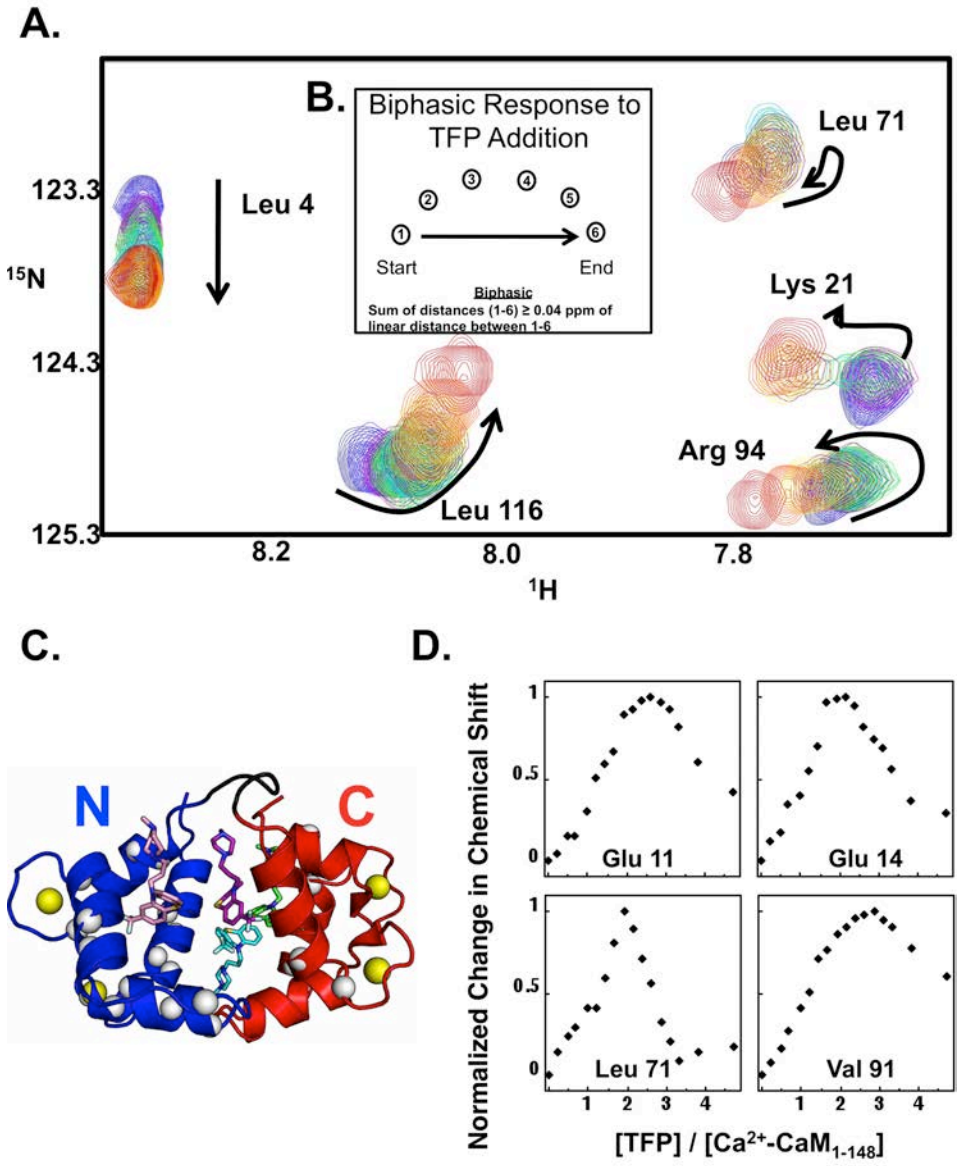

Figure 2.6: Multiple chemical environments observed upon TFP titration of $(Ca^{2+})_4$-CaM A: ^{15}N-HSQC spectrum of uniformly ^{15}N labeled $(Ca^{2+})_4$-CaM titrated with TFP, where arrows represent the movement of each resonance from its initial position. B: Schematic diagram of quantitative criterion for classification of biphasic chemical shift. C: Locations of select residues that underwent a biphasic response upon TFP addition, mapped onto the structure of TFP bound to $(Ca^{2+})_4$-CaM at a 4:1 ratio (1LIN.pdb). D: Normalized chemical shift plots for select individual residues deemed to undergo a biphasic response upon TFP titration of $(Ca^{2+})_4$-CaM. Solution conditions: 10% D_2O, 10 mM imidazole, 100 mM KCl, 50 µM EDTA, 5mM $CaCl_2$, pH 6.5 at 22°C. Users/nmr_mike/Thesis/Chapter_II/Figure2_6.jpg

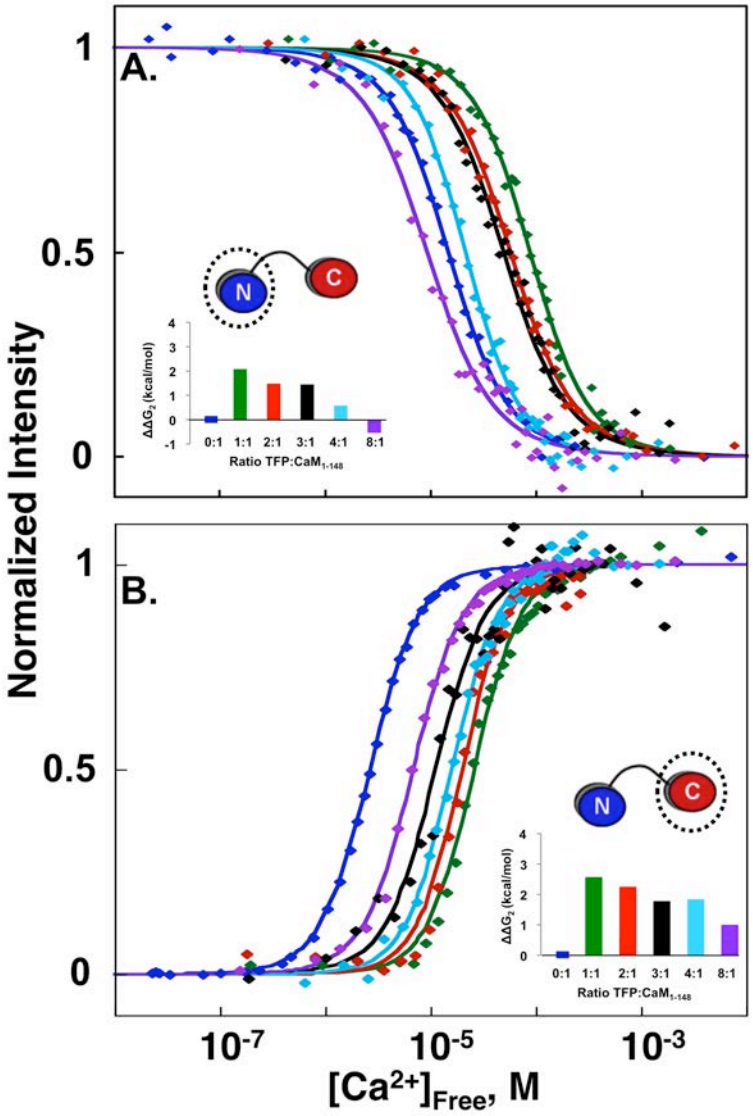

Figure 2.7: Effect of TFP on calcium binding to CaM_{1-148}
Equilibrium calcium titrations of CaM (6 μM) were conducted in the presence of 0 (blue), 6 (green, 1:1), 12 (red, 2:1), 18 (black, 3:1), 24 (cyan, 4:1), or 48 μM (purple, 8:1 TFP:CaM) TFP, and were monitored using the intrinsic fluorescence of CaM. A: phenylalanine fluorescence (250 nm_{ex} and 280 nm_{em}). B: tyrosine fluorescence (277 nm_{ex} and 320 nm_{em}). In B, for 3:1, 4:1 and 8:1 TFP:CaM, the raw signal decreased; it is shown inverted to facilitate comparisons. Solid curves were simulated according to Equation 2.3 and free energies in Table 1; bar graph insets represent ΔΔG2 values in Table 1. Solution conditions: 50 mM HEPES, 100 mM KCl, 5 mM KCl, 0.05 mM EGTA, 1 mM MgCl2, and 6 nM Oregon Green (pH 7.4) at 22°C.
Users/nmr_mike/Thesis/Chapter_II/Figure2_7.jpg

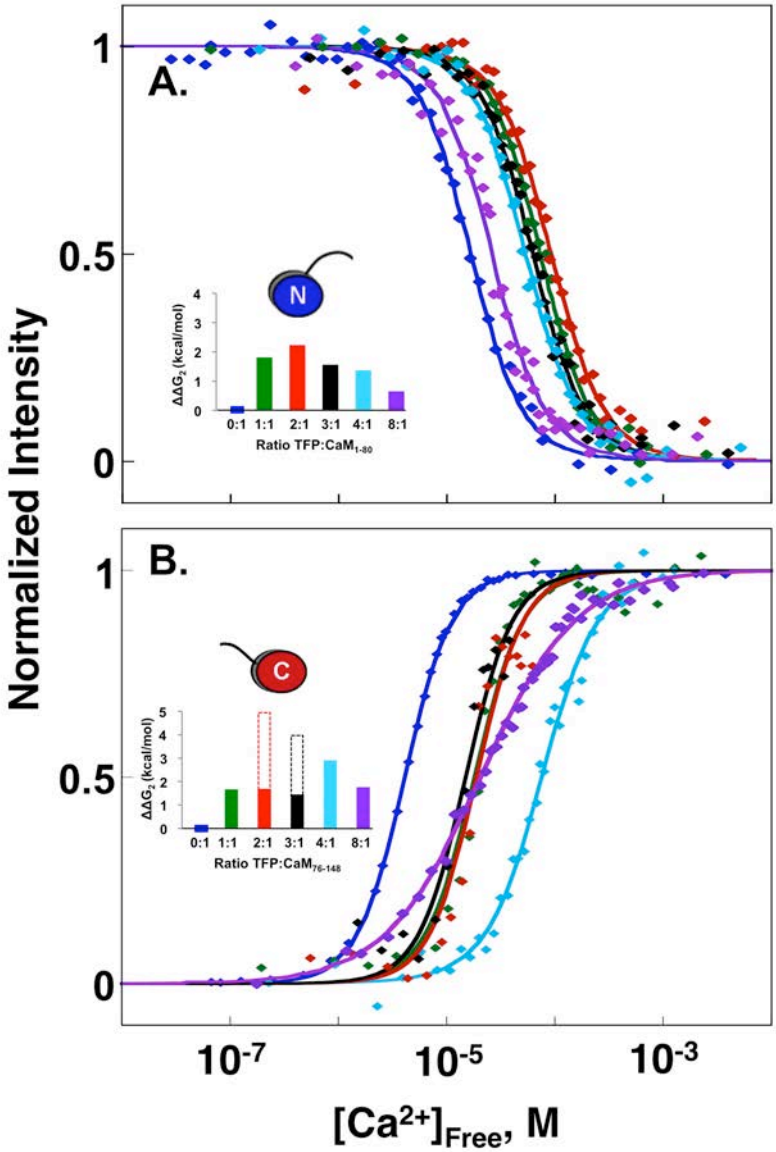

Figure 2.8: Effect of TFP on the calcium binding affinity of CaM_{1-80} and CaM_{76-148} Equilibrium calcium titrations of CaM (6 μM) were conducted in the presence of 0 (blue), 6 (green, 1:1), 12 (red, 2:1), 18 (black, 3:1), 24 (cyan, 4:1), or 48 μM (purple, 8:1 TFP:CaM) TFP, and were monitored using the intrinsic fluorescence of CaM. A: phenylalanine fluorescence (250 nm_{ex} and 280 nm_{em}). B: tyrosine fluorescence (277 nm_{ex} and 320 nm_{em}). In B, for 2:1 and 3:1 TFP:CaM, only the first transition is shown. In B, for 4:1 and 8:1 TFP:CaM, the raw signal decreased; it is shown inverted to facilitate comparisons. Solid curves were simulated according to Equation 2.3 and free energies in Table 1; bar graph insets represent $\Delta\Delta G_2$ values in Table 1. Solution conditions were 50 mM HEPES, 100 mM KCl, 5 mM KCl, 0.05 mM EGTA, 1 mM $MgCl_2$, and 6 nM Oregon Green (pH 7.4) at 22°C.
Users/nmr_mike/Thesis/Chapter_II/Figure2_8.jpg

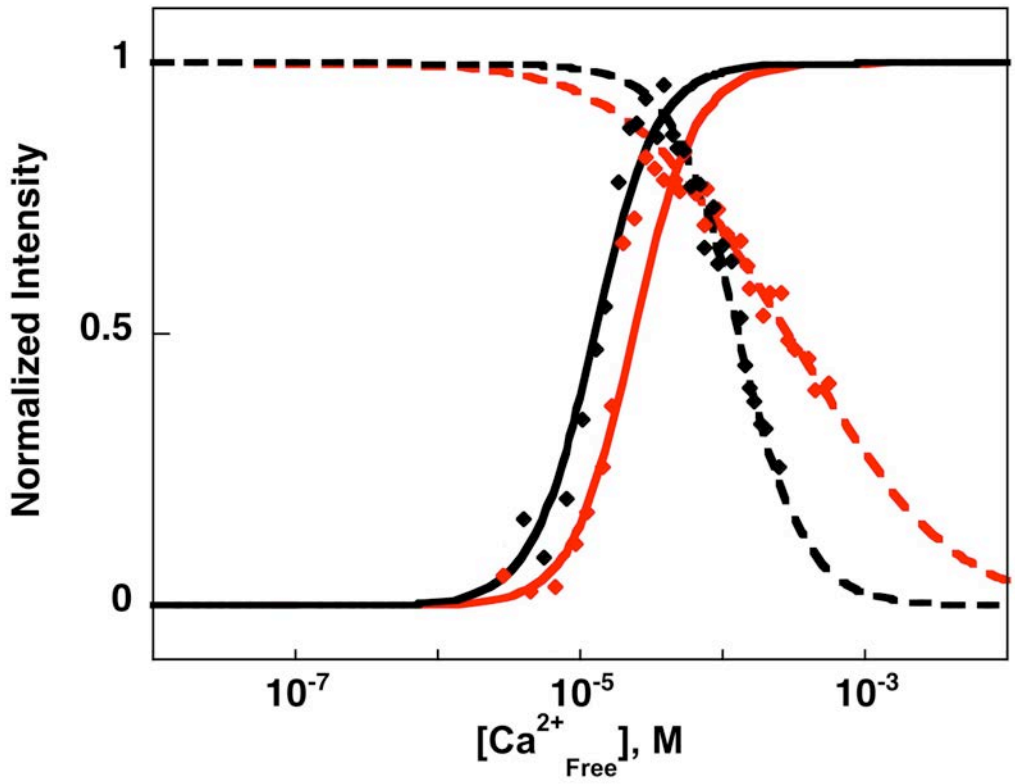

Figure 2.9: Biphasic fluorescence response to calcium binding at intermediate TFP Effect of TFP on calcium titration of $CaM_{76\text{-}148}$ at 12 μM (red, 2:1 TFP:CaM) and 18 μM (black, 3:1 TFP:CaM) monitored using the intrinsic tyrosine fluorescence of CaM (277 nm_{ex} and 320 nm_{em}). Evidence for multiple species, and piecewise analysis described in *Results*. Solid curves for calcium-dependent increase in fluorescence intensity were simulated according to Equation 2.3 and free energies in Table 1; dashed curves correspond to decrease in fluorescence intensity.
Users/nmr_mike/Thesis/Chapter_II/Figure2_9.jpg

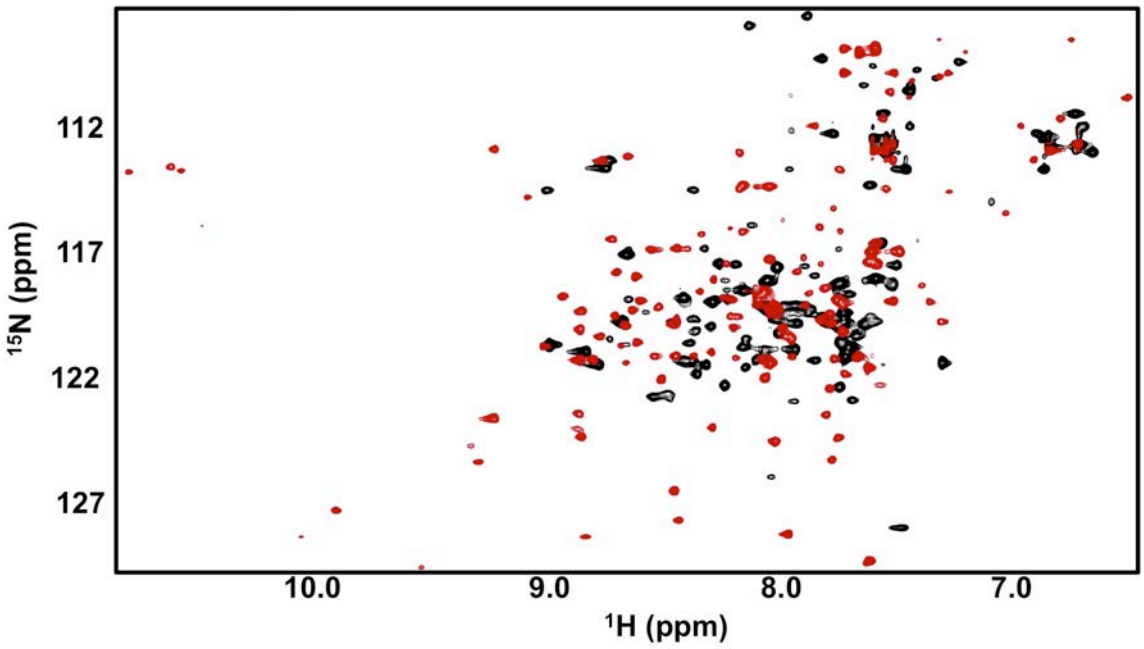

Figure 2.10: Comparison of TFP-saturated apo CaN $(Ca^{2+})_4$-CaM_{1-148}
Overlay of ^{15}N-HSQC spectra of apo CaM (black, 2 TFP:CaM) and $(Ca^{2+})_4$-CaM (red, 4 TFP:CaM). Few peaks overlap, indicating significantly different chemical environments for backbone amides in the structures of apo and $(Ca^{2+})_4$-CaM saturated by TFP.
Users/nmr_mike/Thesis/Chapter_II/Figure2_10.jpg

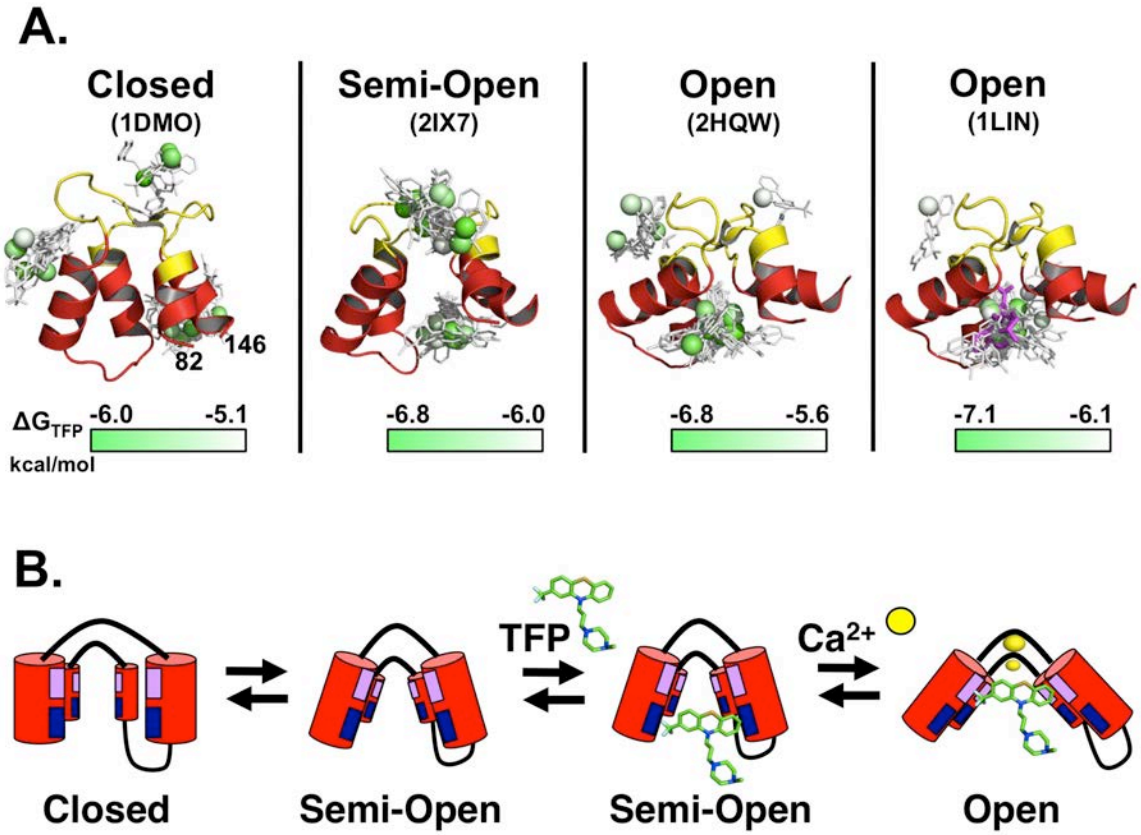

Figure 2.11: Docking and models of TFP binding to the C-domain of CaM
A. TFP Docking to alternative tertiary conformations of apo CaM. Ribbon diagrams of C- domain fragments (residues 82 to 146) represent the "closed" (1DMO.pdb), "semi-open" (2IX7.pdb) and "open" (2HQW, 1LIN.pdb) conformations. Calcium was removed from 2HQW and 1LIN. *AutoDock Vina 1.0.3* [42] predicted positions of TFP binding; 20 models having lowest free energy are shown as sticks. The single sulfur atom of each TFP is shown as a sphere; green corresponds to the most favorable free energy of binding; white is the least favorable. Color thermometer below each set of models indicates the range of energies predicted. The TFP molecule observed at site A of 1LIN.pdb is shown in magenta. Residues in calcium-binding sites are yellow; arrows are included only to orient the viewer to chain direction. **B**. Model of conformational transition of apo C-domain in equilibrium between a "closed" and "semi-open" conformation. Binding of TFP to the blue patches accessible in the "semi-open" conformation is energetically more favorable than binding to "closed" form. TFP binding to the blue occludes hydrophobic patches show in purple of the apo C-domain that are otherwise exposed to solvent. An "open" conformation is adopted upon calcium binding, whether alone or also bound to a drug or protein target exposing hydrophobic patches shown in purple.
Users/nmr_mike/Thesis/Chapter_II/Figure2_11.jpg

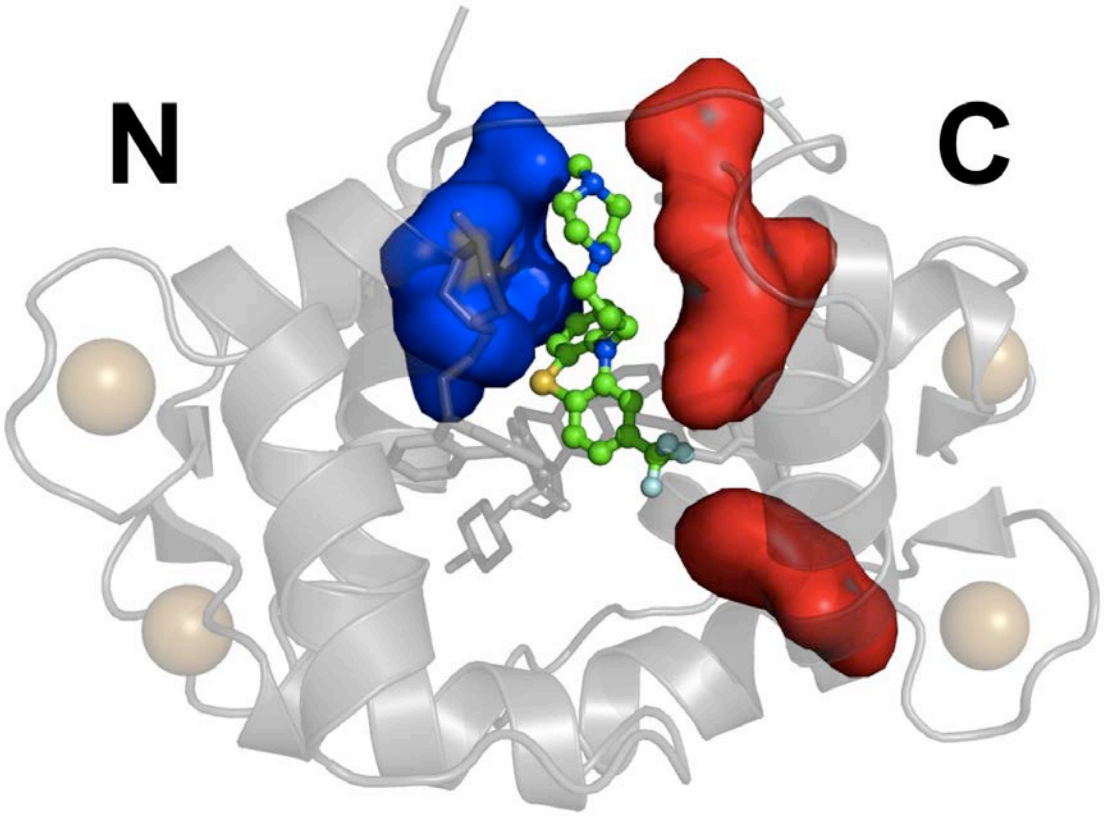

Figure 2.12: Interdomain interactions mediated by TFP
Based on the crystal structure with 4:1 TFP:$(Ca^{2+})_4$-CaM (1LIN.pdb), the trifluoperazine molecule shown in ball-and-stick (green) with fluorine, sulphur, and nitrogen atoms in cyan, yellow, and blue respectively) interacts with residues in both the calcium-saturated N-domain (blue) and C-domain (red). Those within 4 Å were residues 8, 11, 72, 92, 144, 145, TFP 1, and TFP 2. $(Ca^{2+})_4$-CaM backbone (gray), 4 calcium ions (yellow spheres), and three other TFP (gray sticks) are shown.
Users/nmr_mike/Thesis/Chapter_II/Figure2_12.jpg

CHAPTER III

BINDING OF TRIFLUOPERAZINE TO THE C-DOMAIN OF CAM

Introduction

A difficulty encountered in **Chapter II** studies involving TFP binding to apo and $(Ca^{2+})_4$-CaM was found in the added complexity of TFP binding to CaM at stoichiometries greater than 1:1. Binding of TFP at ratios greater that 1:1 complicates structural analysis of TFP induced effects upon CaM as it is difficult to attribute observed changes in CaM to TFP binding at one site, as opposed to another. Further complicating analysis are the allosteric linkages that exist between Ca^{2+} and TFP binding sites if structural changes within CaM can be induced by either direct TFP binding to an area of CaM, or allosterically via propagated change. These complicating factors prompted us to examine how TFP interacted with an isolated C-domain fragment of CaM (CaM_{76-148}).

CaM_{76-148} was appealing to us as studies performed in **Chapter II** showed that TFP preferentially interacted with the C-domain of apo and $(Ca^{2+})_4$-CaM_{1-148}. Choosing to work with isolated CaM_{76-148} reduces that complexity of allosteric interactions that occur between domains of CaM_{1-148} upon TFP binding while still retaining similar Ca^{2+}-binding properties as found in the C-domain of CaM_{1-48}. There is also a common TFP binding site within the C-domain of crystal structures of TFP bound to $(Ca^{2+})_4$-CaM_{1-148} where a significant difference is observed in TFP binding orientation that we would like to resolve why it exists.

The crystal structures of TFP bound to $(Ca^{2+})_4$-CaM differ in the stoichiometry of TFP per molecule of $(Ca^{2+})_4$-CaM (**Figure 2.1c**) (Cook et al., 1994; Vandonselaar et al., 1994a; Vertessy et al., 1998b). These structures also differ in the orientation of the trifluoromethyl group of the TFP molecules common to all 3 TFP bound $(Ca^{2+})_4$-CaM structures . In the structures of TFP bound $(Ca^{2+})_4$-CaM at ratios of 2:1 and 4:1 the

trifluoromethyl group is inserted into the hydrophobic pocket of the C-domain, while in the 1:1 structure it is flipped 180° (**Figure 3.1**). There is no clear explanation as to why the trifluoromethyl would adopt one orientation over the other, as the backbone and side chain conformations of all 3 TFP bound $(Ca^{2+})_4$-CaM structures are nearly indistinguishable (**Figure 3.2**).

Chapter III builds upon thermodynamic studies performed in **Chapter II** to more closely examine the molecular constraints required for TFP binding to apo and $(Ca^{2+})_2$-$CaM_{76\text{-}148}$. This chapter presents structural studies of apo and $(Ca^{2+})_2$-$CaM_{76\text{-}148}$ using NMR and X-ray crystallography respectively. Using NMR spectroscopy we have assigned backbone and side chain nuclei of apo $CaM_{76\text{-}148}$ in the absence and presence of a 1:1 ratio of TFP, allowing for quantification of the residue specific changes in chemical shift. X-ray crystallography was used to determine the structure of TFP bound to $(Ca^{2+})_2$-$CaM_{76\text{-}148}$. Findings reported here reveal residue specific changes and interactions associated with TFP binding to apo and $(Ca^{2+})_2$-$CaM_{76\text{-}148}$.

Materials and Methods

Protein Overexpression

IPTG-induced CaM overexpression was performed using transformed *E. coli* BL21(DE3) cells containing the recombinant pT7-7 vector expressing the C-domain of *Rattus Norvegicus* CaM. Proteins were overexpressed in Luria-Bertani broth. CaM was then purified as previously described by Putkey et al. (Putkey et al., 1985). The recombinant proteins were 97-99% pure as judged by silver-stained SDS-PAGE gels. Protein concentrations were determined by UV spectroscopy of protein denatured with NaOH or native at pH 7.4 (Crouch and Klee, 1980).

Crystallography Materials and Methods

Crystallization of TFP-bound to $(Ca^{2+})_2$-CaM_{76-148} was performed by adding a 10-fold molar excess of TFP to 500µl of ~10mg/ml of CaM_{76-148} in 50mM HEPES, 100mM KCl, 1mM $MgCl_2$, 5mM NTA, 50µM EGTA, pH 7.4, with 500µl of 200mM potassium thiocyanate, 20% polyethylene glycol 3350, pH 6.64 (Solution PEG 62 Qiagen) as a hanging drop in a 96-well tray. The tray was incubated at 15° C for ~8 months, at which time a single rod shaped crystal was observed. The crystal was cryo-protected with mother liquor containing 10% ethylene glycol prior to being flash-frozen at 100 K. Data were collected on this crystal at 100 K at the 4.2.2 synchrotron beamline at the Advanced Light Source at the Ernest Orlando Lawrence Berkeley National Laboratory, with a 150 mm crystal-to-detector distance and the assistance of Jay Nixx (beam-line manager). The program d*TREK was used to analyze and scale the data (Pflugrath, 1999). The monoclinic crystals diffracted to a resolution of 1.9 Å and were of the space group $P2_1$. Molecular replacement was performed using the extracted C-domain of TFP bound $(Ca^{2+})_4$-CaM_{1-148} (1LIN.pdb) as a template with the program Phaser (Read, 2001). TFP and Ca^{2+} were removed from the template prior to use in molecular replacement. Refinement was performed using the program Refmac5 of the CCP4 program suite (Murshudov et al., 1997). Coot was used for molecular visualization and model building (Emsley and Cowtan, 2004). Ca^{2+} and TFP were modeled into clearly visible electron density, water molecules were finally added to the structure using Coot, followed by manual editing. Structure validation was performed using the WhatIf Web Server (http://swift.cmbi.ru.nl/servers/html/index.html).

Overexpression and Purification of Isotope Enriched CaM

All isotopes were obtained from Cambridge Isotope Laboratories (Andover, MA). IPTG-induced CaM overexpression was performed using transformed BL21(DE3) cells

containing the recombinant pET vector expressing the C-domain of *Paramecium* CaM (a gene generously provided by C. Kung, University of Wisconsin, Madison, WI). ^{15}N-labeled proteins were overexpressed in minimal medium, using 2 g/L unlabeled glucose as a carbon source and 1g/L $^{15}NH_4Cl$ as the sole nitrogen source. Double labeled (^{13}C- and ^{15}N-) proteins were produced using 2g/L ^{13}C-glucose as the sole carbon source and 1 g/L $^{15}NH_4Cl$ as the sole nitrogen source. CaM was then purified as previously described by Putkey et al. The recombinant proteins were 97-99% pure as judged by silver-stained SDS-PAGE. Protein concentrations were determined by UV spectroscopy of protein denatured with NaOH or native at pH 7.4 (Beaven and Holiday, 1952).

Assignment of Backbone and Side chain Resonances

The NMR spectra apo $CaM_{76\text{-}148}$ ± TFP were collected at 25 ^{o}C on a Bruker Avance II 500 or 800 NMR spectrometer. The ^{1}H, ^{15}N, and ^{13}C resonances of the backbone were assigned using triple resonance experiments (HNCA, HN(CO)CA, HNCACB, HN(CO)CACB, HNCO, and HN(CA)CO) (Yamazaki et al., 1994) with the uniformly ^{15}N and ^{13}C-labeled CaM in complex with unlabeled TFP. $^{1}H_{\alpha}$ resonances were assigned from an ^{15}N-edited TOCSY spectrum using an uniformly ^{15}N-labeled protein (Clore and Gronenborn, 1994) and from HA(CACO)NH experiment using an uniformly ^{15}N and ^{13}C-labeled sample. The side chain signals were assigned from 3D H(CCO)NH-TOCSY, C(CO)NH-TOCSY, HCCH-TOCSY, ^{15}N-edited TOCSY, and ^{15}N or ^{13}C-edited NOESY spectra (Clore and Gronenborn, 1994; Fesik and Zuiderweg, 1988).

Quantification of ^{15}N-apo $CaM_{76\text{-}148}$ Chemical Shifts due to TFP Addition

To determine the change in chemical shift upon TFP binding to apo $CaM_{76\text{-}148}$, chemical-shift changes in both the ^{1}H and ^{15}N dimensions were quantified using the modified Pythagorean theorem previously described by Jaren et al., 2002 shown in **Equation 3.1**.

$$\Delta ppm = \sqrt{(\Delta^{1}Hppm)^{2} + (0.10134 \bullet \Delta^{15}Nppm)^{2}} \qquad (3.1)$$

In this equation, Δppm refers to the linear change of a specific resonance peak from its initial starting position in apo $CaM_{76\text{-}148}$.

Results

Structure of TFP Bound $(Ca^{2+})_2$-$CaM_{76\text{-}148}$

X-ray crystallography studies of TFP bound to $(Ca^{2+})_2$-$CaM_{76\text{-}148}$ were refined to 2.1 Å resolution with statistical measures of the goodness-of-fit listed in **Table 1**. It is important to point out that the % completeness value (80.92%) reported in this table is not ideal. The reason for this lower than expected value is due to the presence of an ice ring in the data that needed to be removed to properly index and scale the dataset resulting in the loss of some of the diffraction data. Although this value is not ideal, it was sufficient to provide a usable electron density map for model building.

The structure revealed that there were 2 (Ca^{2+})-$CaM_{76\text{-}148}$ and 4 TFP molecules per asymmetric unit (**Figure 3.3a**). The conformations adopted by the 2 $(Ca^{2+})_2$-$CaM_{76\text{-}148}$ chains were very similar to each other with an all atom RMSD of 0.46 Å (**Figure 3.3b**). The interhelical angles adopted between helices E-F of TFP bound $(Ca^{2+})_2$-$CaM_{76\text{-}148}$ chains A and B were 79.0° and 82.9° respectively, while interhelical angles of 89.7° (chain A) and 88.4°(chain B) were observed for helices G-H. Consistent with other structures of $(Ca^{2+})_4$-$CaM_{1\text{-}148}$ either with or without a bound target, both chains of TFP bound $(Ca^{2+})_4$-$CaM_{76\text{-}148}$ adopt an "open" domain conformation.

As previously stated and shown in **Figure 3.3b,** 4 TFP molecules were found within the asymmetric unit. Both $(Ca^{2+})_2$-$CaM_{76\text{-}148}$ chains share a common TFP-binding site located within each of their hydrophobic pockets. Although each (Ca^{2+})-$CaM_{76\text{-}148}$ chain has a TFP molecule bound at a common position, the orientation of TFP within the hydrophobic pocket is different dependent upon the $(Ca^{2+})_2$-$CaM_{76\text{-}148}$ chain examined (**Figure 3.4**). Examination of residues within hydrophobic pockets of $(Ca^{2+})_2$-$CaM_{76\text{-}148}$

that are within 4 Å of TFP that may account for the 180° flip of TFP between $(Ca^{2+})_2$-CaM_{76-148} chains indicate that most of the residues are unchanged with the exception of M144 (**Figure 3.5**).

In addition to the 2 TFP molecules that were observed to bind in the hydrophobic pockets of $(Ca^{2+})_2$-$CaM_{76-148,}$ 2 additional TFP molecules were observed within the asymmetric unit. Analysis of contacts within 4 Å of these TFP molecules indicate that they largely interact with other TFP molecules and made few interactions with $(Ca^{2+})_2$-CaM_{76-148}, compared to TFP molecules found within the hydrophobic clefts of $(Ca^{2+})_2$-CaM_{76-148} (**Figure 3.6**).

This structural study unequivocally shows that TFP-binding to $(Ca^{2+})_2$-CaM_{76-148} does not alter the "open" backbone conformation of $(Ca^{2+})_2$-CaM_{76-148} observed in the absence of TFP. Previous studies conducted in **Chapter II**, indicated that a binding interface used by the D-domain of apo CaM_{1-148} for TFP binding was distinct from those of apo CaM_{1-148} alone and that of TFP-bound $(Ca^{2+})_2$-$CaM_{76-148.}$ To more closely examine the apo CaM_{76-148} TFP binding interface in-depth solution NMR experiments were required.

TFP-Induced Changes of apo CaM_{76-148} as Monitored by ^{15}N-HSQC Spectroscopy

Due to the inherent flexibility found within the Ca^{2+}-binding loops of apo CaM_{76-148}, solution NMR methods were used to examine how TFP interacts with apo CaM_{76-148} at the structural level. **Figure 3.7** shows an overlay of spectra of apo CaM_{76-148} without and with TFP at a 1:1 apo CaM_{76-148}:TFP ratio. TFP binding to apo CaM_{76-148} was observed to be in fast exchange on the NMR time scale due to its weak (~1 μM) binding affinity. TFP binding induced significant chemical shift perturbations of apo CaM_{76-148} amide resonances, as shown in **Figure 3.7.** ^{15}N-HSQC peak assignments of apo CaM_{76-148} in the presence and absence of TFP were determined via 3-dimensional NMR

experiments described in the materials and methods resulting in ~95% assignment of backbone resonances.

Quantification of chemical shifts of apo CaM_{76-148} amide resonances due to TFP binding resulted in an average chemical shift of 0.047 ppm. Individual residue chemical shift values are shown in **Figure 3.8** where it can be observed that TFP binding did not shift apo CaM_{76-148} resonances in a uniform manner, but rather causes shifts at unique positions. Of the 73 amino acids that comprise CaM_{76-148}, 21 were observed to have a chemical shift greater that 0.05 ppm upon TFP addition. Although the structure of TFP-bound apo CaM_{76-148} is unknown, it is likely that TFP binds to an exposed hydrophobic patch of apo CaM_{76-148} comprised of hydrophobic residues identified in **Figure 3.8**. Computational docking of TFP to the C-domain of CaM described in **Chapter** II predicted that TFP bound within the shallow hydrophobic cleft of a "semi-open" conformation composed of similar hydrophobic residues identified here.

The location and magnitude of these chemical shifts have been mapped onto the solution structure (1F71.pdb) of apo CaM_{76-148} (**Figure 3.8)**, where it can be observed that although sequentially distant in primary sequence, many of the TFP perturbed residues are located near each other spatially. As shown in **Figure 3.8**, apo CaM_{76-148} helices F-H as well as the Ca^{2+} binding loops contain resonances that are significantly (>0.05ppm) perturbed, indicating that these regions are either directly or allosterically perturbed upon TFP binding.

Dynamics of TFP Bound apo CaM_{76-148} Monitored with T_2 Relaxation Spectroscopy

The change in overall size of apo CaM_{76-148} upon TFP binding was investigated using T_2 NMR relaxation experiments. Comparison of average amide T_2 relaxation times of apo CaM_{76-148} with (147 ± 79.90 msec) and without TFP (161 ± 59.46 msec), indicate that TFP binding to apo CaM_{76-148} causes an increase in hydrodynamic radius. Shown in

Figure 3.9, are the calculated individual T_2 amide relaxation times for free and TFP bound apo $CaM_{76\text{-}148}$. As expected the N- and C-termini of both TFP free and TFP bound apo $CaM_{76\text{-}148}$ have significantly longer T_2 relaxation times indicative of their lack of defined secondary structure. Consistent with the analysis of ^{15}N-HSQC spectra of TFP binding to apo $CaM_{76\text{-}148}$ presented in this chapter, the T_2 relaxation times apo $CaM_{76\text{-}148}$ of residues within helices F-G, and Ca^{2+} binding loops of CaM are increased upon TFP addition (**Figure 3.10**).

Discussion

The C-domains of apo and $(Ca^{2+})_4$-CaM can bind to their targets using a variety of conformations described previously in **Chapter II**. To simplify structural studies of TFP interacting with the C-domain of apo and $(Ca^{2+})_4$-$CaM_{1\text{-}148}$, the C-domain fragment ($CaM_{76\text{-}148}$) was used. NMR studies presented in this chapter address residue-specific changes in apo $CaM_{76\text{-}148}$ upon TFP addition. The crystal structure of TFP bound $(Ca^{2+})_2$-$CaM_{76\text{-}148}$ consolidates differing observations of the location of the trifluoromethyl group of the TFP common in all observed structures, as well as provides for the first time a molecular basis for the trifluoromethyl group location.

Protein Crystallography of $(Ca^{2+})_2$-$CaM_{76\text{-}148}$-TFP Complex

Crystallization of TFP bound to $(Ca^{2+})_2$-$CaM_{76\text{-}148}$ revealed that TFP binds within the hydrophobic cleft of the isolated C-domain in a similar manner to TFP binding to $(Ca^{2+})_4$-$CaM_{1\text{-}148}$. In the asymmetric unit, 4 TFP molecules were found. The TFP molecules were numbered based on their order from left to right when chain A when Chain A is position on the left and chain B on the right as depicted in **Figure 3.3**. TFP #2 and TFP #3 are likely crystallization artifacts, as both of these TFP molecules made few interactions with either chain A or B compared to TFP bound within the clefts of $(Ca^{2+})_2$-$CaM_{76\text{-}148}$ (**Figure 3.6**). Examination of the asymmetric unit reveals that these bound

TFP molecules function to create a continuous array of TFP molecules between chains A and B (**Figure 3.3a**). This array is similar to the way TFP molecules are positioned in the 4:1 TFP-$(Ca^{2+})_4$-CaM_{1-148} structure, although the $(Ca^{2+})_2$-CaM_{76-148} domains are rotated 180° relative to each other (**Figure 2.1c, Figure 3.3**). This rotation is likely the result of the lack of covalent linkage between the C-domain fragments which would otherwise be present in $(Ca^{2+})_4$-CaM_{1-148}.

Protein chains A and B have a common TFP molecule found in each of their hydrophobic pockets although the location of the TFP's trifluoromethyl groups are flipped 180° relative to each other (**Figure 3.4**). Previous structures of TFP bound $(Ca^{2+})_4$-CaM_{1-148} report that the difference in location of the trifluoromethyl group at the common TFP binding site was reported as improperly assigned electron density (Cook et al., 1994; Vandonselaar et al., 1994a; Vertessy et al., 1998a). These structures were determined at 2.45 (1:1), 2.74 (2:1), and 2.0 Å (4:1) resolution, and only contained one molecule of $(Ca^{2+})_4$-CaM_{1-148} per unit cell. The electron density of the TFP binding site in our 1.9 Å resolution structure which contains two molecules of $(Ca^{2+})_2$-CaM_{76-148} per asymmetric unit clearly indicates that the trifluoromethyl group at the common TFP binding site can occupy both orientations (**Figure 3.11**).

Superposition of chain A or B of $(Ca^{2+})_2$-CaM_{76-148} with the TFP bound C-domain of $(Ca^{2+})_4$-CaM_{1-148} (1CTR.pdb and 1LIN.pdb) shows that the backbone of the C-domain of CaM in CaM_{76-148}, and CaM_{1-148} are similar (RMSD < 0.9Å). However, differences were observed between TFP-bound $(Ca^{2+})_2$-CaM_{76-148}, and $(Ca^{2+})_4$-CaM_{1-148} at the location of TFP binding, and location of the trifluoromethyl groups (Chain A vs. 1:1 CaM_{1-148}:TFP and Chain B vs. 4:1 CaM_{1-48}:TFP) (**Figure 3.12**). Superposition of chains A and B revealed that nearly identical conformations were adopted by both chains as well as the residues within 4Å of the common TFP binding sites in both chains (**Figure 3.4, 3.5**). Slight differences in the structure of $(Ca^{2+})_2$-CaM_{76-148} formed by chains A and B were seen outside of the hydrophobic cleft. Shown in **Figure 3.13** is a Chimera

(Pettersen et al., 2004) generated all-atom morph between chains A and B which depicts that magnitude of change between chains.

The most significant difference between chain A and B is the orientation of the side chain of M144 which appears to act as a selection gate to control whether the trifluoromethyl group can be accommodated within the hydrophobic pocket of $(Ca^{2+})_2$-CaM_{76-148} (**Figure 3.5**). Variability in the side chain conformation of M144 is consistent with other structures of $(Ca^{2+})_4$-CaM_{1-148} bound to drugs or peptides. Side chain methyl dynamics measurements of M144 indicate that it is highly dynamic with respect to other CaM Met residues (Chen et al., 1993; Ehrhardt et al., 1995). In a comparison of 17 compact CaM-drug or CaM-peptide complexes, a tetrad of CaM of residues termed FLMM (L92, L105, M124, M144) was found to consistently contact the ligand for the C-domain in all complexes examined (Ataman et al., 2007). Of the FLMM tetrad residues, the side chain of M144 was the most variable in its closest approach distance when interacting with the hydrophobic anchor residue of the ligand, as well as most variable in terms of amino acid identity in 102 CaM sequences (Ataman et al., 2007). Similar variability conservation of a Met residue in the FLMM tetrad at position 144 was observed in a computational study in which the hydrophobic cleft of CaM was redesigned to improve target binding affinity (Shifman and Mayo, 2002; Shifman and Mayo, 2003). The binding site for TFP within the hydrophobic cleft of the C-domain of CaM is not well defined based on the dynamic nature of Met 144 as its conformation solely selects the orientation of TFP that can be accommodated by the hydrophobic cleft. These observations indicate that the dynamic nature of Met144 results in multiple modes of TFP binding that are used by the C-domain of $(Ca^{2+})_4$-CaM.

This structure helps to resolve controversy within the field when comparing the location of the common TFP binding site found in each of the full length structures of TFP bound to $(Ca^{2+})_4$-CaM_{1-148} at 1:1, 2:1, and 4:1 ratios. It shows that TFP employs 2 modes of binding to the C-domain of CaM, as both orientations of the trifluoromethyl

group are observed within the same unit cell. Previous studies with $(Ca^{2+})_4$-CaM_{1-148} have shown 2 different TFP binding orientations in separate protein crystals obtained from differing crystallization solutions, whereas our findings are from a single crystal and therefore cannot be a result of difference in solution conditions. This structure also indicates that both conformations of TFP have similar binding affinities for the C-domain as protein crystallization requires molecules to adopt low energy conformations to form an ordered crystal lattice. If one of the CaM conformations observed had a significantly more favorable energy than the other, it would be unlikely for both a high and low energy conformation to co-crystallize together.

TFP-Induced Changes of apo CaM_{76-148} as Monitored by ^{15}N-HSQC Spectroscopy

To examine the effect of TFP upon individual residues of apo CaM_{76-148} we have used ^{15}N-HSQC chemical shift mapping to determine TFP induced changes in the chemical environments of residues within apo CaM_{76-148}. **Figure 3.7** shows an overlay of ^{15}N-HSQC spectra of apo CaM_{76-148} recorded in the absence and presence of TFP, where the quantified average change in chemical shift upon TFP addition to apo CaM_{76-148} was 0.047 ppm. If TFP interacted in a nonspecific manner with apo CaM_{76-148}, all residues would have individual Δppm values of ~0.047, but comparison of the average Δppm with individual residue values indicates that TFP selectively interacts with specific residues of apo CaM_{76-148} (**Figure 3.8**). This observation is in agreement with observations made in **Chapter II** that TFP interacts with a selective set of apo CaM C-domain residues. TFP binding to apo CaM_{76-148} perturbs residues located near the hydrophobic cleft of apo CaM_{76-148} as well as residues within the Ca^{2+}-binding loops of sites III and IV of apo CaM_{76-148} (**Figure 3.8**). This result provides direct evidence of allosteric linkage between TFP and Ca^{2+} binding to CaM_{76-148}, consistent with Ca^{2+} titration data in **Chapter II**,

which indicated that TFP at a 1:1 ratio lowered the Ca^{2+}-binding affinity of $CaM_{76\text{-}148}$ by 2.56 kcal/mol.

TFP-Induced Changes of apo $CaM_{76\text{-}148}$ as Monitored by T_2 Relaxation

Comparison of average T_2 relaxation times of apo $CaM_{76\text{-}148}$ and TFP bound apo $CaM_{76\text{-}148}$ (161 ± 59 and 147 ± 79 msec, respectively) indicates that TFP binding to apo $CaM_{76\text{-}148}$ induces a conformational change within apo $CaM_{76\text{-}148}$. Due to the inverse relationship between T_2 time and molecular weight (↑ T_2 time = ↓ molecular tumbling), TFP binding causes apo $CaM_{76\text{-}148}$ to tumble at a slower rate in solution (Palmer, 2001). This conformational change is interpreted to be due to TFP binding resulting in a "semi-open" conformation of apo $CaM_{76\text{-}148}$ that was previously in a "closed" conformation. The average T_2 values of apo $CaM_{76\text{-}148}$ and TFP bound apo $CaM_{76\text{-}148}$ also indicated that both molecules are found as monomers in solution. It may also possibly however unlikely that the change in T_2 time after TFP addition could be a result of aggregation, though visual inspection of the sample indicated that no precipitate was present. An orthogonal approach proposed for future studies to verify the absence of precipitate in the NMR sample would be to use dynamic light scattering or analytical ultracentrifugation to verify

Table 3.1: Data collection and refinement statistis of $(Ca^{2+})_2$-CaM_{76-148}:TFP complex

Data Collection Parameters	
Temperature (K)	100
Wavelength (Å)	1.033
Space Group	P 21
Unit cell parameters	
a, b, c (Å)	24.59, 85.54, 35.35
α, β, δ (Å)	90.00, 93.03, 90.00
Resolution (Å)	22.181 – 2.1
I/Iσ	6.0
Completeness (%)	80.92
R_{merge} (%)	0.091
Redundancy	3.53
Refinement Details	
Resolution (Å)	2.1
R_{work}/R_{free} (%)	1
Number of atoms	2194
Protein	1969
Ligand	139
Water	86
B-factor average ($Å^2$)	
Protein (main chain)	28.55
TFP	33.00
Water	31.08
RMS deviation from ideal geometry	
Bond lengths (Å)	0.009
Bond angles (°)	1.277
Dihedral angles (°)	22.020
Planarity (°)	0.004
Chirality (°)	0.100
Ramachandran plot (% residues)	
Most Favored	100
Additionally allowed	0
Disallowed	0

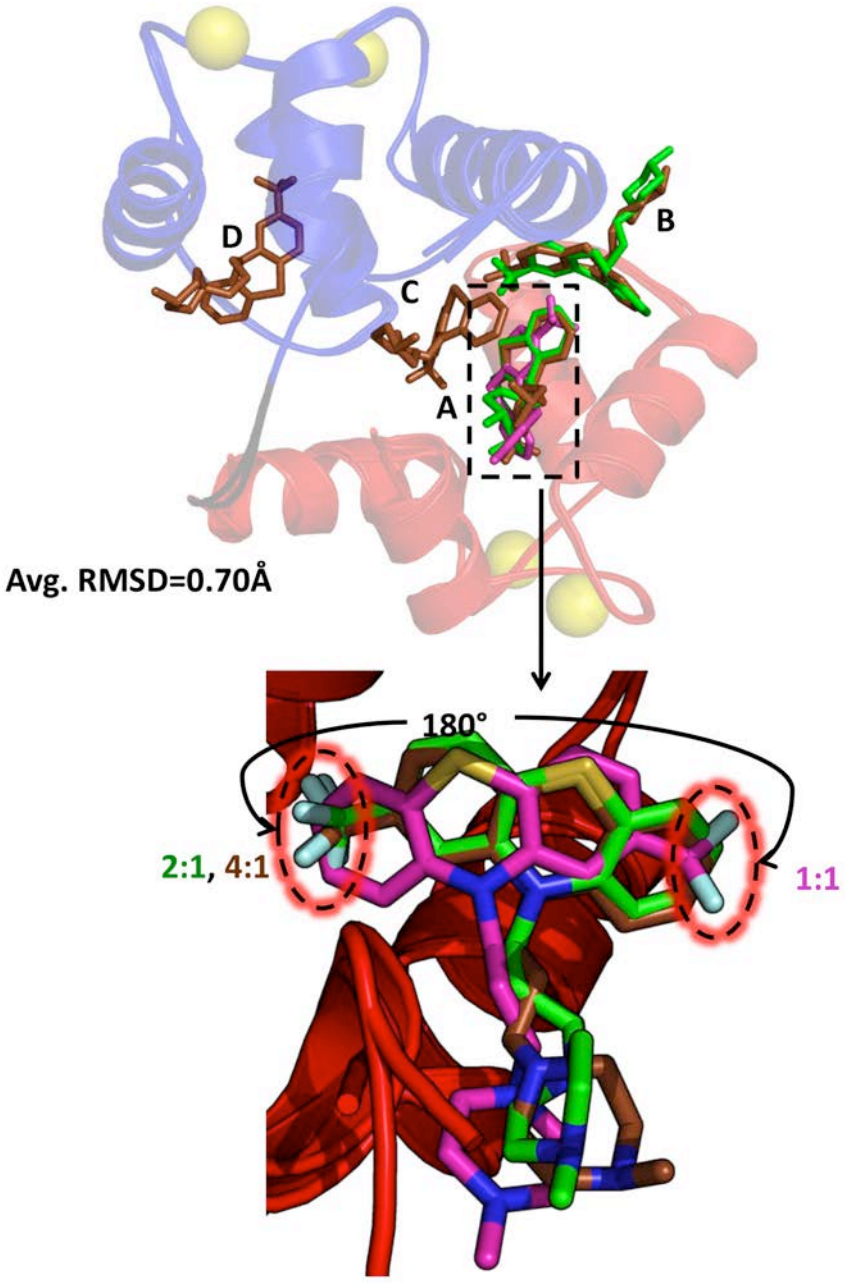

Figure 3.1: Superposition of TFP:$(Ca^{2+})_4$-CaM_{1-148} structures
Superposition of crystallographically derived structures of TFP:$(Ca^{2+})_4$-CaM_{1-148} with drug:protein ratios of 1:1 (1CTR.pdb), 2:1 (1A29.pdf), and 4:1 (1LIN.pdb). The TFP-binding sites are labeled A (green), B (magenta), C (brown) and D (orange). TFP-binding sites A and B are located in the C-domain (backbone red), site C bridges the two domains, and site D is located in the N-domain (backbone blue). The 180° flip of TFP molecules at TFP binding site A (dashed square) results in the trifluoromethyl group of TFP being found in 2 locations (dashed ovals).
Users/nmr_mike/Thesis/Chapter_III/Figure3_1.jpg

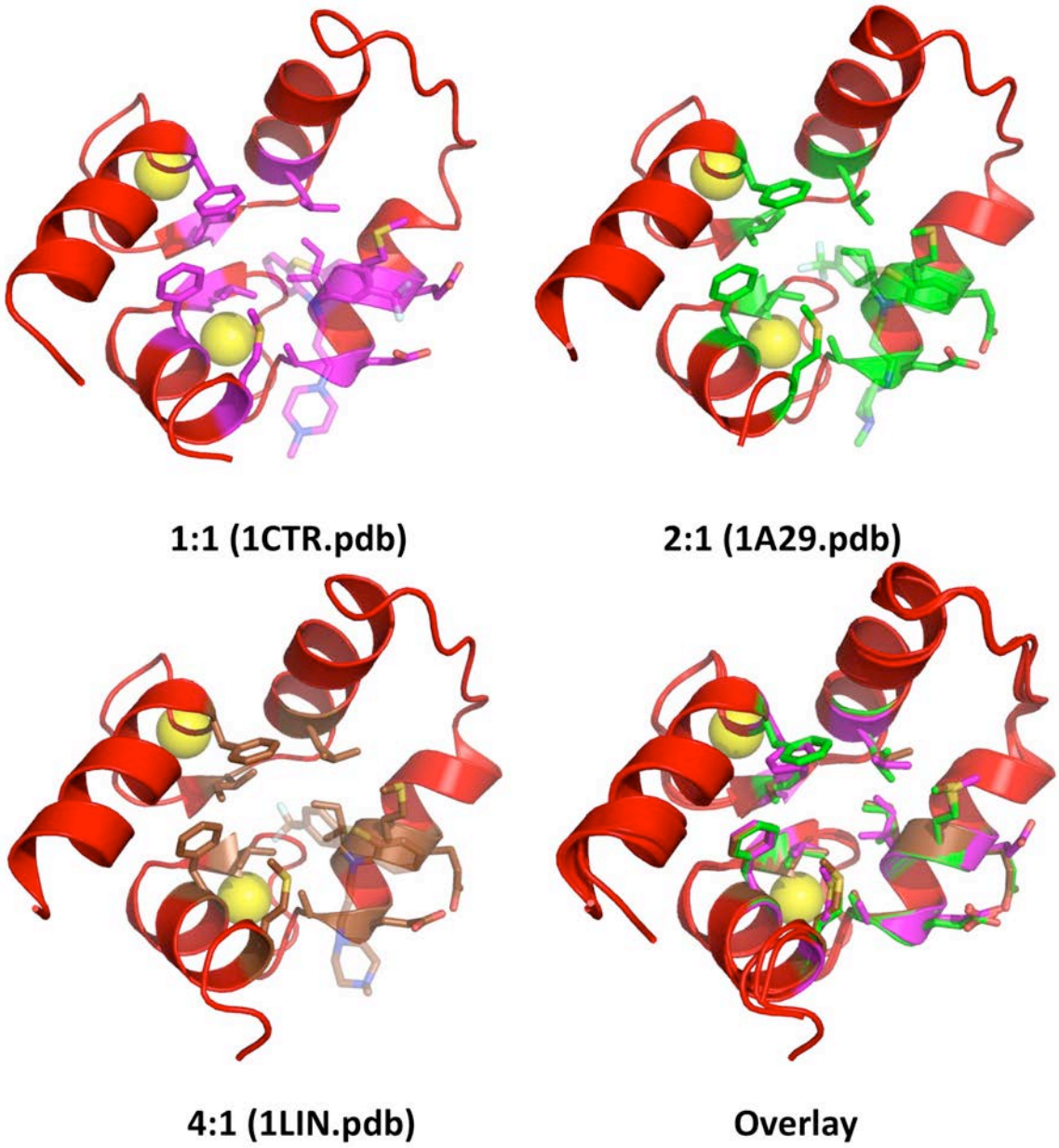

Figure 3.2: Side chain Orientations of $(Ca^{2+})_4$-CaM_{1-148} when binding TFP at site A
A-C: Isolated residues of $(Ca^{2+})_4$-CaM_{1-148} C-domain (red) bound to TFP within 4 Å of TFP bound at site A (transparent sticks) with Ca^{2+} ions shown as yellow spheres. D: Superposition of isolated C-domains of 1:1, 2:1, and 4:1 TFP:$(Ca^{2+})_4$-CaM_{1-148} shown in panels A-C to illustrate that nearly identical binding interfaces and side chain conformations are used when binding TFP at site A.
Users/nmr_mike/Thesis/Chapter_III/Figure3_2.jpg

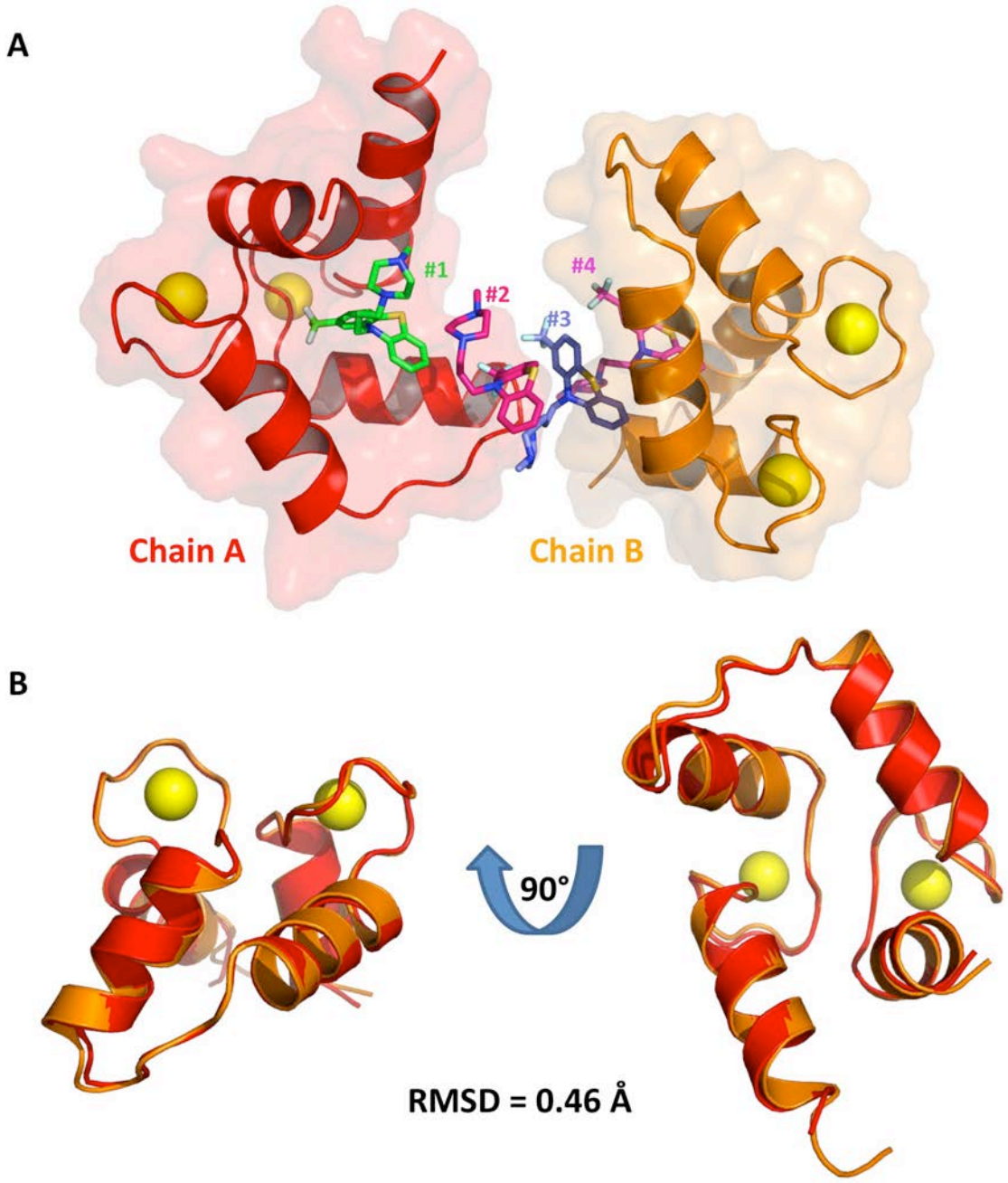

Figure 3.3: Crystal structure of TFP bound $(Ca^{2+})_2$-$CaM_{76\text{-}148}$
A: $(Ca^{2+})_2$-$CaM_{76\text{-}148}$ chains A and B are shown in red, and orange respectively while TFP molecules is depicted in sticks, Ca^{2+} are yellow spheres. B: Superposition of $(Ca^{2+})_2$-$CaM_{76\text{-}148}$ chains A and B shown in red and orange respectively.
Users/nmr_mike/Thesis/Chapter_III/Figure3_3.jpg

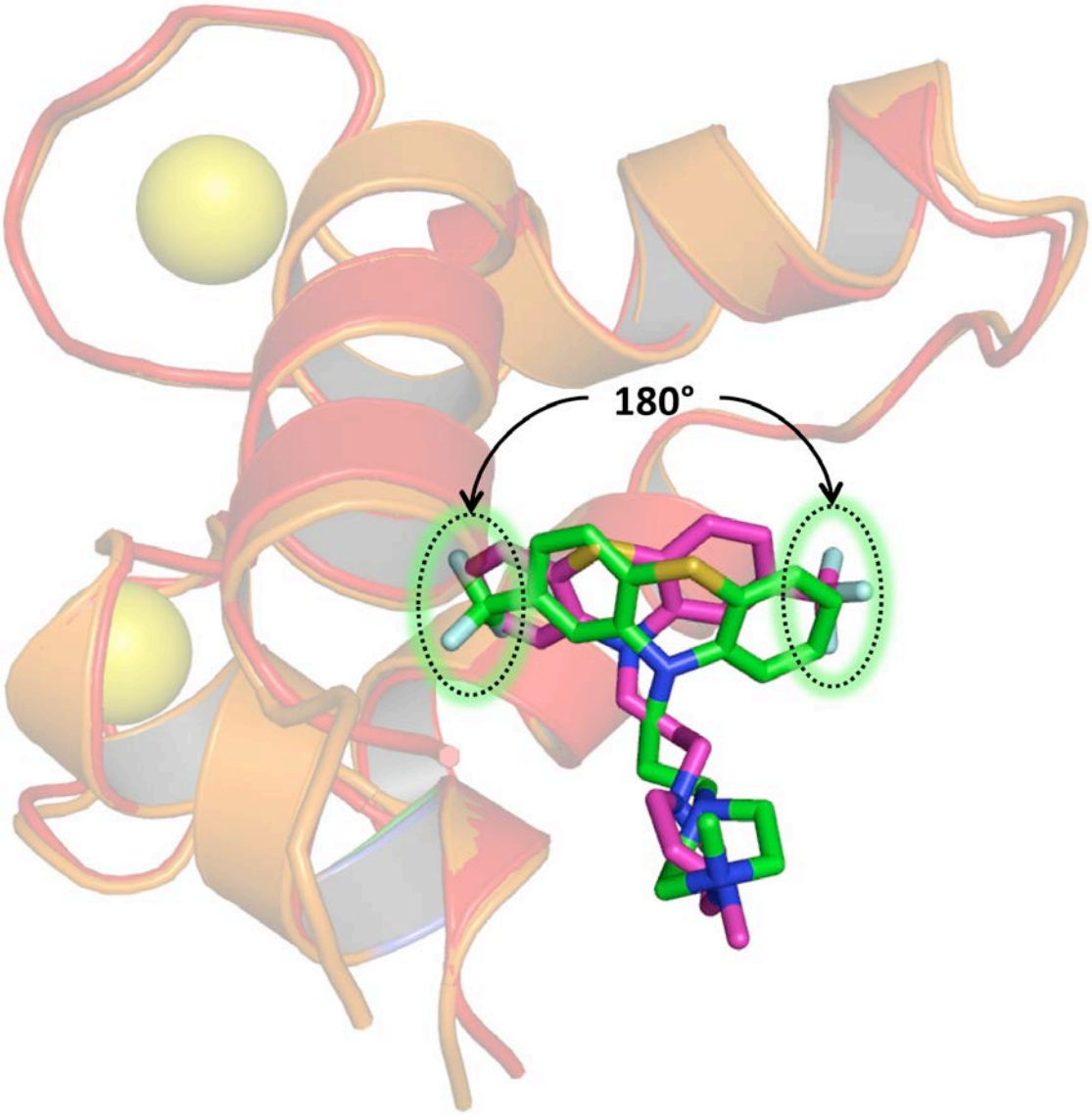

Figure 3.4: Comparison of common TFP binding sites within $(Ca^{2+})_2$-CaM_{76-148}
Superposition of TFP (sticks) bound to $(Ca^{2+})_2$-CaM_{76-148} chains A and B colored red and orange respectively. The TFP molecules associated with chains A and B are colored green and magenta respectively where the 180° flip in the location of the trifluoromethyl of TFP is indicated by dashed circles.
Users/nmr_mike/Thesis/Chapter_III/Figure3_4.jpg

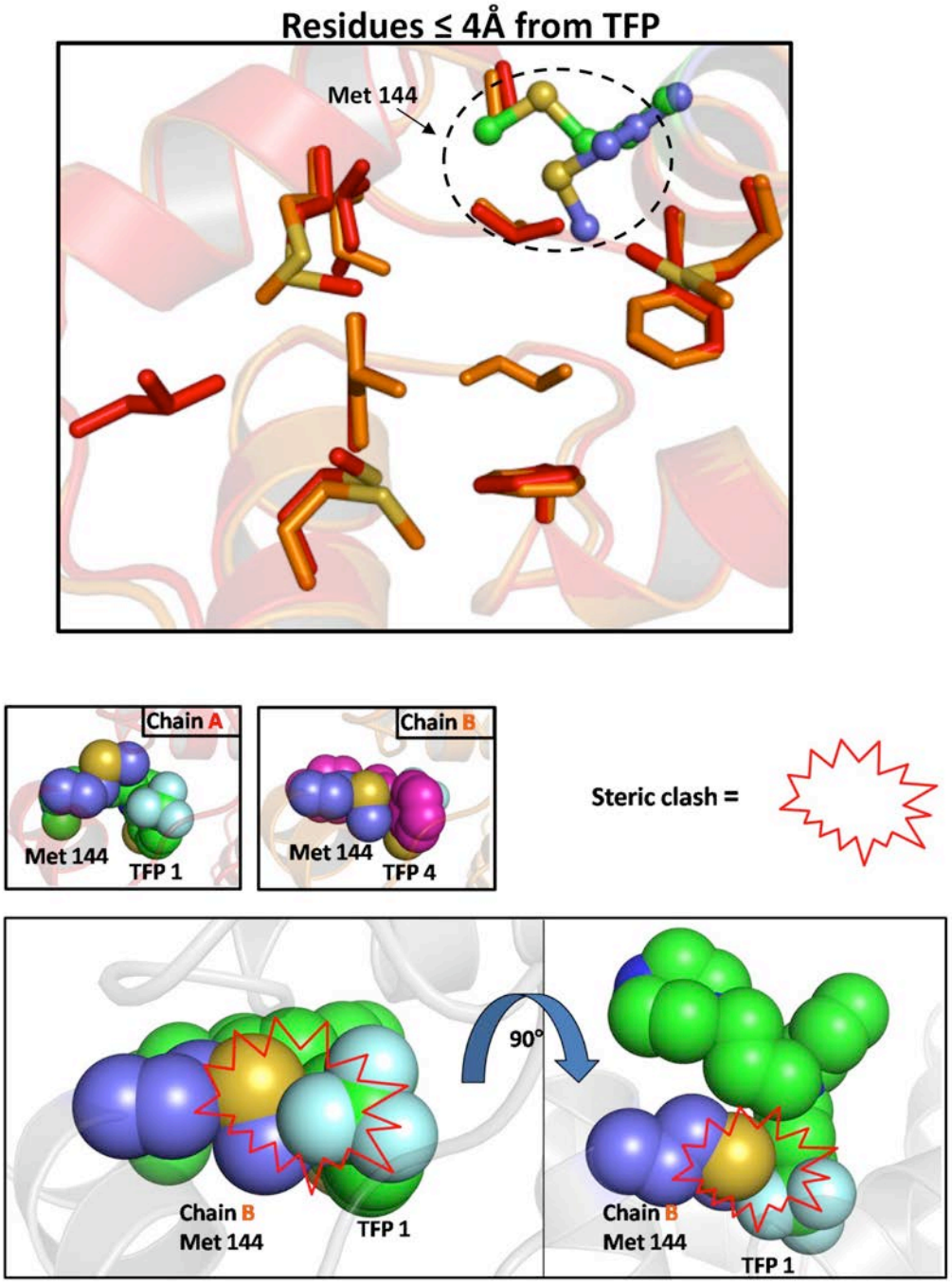

Figure 3.5: Met 144 gating determines TFP orientation
A: Superposition of $(Ca^{2+})_2$-$CaM_{76\text{-}148}$ chains A and B colored red and orange respectively, where residues within 4 Å of TFP are shown as sticks. Shown in ball and stick are the conformations adopted by Met 144 of chains A and B colored green and slate respectively. B: Space-filling representation of Met 144 conformations in relation to TFP. Modeled steric clash between Met 144 side chain conformation found in chain B when TFP #1 from chain A is superimposed into the binding site of TFP 4.
Users/nmr_mike/Thesis/Chapter_III/Figure3_5.jpg

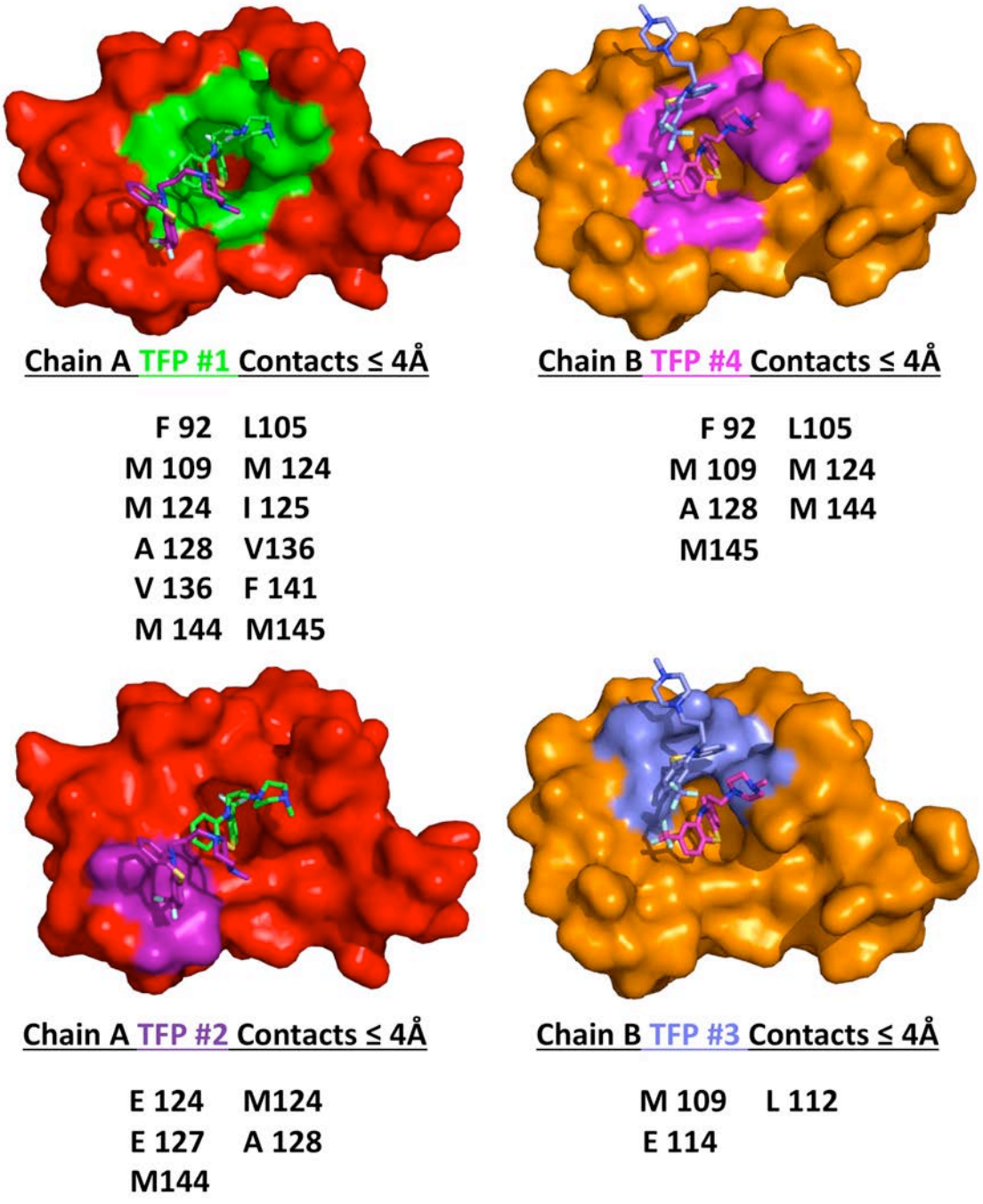

Figure 3.6: Contacts made by TFP molecules with $(Ca^{2+})_2$-CaM_{76-148}
The molecular surface of $(Ca^{2+})_2$-CaM_{76-148} chains A and B are shown as red and orange respectively, where portions are colored according to the respective TFP examined to indicate areas of $(Ca^{2+})_2$-CaM_{1-148} that are within 4 Å
Users/nmr_mike/Thesis/Chapter_III/Figure3_6.jpg

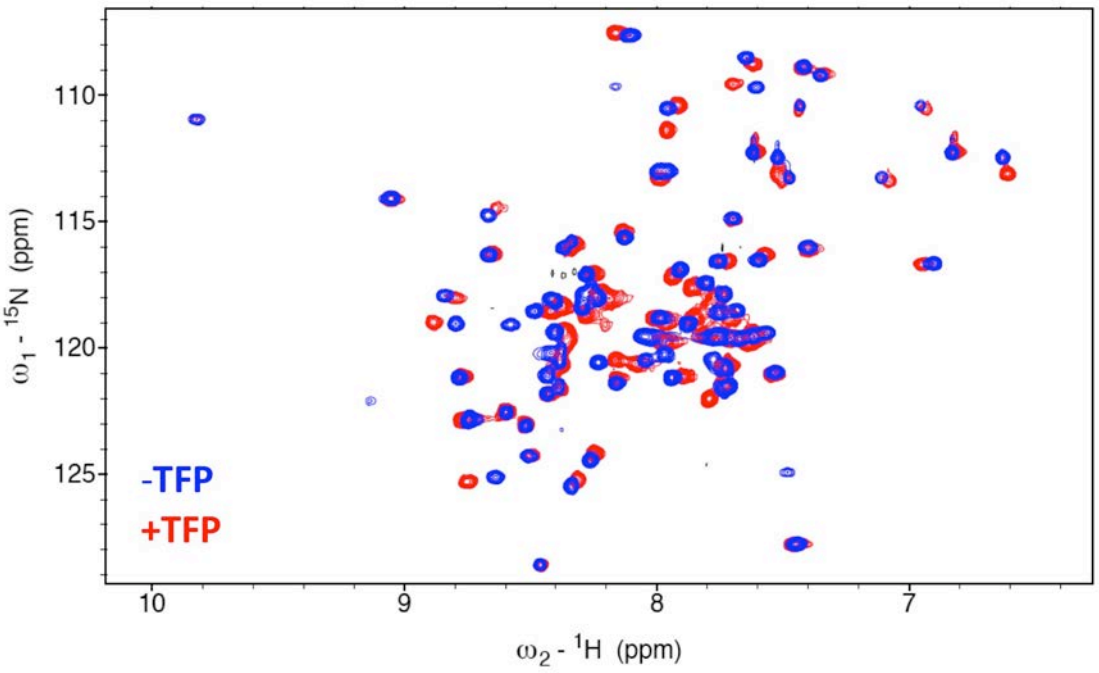

Figure 3.7: ^{15}N-HSQC spectrum of apo $CaM_{76\text{-}148}$ showing the effect of TFP binding Overlaid ^{15}N-HSQC spectra of apo $CaM_{76\text{-}148}$ alone (blue) and in the presence of TFP (red)
Users/nmr_mike/Thesis/Chapter_III/Figure3_7.jpg

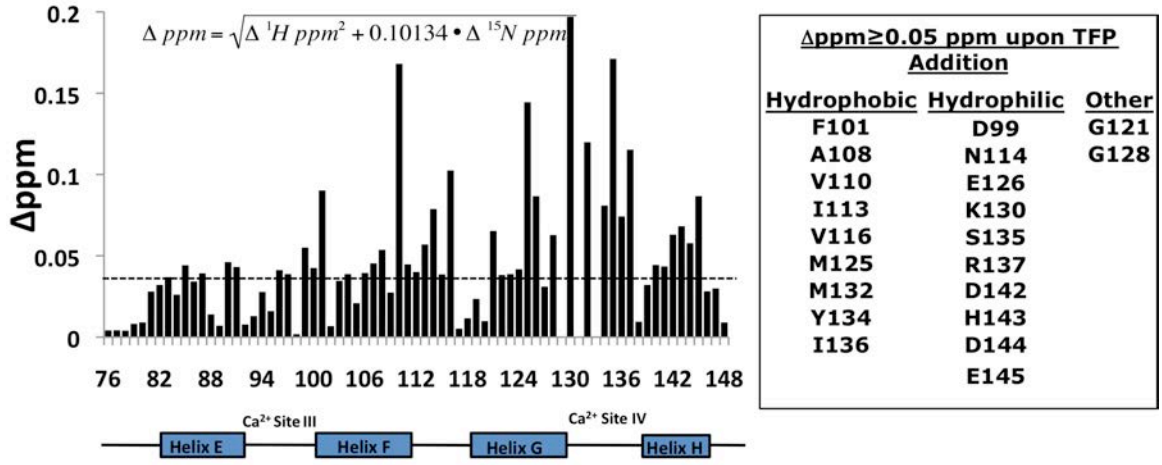

Figure 3.8: Change in amide chemical shift of apo $CaM_{76\text{-}148}$ upon TFP addition
The difference in chemical shift value (Δppm) is plotted for each assigned apo $CaM_{76\text{-}148}$ residue (absent bar represents unassigned residue), dashed line represents average value of TFP induced change in chemical shift of 0.047 ppm. The apo $CaM_{76\text{-}148}$ structure is shown as a cartoon with the Cα atoms of residues whose quantified chemical shift upon TFP addition was greater than 0.05 ppm shown as spheres.
Users/nmr_mike/Thesis/_Chapter_III/Figure3_8.jpg

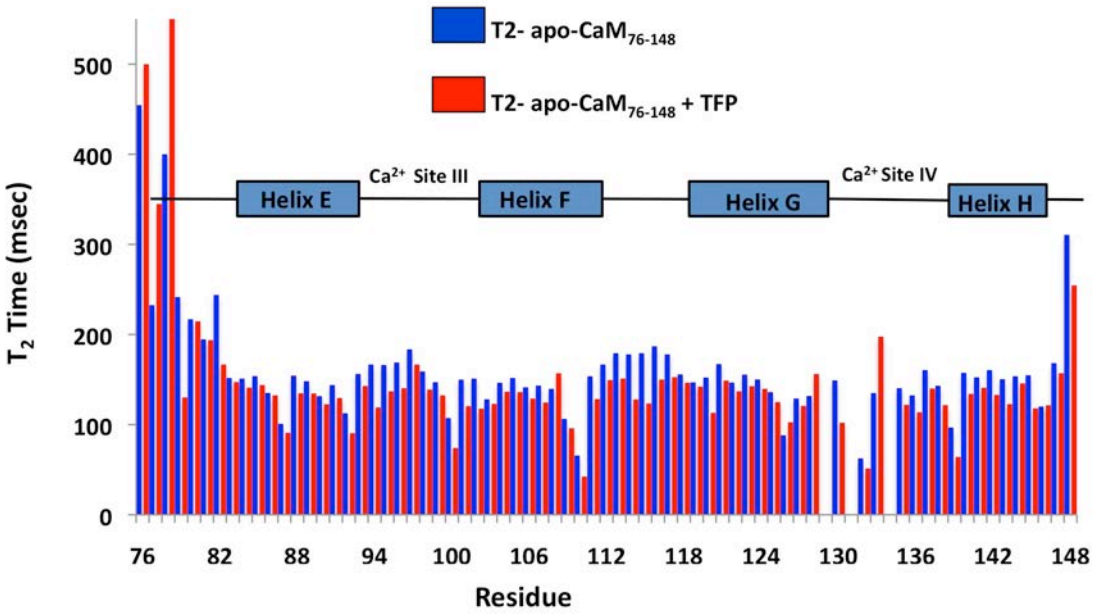

	w/out TFP	w/ TFP
Average T_2	161 ± 59	147 ± 79
Median T_2	152	135

↓ T_2 time = ↑ Hydrodynamic radius

TFP addition decreases T_2 time

Figure 3.9: T_2 Values for apo $CaM_{76\text{-}148}$ in the absence and presence of TFP
Users/nmr_mike/Thesis/Chapter_III/Figure3_9.jpg

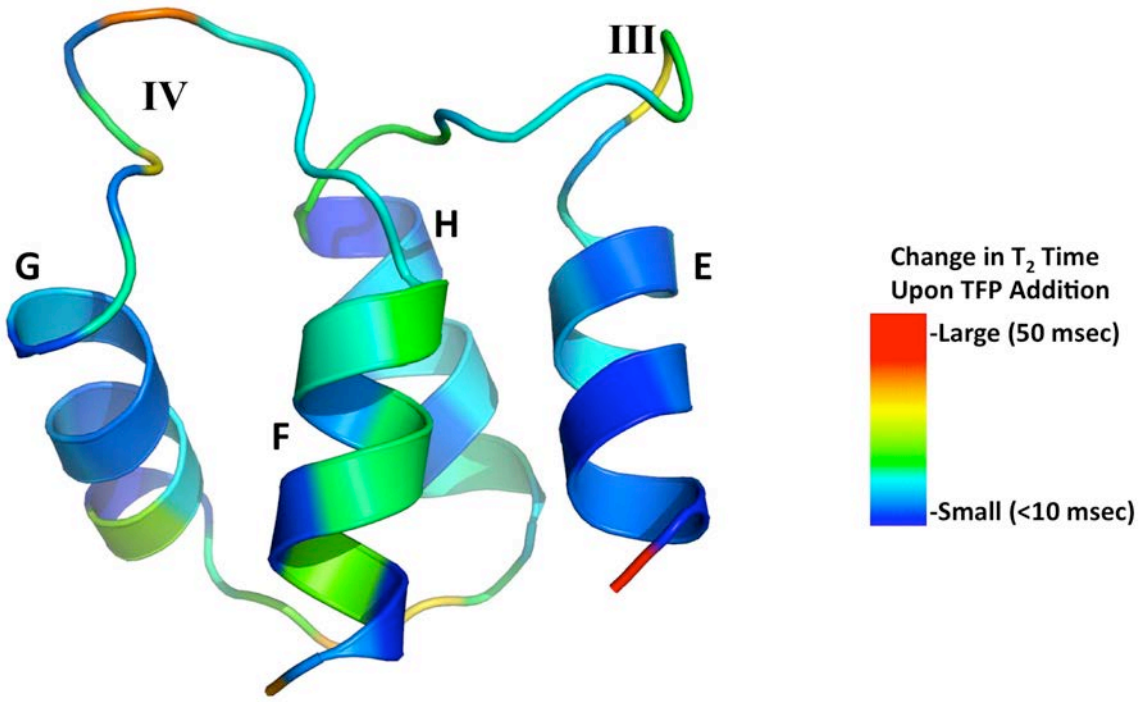

Figure 3.10: Change in T_2 values of apo $CaM_{76\text{-}148}$ upon TFP addition mapped upon the structure of apo $CaM_{76\text{-}148}$
Apo $CaM_{76\text{-}148}$ is shown as a cartoon with labeled helices and Ca^{2+} binding sites.
Users/nmr_mike/Thesis/Chapter_III/Figure3_10.jpg

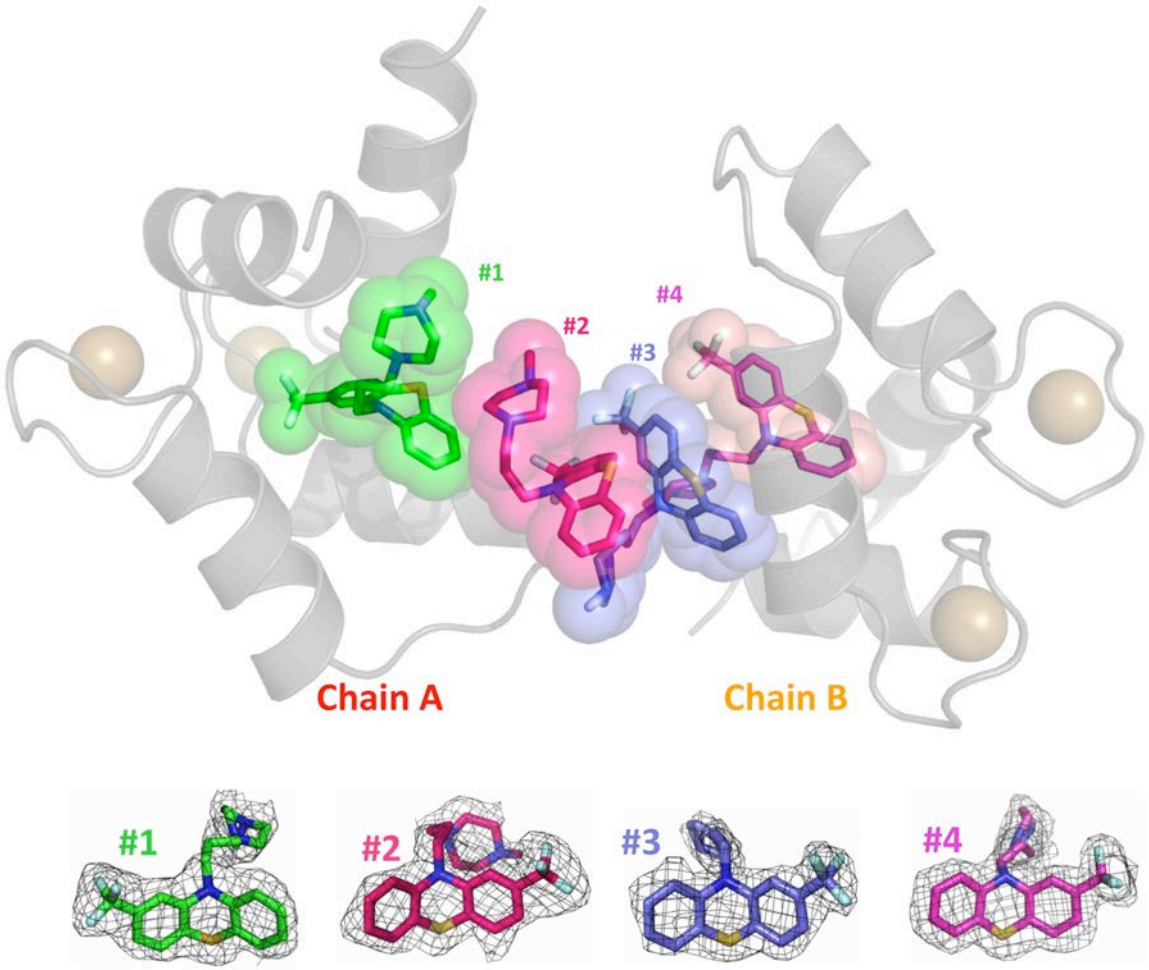

Figure 3.11: Electron density of TFP binding sites in $(Ca^{2+})_2$-$CaM_{76\text{-}148}$
The asymmetric unit of $(Ca^{2+})_2$-$CaM_{76\text{-}148}$ bound to TFP where chains A and B are shown in red and orange respectively, while TFP are shown as sticks. The electron density for TFP molecules in upper panel is displayed at 2σ over each modeled TFP (lower panel).
Users/nmr_mike/Thesis/Chapter_III/Figure3_11.jpg

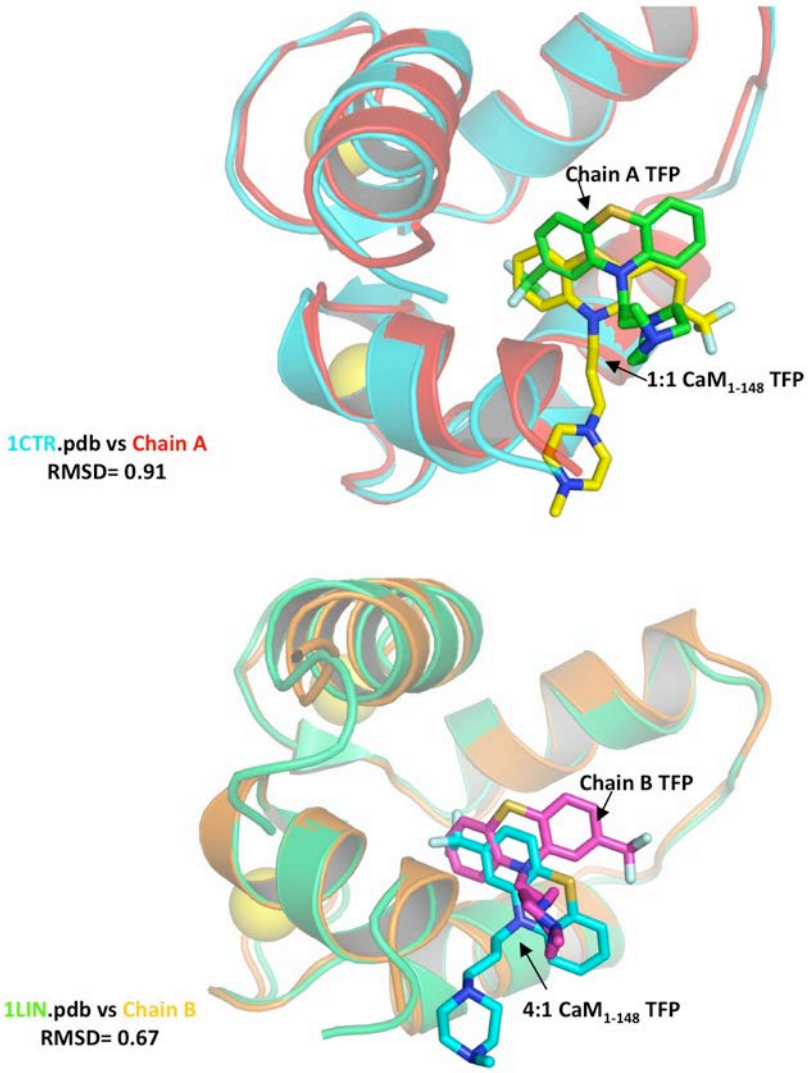

Figure 3.12: Superposition of common TFP binding sites in $(Ca^{2+})_2$-CaM_{76-148} and $(Ca^{2+})_4$-CaM_{1-148}
Superpositions of Isolated C-domains of TFP:(Ca^{2+})-CaM_{1-148} at 1:1 and 4:1 ratios shown in cyan and light green respectively onto TFP bound (Ca^{2+})-CaM_{76-148} chains A and B colored red and orange respectively.
Users/nmr_mike/Thesis/Chapter_III/Figure3_12.jpg

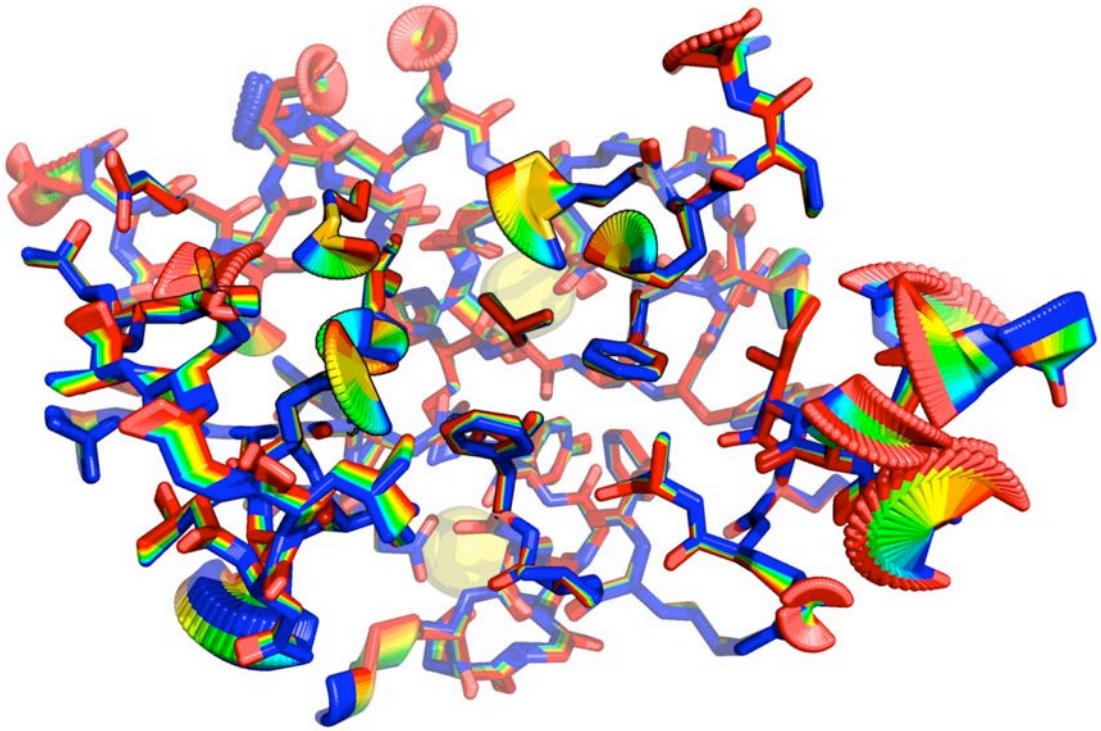

Figure 3.13: Structural morph between chain A and B or TFP-bound $(Ca^{2+})_2$-$CaM_{76\text{-}148}$ UCSF Chimera generated morph between chain A (red) and chain B (blue), indicating areas of similarity and divergence between chains.
Users/nmr_mike/Thesis//Chapter_III_figures/Figure3_13.jpg

CHAPTER IV

BINDING OF $NA_V1.2_{IQP}$ TO THE C-DOMAIN OF APO CAM

Introduction

The voltage-dependent sodium channel type II ($Na_v1.2$) is necessary for the propagation of action potentials along unmyelinated axons that are found primarily in neuronal and muscle tissues (Schaller and Caldwell, 2003; Trimmer and Rhodes, 2004). $Na_v1.2$ has one α-subunit (260 kDa) and one or more β-subunits (33−36 kDa each) (Catterall, 2000b). The α-subunit is comprised of four homologous transmembrane domains (I−IV) that are the pore-forming entity of the channel, as well as intracellular domains that play a vital role in control of channel gating (Cormier et al., 2002; Herzog et al., 2003; Mantegazza et al., 2001). Inactivation or closing of $Na_v1.2$ requires an interaction between two regions of the α-subunit: the intracellular loop that connects domains III and IV and the C-terminal tail (Catterall, 2000a; Cormier et al., 2002; Deschênes et al., 2001; Herzog et al., 2003).

The membrane-proximal half of the C-terminal tail of $Na_v1.2$ has been modeled to contain six α-helices. Patch clamp studies have shown that deletion of the putative sixth α-helix region slows recovery from inactivation by maintaining the channel in a closed, inactivated state (Cormier et al., 2002; Herzog et al., 2003; Mantegazza et al., 2001). A sequence (residues 1901 to 1927, $Na_v1.2_{IQp}$) within the putative sixth α-helix also contains a classical calmodulin-binding IQ-motif (IQxxxBGxxxB), where X is any amino acid, and B is either Arg or Lys (**Figure 4.1a**) (Mori et al., 2003; Mori et al., 2000). IQ-motifs found in many proteins such as myosins, neuronal growth proteins, and ion channels have been characterized to bind preferentially to apo (calcium-depleted) calmodulin (CaM) (Bayley et al., 2003; Gerendasy et al., 1995; Houdusse et al., 2006; Liu and Storm, 1990; Mori et al., 2003; Mori et al., 2000; Mori et al., 2004; Shah et al.,

2006). CaM is a small intracellular calcium sensor that is essential to many eukaryotic signal transduction pathways (Klee, 1988; Wang et al., 1980; Yagi et al., 1990; Yap et al., 2000).

CaM has two homologous domains (N- and C-domains) that are 4-helix bundles connected by a flexible linker (**Figure 4.1b**) (Babu et al., 1988; Evans and Shea, 2009; Sorensen and Shea, 1997). Each domain binds two Ca^{2+} ions cooperatively in neighboring EF-hand motifs, giving rise to a total of 4 bound Ca^{2+} ions per molecule of CaM (Pedigo and Shea, 1993; Sorensen et al., 2002b). Although the two domains are similar in sequence and structure, the N-domain binds Ca^{2+} more weakly than the C-domain in the absence of allosteric effectors (Newman and Shea, 2006; Newman, 2008; Vanscyoc and Shea, 2001b). Changes in intracellular Ca^{2+} levels are linked to many cellular events by the effect of Ca^{2+} on CaM: binding triggers conformational changes that expose hydrophobic surfaces in both domains of CaM, altering the free energy of association with many target proteins (Crivici and Ikura, 1995; Sorensen and Shea, 1997). Several high resolution structures of $(Ca^{2+})_4$-CaM bound to an IQ-motif show that it adopts a compact ellipsoidal conformation. That conformation has also been observed when calcium-saturated CaM is bound to target regions of most known cyclases, phosphatases, cytoskeletal motors and ion channels (Tjandra et al., 1999). Besides the IQ-motif, the most common CaM-binding sequence is a Basic Amphipathic Alpha-helix (BAA) motif, where the domains of $(Ca^{2+})_4$-CaM adopt an "open" conformation to interact with hydrophobic "anchor" residues located within the BAA motif (**Figure 4.1c**) (Tjandra et al., 1999). There are only two available high-resolution structures showing the apo C-domain of CaM bound to a peptide (**Figure 4.1d, 4.1e**): CaM bound to a fragment of myosin V (2IX7) or of the SK channel (1G4Y). Only one of those (2IX7) contains an IQ-motif. However, in both complexes, the apo C-domain of CaM adopted a "semi-open" conformation in which interhelical angles are smaller than those of $(Ca^{2+})_4$-CaM (Houdusse et al., 2006; Schumacher et al., 2001).

All ten human isoforms of the voltage-dependent sodium channel contain a single IQ-motif necessary for regulation by CaM (Yu and Catterall, 2003). Previous studies conducted by the Shea laboratory (Theoharis et al., 2008) showed that both apo and calcium-saturated CaM bind to $Na_v1.2_{IQp}$ with high affinity (i.e., dissociation constants near nanomolar). However, the two homologous domains of CaM have different roles when interacting with $Na_v1.2_{IQp}$ (Theoharis et al., 2008). Circular dichroism and fluorescence spectroscopy showed that $Na_v1.2_{IQp}$ binds preferentially to the C-domain of apo CaM which selectively lowers the calcium-binding affinity of sites III and IV, while having little effect on sites I and II.

To examine the molecular basis of the preferential binding of apo CaM to $Na_v1.2_{IQp}$, and the roles of each domain of CaM, we used heteronuclear NMR to determine residue-specific responses of CaM to binding the IQ-motif. HSQC spectra showed that, under apo conditions, the C-domain of CaM was necessary and sufficient to bind $Na_v1.2_{IQp}$, while resonances corresponding to the N-domain of CaM were not affected. NMR studies of ^{13}C-^{15}N-labeled CaM were then used to determine a set of high-resolution models of a C-domain fragment of apo CaM (CaM_{76-148}) bound to $Na_v1.2_{IQp}$. This set of structures revealed that apo CaM_{76-148} adopts a "semi-open" conformation when bound to $Na_v1.2_{IQp}$ similar to the C-domains of either apo CaM, CaM-like proteins, or essential light chain (ELC) when bound to IQ-motifs in myosin (Houdusse et al., 2006; Swindells and Ikura, 1996; Terrak et al., 2003). It also demonstrated the importance of two Tyr residues in the sequence of $Na_v1.2_{IQp}$; these are conserved in most IQ-motifs of all isoforms of voltage-dependent sodium channels. Although both $Na_v1.2_{IQp}$ and CaM are very polar, the interface was dominated by hydrophobic interactions. This was consistent with results from NaCl titrations of the apo CaM-IQ complex which remained unperturbed in the presence of elevated levels of NaCl (up to 650 mM).

Although $Na_v1.2_{IQp}$ tightly associates with $(Ca^{2+})_4$-CaM, NMR studies showed that participating residues changed dramatically, consistent with an interaction interface

like that found for a peptide bound to an "open" domain of CaM. However, for both apo and calcium-saturated CaM, ^{15}N-HSQC and fluorescence anisotropy revealed that the N-domain of CaM did not interact with $Na_v1.2_{IQp}$. This suggests that its preferred binding site lies elsewhere in the sequence $Na_v1.2$. Analysis of conserved contact residues in all available high-resolution structures of apo CaM, apo ELC, or apo CaM-like proteins in complex with canonical IQ-motifs suggested that all of the IQ motifs bind with a similar polarity, having the amino-terminus closer to the EF-hand, and the C-terminus closer to the G-H hand of that domain.

Materials and Methods

Overexpression and Purification of Calmodulin

All isotopes were obtained from Cambridge Isotope Laboratories (Andover, MA). IPTG-induced CaM overexpression was performed using transformed *E. coli* BL21(DE3) cells containing the recombinant pT7-7 vector expressing either the full length or the C-domain of *Paramecium* CaM (a gift from C. Kung, University of Wisconsin, Madison, WI).^{15}N-labeled proteins were overexpressed in minimal medium, using 2 g/L unlabeled glucose as a carbon source and 1g/L $^{15}NH_4Cl$ as the sole nitrogen source. ^{13}C and ^{15}N-labeled proteins were produced using 2g/L ^{13}C-glucose as the sole carbon source and 1 g/L $^{15}NH_4Cl$ as the sole nitrogen source. CaM was then purified as previously described by Putkey et al (Putkey et al., 1985). The recombinant proteins were 97-99% pure as judged by silver-stained SDS-PAGE gels. Protein concentrations were determined by UV spectroscopy of protein denatured with NaOH (Beaven and Holiday, 1952) or native at pH 7.4 (Crouch and Klee, 1980).

Prepared $Na_v1.2_{IQp}$

A peptide (Nav1.2IQp:KRKQEEVSAIVIQRAYRRYLLKQKVKK 3.36kDa) representing residues 1901-1927 of the α-subunit of $Na_v1.2$ was custom-synthesized by

the GenScript Corporation (Scotch Plains, NJ). The peptide was evaluated to be at least 95% pure by HPLC analysis and MALDI-TOF mass spectrometry.

^{15}N-HSQC Monitored $Na_v1.2_{IQp}$ and Ca^{2+} Titration of CaM_{1-148}

^{15}N-HSQC spectroscopy was used to monitor titration of $Na_v1.2_{IQp}$ into ^{15}N-labeled apo CaM_{1-148} (400 μM) in 10 mM D_4-imidazole, 100 mM KCl, 50 μM D_{16}-EDTA, 0.01% NaN_3, pH 6.5. Upon $Na_v1.2_{IQp}$ saturation of apo CaM_{1-148}, $CaCl_2$ was titrated into the sample to a final concentration of 5mM. $Na_v1.2_{IQp}$ and Ca^{2+} saturation of CaM_{1-148} were confirmed by plateaus in the intensity of peaks corresponding to either the $Na_v1.2_{IQp}$:apo CaM_{1-148} or $Na_v1.2_{IQp}$:$(Ca^{2+})_4$-CaM_{1-148}.

Preparation of ^{13}C/^{15}N-CaM76-148:$Na_v1.2_{IQp}$ Complex

A ^{15}N-HSQC monitored titration of ^{12}C/^{14}N-$Na_v1.2_{IQp}$ into ^{13}C /^{15}N-apo CaM_{76-148} was performed to ensure saturation of apo CaM_{76-148} by $Na_v1.2_{IQp}$ as determined by a plateau in the intensity of peaks corresponding the apo CaM_{76-148}:$Na_v1.2_{IQp}$ complex and the disappearance of peaks corresponding to apo CaM_{76-148} alone. The sample was then applied to a 200 mL G50 Superdex column. Complex containing fractions were pooled, buffer exchanged into 10 mM D_4-imidazole, 100 mM KCl, 50 μM D_{16}-EDTA, 0.01% NaN_3, pH 6.5 and concentrated to 1.5 mM. Nitrogen-based experiments were conducted in the previously described buffer conditions in 90% H_20 / 10% D_20, while carbon-based experiments were conducted in 100% D_2O. All spectra with the exception of amide exchange were conducted with Shigemi (Allison Park, PA) microscale NMR tubes whose magnetic susceptibility was matched to D_2O.

^{15}N-HSQC Monitored Amide Exchange of ^{15}N-CaM76-148:$Na_v1.2_{IQp}$ Complex

A 480 μl sample of 1.5 mM ^{15}N-CaM_{76-148}:$Na_v1.2_{IQp}$ complex in 10 mM D_4-imidazole, 100 mM KCl, 50 μM D_{16}-EDTA, 0.01% NaN_3, pH 6.5 that had been prepared in H_2O was lyophilized in a Speed-Vac Model VG-5 (Savant). After lyophilization the complex was then resuspended with 480 μl of 99.96% D_2O (Cambridge Isotope Laborotories, Andover, MA) from a freshly broken ampoule. The pH of the sample was not adjusted after addition of D_2O, and assumed to be 7.4 as HMQC spectra taken of the sample prior to lyophilization in H_2O were identical to that of the D_2O spectrum. The resuspended sample was placed immediately in a Bruker 500 MHz Avance II spectrometer and data acquisition began within 5 minutes. ^{15}N-HSQC spectra were acquired at 30 minute intervals for 23 hours. Spectra were processed with NMRPipe (Delaglio et al., 1995b) and individual peak intensities were determined with Sparky (Goddard and Kneller). Peak intensity decays times were fit to a mono-exponential decay model (**Equation 4.1**) using the Solver function within Microsoft Excel**.**

$$I = I_0 e^{-(t-t_0)/\tau} + b \tag{4.1}$$

In this equation, I represents the intensity at time t, I_0 is the initial intensity at time zero, t_0 is time zero, τ is the apparent lifetime, and b is a constant representing the offset intensity of the baseline.

NMR Spectroscopy for Structure Determination

The NMR spectra were collected at 25 ^{o}C on a Bruker Avance II 500 or cryo-probe equipped 800 MHz NMR spectrometers. The ^{1}H, ^{15}N, and ^{13}C resonances of the apo CaM_{76-148} backbone were assigned using triple resonance experiments (HNCA, HN(CO)CA, HNCACB, HN(CO)CACB, HNCO, and HN(CA)CO) (Yamazaki et al., 1994) with the uniformly ^{15}N and ^{13}C-labeled apo CaM_{76-148} in complex with unlabeled $Na_v1.2_{IQp}$. $^{1}H_{\alpha}$ resonances were assigned from an ^{15}N-edited TOCSY spectrum using a

uniformly ^{15}N-labeled protein (Clore and Gronenborn, 1994) and from HA(CACO)NH experiment using a uniformly ^{15}N and ^{13}C-labeled sample. The side chain signals were assigned from 3D H(CCO)NH-TOCSY, C(CO)NH-TOCSY, HCCH-TOCSY, ^{15}N-edited TOCSY, and ^{15}N or ^{13}C-edited NOESY spectra (Clore and Gronenborn, 1994; Fesik and Zuiderweg, 1988). The unlabeled $Na_v1.2_{IQp}$ resonances were assigned from several 2D doubly ^{14}N and ^{12}C-filtered NOESY and TOCSY spectra acquired with mixing times of 80 to 120 ms for NOESY and 26 to 46 ms for TOCSY (Ikura and Bax, 1992; Vuister et al., 1994). The intermolecular NOEs were assigned from the ^{13}C-edited and ^{12}C,^{14}N-filtered 3D NOESY spectrum acquired with a mixing time of 140 ms (Vuister et al., 1994). All NMR spectra were processed with the NMRPipe program (Delaglio et al., 1995a) and analyzed using NMRView (Johnson and Blevins, 1994) and Sparky (Goddard and Kneller).

Apo $CaM_{76\text{-}148}$:$Na_v1.2_{IQp}$ Structure Calculations

Structures of the apo $CaM_{76\text{-}148}$:$Na_v1.2_{IQp}$ complex were generated using a torsion-angle molecular dynamics protocol (Karimi-Nejad et al., 1998; Stein et al., 1997) with the CNS program (Brunger et al., 1998). Structure calculations employed a total of 1812 NMR-derived distance restraints from the analysis of 3D ^{15}N- and ^{13}C-resolved NOESY spectra acquired with a mixing time of 120 ms (Fesik and Zuiderweg, 1988). The NOE-derived distance restraints were given upper bounds of 3.0, 4.0, 5.0, and 6.0 Å based upon the measured NOE intensities. From an analysis of the amide exchange rates measured from a series of ^{15}N/^{1}HN HSQC spectra recorded after the addition of D_2O, 47 hydrogen bonds from the α-helices were included in the structural calculations. In addition, 44 ϕ and Ψ angular restraints derived from an analysis of the C, N, C_α, H_α, and C_β chemical shifts using the TALOS program (Cornilescu et al., 1999a; Shen et al., 2009b) were included in the structural calculations. A square-well potential was employed to constrain the NMR-derived distance restraints with F_{NOE} set to 150 and 50

kcal mol^{-1} $Å^{-2}$ during the stages of high temperature and slow-cooling Torsion Angle Dynamics (TAD) and the final stage of conjugate gradient minimization, respectively. Force constants of 100 and 200 kcal mol^{-1} rad^{-2} were applied to all torsional restraints during the stage of high temperature TAD and the rest stages of structural calculations, respectively.

Quantification of chemical shifts due to $Na_v1.2_{IQp}$ or Ca^{2+} addition

To determine the change in chemical shift upon $Na_v1.2_{IQp}$ binding to apo CaM_{76-148}, or Ca^{2+} binding to apo CaM_{1-148}, chemical-shift changes in both the ^1H and ^{15}N dimensions were quantified using the modified Pythagorean theorem shown in **Equation 4.2**, as described previously (Jaren et al., 2002).

$$\Delta ppm = \sqrt{(\Delta^1 Hppm)^2 + (0.10134 \bullet \Delta^{15} Nppm)^2} \quad (4.2)$$

In this equation, Δppm refers to the linear change of a specific resonance peak from its initial starting position in the reference spectrum.

NaCl Titration of apo CaM-$Na_v1.2_{IQp}$ Complex

Fluorescence anisotropy was used to examine the [NaCl] dependence of $Na_v1.2_{IQp}$ binding to either apo CaM_{76-148} or apo CaM_{1-148}. A Fluorolog 3 (Jobin Yvon, Horiba) spectrofluorimeter, equipped with dual auto-assembly Glan-Thompson polarizers was used to monitor the anisotropy change of a fluorescein-labeled $Na_v1.2_{IQp}$ in 50mM HEPES, 1mM $MgCl_2$, 5mM NTA, 50μM EGTA, pH 7.4 as it was titrated at 25 °C to a 1:1.2 ratio of $Na_v1.2_{IQp}$ to either apo CaM_{76-148} or apo CaM_{1-148}. The complex was then titrated with 50mM HEPES, 5M NaCl, 1mM $MgCl_2$, 5mM NTA, 50μM EGTA, pH 7.4. The anisotropy of fluorescein-labeled $Na_v1.2_{IQp}$ was monitored using λ_{ex} 498 nm and λ_{em} 520 nm with 2 nm excitation and 10 nm emission bandpasses. Anisotropy (r) was calculated as shown in **Equation 4.3**, described previously (Akyol et al., 2004)

$$r = \frac{I_{VV} - G \bullet I_{VH}}{I_{VV} + 2G \bullet I_{VH}} \quad (4.3)$$

where I_{VV} and I_{VH} are the intensities of vertically or horizontally emitted light upon vertical excitation respectively, and G is the instrument correction factor ($G = I_{HV} / I_{HH}$).

Results

The C-domain of apo $CaM_{1\text{-}148}$ is Necessary and Sufficient to Bind $Na_v1.2_{IQp}$

Previous studies showed that both $CaM_{1\text{-}148}$ and a C-domain fragment ($CaM_{76\text{-}148}$) exhibit tight, calcium-independent binding to $Na_V1.2_{IQp}$ ($K_d \leq 10$ nM), whereas an N-domain fragment of CaM ($CaM_{1\text{-}80}$) binds weakly ($K_d \sim 1$ mM), regardless of calcium concentration (Theoharis et al., 2008). To understand the structural differences at interfaces responsible for these affinities, ^{15}N-HSQC spectra were collected of apo $CaM_{1\text{-}148}$ ± $Na_v1.2_{IQp}$ for comparison to spectra of apo $CaM_{1\text{-}80}$ and apo $CaM_{76\text{-}148}$:$Na_v1.2_{IQp}$ complex. When spectra of apo CaM ± $Na_v1.2_{IQp}$ were overlaid (**Figure 4.2a**), many of the observed peaks for the apo $CaM_{1\text{-}148}$:$Na_v1.2_{IQp}$ complex were shifted relative to apo $CaM_{1\text{-}148}$ alone. Analyzing spectral overlap indicated that the chemical environment of the amide groups of the C-domain were all perturbed upon $Na_v1.2_{IQp}$ addition, while those of the N-domain of apo $CaM_{1\text{-}148}$ were unperturbed by the peptide.

When spectra of the apo $CaM_{76\text{-}148}$:$Na_v1.2_{IQp}$ complex (**Figure 4.2b**) or apo $CaM_{1\text{-}80}$ (**Figure 4.2c**) were compared to the spectrum of apo $CaM_{1\text{-}148}$ bound to $Na_v1.2_{IQp}$, it was seen that the spectra were additive. Nearly all of the peaks in the samples of apo $CaM_{76\text{-}148}$:$Na_v1.2_{IQp}$ and apo $CaM_{1\text{-}80}$ alone overlaid upon the full set of those observed for the apo $CaM_{1\text{-}148}$:$Na_v1.2_{IQp}$ complex. These results indicated that the interaction of apo $CaM_{1\text{-}148}$ with $Na_v1.2_{IQp}$ was mediated solely via the C-domain because the spectrum of apo $CaM_{1\text{-}148}$:$Na_v1.2_{IQp}$ complex could be reproduced by combining the spectra of apo $CaM_{1\text{-}80}$ and apo $CaM_{76\text{-}148}$:$Na_v1.2_{IQp}$ complex as seen in **Figure 4.2d**.

Previous studies of $Na_v1.2_{IQp}$ binding to CaM showed similar affinities for apo $CaM_{76\text{-}148}$ or apo $CaM_{1\text{-}148}$ indicating that the interaction of $Na_v1.2_{IQp}$ with apo CaM is mediated solely by the C-domain. These previous data, coupled with the new residue-specific observation that the N-domain of apo $CaM_{1\text{-}148}$ was unperturbed by $Na_v1.2_{IQp}$ binding prompted using NMR to determine the structure of apo $CaM_{76\text{-}148}$ bound to $Na_v1.2_{IQp}$. Relative to using full-length CaM this complex reduced spectral complexity while still capturing the complete high-affinity binding interface that would exist in the apo $CaM_{1\text{-}148}$:$Na_v1.2_{IQp}$ complex.

Comparison and quantification of ^{15}N-HSQC spectra of apo $CaM_{76\text{-}148} \pm Na_v1.2_{IQp}$ indicated significant perturbation (average Δppm for all residues was 0.51) upon addition of $Na_V1.2_{IQp}$ (**Figure 4.3a and 4.3b**). It is of interest to point out that that $Na_v1.2_{IQp}$ addition dramatically increased dispersion of ^{15}N-HSQC peaks (**Figure 4.3a**) by breaking the symmetry of similar chemical environments of homologous residues in the paired EF-hands of apo $CaM_{76\text{-}148}$. Mapping of chemical shift perturbations upon the structure of apo $CaM_{76\text{-}148}$ bound to $Na_v1.2_{IQ}$ indicated that the highest chemical shift perturbation (average Δppm of 1.47) was located in the loop region (residues 108-117) between helices F and G which is in close proximity to the Gln (Q) of the IQ-motif (**Figure 4.3c**).

Hydrogen/Deuterium Backbone Amide Exchange

Analysis of hydrogen/deuterium (H-D) backbone amide exchange of the apo $CaM_{76\text{-}148}$:$Na_v1.2_{IQp}$ complex was performed to observe the location of persistent hydrogen bonds. These were used as structural restraints, and were analyzed to determine apparent amide exchange rates that correlate with protein packing and flexibility. A total of 30 amide resonances were detected ~30 minutes after addition to D_2O to a lyophilized sample of the apo $CaM_{76\text{-}148}$:$Na_v1.2_{IQp}$ complex. Their identities were included as hydrogen bonding restraints for structure calculations. Apparent amide exchange rates (listed in **Table 4.1**) were calculated from peak decays such as those

shown in **Figure 4.4a,** fit to a mono-exponential decay (Eq. 1, **Figure 4.4b)** and mapped onto the structure of the apo $CaM_{76\text{-}148}$:$Na_v1.2_{IQp}$ complex (**Figure 4.4c**). The residues with observable exchange rates indicate persistent secondary structure elements. These locations in combination with residue-specific dihedral angles calculated via TALOS (Cornilescu et al., 1999b; Shen et al., 2009a) from backbone chemical shifts were consistent with the pattern of secondary structure elements found in a 4-helix bundle with two anti-parallel β-sheets.

Determination of apo $CaM_{76\text{-}148}$:$Na_v1.2_{IQp}$ Structure

The structural statistics of the final apo $CaM_{76\text{-}148}$:$Na_v1.2_{IQp}$ complex structure are presented in **Table 4.2**. Favorable linewidths and dispersion exhibited in the NMR spectra greatly facilitated chemical shift assignment and NOE analysis as compared to analysis of CaM alone. Nearly complete ^{1}H, ^{13}C, and ^{15}N resonance assignments were obtained for apo $CaM_{76\text{-}148}$ when bound to $Na_v1.2_{IQp}$. This structure was determined based on 1974 unambiguous restraints comprised of 457 intra-residue, 298 short (+1), 300 medium (2-4), 331 long (5+), 245 intra-peptide,188 intermolecular, 46 hydrogen bonds, and 109 dihedral angles. The distribution of restraints was in agreement with the occurrences of residues in a secondary structure element, where a higher number of restraints were observed in α-helical and β-sheet regions than in the loop regions that contain Ca^{2+}-binding sites III and IV. **Figure 4.5a** presents a superposition of the family of 20 lowest energy structures of $Na_v1.2_{IQp}$ bound to apo $CaM_{76\text{-}148}$ that best satisfied the experimental restraints. The interhelical angles as calculated by UCSF Chimera (Pettersen et al., 2004) between helices E-F and G-H of these structures were 77.4° ± 1.7 and 78.0° ± 2.3 respectively.

The structure of the apo $CaM_{76\text{-}148}$:$Na_v1.2_{IQp}$ complex was well defined, as reflected by the low value of the ensemble RMSD (0.65 ± 0.06 Å) and is of good quality, as indicated by the Ramachandran statistics and energetic terms listed in **Table 4.2**.

Frayed termini were observed at the N- and C-termini of apo $CaM_{76\text{-}148}$ and $Na_v1.2_{IQp}$ in **Figure 4.5a**. This was attributed to the absence of observable NOEs for these residues, and lack of assignments for peptide residues 1901-1903, 1922-1923, and 1926-1927.

Interaction Interface of $Na_v1.2_{IQp}$ with apo $CaM_{76\text{-}148}$

The hydrophobic interface between apo $CaM_{76\text{-}148}$ and $Na_v1.2_{IQp}$ was well defined as judged by the positions of interacting residues shown in **Figure 4.5b.** The change in solvent accessible hydrophobic surface between apo $CaM_{76\text{-}148}$ and $Na_v1.2_{IQp}$ was calculated using GETAREA (Fraczkiewicz and Braun, 1998). Upon binding the peptide, 1393 $Å^2$ (751 $Å^2$ $Na_v1.2_{IQp}$, 642 $Å^2$ apo $CaM_{76\text{-}148}$) of solvent accessible hydrophobic surface area was buried. In apo $CaM_{76\text{-}148}$, a subset of hydrophobic residues that consisted of A88, V91, F92, L112 and M145 accounted for 43% of the buried surface, while in $Na_v1.2_{IQp,}$ hydrophobic residues V1911, I1912, Y1916, Y1919, and L1920 accounted for 53.5% of the buried surface area.

In addition to hydrophobic interactions, favorable electrostatic interactions were observed between apo $CaM_{76\text{-}148}$ and $Na_v1.2_{IQp.}$ Shown in **Figure 4.5c** are the electrostatic surface potentials calculated by APBS (Baker et al., 2001) for coordinates of apo $CaM_{76\text{-}148}$ and $Na_v1.2_{IQp}$ corresponding to their conformation in the complex. Examination of the electrostatic potentials of solvent-accessible regions clearly showed that charge complementarity is present between the negatively charged apo $CaM_{76\text{-}148}$ and the positively charged $Na_v1.2_{IQp}$.

All contacts between apo $CaM_{76\text{-}148}$ and $Na_v1.2_{IQp}$ that were within 4.5 Å were tabulated using the program *Contacts of Structural Units (CSU)* (Sobolev et al., 1999) and are shown in **Figure 4.6a**. The interactions of the IQ residues (I1912 and Q1913) with apo $CaM_{76\text{-}148}$ were of special interest due to their highly conserved nature in IQ-motifs as shown in **Figure 4.1a** and could be investigated on the basis of numerous NOEs such as those shown in **Figure 4.6b** and **4.6c**. As indicated in the CSU analysis and

displayed in **Figure 4.6d**, I1912 inserted directly into the shallow hydrophobic pocket of apo $CaM_{76\text{-}148}$. As shown in **Figure 4.6e,** Q1913 is positioned to form hydrogen bonds with backbone atoms of residues L112 and E114 that are in the loop connecting helices F and G of apo $CaM_{76\text{-}148}$. A comparison of CaM sequences in 102 eukaryotic species (Ataman et al, Supplementary Table 1) showed that residue E114 and its preceding residue, G113, were identical in all species; while L112 was highly conserved (found in 91 of 102 sequences).

Effect of Ca^{2+} upon apo $CaM_{1\text{-}148}$:$Na_v1.2_{IQp}$ Complex

^{15}N-HSQC NMR spectroscopy was used to examine whether apo $CaM_{1\text{-}148}$ bound to $Na_v1.2_{IQp}$ undergoes a structural transition as a result of Ca^{2+} binding. Shown in **Figure 4.7a** are spectral overlays of apo $CaM_{1\text{-}148}$ (red) and $(Ca^{2+})_4$-$CaM_{1\text{-}148}$ (black). Comparison of these indicated a significant change in the chemical environment of apo $CaM_{1\text{-}148}$ resonances within the apo $CaM_{1\text{-}148}$:$Na_v1.2_{IQp}$ complex upon Ca^{2+} addition. To determine whether the chemical shifts observed upon Ca^{2+} addition to the apo $CaM_{1\text{-}148}$:$Na_v1.2_{IQp}$ complex are due to Ca^{2+} induced release of $Na_v1.2_{IQp}$, the spectrum of free $(Ca^{2+})_4$-$CaM_{1\text{-}148}$ was compared to the spectrum of the $(Ca^{2+})_4$-$CaM_{1\text{-}148}$:$Na_v1.2_{IQp}$ complex (**Figure 4.7a**). Lack of spectral overlap in **Figure 4.7a** indicated that both apo $CaM_{1\text{-}148}$ and $(Ca^{2+})_4$-$CaM_{1\text{-}148}$ were bound to $Na_v1.2_{IQ}$, but that their structures were significantly different.

Shown in **Figures 4.7b, 4.7c, and 4.7d** are plots showing the HSQC signal for selected resonances of the N- and C-domain of apo $CaM_{1\text{-}148}$ when bound to $Na_v1.2_{IQp}$ at successively higher levels of calcium during a titration. Shown in **Figure 4.7b** are residues of the N-domain of apo $CaM_{1\text{-}148}$ that were uniformly in fast-exchange over the course of the calcium titration. The normalized change in chemical shift plotted against the equivalents of calcium added indicated that most residues within the N-domain titrated fully between 0 and 2 Ca^{2+} equivalents.

Observation of changes in position and intensity of C-domain peaks during the calcium titration (**Figure 4.7c**) revealed that they were in intermediate or slow exchange. For those, calcium-dependent change in intensities of peaks were used to determine their relative populations over the course of the titration. For apo $CaM_{1\text{-}148}$ bound to $Na_v1.2_{IQp}$, peaks corresponding to the C-domain of the apo state broadened beyond the limit of detection after addition of 2 Ca^{2+} equivalents (**Figure 4.7c).** Although amide backbone assignments for the C-domain of $(Ca^{2+})_4$-$CaM_{1\text{-}148}$ bound to $Na_v1.2_{IQp}$ are unknown, peaks that appeared at the midpoint of the Ca^{2+} titration are likely to correspond to residues located within the C-domain of $(Ca^{2+})_4$-$CaM_{1\text{-}148}$. When the intensities of these peaks were plotted against the ratio of $[Ca^{2+}]/[CaM_{1\text{-}148}{:}Na_v1.2_{IQp}]$, increases in peak intensity were observed at higher calcium stoichiometries than were chemical shift changes. These data indicated that when bound to $Na_v1.2_{IQp}$ the N- and C-domains of $CaM_{1\text{-}148}$ bind 2 Ca^{2+} per domain, where the N-domain has a slightly more favorable Ca^{2+}-binding affinity than the C-domain, consistent with species population simulations conducted previously (Theoharis et al., 2008).

Effect of Ca^{2+} upon Molecular Size of $CaM_{1\text{-}148}$:$Na_v1.2_{IQp}$ Complex

To examine whether Ca^{2+} binding causes the N-domain of the $(Ca^{2+})_4$-$CaM_{1\text{-}148}$ to collapse onto $Na_v1.2_{IQp}$ forming a compact ellipsoidal structure, $CaCl_2$ was titrated into a solution of preformed apo $CaM_{1\text{-}148}$:$Na_v1.2$ complex and monitored with fluorescence anisotropy. As shown in **Figure 4.8a**, apo $CaM_{1\text{-}148}$ bound to the fluoresceinated $Na_v1.2_{IQp}$ stoichiometrically at a 1:1 ratio. Following complex formation, the apo CaM-IQ complex was titrated with 10 mM $CaCl_2$ in matching buffer (**Figure 4.8a**). No significant decrease in fluorescence anisotropy was observed, indicating that $(Ca^{2+})_4$-$CaM_{1\text{-}148}$ maintains the hydrodynamic behavior of apo $CaM_{1\text{-}148}$ bound to fl-$Na_v1.2_{IQp}$.

This suggested that $(Ca^{2+})_4$-CaM does not adopt a compact ellipsoidal structure when bound to $Na_v1.2_{IQp}$ on the basis of raw anisotropy.

Effect of Na^+ upon $Na_v1.2_{IQp}$ Binding to CaM

$Na_v1.2$ and other proteins in the plasma membrane experience a large fluctuation in Na^+ ion concentration during $Na_v1.2$ gating. Thus, it was of interest to determine whether NaCl affected the affinity of $Na_v1.2_{IQp}$ for apo or calcium-saturated CaM. Shown in **Figure 4.8b** are NaCl titrations of complexes of $Na_v1.2_{IQp}$ binding apo CaM_{76-148} or apo CaM_{1-148} as monitored by fluorescence anisotropy to examine the NaCl dependence of $Na_v1.2_{IQp}$ dissociation. Both apo CaM_{76-148} and apo CaM_{1-148} bound to the fluoresceinated $Na_v1.2_{IQp}$ stoichiometrically at a 1:1 ratio. Saturation of $Na_v1.2_{IQp}$ was ensured by the addition of a slight excess of either apo CaM_{76-148} or apo CaM_{1-148}, then the complex was titrated with NaCl in matching buffer to cover a range from 0 to 650 mM NaCl (**Figure 4.8b**). This NaCl range was used in attempt to dissociate apo CaM from $Na_v1.2_{IQp}$, but proved unsuccessful as the cuvette volume limited the amount of NaCl solution that could be added resulting in 650 mM being the maximum NaCl examined. In NaCl titrations of complexes of $Na_v1.2_{IQp}$ bound to apo CaM_{76-148} and apo CaM_{1-148}, the anisotropy of $Na_v1.2_{IQp}$ was unchanged by NaCl, which indicated a negligible effect on $Na_v1.2_{IQp}$ dissociation from CaM at the final concentration of peptide and protein.

Discussion

The voltage-dependent sodium channel $Na_v1.2$ contains a CaM-binding IQ-motif that is required for proper regulation of its physiological function. The high-resolution solution structure of apo CaM_{76-148} bound to $Na_v1.2_{IQps}$ presented here demonstrates that apo CaM_{76-148} adopts a "semi-open" conformation when bound to $Na_v1.2_{IQp}$, and that it binds such that the F-G loop interacts directly with the glutamine residue of the IQ motif. The structure of this apo CaM_{76-148}:$Na_v1.2_{IQp}$ complex provides a foundation for studying

other isoforms of voltage-dependent ion channels that interact preferentially with the C-domain of apo CaM.

A "semi-open" apo C-domain Binds $Na_v1.2_{IQp}$.

Shown in **Figure 4.9a** are superpositions of the backbone of (a) apo CaM_{76-148} bound to $Na_v1.2_{IQp}$ determined in this study (b) the C-domains of two apo CaM_{1-148} molecules bound to two neighboring IQ-motifs found in myosin V (2IX7.pdb), (c) apo CaM-like proteins bound to IQ-motifs of MYO2P (1M46.pdb, 1M45.pdb, and 1N2D.pdb) and (d) ELC bound to myosin heavy chain. A feature common to all of these structures is that each set of paired EF-hands of the C-domain adopts a "semi-open" conformation when bound to its respective IQ-motif. Another feature common to all structures shown in **Figure 4.9a** is that residues located at positions "0" and "1" (defined in **Figure 4.1a**) of the IQ-motif interact with a similar subset of residues in the apo C-domain. These conserved structural features are also reflected in the sequence conservation of the IQ-motif at these positions **Figure 4.1a**.

At position "0" we observed that a hydrophobic residue (often a branched chain) is necessary to insert into the exposed hydrophobic core of the "semi-open" C-domain, burying what would otherwise be solvent exposed hydrophobic surface. The absolute conservation of Gln at position "1" of canonical IQ-motifs is reflected by hydrogen bonding interactions made between the carboxamide of Gln at position "1" and the backbone of residues found within the loop connecting helices F and G as shown in **Figure 4.6e**. Formation of this hydrogen bonding network between Gln at position "1" and the backbone of the loop residues account for the large amide chemical shift at this position observed in the ^{15}N-HSQC spectrum shown in **Figure 4.3a, 4.3b, and 4.3c**.

A "Semi-open" apo C-domain is used to Bind a Non IQ-motif Containing Target

There is an example of 1 apo C-domain bound to a peptide that does not have an IQ-motif in the structure of partially Ca^{2+}-saturated CaM bound to a peptide derived from the small conductance potassium channel (SK-Channel) (Schumacher et al., 2001). When $Na_v1.2_{IQp}$ bound apo $CaM_{76\text{-}148}$, and the apo C-domain of CaM bound to the SK-channel peptide (SK_p) were overlaid (**Figure 4.9b**), both adopt "semi-open" domain conformations. This structural similarity indicates that an IQ-motif is sufficient but not necessary to induce a "semi-open" apo C-domain conformation. Additionally the structural similarity in **Figure 4.9b,** suggests that a "semi-open" C-domain conformation is not exclusive to IQ-motifs alone but quite possibly all motifs that bind to the C-domain of apo CaM.

Although the SK-Channel does not contain an IQ-motif, it shares key features seen in IQ-motif bound structures of apo CaM, CaM-like proteins, and ELC. **Figures 4.9a,** and **4.9b**, show that a carboxamide-containing side chain of Gln (IQ-motif) or Asn (SK_p) are required to form a hydrogen bond with the backbone of loop residues located between the F and G helices of CaM. This conserved hydrogen-bonding network between the side chain carboxamide and loop backbone of CaM helps to determine the α-helical register of the IQ-motif or SK_p relative to the apo C-domain.

The similarity in α-helical register between the IQ-motif and SK_p was also apparent in a conserved hydrophobic interaction between either I1912 ($Na_v1.2_{IQp}$) or L428 (SK_p) and the core of the apo C-domain (**Fig 4.9b**). Due to the polarity of the N- and C-terminus of their respective motifs, I1912 or L428 differ in primary sequence position relative to the highly conserved carboxamide side chain used to hydrogen bond to the backbone of residues L112 and E114 of CaM (**Figure 4.9b**). For ease in describing the reversal in polarity between $Na_v1.2_{IQp}$ and SK_p relative to the C-domain, we have termed the interactions of $Na_v1.2_{IQp}$ and SK_p with apo $CaM_{76\text{-}148}$ as ${}_NF\text{-}G_C$ and

$_{C}$F-G$_{N}$ respectively. These terms result from positioning the 4-helix bundle of the C-domain as depicted in **Figure 4.9c**, where dependent upon polarity of the peptide N- and C-terminus relative to helices F and G of CaM either a $_{N}$F-G$_{C}$ or $_{C}$F-G$_{N}$ orientation is adopted.

When an $_{N}$F-G$_{C}$ orientation is adopted, as in the interaction of apo CaM with $Na_v1.2_{IQp}$, the conserved hydrophobic residue (I1912) that inserts in the core of apo $CaM_{76\text{-}148}$ precedes the conserved carboxamide-containing residue (Q1913). However if the peptide polarity is reversed as seen the $_{C}$F-G$_{N}$ orientation of SK_p relative to the C-domain of apo-CaM, the residue homologous to I1912 of $Na_v1.2_{IQp}$, (L428) is located 2 amino acids away on the C-terminal side of the carboxamide-containing residue (N426).

Canonical IQ-motifs Bind to apo CaM using Similar Orientations

Shown in **Figure 4.10** are structures of apo and $(Ca^{2+})_4$-CaM bound to IQ-motif containing peptides derived from various targets, where the directionality of the target interaction with CaM is depicted with right or left arrows respectively. Depicted in **Figure 4.9a,** are conserved interactions made by all apo CaM or apo CaM-like proteins when bound to IQ-motifs. These conserved features consist of a hydrophobic interaction at IQ-motif position "0" of the peptide contacting the core of CaM as well as the hydrogen bond network between the ultra-conserved Gln residue at position "1" and CaM loop residues L112 and E114 or their CaM-like protein equivalent. If these conserved interactions are maintained throughout all canonical apo CaM binding motifs then all canonical IQ-motifs must bind to the C-domain of apo CaM in a $_{N}$F-G$_{C}$ orientation.

Examination of the binding orientation of $(Ca^{2+})_4$-CaM bound to IQ-motif containing structures is less clear as structures of $(Ca^{2+})_4$-CaM bound to the IQ-motifs of $Ca_v2.1$ and 2.3 differ as to the peptide orientation relative to $(Ca^{2+})_4$-CaM (**Figure 4.10**) . $Ca_v2.1$ and 2.3 peptides of differing length as well as different crystallization conditions

were used to obtain these structures which may account for this discrepancy (Fallon et al., 2009; Fallon et al., 2005; Halling et al., 2009; Houdusse et al., 2006; Kim et al., 2008; Mori et al., 2008; van Petegem et al., 2005). We propose apo and $(Ca^{2+})_4$-CaM bind to $Na_v1.2_{IQp}$ and canonical IQ-motifs where a Gln is located at position "1" in a $_NF$-G_C orientation. The alternative would require CaM to release from its anti-parallel orientation to the IQ-motif upon Ca^{2+} influx, and reorient itself into a parallel arrangement for binding to occur.

Role of the N-domain of CaM_{1-148} in $Na_v1.2$ Regulation

^{15}N-HSQC and fluorescence anisotropy monitored Ca^{2+} titration studies shown in **Figures 4.7a** and **4.8a**, indicated that the N-domain of both apo and $(Ca^{2+})_4$-CaM_{1-148} do not interact with $Na_v1.2_{IQp}$. These observations are consistent with previous studies that indicated that a region consisting of residues 1913-1938 in $Na_v1.2$ contains a second CaM-binding BAA-motif ($Na_v1.2_{BAA}$) (Mori et al., 2003; Mori et al., 2000). Based on results presented here, we propose the model presented in **Figure 4.9d**.

In this model, only the "semi-open" C-domain of apo CaM interacts with the IQ-motif of $Na_v1.2$, while under Ca^{2+}-saturating conditions both CaM N- and C-domains adopt "open" conformations when they bind to the BAA and IQ-motifs of $Na_v1.2$ respectively. This model is supported by observations in **Figure 4.2** where only the C-domain CaM_{1-148} is perturbed upon $Na_v1.2_{IQp}$ addition, while **Figure 4.3** shows that the apo C-domain adopts a "semi-open" conformation when bound to $Na_v1.2_{IQp}$. Support for the proposed $(Ca^{2+})_4$-CaM_{1-148} interactions with $Na_v1.2$ are drawn from **Figure 4.7** which indicated CaM_{1-148} binds 4 Ca^{2+} ions and **Figure 4.8a**, which showed that the N-domain of $(Ca^{2+})_4$-CaM_{1-148} does not interact with $Na_v1.2_{IQp}$ by collapsing upon it after Ca^{2+} addition. These observations coupled with studies by Mori et al. (Mori et al., 2003) which showed that $(Ca^{2+})_4$-CaM_{1-148} bound to both $Na_v1.2_{IQp}$ and $Na_v1.2_{BAA}$, while only

apo $CaM_{1\text{-}148}$ bound to $Na_v1.2_{IQp}$ provide strong evidence for the model proposed in **Figure 4.9d .**

Future studies will focus on uncovering the mechanistic role that CaM plays in $Na_v1.2$ regulation under Ca^{2+}-saturating conditions as well as determination of structures of larger intracellular regions of $Na_v1.2$ in complex with CaM. To accomplish these goals, studies to establish the location of the N-domain binding site within $Na_v1.2$, coupled with structure determination of $(Ca^{2+})_4$-CaM in complex with a peptide that contains both the N-domain binding site and $Na_v1.2_{IQp}$ are proposed.

Table 4.1:Apparent amide exchange rates of apo $CaM_{76\text{-}148}$ when bound to $Na_v1.2_{IQp}$

Residue	Rate*	Error*
86	69.1	0.9
87	138.9	1.5
88	162.9	1.7
89	180.6	2.4
90	122.9	1.1
91	16.7	0.3
92	185.6	2.0
93	43.8	0.8
99	85.6	0.9
100	382.6	5.5
103	247.4	26.2
105	3.6	0.5
106	30.9	0.4
108	70.7	1.1
109	125.1	2.4
110	17.9	0.4
111	141.4	7.8
112	20.2	0.4
116	15.1	0.4
117	21.0	0.8
118	92.1	6.3
120	25.9	0.4
121	243.7	3.1
122	233.0	2.4
123	57.4	1.0
124	384.2	7.1
125	965.9	36.0
126	128.7	2.9
136	34.2	1.0
138	54.9	1.6
139	6.4	0.2
140	17.7	0.2
142	1223.6	46.4
143	408.3	6.6
144	139.0	1.6
145	126.9	1.5
146	69.6	1.0

*Values reported in minutes

Table 4.2:Structural statistics and root-mean-square deviation for 20 structures of apo $CaM_{76\text{-}148}$:$Na_v1.2_{IQp}$ complex

Structural statistics[a]	<SA>	$<SA>_r$
Rmsd from experimental distance restraints (Å)[b]		
All (1865)	0.008 ± 0.001	0.007
CaM intra-residue (457)	0.007 ± 0.002	0.005
CaM sequential (298)	0.005 ± 0.004	0.003
CaM medium range (300)	0.009 ± 0.002	0.008
CaM long range (331)	0.006 ± 0.001	0.005
Intra-peptide (245)	0.005 ± 0.002	0.003
CaM-peptide intermolecular (188)	0.012 ± 0.002	0.011
hydrogen bond (46)	0.016 ± 0.001	0.021
Rmsd from experimental torsional angle restraints (deg)[c]		
ϕ and ψ angles (109)	0.3 ± 0.03	0.2
CNS potential energies (kcal mol^{-1})		
E_{tot}	89 ± 4.8	80
E_{bond}	5 ± 0.5	1
E_{ang}	65 ± 2.9	62
E_{imp}	5 ± 0.6	4
E_{repel}	6 ± 1.2	6
E_{noe}	6 ± 1.2	5
E_{cdih}	1 ± 0.1	1
Cartesian coordinate rmsd (Å)	N, C_a, and C’	all heavy
<SA> vs. <SA> [d]	0.31 ± 0.05	0.95 ± 0.11

[a]Where <SA> is the ensemble of 20 NMR-derived solution structures of CaM/peptide; $<SA>$ is the mean atomic structure; $<SA>_r$ is the energy-minimized average structure. The CNS F_{repel} function was used to simulate van der Waals interactions using a force constant of 4.0 kcal mol^{-1} $Å^{-4}$ with the atomic radii set to 0.8 times their CHARMM values (Brooks et al., 1983)(Brooks, Bruccoleri et al. 1983)

[b]Distance restraints were employed with a square-well potential (F_{noe} = 50 kcal mol^{-1} $Å^{-2}$). Hydrogen bonds were given bounds of 1.8-2.4 Å (H-O) and 2.7-3.3 Å (N-O). No distance restraint was violated by more than 0.3 Å in any of the final structures.

[c]Torsional restraints were applied with values derived from an analysis of the C’, N, C_a, H_a, and C_b chemical shifts using the TALOS program. Force constant of 200 kcal mol^{-1} rad^{-2} was applied for all torsional restraints.

[d]Rmsd for CaM protein residues 80-128 and 134-146 and peptide residues 1905-1920.

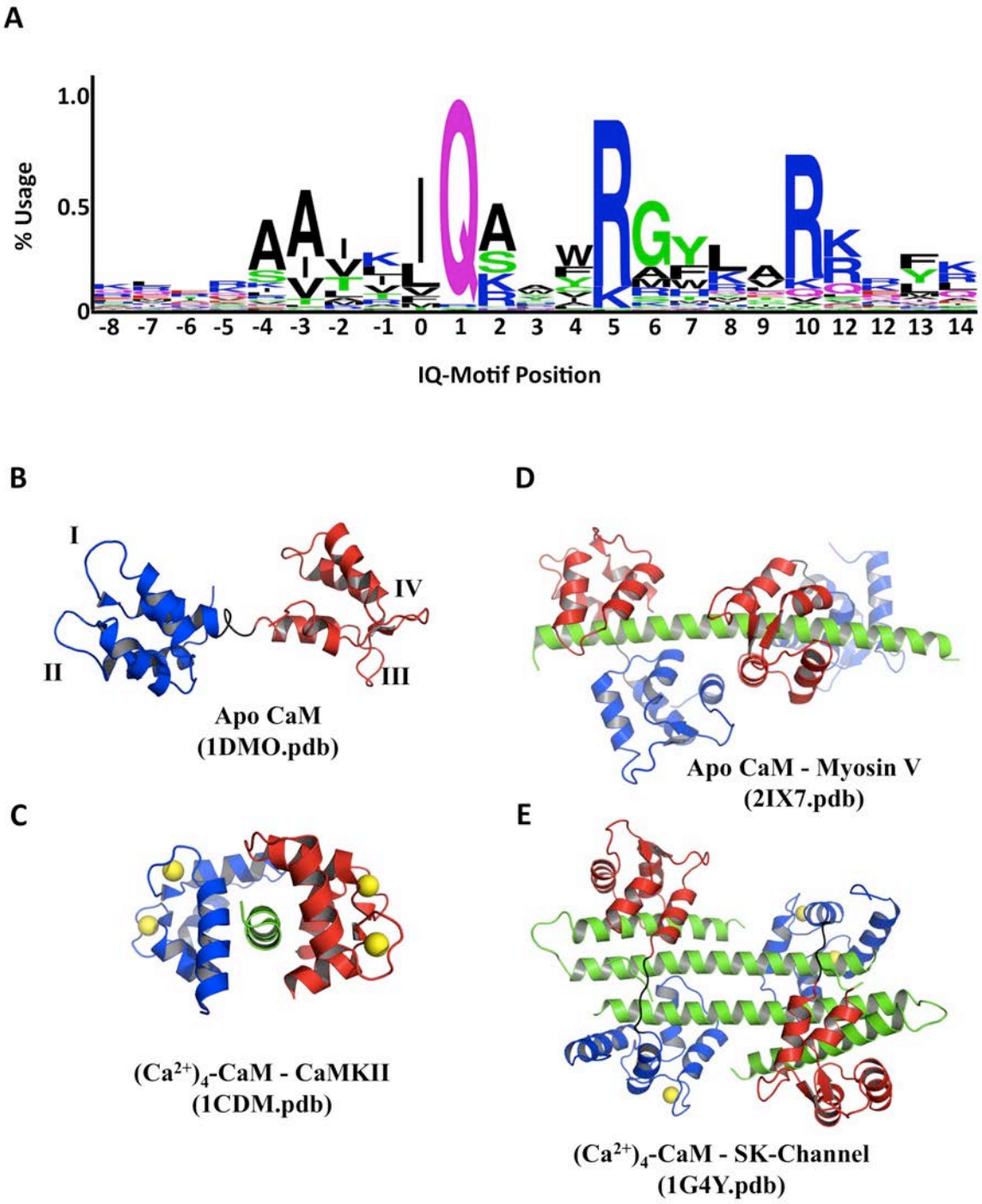

Figure 4.1: CaM and target interaction background
A: Consensus sequence of 208 canonical IQ-motifs derived from 108 proteins of the human genome. **B-C**: Structures of CaM (residues 1-75 blue, 76-80 black, 81-148 red) in the absence and presence of peptide targets (green, Ca^{2+} yellow spheres).
/Users/nmr_mike/Thesis/Chapter_IV/Figure4_1.jpg

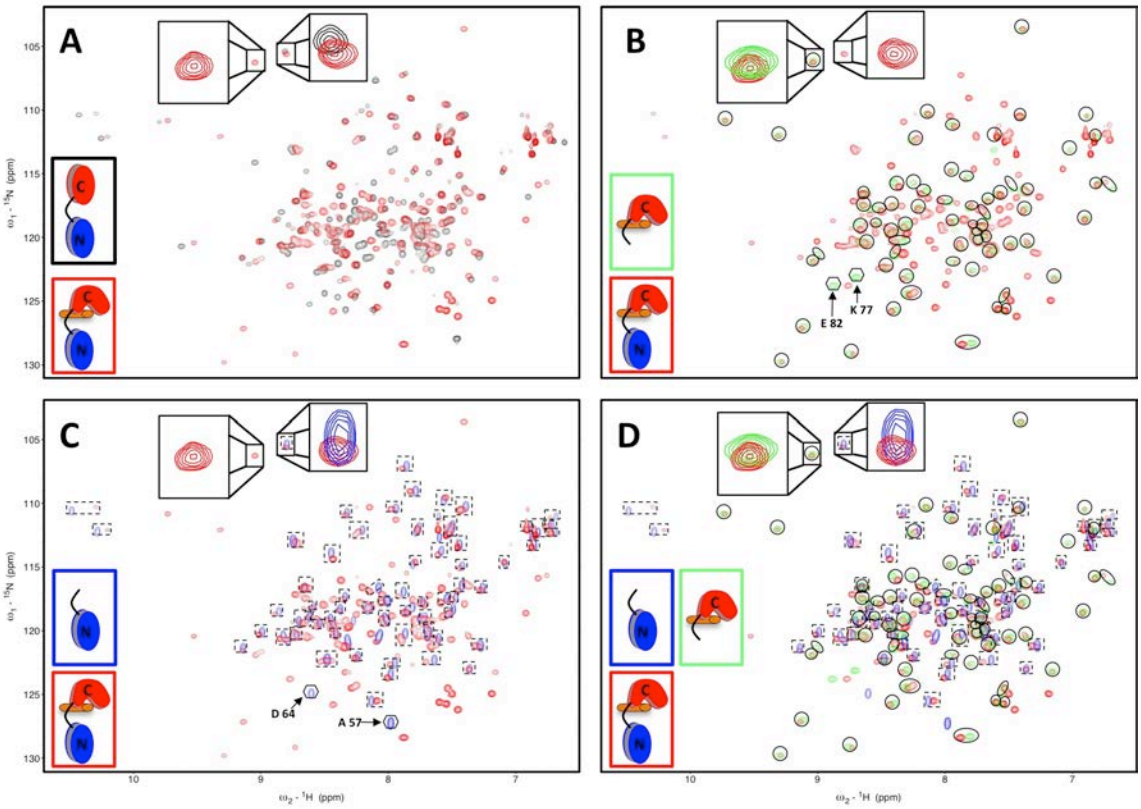

Figure 4.2: ^{15}N-HSQC Spectra of apo CaM_{76-148} and apo CaM_{1-148} bound to $Na_v1.2_{IQp}$ **A:** Overlaid ^{15}N-HSQC spectra of apo CaM_{1-148} alone (black) and apo CaM_{1-148} bound to $Na_v1.2_{IQp}$ (red). **B:** Overlaid ^{15}N-HSQC spectra of apo CaM_{76-148} (green) and apo CaM_{1-148} when bound to $Na_v1.2_{IQp}$. Overlapping resonances are indicated in solid circles, while non-overlapping residues of apo CaM_{76-148} bound $Na_v1.2_{IQp}$ are indicated by solid hexagons. **C:** Overlaid ^{15}N-HSQC spectra of apo CaM_{1-80} (blue) and apo CaM_{1-148} bound to $Na_v1.2_{IQp}$ (red). Overlapping resonances are indicated by dashed squares, while non-overlapping apo CaM_{1-80} resonances are indicated by solid hexagons. **D:** Overlaid ^{15}N-HSQC spectra of apo CaM_{1-80} (blue), apo CaM_{76-148} bound to $Na_v1.2_{IQp}$ (green), and apo CaM_{1-148} bound to $Na_v1.2_{IQp}$ bound to $Na_v1.2_{IQp}$. Resonances of apo CaM_{1-80} which overlap with those of apo CaM_{1-148} bound to $Na_v1.2_{IQp}$ are shown in dashed squares, while resonances of apo CaM_{76-148} bound to $Na_v1.2_{IQp}$ that overlay onto apo CaM_{1-148} bound to $Na_v1.2_{IQp}$ are shown in solid circles.
Users/nmr_mike/Thesis/Chapter_IV/Figure4_2.jpg

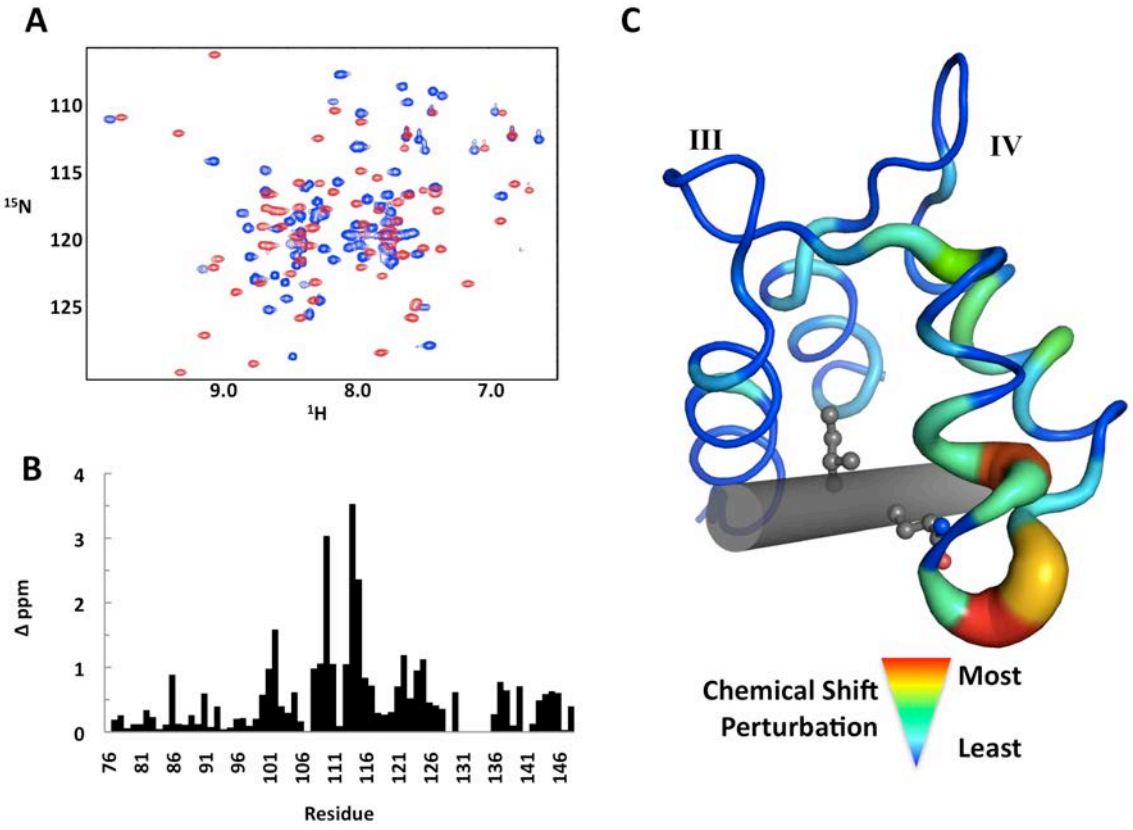

Figure 4.3: $Na_v1.2_{IQp}$ binding to apo $CaM_{76\text{-}148}$ quantified by ^{15}N-HSQC spectroscopy **A:** Overlaid ^{15}N-HSQC spectra of apo $CaM_{76\text{-}148}$ (blue) and apo $CaM_{76\text{-}148}$ bound to $Na_v1.2_{IQp}$ (red). **B:** Quantified apo $CaM_{76\text{-}148}$ amide proton chemical shifts upon $Na_v1.2_{IQp}$ addition. **C:** Magnitude of $Na_v1.2_{IQp}$ induced chemical shift mapped to the structure of apo $CaM_{76\text{-}148}$ bound to $Na_v1.2_{IQp}$ (gray rod) with I and Q residues of the IQ-motif shown in ball and stick.
Users/nmr_mike/Thesis/Chapter_IV/Figure4_3.jpg

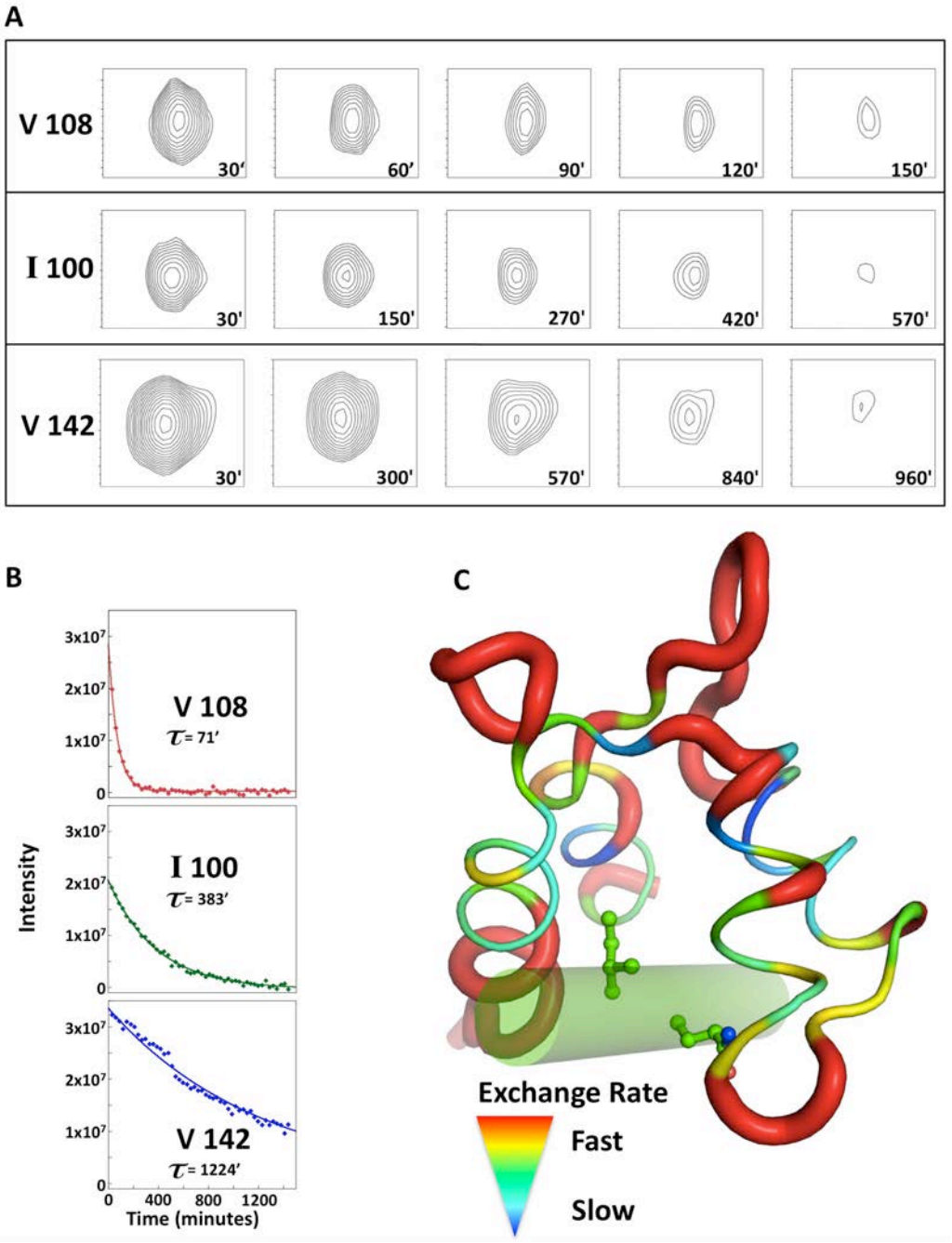

Figure 4.4: ^{15}N-HSQC-monitored amide exchange of apo $CaM_{76\text{-}148}$:$Na_v1.2_{IQp}$ complex **A**: ^{15}N-HSQC monitored amide exchange series of select residues peak intensities as a function of exchange time corresponding to different exchange regimes. **B:** Fitted exchange curves and rates for residues shown in panel A. **C:** Magnitude of observed exchange rates mapped to the structure of apo $CaM_{76\text{-}148}$ bound to $Na_v1.2_{IQp}$ (green rod) with I and Q residues of the IQ-motif shown in ball and stick.
Users/nmr_mike/Thesis/Chapter_IV/Figure4_4.jpg

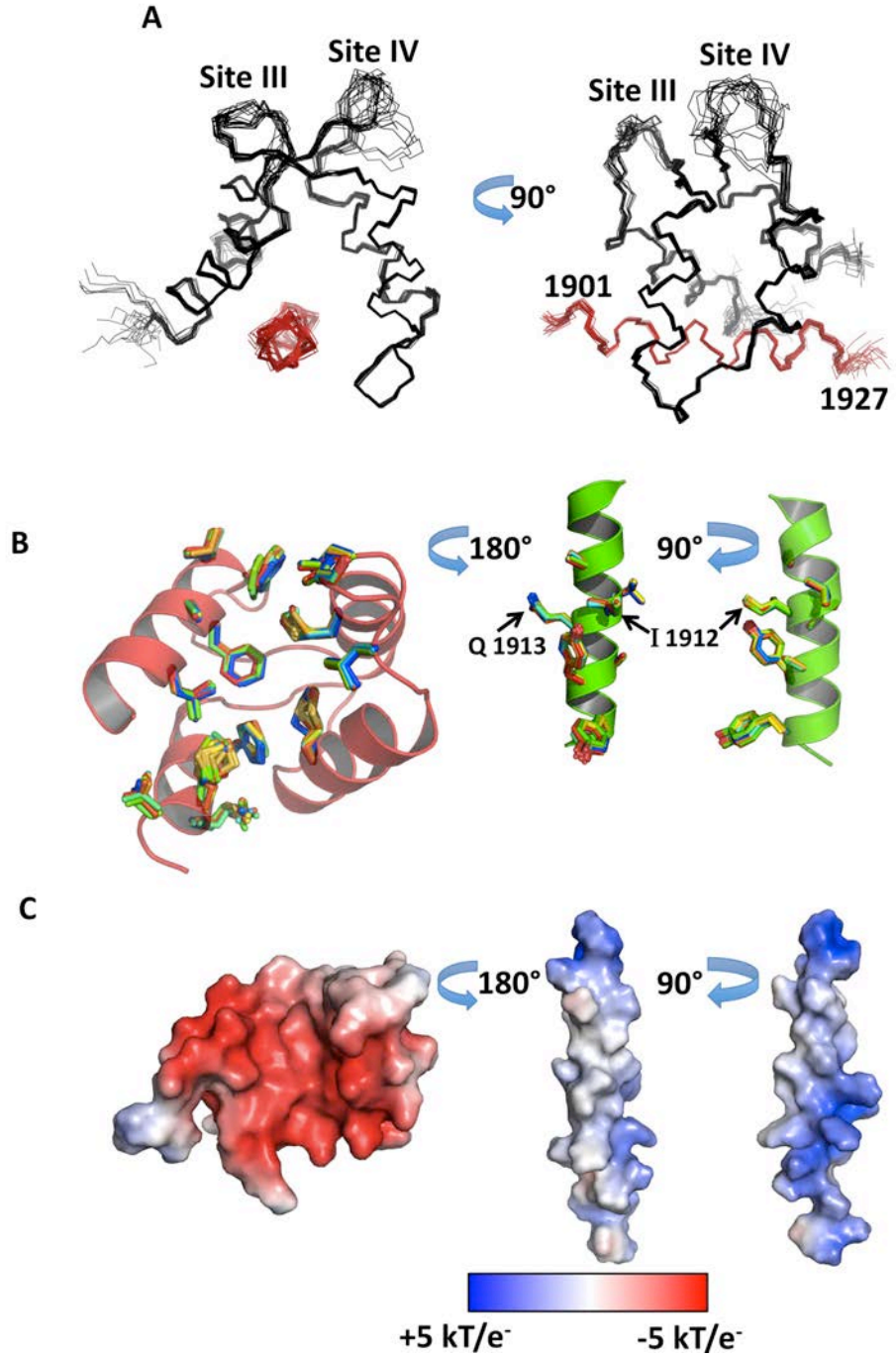

Figure 4.5: Solution structure of apo $CaM_{76\text{-}148}$ bound to $Na_v1.2_{IQp}$
A: Ensemble of 20 lowest energy structures of apo $CaM_{76\text{-}148}$ (black) bound to $Na_v1.2_{IQp}$ (red) **B:** Hydrophobic interaction interfaces of 20 lowest energy structures of apo $CaM_{76\text{-}148}$ (red) bound to $Na_v1.2_{IQp}$ (green). **C:** Electrostatic potentials of apo $CaM_{76\text{-}148}$ (left), and $Na_v1.2_{IQp}$ (middle, and right) in 150mM NaCl, pH 6.5.
Users/nmr_mike/Thesis/Chapter_IV/Figure4_5.jpg

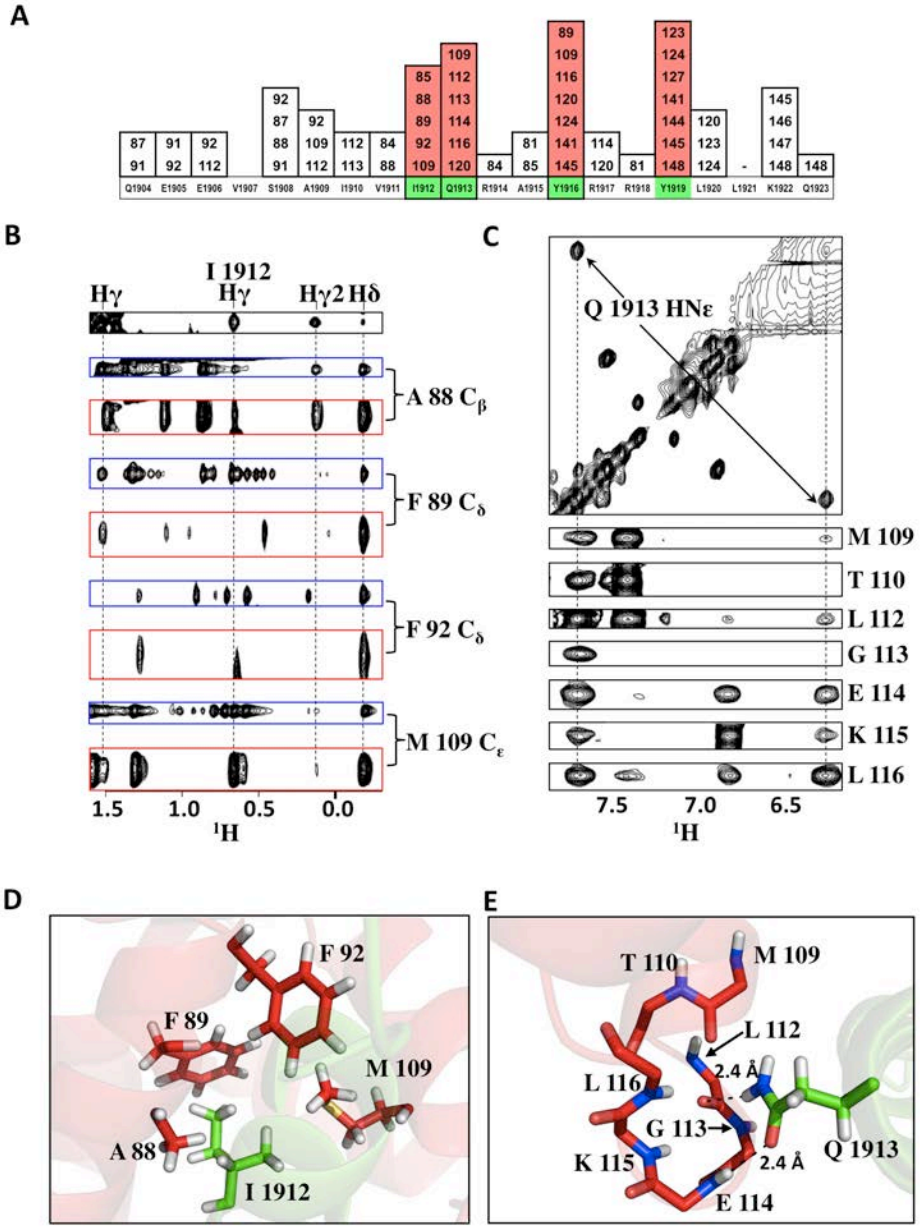

Figure 4.6: Binding interfaces of apo $CaM_{76\text{-}148}$ and $Na_v1.2_{IQp}$
A: apo $CaM_{76\text{-}148}$ residues (red) ≤ 4.5 Å of $Na_v1.2_{IQp}$ (black) **B:** Select NOE peak between I1912 of $Na_v1.2_{IQp}$ and apo $CaM_{76\text{-}148}$ where individual residue unfiltered and filtered ^{13}C-NOESY spectral strips are outlined in blue and red respectively. **C:** Select NOE peaks between Q1913 of $Na_v1.2_{IQp}$ and apo $CaM_{76\text{-}148}$, where individual ^{15}N-NOESY spectral strips are outlined in black. **D:** Location of apo $CaM_{76\text{-}148}$ residues shown in panel B in relation to I1912. **E:** Location of apo $CaM_{76\text{-}148}$ residues shown in panel C in relation to Q1913, shown in dashed lines are hydrogen bonds made by the carboxamide of Q1913 to the backbone of residues L112, and E114.
Users/nmr_mike/Thesis/Chapter_IV/Figure4_6.jpg

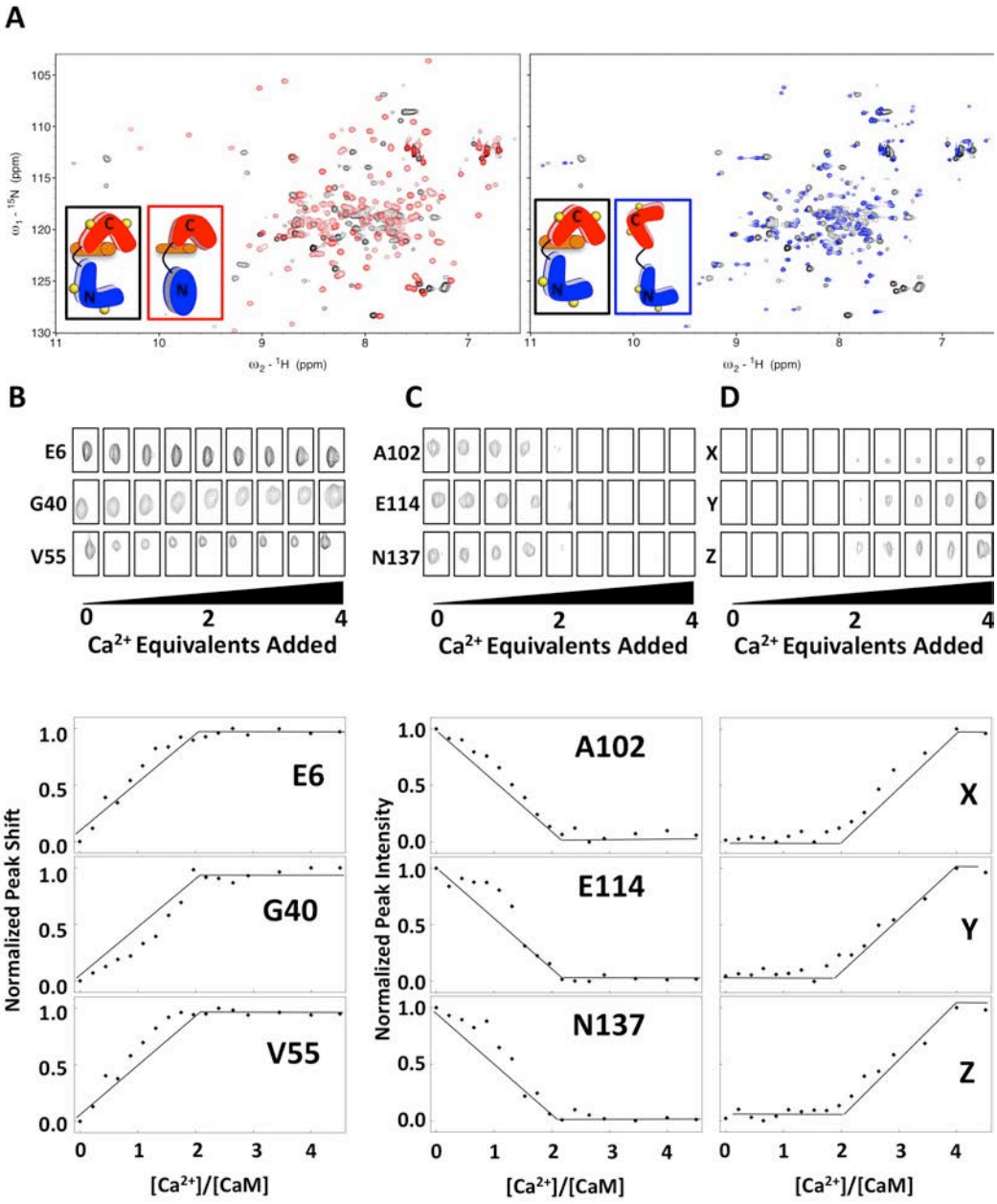

Figure 4.7: Effect of Ca^{2+} upon apo $CaM_{76\text{-}148}$ when bound to $Na_v1.2_{IQp}$
A: ^{15}N-HSQC spectral overlay of apo (red) and $(Ca^{2+})_4$-$CaM_{1\text{-}148}$ (black) bound to $Na_v1.2_{IQp}$ (left). ^{15}N-HSQC spectral overlay of apo $CaM_{1\text{-}148}$ (blue) and $(Ca^{2+})_4$-$CaM_{1\text{-}148}$ bound to $Na_v1.2_{IQp}$ (right). **B:** ^{15}N-HSQC Monitored Ca^{2+} titration of select N-domain residues (upper) with quantified change in chemical shift as Ca^{2+} was added (lower). **C:** ^{15}N-HSQC Monitored Ca^{2+} titration of select C-domain residues (upper) with quantified change in chemical shift as Ca^{2+} was added (lower), lines are added to guide the eye. **D:** ^{15}N-HSQC Monitored Ca^{2+} titration of residues from the C-domain of CaM, but whose individual residue identity is unknown (upper) with quantified change in chemical shift as Ca^{2+} was added (lower)Users/nmr_mike/Thesis/Chapter_IV/Figure4_7.jpg

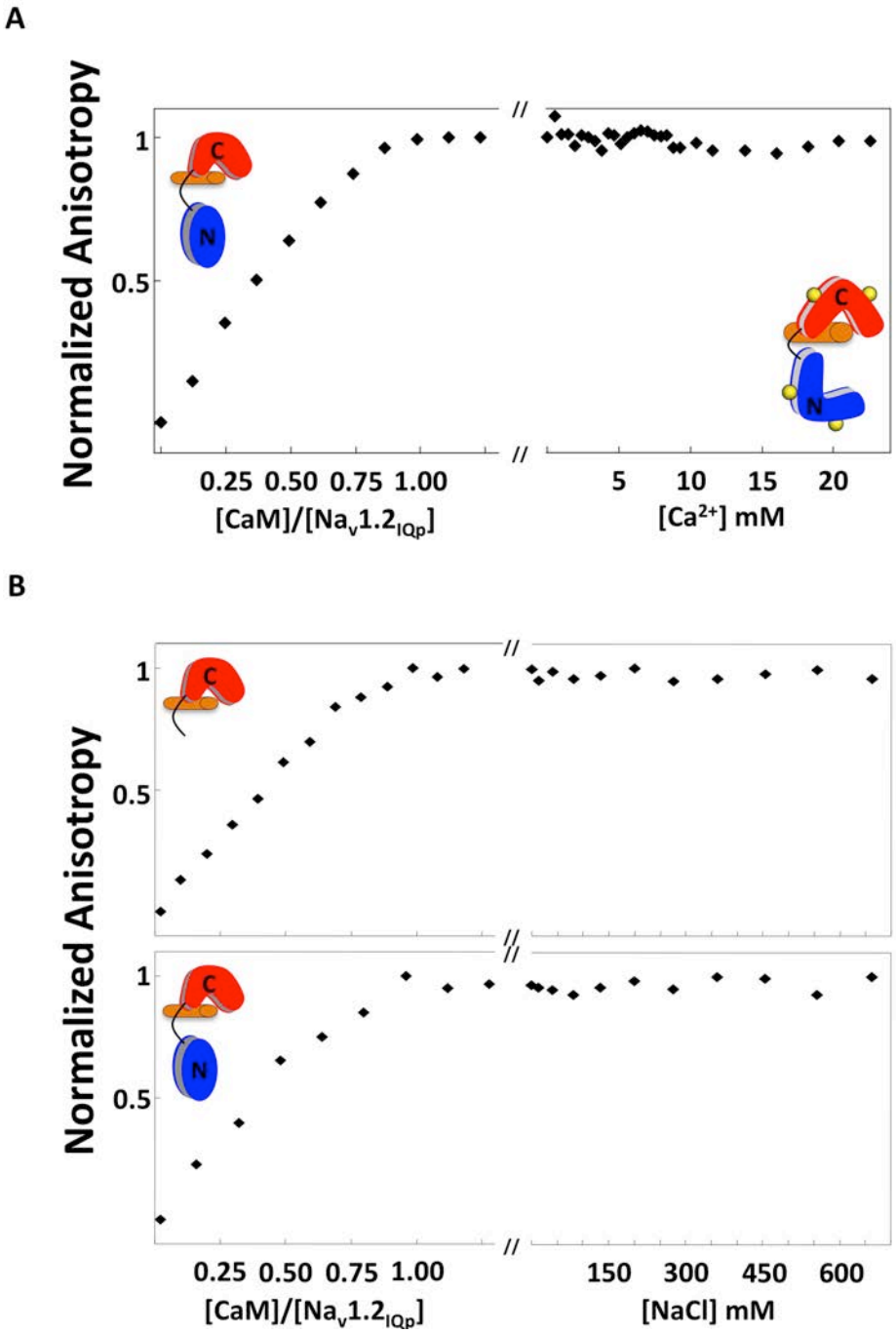

Figure 4.8: Fluorescence anisotropy monitored titration of apo CaM bound to $Na_v1.2_{IQp}$
A: Fluorescence anisotropy monitored apo CaM_{1-148} titration of fluoresceinated $Na_v1.2_{IQp}$ (left) followed by $CaCl_2$ titration of apo CaM_{76-148}:$Na_v1.2_{IQp}$ complex (right).
B: Fluorescence anisotropy monitored of fluoresceinated $Na_v1.2_{IQp}$ (left) with apo CaM followed by NaCl titration of the apo CaM:$Na_v1.2_{IQp}$ complex (right).
Users/nmr_mike/Thesis/Chapter_IV/Figure4_8.jpg

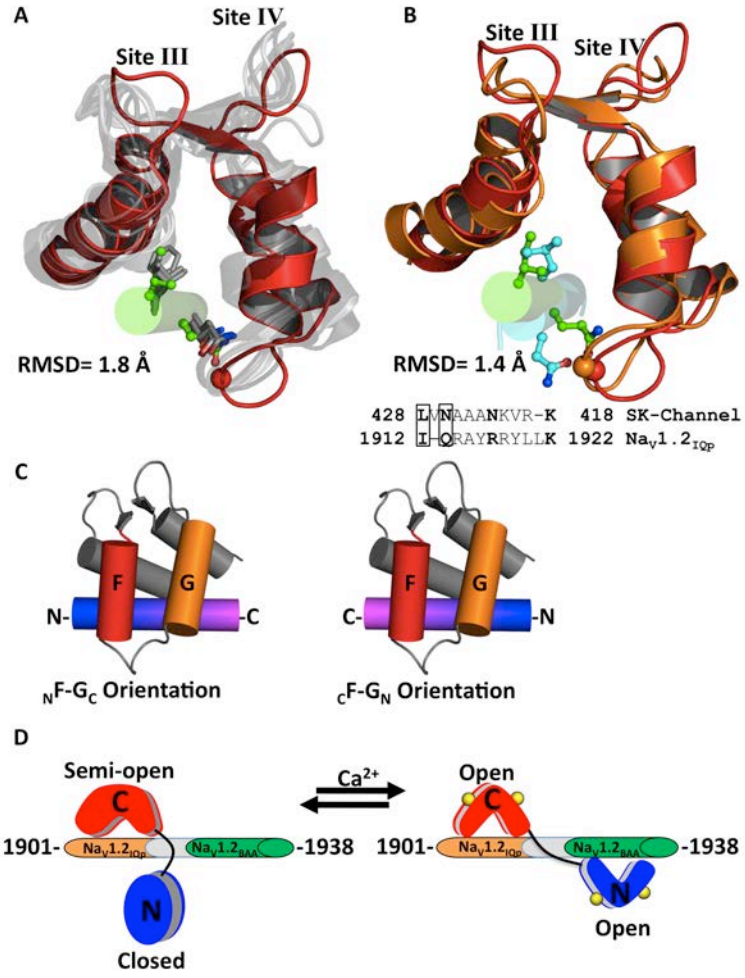

Figure 4.9: Superposition of target bound apo CaM and CaM-like protein C-domains **A:** Superposition of apo $CaM_{76\text{-}148}$ (red):$Na_v1.2_{IQp}$ (green rod) complex onto C-domains of apo CaM and apo CaM-like proteins (gray) bound to canonical IQ-motifs. I and Q residues of all IQ-motifs are shown in sticks, the Cα atom of residue 113 is shown as a sphere as a point of reference. Pdb files used in overlay 2IX7, 1M45, 1M46, 1ND2, and 3JVT. **B:** Superposition of apo $CaM_{76\text{-}148}$ (red):$Na_v1.2_{IQp}$ (green rod) complex and the C-domain of partially Ca^{2+}-saturated $CaM_{1\text{-}148}$ (orange) bound to the SK-Channel peptide (cyan). Residues at positions I and Q of IQ-motif and their SK-channel homologs are shown in sticks, the Cα atom of residue 113 is shown as a sphere as a point of reference. The aligned primary sequences of $Na_v1.2_{IQp}$ and SK-channel are shown where residues at IQ-motif defining position are shown in bold, and essential IQ-motif residues or their homolog are boxed. **C:** Structural depiction of naming scheme used to describe peptide polarity when interacting with the C-domain of CaM. The N- and C-termini of a peptide (blue and magenta respectively) can orient themselves in 2 possible ways with respect to helices F (red) and G (orange) of the C-domain resulting in either a $_NF\text{-}G_C$ or $_CF\text{-}G_N$ orientation. **D:** Proposed model of $CaM_{1\text{-}148}$ interaction with the C-terminal tail of $Na_v1.2$ under apo and Ca^{2+}-saturating conditions.
Users/nmr_mike/Thesis/Chapter_IV/Figure4_9.jpg

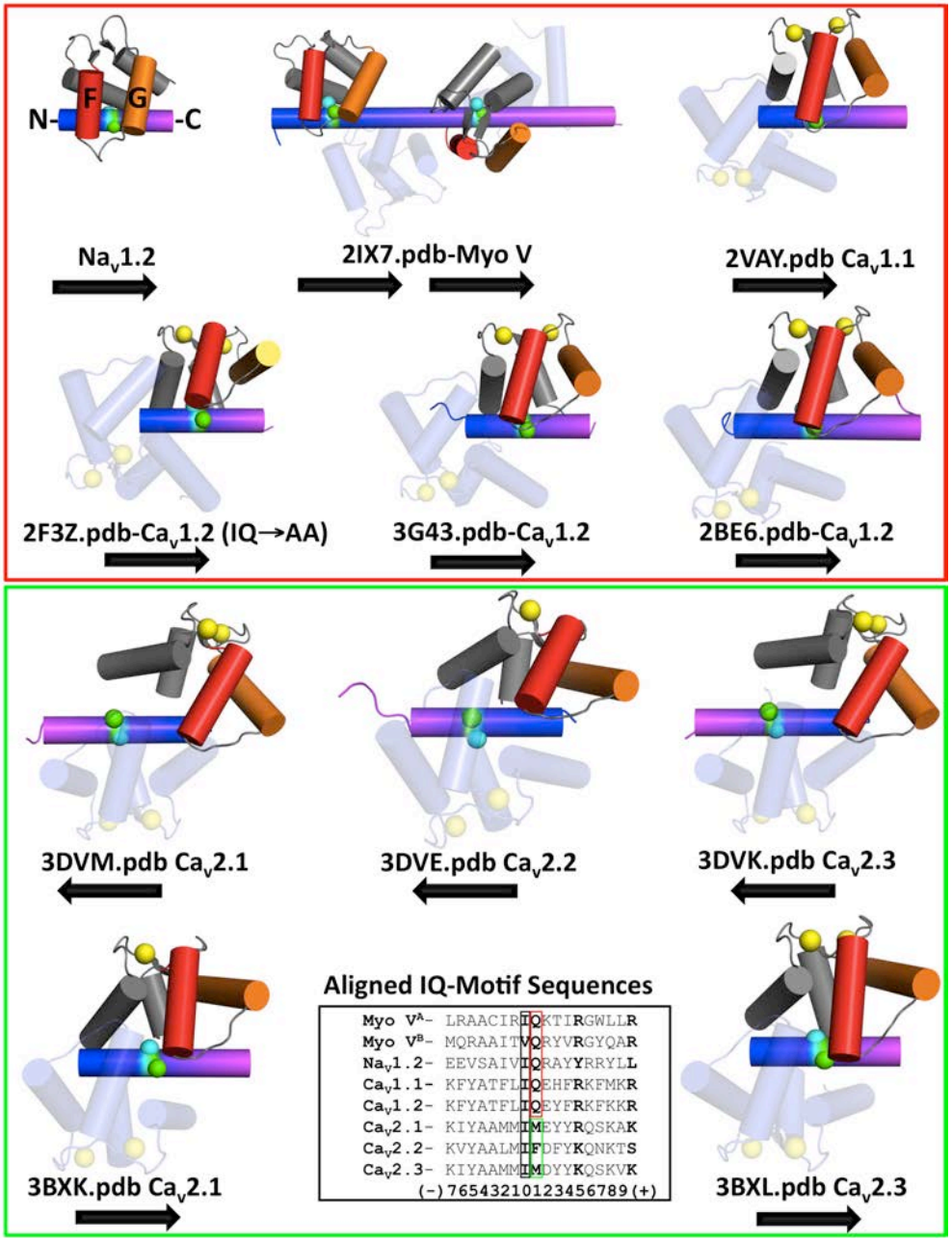

Figure 4.10: Directionality of IQ-motif binding to the C-domain of CaM
The polarity of IQ-motif containing helices is indicated by the color gradient where the N-terminus is shown in blue and C-terminus in purple. CaM helices F and G are colored red and orange, while the I and Q of each IQ-motif are shown as spheres colored cyan and green respectively.
Users/nmr_mike/Thesis/Chapter_IV/Figure4_10.jpg

CHAPTER V

INFLUENCE OF ELECTROSTATIC INTERACTIONS ON CA^{2+} AND TARGET BINDING BY CAM

Introduction

CaM is a Ca^{2+} sensor protein that is essential to eukaryotic signal transduction pathways (Pedigo et al., 1992). Changes in intra-cellular Ca^{2+} levels are linked to cellular events by the effect of Ca^{2+} on CaM: it triggers conformational changes that expose hydrophobic surfaces in both domains of CaM, altering its binding to many target proteins (VanScyoc and Shea, 2001a; Yagi et al., 1990). In addition to the widely accepted role of hydrophobic interactions in recognition and binding of targets by CaM, electrostatic interactions have an important role in these processes as well (André et al., 2004; Linse et al., 1988; Ogawa and Tanokura, 1984). At physiological conditions (pH 7, 100mM KCl) CaM is a negatively charged protein (pI=4) with net charges of -24 (apo) and -16 (Ca^{2+}-saturated) while peptide derivatives from the CaMBD's of its targets typically carry a complementary positive charge ($Na_v1.2_{IQp}$ = +8, $CaMKII_p$ = +6). Compared to hydrophobic interactions alone, electrostatic interaction between CaM and its targets allow for recognition of each other at much greater distances, increasing the rate at which they associate (André et al., 2004; Antosiewicz and McCammon, 1995). The strength of electrostatic attraction between CaM and its targets is particularly interesting as it can be influenced in the cell due to spatial and temporal fluctuations in ionic concentrations due to naturally occurring currents through ion channels(Akyol et al., 2004; Cens et al., 2006; Levitan, 1999; Saimi and Kung, 2002).

Hydrophobic and electrostatic interactions are the major forces responsible for CaM-target recognition and binding affinity (Bayley et al., 1996; Tjandra et al., 1999; Yagi et al., 1990). Electrostatic interactions between CaM and its targets guide hydrophobic surfaces located on CaM and its targets into close proximity so that they can interact. Due to their α-helical character, CaMBD's contain a periodicity within their primary amino acid sequence

producing a hydrophobic face that is buried from the solvent upon binding to CaM and a basic face that remains solvent exposed. This periodicity has resulted in multiple CaM binding motifs that have been characterized based upon the numerical position of the hydrophobic residues within CaMBD's that insert into the hydrophobic pockets of the N- and C-domains of CaM (**Figure 5.1**). This periodicity can also be visualized in helical wheel diagrams of the CaMBDs of proteins regulated by CaM (**Figure 5.2**). The regions between hydrophobic "anchor" positions are enriched with positively charged residues creating charge complementarity between CaM and its target (Yamniuk and Vogel, 2004).

The extent to which electrostatic interactions contribute to CaM-target recognition and binding affinity may significantly change in the cell due to ion fluxes necessary for the generation and propagation of action potentials (Andre et al., 2006; Suizu et al., 1995). The ions that undergo the largest change in intra and extracellular concentration involved in this process are Na^+, K^+, Ca^{2+}, and Cl^-. Shown in **Figure 5.3** is a schematic illustrating the ionic strength and concentration gradients present in a resting cell (Hille, 2001).

Large changes in local intracellular ion concentration occur near ion channels as they open to allow their specific ions to pass through the membrane. Given that CaM is an intrinsic subunit of several known Na^+, K^+, and Ca^{2+} channels, fluctuations in the strength of electrostatic interaction may alter occupancy of CaM at CaMBDs on these channels (Ehlers et al., 1996; Halling et al., 2005; Pitt, 2005; Saimi and Kung, 1994; Theoharis et al., 2008). To investigate whether these fluctuations significantly alter the affinity of CaM binding to $CaMKII_p$ or $Na_v1.2_{IQp}$, fluorescence anisotropy monitored titrations as a function of varied salt were performed.

Poisson-Boltzmann Equation

Electrostatic interactions can be observed between virtually all interacting macromolecules. Creighton has estimated that more than 20% of all amino acids in globular proteins are ionized at physiological pH (Creighton, 1993). Structural methods such as NMR,

and X-ray crystallography are able to provide the spatial arrangement of charged amino acid groups within a protein or protein-ligand complex, allowing for the calculation of electrostatic potentials that can be mapped to the macromolecular surface. Solution of Poisson-Boltzmann equation was first described by Gouy (1910) and Chapman (1913) (Chapman, 1913; Gouy, 1910) allows for the calculation of the electrostatic potential of a macromolecule throughout the calculated space, as well the distribution the local ions around the macromolecule.

The Poisson-Boltzmann equation (**Equation. 5.1**)

$$-\nabla \bullet \varepsilon(\chi)\nabla\phi(\chi) + \kappa^{-2}(\chi)\sinh\phi(\chi) = f(\chi) \qquad (5.1)$$

is a second-order nonlinear elliptic partial differential equation that relates the electrostatic potential (ϕ) to the dielectric properties of the solute and solvent (ε), the ionic strength of the solution and the accessibility of ions to the solute interior (κ^{-2}), and the distribution of solute atomic partial charges (f). To expedite solution of the equation, the nonlinear PBE is often approximated by the linearized PBE (LPBE) by assuming $sinh\phi(\chi) \approx \phi(\chi)$. Pioneering work in this area has been done by many groups including Honig and McCammon. Their studies allow the calculation of electrostatic potentials of macromolecules such as nucleic acids and proteins (Allison et al., 1988; Gilson and Honig, 1988; Honig and Nicholls, 1995; Sharp and Honig, 1990). In addition to visualization of electrostatic potentials of a macromolecule in solutions of varying ionic strength, solution of the linear or non-linear Poisson-Boltzmann equation allows for calculation of macromolecular solvation energies.

Determination of the solvation energies of the macromolecular complex and the individual components that comprise them can be used via linkage analysis to calculate the contribution of electrostatic interactions to overall binding affinity. Multiple ionic strengths can be used to examine the dependence of the electrostatic binding energy on solution ionic strength. This dependence can determined by plotting the electrostatic binding energy (x-axis) versus the log [salt] (y-axis) and fitting a line to the points. The greater the slope of this plot, the more dependent the electrostatic component of binding and by default the overall binding energy of the associating macromolecules are on the ionic strength of the solution.

Materials and Methods

Poisson-Boltzmann calculations

Poisson-Boltzmann calculations were performed using the Adaptive Poisson-Boltzmann Solver (APBS) software package developed by Nathan Baker and coworkers (Baker et al., 2001) to determine the theoretical contribution of electrostatic interactions to the overall binding energy of $(Ca^{2+})_4$-CaM for $CaMKII_p$. Structural coordinates for the $(Ca^{2+})_4$-CaM:$CaMKII_p$ complex were obtained from the pdb file 1CM1.pdb, and missing side chains were added using Swiss-PDBViewer (Guex and Peitsch, 1997). From the previously mentioned file, two separate PDB files were created consisting of $(Ca^{2+})_4$-CaM, and $CaMKII_p$, in the conformation they were observed in the $(Ca^{2+})_4$-CaM:$CaMKII_p$ complex structure. These files were then converted into PQR format and protonated based on their charge states at pH 7.4 using the PDB2PQR webserver (Sobczak et al., 2002).

Identical calculation grid center and length coordinates were used in calculating electrostatic potentials of each molecule or complex. The dimensions of the coarse grid were x=60 Å, y=75 Å, and z=70 Å with a grid spacing of 0.5 Å, while the fine grid was x=41.5 Å, y=52 Å, and z=48 Å with a grid spacing of 0.25, each was centered at x=19.558, y=56.112, and z=74.867. The temperature used in the calculation was 295K, while the dielectric constant values used for the protein and solvent were 4.00 and 78.54. The linearized form of the Poisson-Boltzmann equation was solved using single Debye-Huckel boundary conditions with cubic B-spline charge discretization and surface smoothing, while the spline window was set to 0.3Å.

The [NaCl] or [KCl] was varied in 50mM increments over a range between 0 and 2M, while the keeping the [$CaCl_2$] and [$MgCl_2$] constant to mimic the experimental setup to which these calculations were compared to. The atomic radii of the Ca^{2+}, Mg^{2+}, Cl^-, and (Na^+ or K^+) used in the calculation were 1.97 Å, 1.60 Å, 1.75 Å, 1.86 Å and 2.27 Å respectively, while the solvent radius was 1.4 Å. The atomic radii of the afore mentioned ions were calculated using APBS by iterative rounds of calculation of the solvation energy of the ion and radius adjustment

to match experimentally determined solvation values (Burgess, 1988). The electrostatic potentials of the $(Ca^{2+})_4$-CaM:$CaMKII_p$ complex, $(Ca^{2+})_4$-CaM, and $CaMKII_p$ were then calculated at each [NaCl or KCl]. These electrostatic potentials were then used to determine the electrostatic component of $CaMKII_p$ binding to $(Ca^{2+})_4$-CaM at each [NaCl or KCl] by subtracting the electrostatic energy values determined for $(Ca^{2+})_4$-CaM and $CaMKII_p$ from the value determined for the $(Ca^{2+})_4$-CaM:$CaMKII_p$ complex as shown in **Equation 5.2**.

$$\Delta G_{Electrostatic} = Complex - CaM_{Alone} - Na_v1.2_{IQp} \quad (5.2)$$

The resulting value from this calculation represents the energy of binding/complex formation.

Fluorescence Anisotropy Monitored Titrations of CaM Binding to Either $CaMKII_p$ or $Na_v1.2_{IQp}$ at Varied [NaCl or KCl]

Fluorescence anisotropy monitored titrations of CaM binding to either $CaMKII_p$ or $Na_v1.2_{IQp}$ at varied [NaCl or KCl] were performed to examine how these salts alter the binding affinity of CaM for these peptides. $(Ca^{2+})_4$-CaM_{1-148} binding to fluorescein-labeled $CaMKII_p$, or CaM_{76-148} or CaM_{1-148} binding to fluorescein-labeled $Na_v1.2_{IQp}$ peptide under apo and Ca^{2}-saturating conditions were monitored using a Fluorolog 3 (Jobin Yvon, Horiba) spectrofluorimeter, equipped with dual auto-assembly Glan-Thompson polarizers. The anisotropy of the fluorescein labeled peptides were monitored using λ_{ex} 496 nm and λ_{em} 520 nm with 2bnm excitation and 10nm emission bandpasses. Anisotropy (r) was calculated as shown in **Equation 5.3** as described previously (Akyol et al., 2004),

$$r = \frac{I_{VV} - G \bullet I_{VH}}{I_{VV} + 2G \bullet I_{VH}} \quad (5.3)$$

where I_{VV} and I_{VH} are the intensities of vertically- or horizontally-emitted light upon vertical excitation, respectively, and G is the instrument correction factor ($G= I_{HV}/I_{HH}$). Averages of three readings with a 1-sec integration time at each point were recorded. Samples of 100 nM Fl-

$CaMKII_p$ or 1μM Fl-$Na_v1.2_{IQp}$ in 50 mM HEPES, 100 mM KCl, 50 μM EGTA, 5 mM NTA, 1 mM $MgCl_2$, pH 7.4 in the absence (apo) or presence of 10 mM $CaCl_2$ (Ca^{2+}-saturated) at 22 °C were titrated with concentrated apo or Ca^{2+}-saturated CaM. At least three replicate titrations were conducted for each NaCl or KCl concentration examined as well as for apo and $(Ca^{2+})_4$- CaM_{1-148}. Titrations involving CaM_{76-148} were less well determined and represent only single trials performed as part of exploratory measurements.

Analysis of K_d for CaM Binding to $Na_v1.2_{IQp}$ or $CaMKII_p$

Affinity estimates of CaM for $Na_v1.2_{IQp}$ or $CaMKII_P$ were determined by fitting titration data to a one-site binding model using NONLIN (Johnson and Frasier, 1985). Fractional saturation of $Na_v1.2_{IQp}$ or $CaMKII_p$ was described by **Equation 5.4** as described previously (Akyol et al., 2004):

$$\overline{Y} = \frac{K_a[X_{Free}]}{1 + K_a[X_{Free}]} \tag{5.4}$$

where K_a represents the association constant for CaM binding to CaMKII or $Na_v1.2_{IQp}$, and $[X_{free}]$ is the free concentration of CaM in solution, as calculated from the independent variables (total concentration of X, $[X_{total}]$) and (total concentration of M, $[M_{total}]$) according to the quadratic equation described by **Equation 5.5** as described previously (Akyol et al., 2004):

$$[X_{Free}] = \frac{\sqrt{-b \pm b^2 - 4K_a([-X_{Total}])}}{2K_a} \tag{5.5}$$

where $b = (1 + K_a[M_{Total}] - K_a[X_{Total}])$. Under equilibrium conditions, the concentration of $Na_v1.2_{IQp}$ or CaMKII ($[M_{total}]$) was low relative to the Kd (dissociation constant, 1/Ka) of CaM binding to the peptide. The free concentration of CaM may be approximated by the total (i.e., $[X_{free}]$ at $[X_{total}]$. This allows for an accurate estimate of the association constant. Under stoichiometric conditions however, the ligand is limiting and $[X_{free}]$ is estimated iteratively in the nonlinear least squares function for saturation as the best solution to the difference between $[X_{total}]$ (calculated on the basis of the total ligand added) and $[X_{bound}]$ (calculated as the product

of [M_{total}] and $\bar{Y}$). The value of a binding constant estimated in this way is highly correlated with the precision of the numerical value measured for [M_{total}]; therefore, the dissociation constant of $Na_v1.2_{IQp}$ or $CaMKII_P$ for apo and Ca^{2+}-saturated CaM_{76-148} or CaM_{1-148} in **Tables 5.1 and 5.2** is reported as a limiting value. Experimental variations in the observed endpoints of individual titration curves were accounted for by **Equation 5.6** described previously (Akyol et al., 2004):

$$f(X) = Y_{[X]low} + \overline{Y}_1 \bullet [(Y_{[X]high} - Y_{[X]low}) = Span \tag{5.6}$$

where $\overline{Y}_1$ refers to average fractional saturation of $Na_v1.2_{IQp}$ or CaMKII and $Y_{[X]low}$ corresponds to the intrinsic fluorescence anisotropy of CaMKII or $Na_v1.2_{IQp}$ in the absence of CaM. The *Span* describes the magnitude and direction of signal change upon titration, which describes the difference between the high ($Y_{[X]high}$) and low ($Y_{[X]low}$) endpoints. The *Span* is positive for an increasing signal and negative for a decreasing signal.

In most titrations, the upper and lower endpoints were well defined experimentally. However, in the equilibrium titrations of $Na_v1.2_{IQp}$ with apo and $(Ca^{2+})_2$-CaM_{76-148} at 300mM KCl the fluorescence anisotropy of $Na_v1.2_{IQp}$ did not reach a plateau at the final CaM concentration tested. To estimate the final anisotropy that might have been reached if $Na_v1.2_{IQp}$ had become saturated with apo and $(Ca^{2+})_2$-CaM_{76-148}, the end points of the same titrations done at 100 mM KCl were used. The endpoint ($Y_{[X]high}$) was fixed at this value in the nonlinear least squares analysis of the affected titrations.

To illustrate the degree of precision which we were able to place on the limiting K_d values of stoichiometric titrations reported in this chapter binding curves corresponding to K_d values of 1, 10, 25, and 50 nM were simulated and are shown in **Figure 5.5**. These curves were simulated assuming a 1μM peptide concentration and plotted against either log $[CaM]_{total}$, or [CaM]/[Peptide]. Plotted upon each graph are identical data points of a $(Ca^{2+})_4CaM_{1-148}$ titration of $Na_v1.2_{IQp}$ where the [$Na_v1.2_{IQp}$] concentration was 1 μM to demonstrate how the representation of the same data points change dependent upon how the x-axis is displayed.

Results

Fluorescence Anisotropy Monitored CaM Titrations of $Na_v1.2_{IQp}$

As shown in **Figures 5.4** and **5.6**, CaM titrations of $Na_v1.2_{IQp}$ monitored by fluorescence anisotropy were used to determine the binding affinities of CaM_{78-148} and CaM_{1-148} for $Nav1.2_{IQp}$ under apo and Ca^{2+}-saturating conditions at varied NaCl (CaM_{1-148} only) and KCl concentrations. Reported in Table 5.2 are estimated binding affinities for CaM_{76-148} and CaM_{1-148} for $Nav1.2_{IQp}$. It should be noted that the value of CaM_{76-148} titration of $Na_v1.2_{IQp}$ is the result of a single trial performed as part of initial exploratory study of salt effects on the affinity of $Na_v1.2_{IQp}$ binding to CaM_{76-148}.

A common feature present for all titrations of CaM_{1-148} was that $Nav1.2_{IQp}$ binding was observed to be in a stoichiometric binding regime regardless of the salt (NaCl, or KCl) used (**Figure 5.3**). Increasing the KCl concentration shifted $Na_v1.2_{IQp}$ binding to both apo and $(Ca^{2+})_2$-CaM_{76-148} from a stoichiometric to equilibrium binding regime (**Figure 5.2**) The stoichiometry of $Nav1.2_{IQp}$ binding to either CaM_{76-148} or CaM_{1-148} was determined to be 1:1 under both apo and Ca^{2+}-saturating conditions. A decrease in $Na_v1.2_{IQp}$ binding affinity was observed as the concentration of salt was increased in all titrations (**Figures 5.1**, and **5.2**). Comparison of changes in free energy of $Nav1.2_{IQp}$ binding at varied salt concentrations showed that NaCl induced larger changes in $Nav1.2_{IQp}$ binding affinity than KCl (**Table 5.2**) for both apo and $(Ca^{2+})_4$-CaM_{1-148}.

Although additional trials of CaM_{76-148} titrations of $Na_v1.2_{IQp}$ are needed to confirm the values of these initial findings, when changes in $Na_v1.2_{IQp}$ binding affinities at 100mM and 300mM KCl were compared for CaM_{76-148} and CaM_{1-148}, larger changes are observed for CaM_{76-148} than CaM_{1-148} (**Table 5.2**).

Fluorescence Anisotropy Monitored CaM Titrations of $CaMKII_p$

As shown in **Figure 5.3** CaM titrations of $CaMKII_p$ monitored by fluorescence anisotropy were used to determine the binding affinity of $(Ca^{2+})_4$-CaM_{1-148} for $CaMKII_p$ at varied NaCl and KCl concentrations. Reported in **Table 5.1** are estimated binding affinities of $CaMKII_p$ for $(Ca^{2+})_4$-CaM_{1-148}. A common feature present for all titrations was that $CaMKII_p$ binding was observed to be in a stoichiometric binding regime regardless of the salt (NaCl, or KCl) used (**Figure 5.3**). The stoichiometry of $CaMKII_p$ to either $(Ca^{2+})_4$-CaM_{1-148} was determined to be 1:1. Though stoichiometric, a decrease in $CaMKII_p$ binding affinity was observed as the concentration of either NaCl or KCl was increased. Comparison of changes in free energy of $CaMKII_p$ binding at varied salt concentrations showed that NaCl induced larger changes in $CaMKII_p$ binding affinity than KCl (**Table 5.1**) for $(Ca^{2+})_4$-CaM_{1-148}.

Electrostatic Binding Energy of CaMKII for $(Ca^{2+})_4$-CaM_{1-148} Calculated via APBS

To predict the effect of NaCl and KCl on the binding affinity of $CaMKII_p$ for $(Ca^{2+})_4$-CaM_{1-148}, Poisson-Boltzmann calculations were performed at varied NaCl and KCl concentrations (25 mM–1000 mM). Both NaCl and KCl lowered the binding affinity of $CaMKII_p$ for $(Ca^{2+})_4$-CaM in a concentration dependent manner shown in **Figure 5.4a**. Though both NaCl and KCl lowered the affinity of $CaMKII_p$ for $(Ca^{2+})_4$-CaM, NaCl induced a greater change in affinity at concentrations ranging from 25-400 mM than KCl (**Figure 5.4a**). Comparison of $\Delta\Delta G_{NaCl\text{-}KCl}$ values of $CaMKII_p$ binding at salt concentrations greater than 400 mM indicated a convergence in the degree to which Na^+ or K^+ reduce the binding affinity of $CaMKII_p$ (**Figure 5.4a**). Shown in **Figure 5.4b** are structures of $(Ca^{2+})_4$-CaM_{1-148} and $CaMKII_p$ whose solved exposed surfaces are colored according to their electrostatic potential at varied NaCl or KCl concentrations.

Discussion

CaM is a negatively charged protein (pI=4) that binds to CaMBD sequences that are enriched in positive charge. The interaction of charged particles in solution can be lessened by electrostatic shielding by the addition of salt. Results presented in **Chapter V** indicate that increasing the concentration of NaCl or KCl lowered the binding affinity of targets for CaM. Examination of values determined for $CaMKII_p$ and $Na_v1.2_{IQp}$ binding to CaM at the same NaCl or KCl concentration indicated that the Na^+ ion induced a larger effect on $CaMKII_p$ or $Na_v1.2_{IQp}$ binding affinity than the K^+ ion.

Poisson-Boltzmann calculations of $CaMKII_p$ binding to $(Ca^{2+})_4$-CaM_{1-148} indicated that both NaCl and KCl reduced the binding affinity of $CaMKII_p$ for $(Ca^{2+})_4$-CaM, with NaCl having a larger effect than KCl up to 400 mM. Calculation of NaCl and KCl effects on $CaMKII_p$ binding to $(Ca^{2+})_4$-CaM_{1-148} at concentrations greater than 400 mM showed a decrease in Na^+ or K^+ ion specific effects indicating a general ion effect applies at salt concentrations above 400 mM. The onset of a general salt effect as NaCl or KCl progress past 400 mM represents a saturation of $(Ca^{2+})_4$-CaM_{1-148} and $CaMKII_p$ surfaces with either salt, after which Na^+ or K^+ ion specific effects become less pronounced.

Results obtained in this chapter show that electrostatic interactions between CaM and its targets $CaMKII_p$ and $Na_v1.2_{IQp}$ are influenced by changes in solvent ionic strength, influencing their binding affinity for each other. A caveat of this observation is that although the peptide binding affinity of CaM was decreased by increasing the salt concentration, the binding affinity of CaM for $CaMKII_p$ and $Na_v1.2_{IQp}$ remained at levels where they would remain associated with CaM in the cell. Together these observations suggest that CaM and its targets have evolved binding surfaces whose molecular interfaces rely on interactions that are largely independent of changes in intracellular salt concentration.

Salt Dependence of $Na_v1.2_{IQp}$ Binding to apo and (Ca^{2+})-CaM

Titrations of $Na_v1.2_{IQp}$ binding to CaM at varied NaCl and KCl concentrations showed differential effects upon the $Na_v1.2_{IQp}$ binding affinity of CaM. In all cases titrations done in the presence of NaCl showed a greater decrease in the binding affinity of $CaMKII_p$ or $Na_v1.2_{IQp}$ for CaM than those done in KCl. This effect can be directly attributed to differences between interactions of the Na^+ or K^+ ion and the CaM:target complex. Comparison of the radii of the Na^+ and K^+ ion indicate that the Na^+ ion has a greater charge density than the K^+ ion (Hille et al. 2001). This characteristic allows for stronger attraction, and greater access to negatively charged cavities found within CaM and either $CaMKII_p$ or $Na_v1.2_{IQp}$ than the larger K^+ ion. These results suggest that as K^+ ions exchange for Na^+ ions during an action potential, the affinity of CaM for its targets decreases.

Comparison of salt effects on the binding affinity of $Na_v1.2_{IQp}$ for apo and $(Ca^{2+})_4$-CaM_{1-148} showed that the binding affinity of $Na_v1.2_{IQp}$ for apo CaM_{1-148} was decreased to a greater extent than for $(Ca^{2+})_4$-CaM_{1-148} (**Table 5.2**). This effect is attributed to the electrostatic component of the overall $Na_v1.2_{IQp}$ binding affinity for apo CaM_{1-148} comprising a greater percentage than $(Ca^{2+})_4$-CaM. This difference in contribution of electrostatic interactions to the overall binding affinity is likely due to apo CaM_{1-148} have a greater overall net negative charge of -24 compared to -16 of $(Ca^{2+})_4$-CaM_{1-148} due to Ca^{2+} binding.

Preliminary trials of both apo and $(Ca^{2+})_2$-CaM_{76-148} at 100 and 300 mM KCl showed a more pronounced change in the affinity of $Na_v1.2_{IQp}$ than what was observed for apo and $(Ca^{2+})_4$-CaM_{1-148}. Additional trials are necessary to confirm the significance of these observed values. Based on the available data for CaM_{76-148}, addition of KCl caused a larger decrease in $Na_v1.2_{IQp}$ affinity for both apo and $(Ca^{2+})_2$-CaM_{76-148} than apo and $(Ca^{2+})_4$-CaM_{1-148} with the largest decrease in $Na_v1.2_{IQp}$ binding affinity seen in apo CaM_{76-148} (**Table 5.2**). The greater effect of KCl upon CaM_{76-148} than CaM_{1-148} may be attributed to KCl induced structural changes specific to CaM_{76-148} that are not found in CaM_{1-148}. This differential effect is consistent with previous

studies that showed that when separated, the domains of CaM do not behave in an identical manner as when they are covalently linked (Sorensen et al., 2002a; Sorensen and Shea, 1998).

Evaluation of calculated versus experimentally observed changes in the binding affinity of $CaMKII_p$ for $(Ca^{2+})_4$-CaM indicates qualitative effects similar to those described previously for $Na_v1.2_{IQp}$ binding. In both experimental and calculated measurements, increasing NaCl or KCl concentrations decreased the affinity of $CaMKII_p$ for $(Ca^{2+})_4$-CaM. Quantitative comparison of calculated values determined for $CaMKII_p$ binding to $(Ca^{2+})_4$-CaM showed that the salt dependence of $CaMKII_p$ binding to $(Ca^{2+})_4$-CaM is overestimated. Shown in **Figure 5.9** are the salt dependence slopes of experimentally observed and calculated changes in $CaMKII_p$ binding affinity for $(Ca^{2+})_4$-CaM. This difference between observed and predicted results represents a significant overestimate in the calculated salt dependence of $CaMKII_p$ binding to $(Ca^{2+})_4$-CaM.

Comparison of APBS calculated salt dependence slopes of $(Ca^{2+})_4$-CaM binding to $CaMKII_P$ (6.7-6.8) with that calculated for DNA binding to the Lambda repressor DNA binding domain (4.6) indicates a significantly greater salt dependence in the CaM-$CaMKII_p$ system (Sharp et al., 1995). Like $CaMKII_p$ binding to CaM, both DNA and the lambda repressor DNA binding domain are oppositely charged macromolecules indicating a significant contribution of electrostatic forces to the overall binding affinity (Sharp et al., 1995). It is of interest to note that unlike CaM binding $CaMKII_p$, the structure of the DNA binding domain of the lambda repressor does not undergo a large conformational change upon DNA binding (Beamer and Pabo, 1992; Pervushin et al., 1996).

The calculated overestimate in salt dependence of $CaMKII_p$ binding to $(Ca^{2+})_4$-CaM is likely due to multiple factors. APBS calculations do not take into account conformational changes that are known to occur within $(Ca^{2+})_4$-CaM and $CaMKII_p$ upon binding. CaM is a very flexible molecule whose conformation changes it from an extended conformation in the unbound state to a collapsed structure when bound to a target (**Figure 1.4**). CD data of $CaMKII_p$ peptide in the absence of CaM indicates that it does not form a persistent α-helix in solution (Shifman

and Mayo, 2002). Another factor that may also contribute the discrepancy between observed and predicted salt dependence values are structural differences that may be present at one salt concentration but not at others.

The discrepancy between predicted salt effects from calculated and observed values suggest that conformational changes occur upon peptide binding or salt-induced structural changes of $CaMKII_p$ to $(Ca^{2+})_4$-CaM, that are not captured by the structures used in these calculations. These results further demonstrate that a folding transition must occur upon $CaMKII_p$ (unstructured) binding to $(Ca^{2+})_4$-CaM (extended) and the final compact ellipsoidal structure of $(Ca^{2+})_4$-CaM bound to $CaMKII_p$ (**Figure 1.4**) (Tse et al., 2007).

Table 5.1: Calculated effect of salt on $CaMKII_p$ binding to $(Ca^{2+})_4$-CaM_{1-148}

[Salt], mM	K_d (KCl)	K_d (NaCl)	Fold Difference (K_d KCl/ K_d NaCl)
50	10 nM (-10.8*)	12 nM (-10.7*)	0.83
100	14 nM (-10.6*)	16 nM (-10.5*)	0.88
200	29 nM (-10.2*)	47 nM (-9.9*)	0.62
300	55 nM (-9.8*)	85 nM (-9.5*)	0.65

*Values reported in kcal/mol

Table 5.2: Effect of salt on $Na_v1.2_{IQp}$ binding to apo and (Ca^{2+})-CaM

CaM_{1-148}

[Salt], mM	apo K_d (KCl)	(Ca^{2+}) K_d (KCl)	apo/Ca^{2+}	apo K_d (NaCl)	(Ca^{2+}) K_d (NaCl)	apo/Ca^{2+}
100	≤10 nM (≤-10.8*)	≤10 nM (≤-10.8*)	1	≤1 nM (≤-10.8*)	≤51 nM (≤-9.8*)	0.02
300	≤85 nM (≤ -9.5*)	≤62 nM (≤-9.7*)	1.37	≤122 nM (≤ -9.3*)	≤170 nM (-≤9.1*)	0.71

CaM_{76-148}

[Salt], mM	apo K_d (KCl)	(Ca^{2+}) K_d (KCl)	apo/Ca^{2+}	apo K_d (NaCl)	(Ca^{2+}) K_d (NaCl)	apo/Ca^{2+}
100	≤1 nM (≤-10.8*)	≤1 nM (≤-10.8*)	1	--	--	--
300	1 ± 4 μM (-8.1* ±0.2)	2.8 ± 3 μM (-7.5* -±0.3)	0.36	--	--	--

*Values reported in kcal/mol

Table 5.3: Calculated effect of salt on $CaMKII_P$ binding to $(Ca^{2+})_4$-CaM_{1-148}

[Salt], mM	$\Delta G_{Electrostatic}$* (KCl)	$\Delta G_{Electrostatic}$* (NaCl)
0	-11.5	-11.5
25	-9.6	-9.3
50	-8.2	-7.8
75	-7.2	-6.8
100	-6.4	-5.9
150	-5.2	-4.6
200	-4.3	-3.7
300	-3.0	-2.4
400	-2.1	-1.5
500	-1.5	-0.9
600	-1.0	-0.4
700	-0.6	0.1
800	-0.2	0.4
900	0.1	0.7
1000	0.3	0.9

*Values reported in kcal/mol

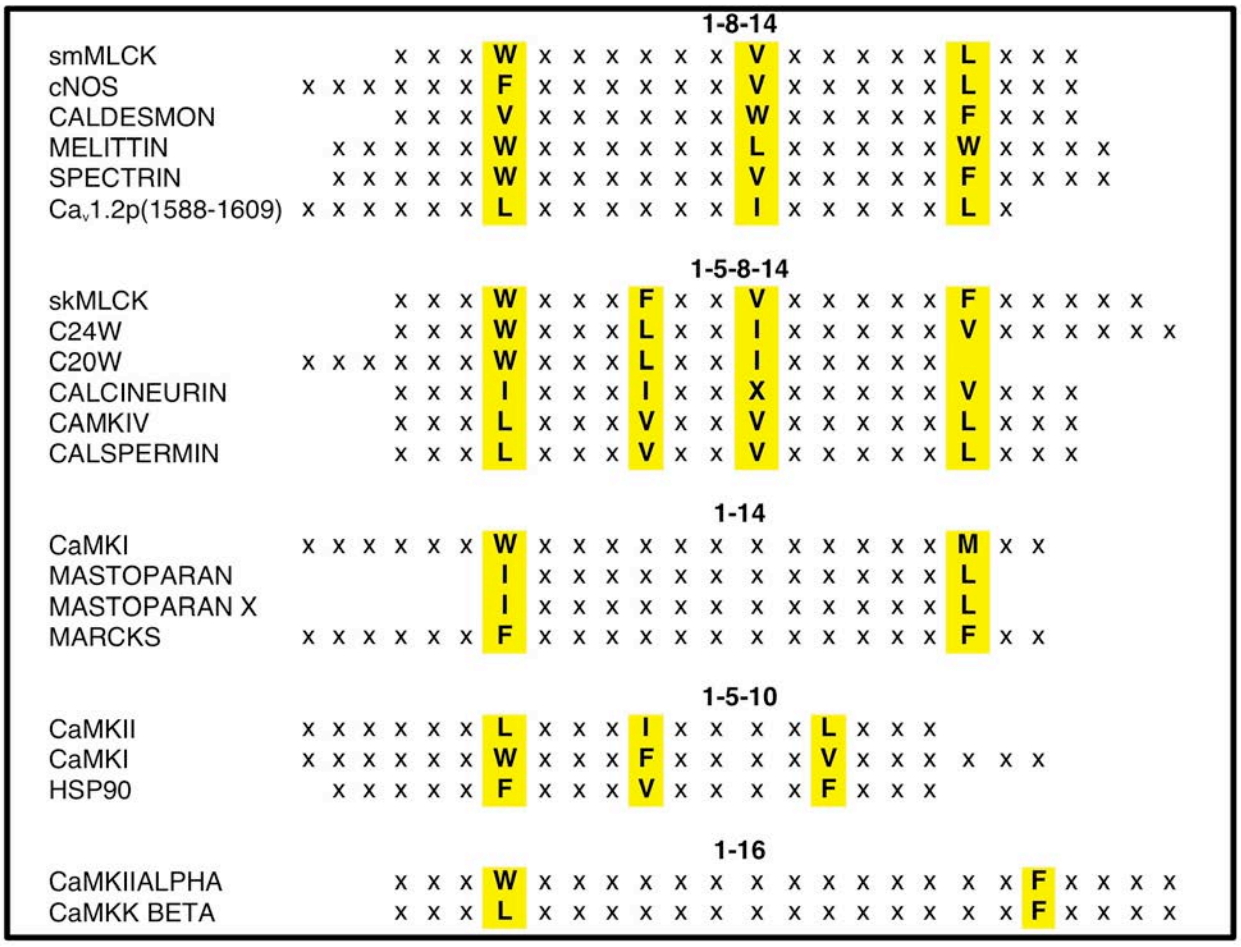

Modified from Yamniuk and Vogel, *Mol. Biotech.* (2004)

Figure 5.1: CaM-binding domains classified by residues used to interact with the N- and C-domain of CaM
Highlighted in yellow are the locations hydrophobic residues that insert into the hydrophobic pockets of CaM exposed upon Ca^{2+} binding. The spacing between these hydrophobic residues dictates the numerically derived name given to each CaMBD.
Users/nmr_mike/Thesis/Chapter_V/Figure5_1.jpg

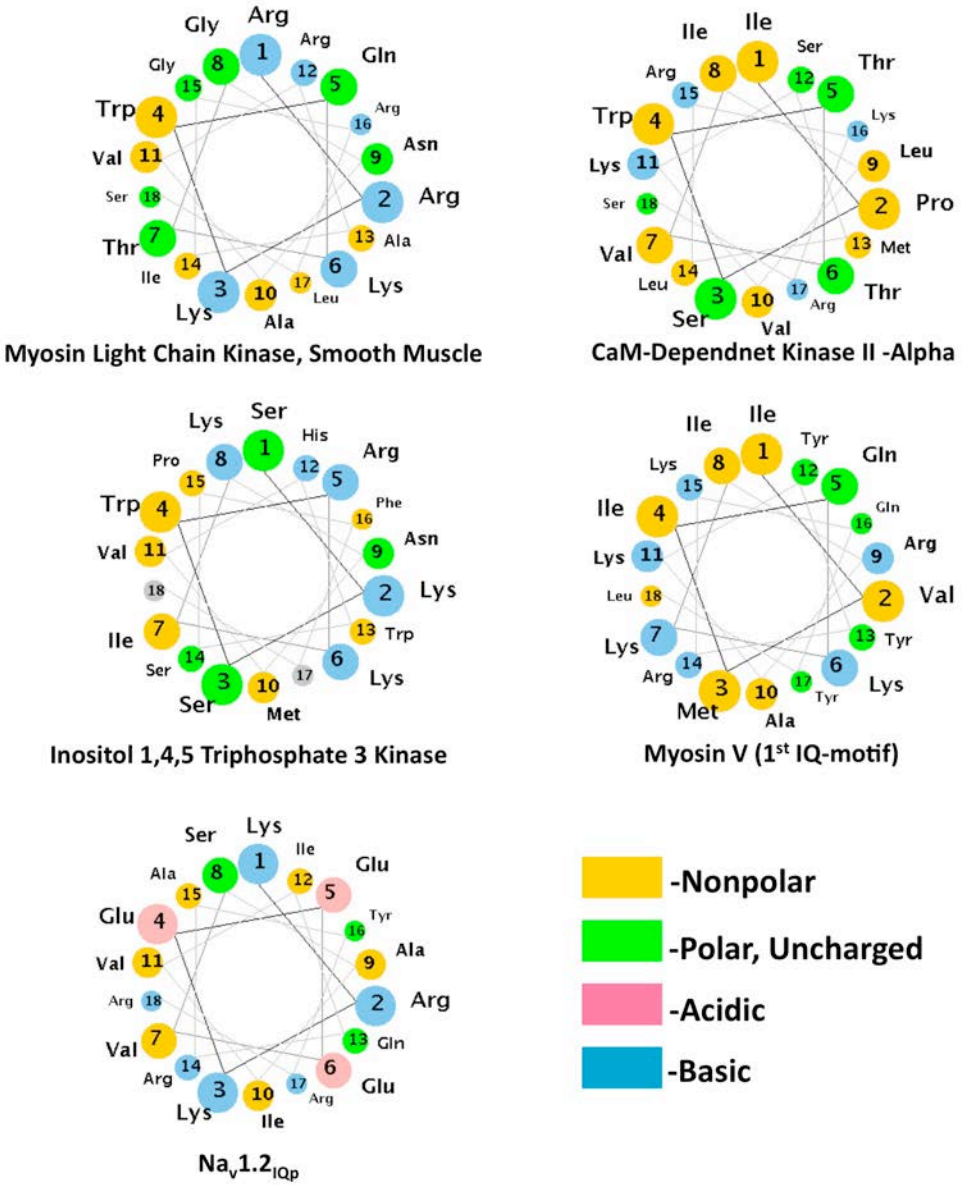

Figure 5.2: Helical Wheel Diagrams of CaM-Binding Domains
Helical wheel diagrams generated using University of Virginia applet http://cti.itc.virginia.edu/~cmg/Demo/wheel/wheelApp.html for various Ca^{2+}-dependent and Ca^{2+}-independent CaMBDs where nonpolar residues are colored according to the scheme depicted above.
Users/nmr_mike/Thesis/Chapter_V/Figure5_2.jpg

[Salt] (mM) in Cellular Environment

Ion	Outside (mM)	Inside (mM)	Ratio (Out/In)
Na^+	145.0	15.0	9.67
K^+	4.0	155.0	0.03
Ca^{2+}	1.5	0.1-0.01	15.0 - 150
Mg^{2+}	2.0	0.5	4.0
Cl^-	123.0	4.2	29.29

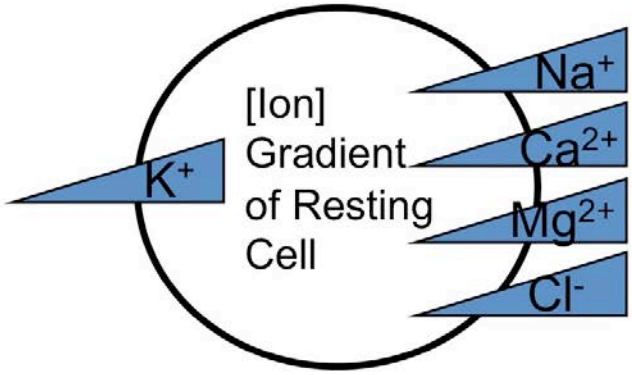

Figure 5.3: Intracellular and extracellular ion concentrations of a resting cell
Intracellular and extracellular ionic strengths of Na^+, K^+, Ca^{2+}, Mg^{2+}, and Cl^- ions are shown (top), while their concentration gradients across the membrane are qualitatively shown below. Upon membrane depolarization ion channels open to allow for ions to pass into or out of the cell dependent upon their concentration gradients (Hille et al. 2001).
Users/nmr_mike/Thesis/Chapter_V/Figure5_3.jpg

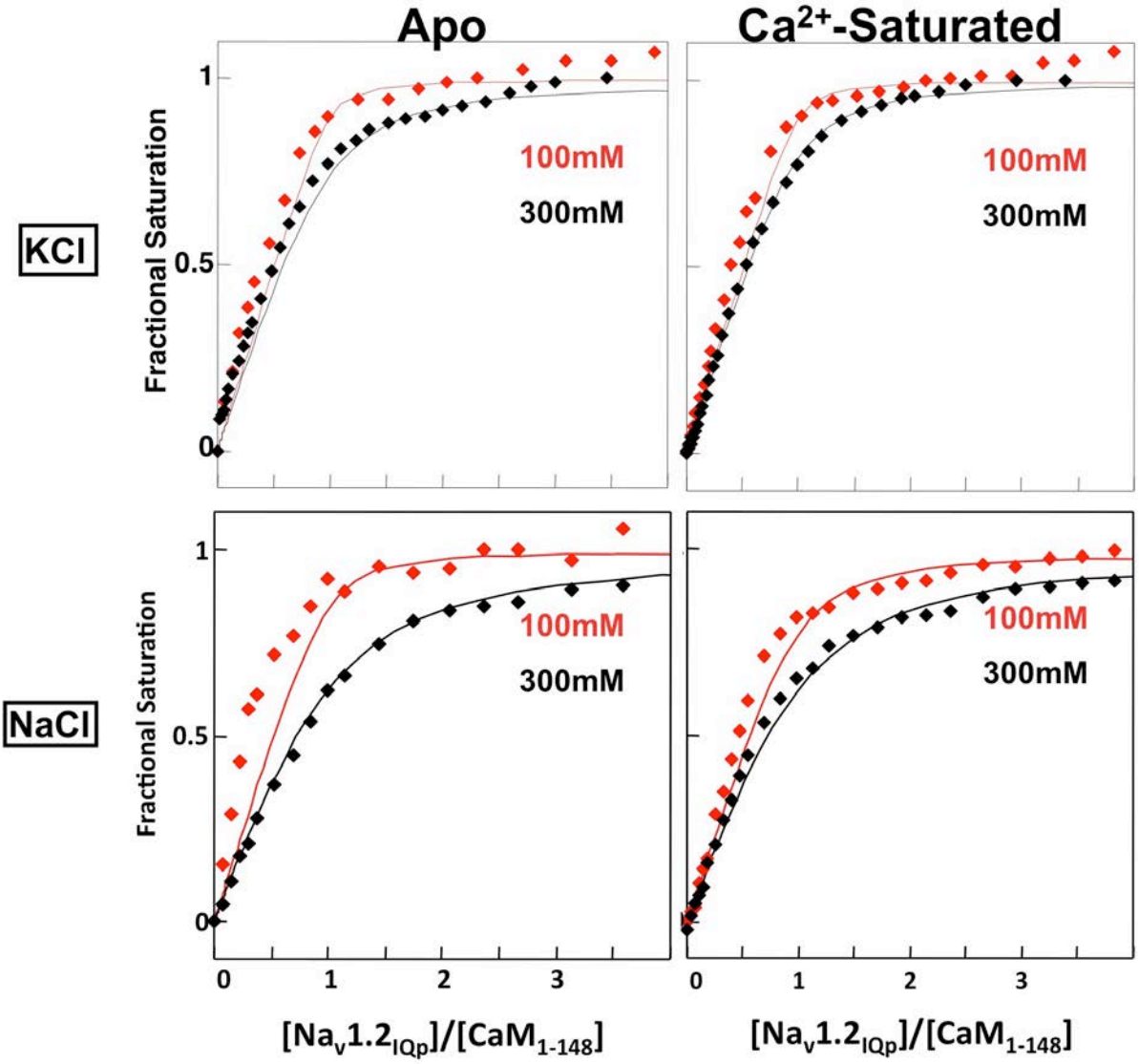

Figure 5.4: Apo or $(Ca^{2+})_4$-CaM_{1-148} titration of $Na_v1.2_{IQp}$ at varied [Salt]
Titrations of $Nav1.2_{IQp}$ with apo or $(Ca^{2+})_4$-CaM_{76-48} are shown. Titrations were conducted at 5 mM $CaCl_2$ or 50 μM EGTA for Ca^{2+}-saturating or apo trials respectively. Shown in red are trials performed at 100 mM [Salt], while trials shown in black were performed at 300 mM [Salt]
Users/nmr_mike/Thesis/Chapter_V/Figure5_4.jpg

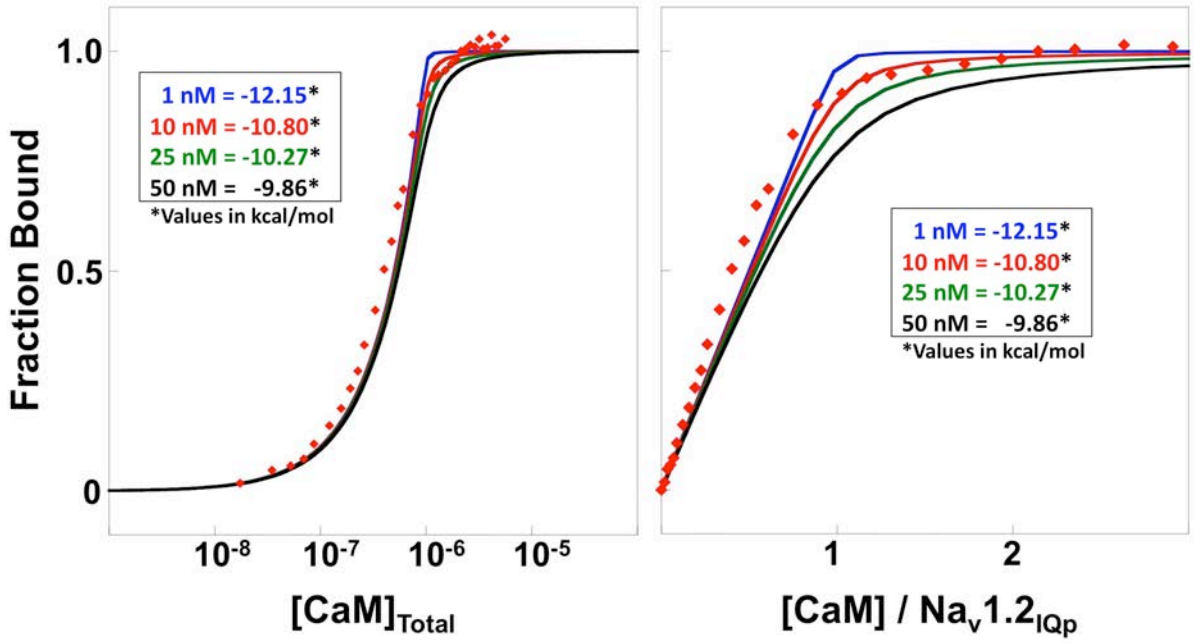

Figure 5.5: Simulated fitting curves used to determine $Na_v1.2_{IQp}$ binding affinity for CaM Both plots display identical data plotted in two different formats. $Na_v1.2_{IQp}$ binding to $(Ca^{2+})_4$-CaM_{1-148} (red diamonds) is shown on the left where the log $[CaM]_{Total}$ is plotted on the x-axis , while on the x-axis of the titration on the right the stoichiometry of [CaM] / $[Na_v1.2_{IQp}]$ is shown. Shown in solid lines are simulated binding curves at varied affinities/binding energies where the $[Na_v1.2_{IQp}]$ was set to 1μM. Note that when stoichiometic data is plotted on a log scale x-axis typically used for equilibrium binding curves that the difference between one possible fit or another is significantly reduced.
Users/nmr_mike/Thesis/Chapter_V/Figure5_5.jpg

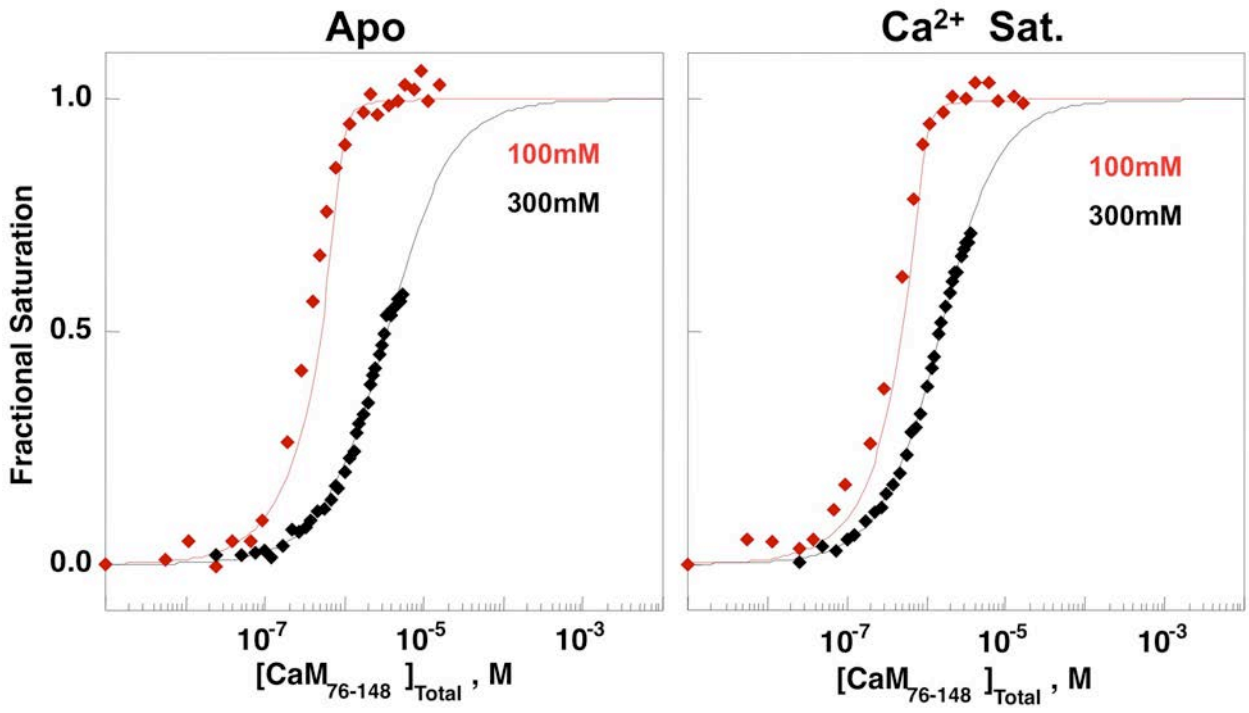

Figure 5.6: Apo or $(Ca^{2+})_2$-CaM_{76-148} titration of $Na_v1.2_{IQp}$ at varied [KCl]
Titrations of $Na_v1.2_{IQp}$ with apo or $(Ca^{2+})_4$-CaM_{76-48} are shown. Titrations were conducted at 5 mM $CaCl_2$ or 50 μM EGTA for Ca^{2+}-saturating or apo trials respectively. Shown in red are trials performed at 100 mM KCl, while trials shown in black were performed at 300 mM KCl.
Users/nmr_mike/Thesis/Chapter_V/Figure5_6.jpg

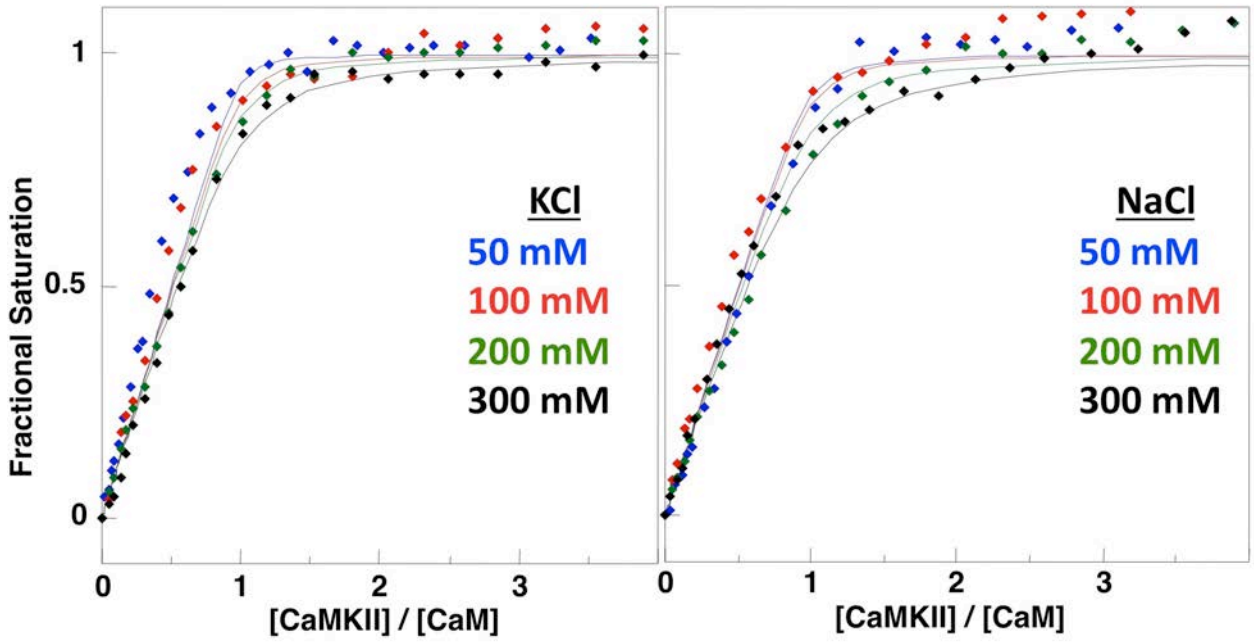

Figure 5.7: $(Ca^{2+})_4$-CaM_{1-148} titration of $CaMKII_p$ at varied [KCl] and [NaCl]
Titrations of $CaMKII_p$ with $(Ca^{2+})_4$-CaM_{1-48} are shown. Titrations were conducted at $CaCl_2$ concentrations of 5mM at 50 mM (blue), 100 mM (red), 200 mM (green), and 300 mM (black) NaCl or KCl.
Users/nmr_mike/Thesis/Chapter_V/Figure5_7.jpg

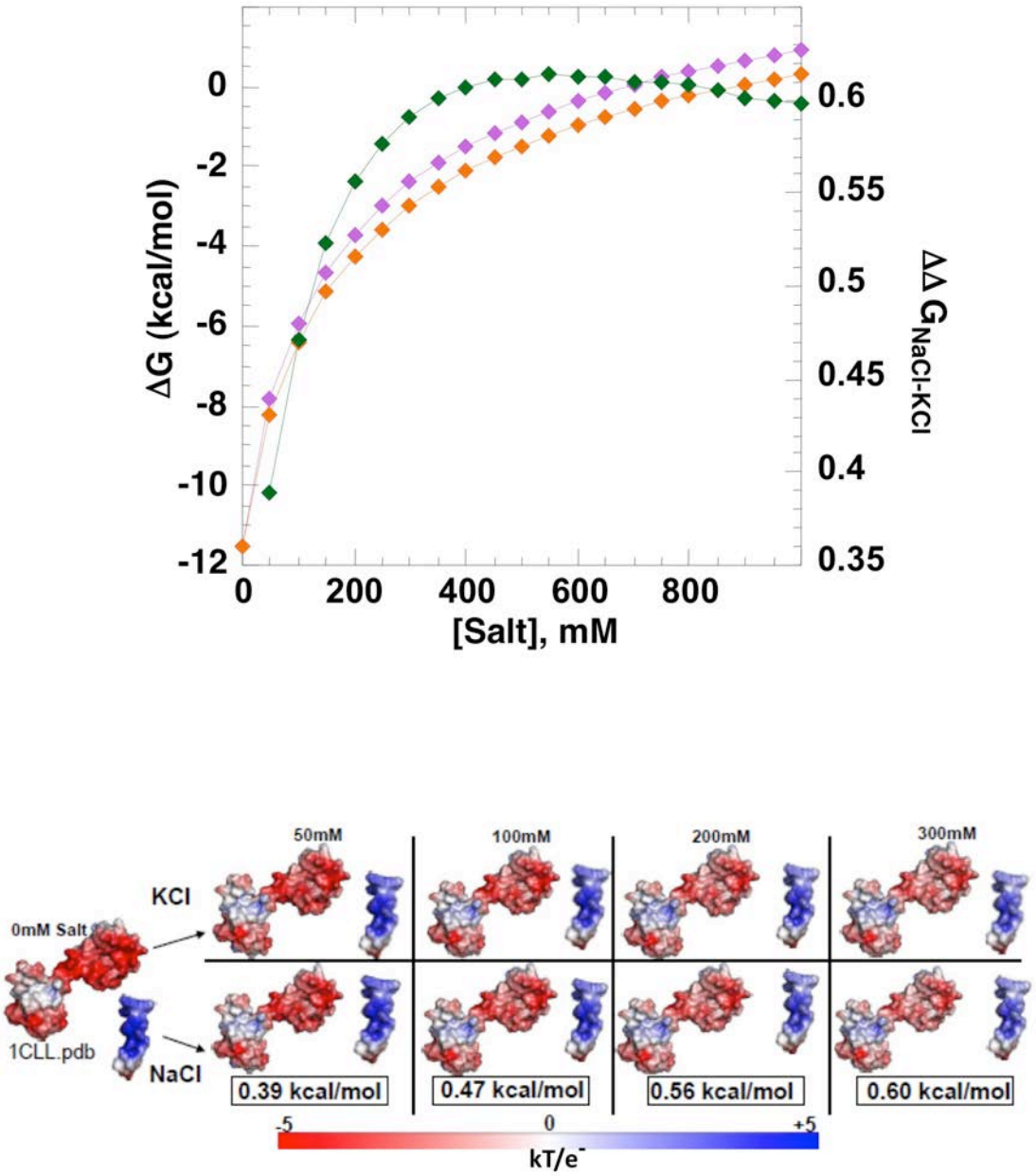

Figure 5.8: Calculated electrostatic binding energies of $CaMKII_p$ for $(Ca^{2+})_4$-CaM_{1-148}
A: Plotted change in $CaMKII_p$ affinity for $(Ca^{2+})_4$-CaM_{1-148} as a function of salt. Plotted on the primary Y-axis are APBS calculated electrostatic binding energies of $CaMKII_p$ for $(Ca^{2+})_4$-CaM_{1-148} as a function of [NaCl] (purple) or [KCl] (orange). Plotted on the secondary Y-axis is the difference between APBS calculated NaCl and KCl binding affinities at similar concentrations (green). **B:** Electrostatic surface potentials of $(Ca^{2+})_4$-CaM_{1-148} and $CaMKII_p$ at varied NaCl and KCl concentrations. Positive surface is colored in blue, while negative surface is shown in red.
Users/nmr_mike/Thesis/Chapter_V/Figure5_8.jpg

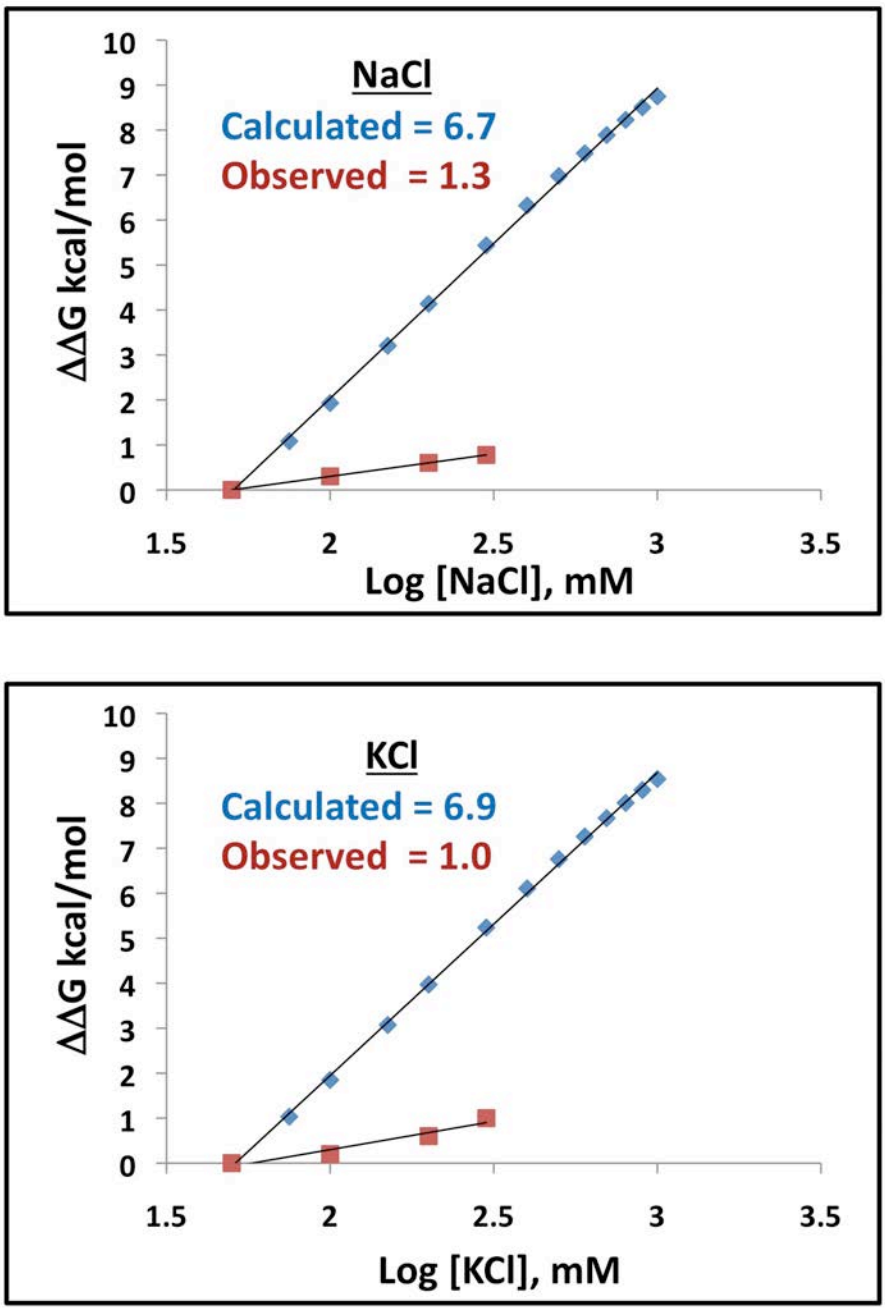

Figure 5.9: Comparison of calculated and observed changes in $CaMKII_p$ binding to $(Ca^{2+})_4$-CaM_{1-148} as a function of salt
Comparison of observed (red) and calculated (light blue) changes in the binding affinity of $CaMKII_p$ for $(Ca^{2+})_4$-CaM_{1-148} as a function of either [NaCl] (upper plot) or [KCl] (lower plot).
Users/nmr_mike/Thesis/Chapter_V/Figure5_9.jpg

CHAPTER VI

SUMMARY AND FUTURE DIRECTIONS

Thesis Summary

The interaction of apo CaM with targets is an emerging area of interest in the CaM research field where historically it was a widely held belief that only $(Ca^{2+})_4$-CaM bound and activated intracellular targets (Cheung, 1980; Klee and Haiech, 1980; Siegel, 1973). Numerous targets such as myosins, ion channels, and growth-associated proteins have been shown to interact with apo CaM via an IQ-motif (Black et al., 2005; Liu and Storm, 1990; Martin and Bayley, 2004; Shah et al., 2006). This thesis investigates how the anti-psychotic drug TFP, and $Na_v1.2_{IQp}$ interact with apo CaM at the molecular level to better understand how apo CaM recognizes and binds such diverse targets. A model of how CaM interacts with both of these targets is presented in **Figure 6.1**.

TFP Binding Induces a Biphasic Response in the Ca^{2+}-Binding Affinity of CaM

Nearly all targets that bind to CaM either naturally occurring or synthetic "tune" its Ca^{2+}-binding affinity in some manner (Peersen et al., 1997). Targets such as $CaMKII_p$, Calcineurin, and the Ryanodine receptor increase the Ca^{2+}-binding affinity of CaM, while IQ-motif containing proteins such as $Na_v1.2$ lower the Ca^{2+}-binding affinity of CaM (Evans and Shea, 2009; Newman and Shea, 2006; Quintana et al., 2005; Theoharis et al., 2008). Unlike these previously mentioned protein targets of CaM, the anti-psychotic drug TFP was shown in Chapter II to both increase and decrease the Ca^{2+}-binding affinity of CaM dependent upon the concentration of TFP examined. To our knowledge this is the first time this behavior has been observed with any allosteric effector of CaM.

The basis of the observed biphasic response can be found in the stoichiometry of TFP binding to CaM. We determined that there are 2 TFP binding sites (one per domain) in apo CaM, while there are 4 TFP binding sites in $(Ca^{2+})_4$-CaM. The TFP induced biphasic response in

Ca^{2+}-binding affinity results from each TFP site having a different binding affinity for apo and $(Ca^{2+})_4$-CaM as shown in Chapter II. TFP at ratios of 1:1 and 2:l have a more favorable binding affinity for apo CaM than $(Ca^{2+})_4$-CaM, and thus via allosteric linkage cause the Ca^{2+}-binding affinity of CaM to become less favorable. TFP:CaM ratios of 3:1 and 4:1, are achieved in the Ca^{2+}-bound state only, because of this the Ca^{2+}-bound state of CaM is selectively stabilized over the apo state resulting in a more favorable Ca^{2+}-binding affinity. To further probe the basis of this biphasic response, TFP titrations of $(Ca^{2+})_4$-CaM were performed. We observed biphasic responses in the chemical shift of residues located at the interface between the N- and C-domain of CaM as well as in residues in close (< 4 Å) proximity to multiple TFP binding sites, corroborating the biphasic response seen in Ca^{2+}-binding measurements.

CaM uses Distinct Interfaces to Bind TFP under apo and Ca^{2+}-Saturating Conditions

Ca^{2+}-titrations of CaM at multiple ratios of TFP performed in Chapter II, indicated that the Ca^{2+}-binding affinity of the C-domain of CaM was affected to a greater extent than that of the N-domain. It was clear in ^{15}N-HSQC spectra taken of TFP bound to apo and $(Ca^{2+})_4$-CaM that TFP induced non-equivalent chemical shifts which were dependent upon the Ca^{2+}-ligation state of CaM. Consistent with Ca^{2+}-titration data, quantification of N- and C-domain ^{15}N-HSQC chemical shifts of apo and $(Ca^{2+})_4$-CaM indicated that in both cases the C-domain of CaM was perturbed to a greater extent than the N-domain. These observations prompted structural studies using the isolated C-domain fragment (CaM_{76-148}) performed in Chapter III to gain insight into the differing molecular interfaces used by apo and $(Ca^{2+})_2$-CaM_{76-148} identified in Chapter II.

The crystal structure of TFP bound to $(Ca^{2+})_2$-CaM_{76-148} directly reveals the molecular binding interface and conformation used by $(Ca^{2+})_2$-CaM_{76-148} when binding TFP. In this structure $(Ca^{2+})_2$-CaM_{76-148} adopts an “open” domain conformation observed in all structures of $(Ca^{2+})_4$-CaM alone or when bound to a target. The TFP binding site is located within the hydrophobic pocket of $(Ca^{2+})_2$-CaM_{76-148} and contacts the FLMM tetrad of residues, both

common features seen in all structures of $(Ca^{2+})_2$-CaM_{76-148} bound to protein or drug targets (Ataman et al., 2007). A unique feature of this structure was that 2 chains of $(Ca^{2+})_2$-CaM_{76-148} were found within the unit cell, and formed a pseudo ellipsoidal structure typically observed when the N- and C-domain of $(Ca^{2+})_4$-CaM_{1-148} bind a target. A desirable future set of experiments would be to determine the ^{1}H, ^{15}N, and ^{13}C assignments of TFP-bound $(Ca^{2+})_2$-CaM_{76-148} to use NMR spectroscopy to observe changes in dynamics upon TFP binding, and compare these changes with areas of chains A and B that differ structurally. This comparison will serve as an orthogonal approach to validate the structural changes observed between chains A and B of $(Ca^{2+})_2$-CaM_{76-148} when bound to TFP, as well as allow for T_1 and T_2 experiments to verify its oligomeric state.

NMR studies of residue-specific changes induced upon TFP binding to apo CaM_{76-148} performed in **Chapter III** indicated that significant structural changes occurred within apo CaM_{76-148} as TFP binds. These residue-specific changes were then mapped to a structure of apo CaM_{76-148} determined in the absences of TFP and clustered onto helices F-H as well as the Ca^{2+}-binding loops. Hydrophobic residues dominate TFP binding perturbed resonances within helices F-H, while polar residues are perturbed in the Ca^{2+}-binding loops. The chemical shifts induced upon TFP addition to apo CaM_{76-148} are most likely a result of 2 different phenomena: 1) direct TFP binding or 2) allosteric linkage. Due to the chemical properties of TFP (hydrophobic small molecule) we hypothesize that TFP interacts directly with hydrophobic residues contained within helices F-H, while it allosterically alters the chemical shifts of the Ca^{2+}-binding loops. Evidence to support this claim was shown in **Chapter II** in which TFP was shown to allosterically alter the Ca^{2+}-binding affinity of CaM_{76-148}, and that it is unlikely that TFP directly competes with Ca^{2+} within the Ca^{2+}-binding loops of CaM_{76-148}.

Although TFP significantly perturbed apo CaM_{76-148} upon binding, the magnitude of change in chemical shifts was much smaller than those observed for TFP binding to C-domain of CaM_{1-148}, suggesting a smaller conformational change occurs under apo conditions. The only conformation observed of the C-domain of apo CaM or CaM-like proteins when bound to a

target has been that of the "semi-open" conformation. We hypothesize that a "semi-open" conformation is used by apo CaM_{76-148} when binding TFP, as this conformation (consistent with magnitude of ^{15}N-HSQC shifts) requires less structural rearrangement than the "open" conformation. The adoption of a "semi-open" conformation is also evidenced by the slight decrease in T_2 relaxation time upon addition of TFP to apo CaM_{76-148}, indicative of a slight increase in molecular size. Future studies are proposed to determine changes in T_2 relaxation rates upon TFP binding to $(Ca^{2+})_2$-CaM_{76-148}. These values would help to confirm that the rate of molecular tumbling due to changes in the hydrodynamic radius of TFP-bound apo CaM_{76-148} is faster that of TFP-bound $(Ca^{2+})_2$-CaM_{76-148}. It is anticipated that the average T_2 rate of apo CaM > TFP-bound apo CaM_{76-148} > TFP-bound $(Ca^{2+})_2$-CaM_{76-148}.

To definitively confirm that CaM uses distinct interfaces to bind TFP under apo and Ca^{2+}-saturating conditions high resolution 3 dimensional structures are required. To this end the we have determined the $(Ca^{2+})_2$-CaM_{76-148} adopts an "open" conformation via x-ray crystallography. The future goal of the work described in Chapter III is to determine the solution structure of TFP bound to apo CaM_{76-148}. These NMR data have been collected and are awaiting assignment and analysis for calculation the structure of TFP bound to apo CaM_{76-148}..

Conservation of Carboxamide-Containing Side chains in apo CaM Binding Motifs

Studies presented in Chapter IV indicated the "semi-open" domain conformation is used by the C-domain of CaM and CaM-like proteins when interacting with targets under apo conditions. The structure of the SK-channel bound to a partially Ca^{2+}-saturated CaM shows that an IQ-motif is not necessary for binding of the C-domain of apo CaM (Figure 4.9) (Schumacher et al., 2004). The one structural feature observed that was conserved by all apo CaM binding motifs was a Gln or Asn residue whose carboxamide-containing side chain was used to make 2 hydrogen bonds to atoms found in the backbone of residues 112 and 114 located within the loop connecting helices F and G of CaM (Figure 4.9).

To examine the necessity of this hydrogen bonding network for apo C-domain binding additional studies are proposed in which mutations of either Gln→Glu ($Na_v1.2_{IQp}$) or Asn→Asp (SK-Channel) will be made at the Q position of the IQ-motif followed by fluorescence anisotropy monitored binding studies. These mutants would test whether 2 hydrogen bonds are required for apo binding of the C-domain of CaM. The aforementioned study (dependent upon the results) could be repeated except instead of Gln→Glu or Asn→Asp mutations, a Glu or Asn →Ala mutation would be made that completely removes the observed hydrogen bond network between apo CaM and the target peptide.

Changes in the Electrostatic Environment of CaM Alters its Interaction with Targets

Studies shown in **Chapter V** indicate that increasing the concentration of NaCl or KCl in solution lowers the affinity of CaM for its target, due to the screening of electrostatic interactions between CaM and the peptide target. Perturbation of the local electrostatic environment of CaM can also be performed by introducing point mutations that introduce, remove or reverse the intrinsic charge of an amino acid. Structural changes due to this type of perturbation of the electrostatic environment of CaM, will be examined with CaM mutants D95G and H135R. These mutants were identified via a genetic screen of viable *Paramecia* that exhibited abnormal chemotactic behavior resulting from impaired ion channel function (Kung et al., 1992; Ling et al., 1992). Exploratory studies of D95G and H135R have identified these over-reactive mutants as ideal candidates for structural studies. $(Ca^{2+})_2$-$CaM_{76\text{-}148}$ H135R was crystallized and diffracted to 2.2 Å, while the ^{15}N-HSQC spectrum of D95G $(Ca^{2+})_2$-$CaM_{76\text{-}148}$ bound to $Na_v1.2_{IQp}$ showed excellent peak dispersion (Figure 6.2).

Future endeavors to determine to these high-resolution structures will allow for direct observations to be made of the effect of D95G or H135R on CaM alone or when in complex with $Na_v1.2_{IQp}$. Either of these structures would be the first of their kind to have been determined from the genetic screen of viable *Paramecium* mutants. These structures would lay the

groundwork for structural based conclusions to be made as to the molecular basis of the altered chemotactic behavior observed in *Paramecium* mutants.

Future Studies

Changes in Met 144 Dynamics upon Binding $(Ca^{2+})_2$-CaM_{76-148}

The residue M144 has previously been identified to adopt the most variable conformations when bound to a target of the FLMM tetrad residues, as well as being the least conserved FLMM tetrad residue in 102 CaM sequences from other species. Studies presented in Chapter III indicated that the side chain dynamics of M144 play a key role in selecting the orientation of TFP within the hydrophobic cleft of $(Ca^{2+})_2$-CaM_{76-148}. To investigate this observation further, ^{13}C-methyl relaxation experiments are proposed to examine changes in relaxation rates of $(Ca^{2+})_2$-CaM_{76-148} upon binding TFP (Palmer, 2001; Wand, 2001). This data would help to clarify at a finer level of detail the amount of molecular motion present within the TFP-binding site of $(Ca^{2+})_2$-CaM_{76-148} as x-ray crystallography only provide static images.

This data could then be incorporated into small molecule docking simulations of drugs to CaM in which highly dynamic residues would be allowed to be flexible, instead of being held rigid as is often done for all residues in docking simulations. This treatment would allow for a more realistic docking simulation to be run, yet be less computationally taxing than allowing all-atom flexibility. On a larger scale, incorporation of *in vitro* data into virtual docking simulations of lead compounds against hub-proteins such as CaM, may benefit pharmaceutical discovery in which off target effects are not desired. Virtual screening of a compound library against every known protein structure is considerably more computationally expensive than screening against a select set of hub-proteins who regulate a myriad of downstream targets. *In silico* identification of compounds that alter the function of hub-proteins such as CaM would save in the cost of bringing a compound to clinical trials by identifying a drug or drugs whose interaction with a network of regulatory pathways could result in an undesired off-target effect.

Determination of Binding Site for N-domain of $(Ca^{2+})_4$-CaM on $Na_v1.2$

Studies presented in **Chapter IV** determined that the N-domain of $(Ca^{2+})_4$-CaM does not bind to $Na_v1.2_{IQp}$, indicating that there is likely to be binding site for the N-domain of $(Ca^{2+})_4$-CaM located in another region of $Na_v1.2$. Future studies will build off of the observations made in Chapter IV by using a peptide array. This array will be composed of overlapping 30-residue peptide sequences derived from the cytoplasmic face of $Na_v1.2$. Following initial identification of a putative N-domain $Na_v1.2$ binding sequence ($Na_v1.2_N$) FRET will be used to confirm that donor-acceptor labeled peptides corresponding to $Na_v1.2_{IQp,}$ and $Na_v1.2_N$ are capable of simultaneously binding to the N- and C-domain of $(Ca^{2+})_4$-CaM. Lastly, comparison of patch clamp currents of $Na_v1.2$ channel mutants in the area of $Na_v1.2_N$, as well as the use of CaM mutants deficient in N-domain Ca^{2+}-binding will be used to verify functional role binding to the N-domain of $(Ca^{2+})_4$-CaM.

Circular Permutation of Charge Residues in $Na_v1.2_{IQp}$

An IQ-motif peptide derived from another sodium channel variant ($Na_v1.5_{IQp}$) is homologous (78%) to $Na_v1.2_{IQp}$ yet binds with a 16-fold lower affinity to Apo-CaM and 200-fold lower affinity to $(Ca^{2+})_4$-CaM than $Na_v1.2_{IQp}$ (Shah et al., 2006). The most notable difference between the two to account for these differences is their charge distribution and overall net charge (**Figure 6.3**). To investigate the role that charge distribution has on the affinity of apo and Ca^{2+}-CaM, charged residues of the $Na_v1.2_{IQp}$ will be mutated. Initially charged residues of the $Na_v1.2_{IQp}$ which are not conserved when compared to $Na_v1.5_{IQp}$ will be mutated to their $Na_v1.5_{IQp}$ counterpart. The effect of the mutant $Na_v1.2_{IQp}$ on its affinity for CaM and effect on Ca^{2+} binding by CaM will then be measured to clarify how apo- and (Ca^{2+})-CaM interact. Pinpointing and then mutating key areas of the $Na_v1.2_{IQp}$ -CaM interface will explain on a molecular level how the Ca^{2+}-affinity of the domains of CaM are "tuned" to perform their physiological functions when bound to IQ-motifs of sodium channel variants (**Figure 1.8**)

In Vitro Evolution of apo CaM Binding IQ-motifs

A fascinating aspect of the IQ-motif (Figure 4.1a) is that with the exception of the Q, it is similar in amino acid composition and spacing with a 1-8-14 BAA motif known to only interact with $(Ca^{2+})_4$-CaM (Yap et al., 2000). Although the IQ-motif as a whole has been characterized to preferentially interact with apo CaM, exceptions to this statement have been observed for IQ motifs found in $Na_v1.5$ and $Ca_v1.2$ ion channels in which more favorable IQ-motif binding is observed for $(Ca^{2+})_4$- than apo CaM (Shah et al., 2006). To explore the sequence requirements of target binding to CaM, phage display will be used to evolve peptide target sequences or varying affinity to apo and $(Ca^{2+})_4$-CaM to.

The selection pool will be composed of a phage library in which unconserved positions of the IQ-motif will be fully randomized at positions indicated with an "X" in the following sequence [x(Q/N)xxx(K/R)xxxx(K/R)], while positions in parenthesis will only carry a binary randomization. Bio-panning will first be carried out against immobilized CaM where initial wash steps will include EGTA to insure enrichment of apo CaM binding sequences. In the last biopanning selection round prior to sequencing, the phage library will be split and selected against either apo or $(Ca^{2+})_4$-CaM using either an EGTA or Ca^{2+} final wash step. After phage sequencing, comparison of these two groups will be made to identify sequences (if any) that only bind to apo CaM, as well as those that are capable of binding both apo and $(Ca^{2+})_4$-CaM. This process will be repeated again with the exception that initial bio-panning will be done in the presence of Ca^{2+} instead of EGTA, to evolve IQ-motif sequences that preferentially bind $(Ca^{2+})_4$-CaM (Figure 6.4) The final result will be 4 pools of CaM binding motifs consisting of sequences that: only bind (Ca^{2+})-CaM, bind apo and $(Ca^{2+})_4$-CaM with preference for $(Ca^{2+})_4$-CaM, bind apo and $(Ca^{2+})_4$-CaM with preference for apo CaM, and sequences that only bind apo CaM.

The results from these experiments would help to resolve uncertainties as to what the sequence determinants of IQ-motifs are that allow them to tune their affinity for the multiple

Ca^{2+}-ligation states of CaM. Comparison of *in vitro* evolutionary results with those of phylogenic trees of IQ-motifs evolved *in vivo* will also provide insight into what evolutionary pressures produced naturally occurring IQ-motifs whose evolution are a result of selection pressure of multiple simultaneous factors.

Examination of Naturally Occurring $Na_v1.2_{IQp}$ R1902C Mutation on CaM

The sodium channel variants contain naturally occurring mutations distributed along multiple areas of the channel sequence that are genetically linked to human disorders. One such mutation R1902C is located within the IQ-motif of $Na_v1.2$ and is associated with familial autism (Weiss et al., 2003). Future studies are proposed to determine if the R1902C mutation alters previously determined Ca^{2+}-binding affinity values of CaM when bound to Wt-$Na_v1.2$, as well as to determine how this mutation alters the binding affinity of $Na_v1.2$ to CaM. Structural studies (SAXS, NMR, or X-ray crystallography) are proposed in combination with other biophysical measurements and techniques (CD, analytical ultracentrifugation, and stokes radius) to determine how R1902C may alter the CaM-$Na_v1.2_{IQp}$ complex. It is well known that binding of targets "tune" the Ca^{2+}-binding affinity of CaM, these investigations may provide the 1st example of how alteration of tuned affinities of CaM result in a human disorder. A better understanding of the fundamental molecular basis of this disorder may aid in improved treatment therapies for individuals carrying the R1902C mutation.

Structure Determination of Larger Intracellular Fragments of $Na_v1.2$ in Complex with CaM

Structural studies involving CaM bound to peptides derived from target proteins have proven useful in the dissection of the molecular interactions made upon binding. Although valuable, these studies fail to capture the overall structural changes that occur within the entire macromolecular complex that result in their function. This lack of overall mechanistic detail is likely to be most pronounced in IQ-motif containing targets such as $Na_v1.2$ where CaM is an

intrinsic subunit under both apo and Ca^{2+}-saturating conditions. Ideally, to fully understand how CaM regulates $Na_v1.2$ gating to allow passage of Na^+ ions across cellular membranes, structures of $Na_v1.2$ bound to CaM in all of their physiologically relevant states are required. Given that the determination of the structure of $Na_v1.2$ represents a significant challenge that has yet to be overcome by structural biologists, it is unlikely that in the near future structures of apo and $(Ca^{2+})_4$-CaM bound to $Na_v1.2$ will be determined. A more tractable path to uncover a deeper mechanistic understanding of how $Na_v1.2$ is regulated by CaM beyond that of peptide studies might be found in structural studies involving intracellular domains of $Na_v1.2$ identified to bind CaM. The IQ-motif of $Na_v1.2$ is found within a larger domain of $Na_v1.2$ theorized to be composed of 6 α-helices, while studies shown in **Chapter 4** indicated that a region outside of $Na_v1.2_{IQp}$ interacted with the N-domain of CaM. For these reasons, future structural studies are proposed to determine the structure of apo and $(Ca^{2+})_4$-CaM bound to $Na_v1.2_{IQp}$ in the context of the entire C-terminal domain of $Na_v1.2$. It is also proposed that dependent upon studies to determine the portion of $Na_v1.2$ that binds the N-domain of CaM, that this segment be included as well. These proposed studies would help to establish spatial constrains upon where intracellular regions of $Na_v1.2$ are located under apo and Ca^{2+}-saturating conditions.

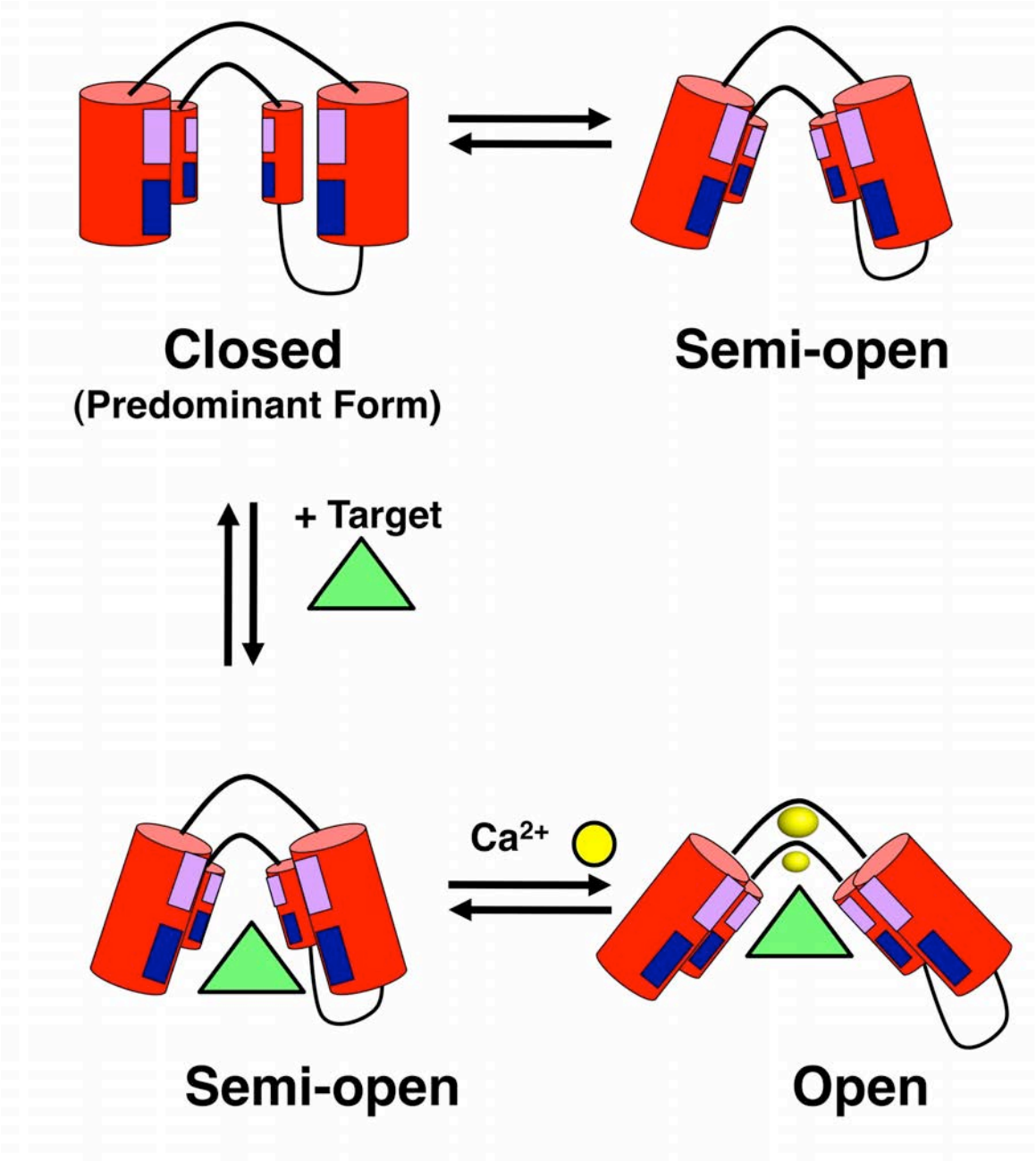

Figure 6.1: Model of apo and $(Ca^{2+})_4$-CaM C-domain conformations used when binding targets The C-domain of CaM is represented as red cylinders which contain two distinct binding surfaces. The purple surface located near the perimeter of the hydrophobic cleft of CaM is used for target (green triangle) binding under apo conditions, while the light purple surface is used when the C-domain is Ca^{2+}-saturated.
Users/nmr_mike/Thesis/Chapter_VI/Figure6_1.jpg

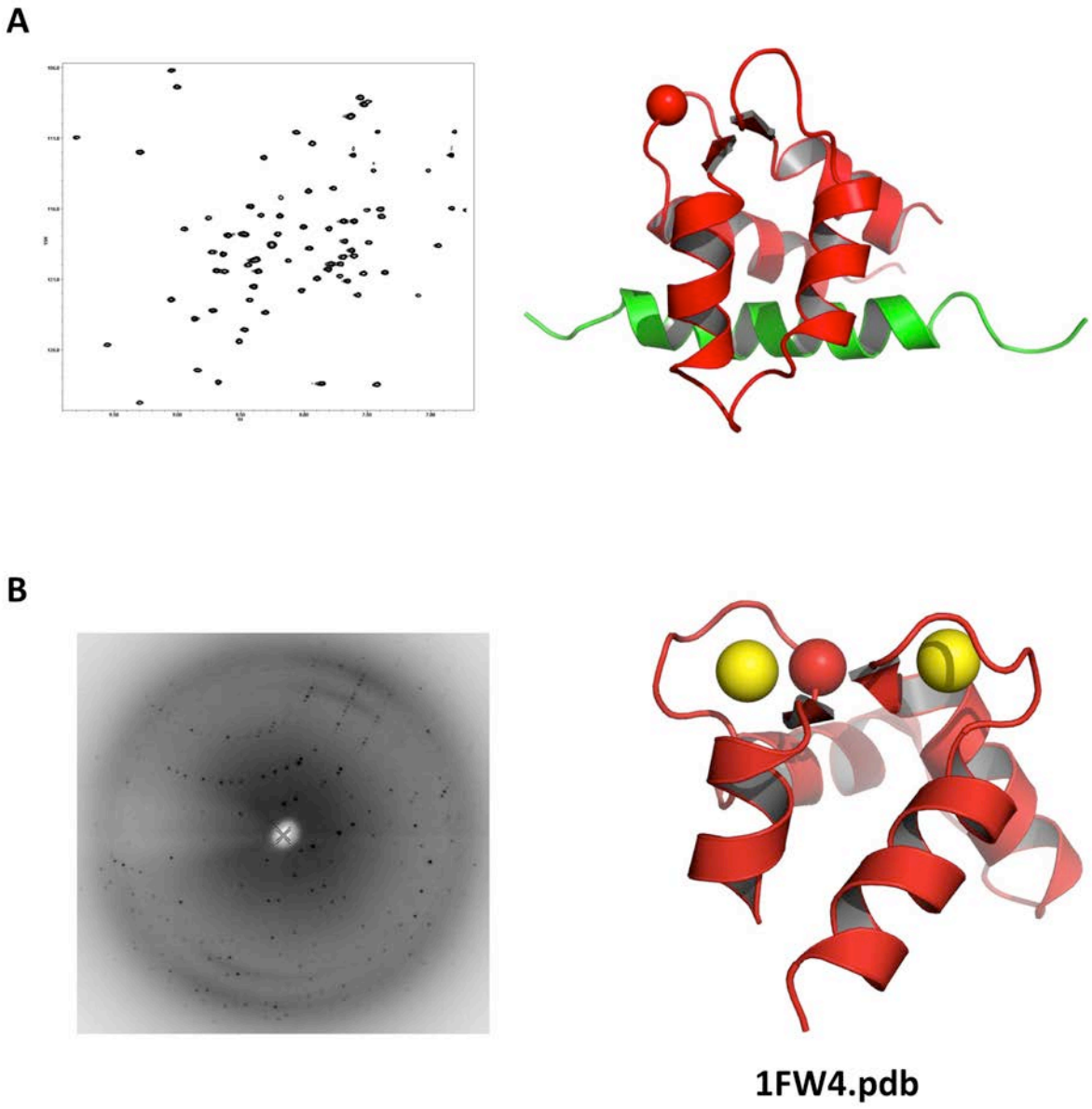

Figure 6.2: ^{15}N-HSQC Spectrum and diffraction image of PCaM Mutants
A: ^{15}N-HSQC spectrum of D95G apo $CaM_{76\text{-}148}$ (red) Bound to $Na_v1.2_{IQp}$ (green), where the location of the D95G mutation is indicated by a red sphere. **B:** Diffraction image of H135R $(Ca^{2+})_2$-$CaM_{76\text{-}148}$. The location of the H135R mutation is shown as a red sphere on the structure of Wt-$CaM_{78\text{-}148}$ (red) where Ca^{2+}-ions are colored yellow.
Users/nmr_mike/Thesis/Chapter_VI/Figure6_2.jpg

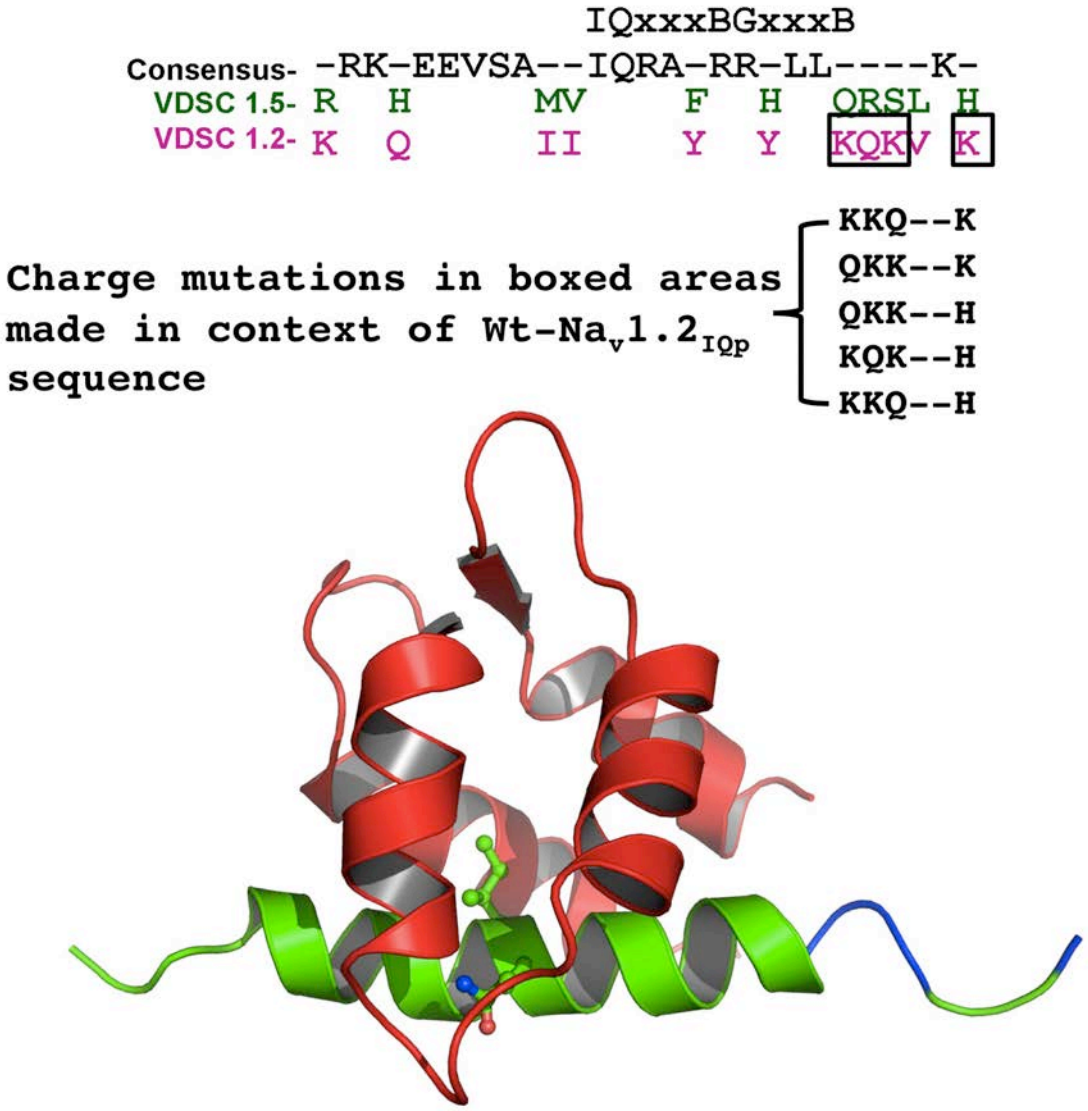

Figure 6.3: Sequence alignment of $Na_v1.2$ and $Na_v1.5$ IQ-motifs
The IQ-motifs of $Na_v1.2$ and $Na_v1.5$ are shown in green and magenta respectively. Boxed areas represent positions that differ in charge, sequences below represent circular permutations of charged residues of $Na_v1.2_{IQp}$ that well be examined via Ca^{2+} titration and fluorescence anisotropy to monitor changes in Ca^{2+} and peptide-binding affinity of CaM.
Users/nmr_mike/Thesis/Chapter_VI/Figure6_3.jpg

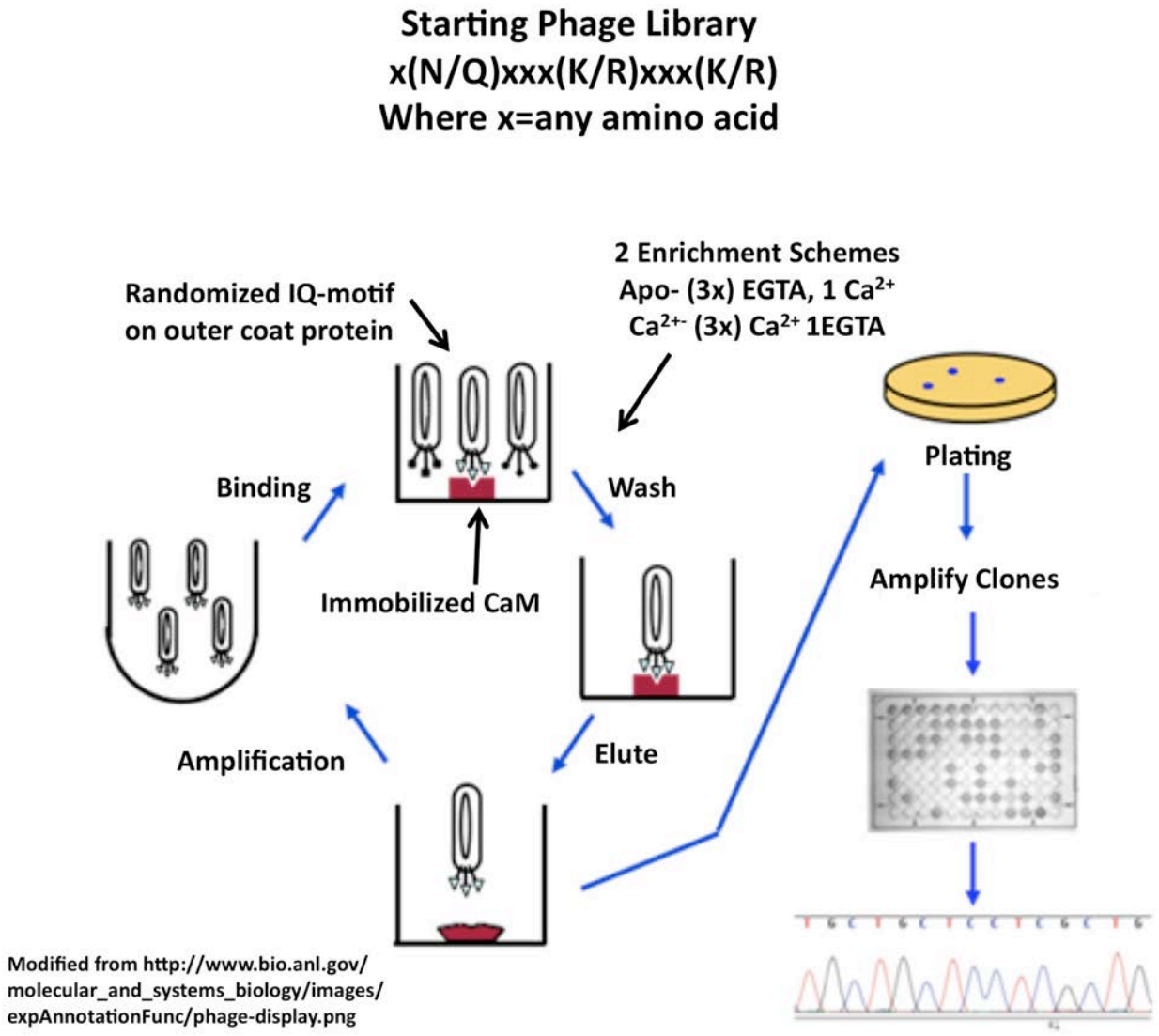

Figure 6.4: Schematic of phage display selection procedure
An initial phage library will be generated and enriched to produce IQ-motifs which either selectively bind to apo or $(Ca^{2+})_4$-CaM.
Users/nmr_mike/Thesis/Chapter_VI/Figure6_4.jpg

APPENDIX A

FORTRAN FUNCTION FOR FITTING FLUORESCENCE ANISOTROPY DATA TO A SIMPLE LANGMUIR BINDING ISOTHERM

The following Fortran function was used in nonlinear least squares analysis of the fluorescence anisotropy data presented in **Chapter II** and **Chapter IV**. Fits using this function were used to determine the association constant of CaM for a synthetic peptide represent the CaM-binding domain of $Na_v1.2_{IQp}$ or $CaMKII_P$. This equation fits to a one-site binding model (**Equation A.1**), using the total concentration of CaM at each point.

$$\overline{Y} = \frac{K_a[X]}{1 + K_a[X]} \qquad (A.1)$$

```
Function FX( Ans, X, ydum, ierr, n)
*
*   fxYvsXt1K.f
*
*   Function for fitting ligand binding to macromolecule
*   when total ligand, rather than free ligand,
*   concentration is known.
*      Model of binding:  Monomer binding to equal and
*           independent site(s).
*      Number of Sites:   Set by ans parameter ans(3)
*       Original function name:  &FNWT1 <831018.1019>
*
*   The ANS vector has the following form:
*     ANS(1) = macromolecule total concentration
*     ANS(2) = Association binding constant for ligand to
*                          macromolecule
*     ANS(3) = N, number of independent sites on
*                          macromolecule
*     ANS(4) = Endpoint at Low X
*     ANS(5) = Endpoint at High X
*
      Real Ans(5), K, MKS

      F = 1.E-7*X   ! free ligand is approximated as a
                                  fraction of total
      MKS = Ans(1)*Ans(2)*Ans(3)
      K   = Ans(2)
```

```
      EndLowX = Ans(4)
      EndHighX = Ans(5)
      Span = EndHighX - EndLowX

      Do 10 i = 1, 500
      gf = -X + F + MKS*F/(1.+K*F)
      gf1 = 1. + MKS/(1.+K*F)/(1.+K*F)
      fold = f
      F = F -gf/gf1

      If(Abs(Fold/F - 1.).lt.1.E-5) Go to 11

10    Continue

11    Fx = EndLowX + Span * F*K/(1.+F*K)

      Return
      End


      SUBROUTINE START(NAME,MAXP,DNAME,MAXD,MAXV)
C
C       THIS ROUTINE IS USED TO SET THE VARIABLE NAMES FOR C          THE
PARAMETERS. THESE NAMES MUST CORRESPOND TO
C            THE VARIABLES USED IN THE FX ROUTINE.

      CHARACTER*8 NAME(5),NAMES(5)
      CHARACTER*8 DNAME(1),DNAMES(1)
      DATA NAMES/'[Mtotal]','Ka (M)  ','# sites ','EndLowX','EndHighX'/
      DATA DNAMES/'dG@22C'/
C
      MAXV=1
C     maxv is the # of independent variables for the fit.
C          This is usually set to 1.  However, to fit multiple  C  sets of data it could be set to 2.  The
second vector C            of X values can then be used to specify which
C     data set is actually being fit. If this is greater
C          than 1 then X in the FX routine must be dimensioned
C          appropriately.
C
      MAXP=5
C          maxp is the # of parameters in model being fit by
C          these routines.
      DO 10 I=1,MAXP
   10 NAME(I)=NAMES(I)
C          NAME is the names of the actual fitting parameters.
```

```
      MAXD=1
C MAXD specifies the number of derived parameters.  A
C derived parameter is simply a quantity that you wish
C evaluated from the fitting answers after the fit is
C finished.  By using this feature the program will
C complete the actual error propagation for the derived
C parameters.  In the current example, we calculate the
C free energy from the Kd.
c
      DO 110 I=1,MAXD
  110  DNAME(I)=DNAMES(I)
c DNAME is the names of the derived parameters.

      RETURN
      END


      subroutine derive(old,new)
C    This routine is used to map the OLD (fitted)
C         parameters into the desired derived (NEW) parameters.
c
       real old(3),new(1)
        new(1) = -0.58646 * 2.303 * alog10(old(2))  !RT at 22C
       return

       end
```

APPENDIX B

FORTRAN FUNCTION FOR ANALYSIS OF CALCIUM-DEPENDENT CHANGES IN FLUORESCENCE THAT DESCRIBE FILLING OF ONLY TWO SITES

The following Fortran function was used for nonlinear least squares analysis to determine the free energies of calcium binding to CaM from calcium-dependent changes in fluorescence during equilibrium calcium titrations. This function uses a model-independent two-site equation (**Equation B.1**) that describes potentially heterogeneous, cooperative sites.

$$\overline{Y} = \frac{K_1[X] + 2K_2[X]^2}{2(1 + K_1[X] + K_2[X]^2)} \qquad \text{(B.1)}$$

```
    FUNCTION FX(ANS,X,Y,INDEX,N)
**********************************************************
*  FX2s2K.mpf
*  Function file for use with nonlin (M.L.Johnson)
*  For analysis of classical 2-site isotherms
*  Resolves macroscopic binding energies at 2 sites
*  Permits resolution of span and Yzero value
*
*  Independent variable:     X = [Ligand] free
*  Dependent variable:  Fractional saturation
*  Parameters or ANS vector elements:
*     ANS(1) = TEMPERATURE IN CENTIGRADE
*     ANS(2) = Macrosopic Delta G for 1 bound
*     ANS(3) = Macrosopic Delta G for 2 bound
*     ANS(4) = Span
*     ANS(5) = Y infinity
*
**********************************************************
*
    DIMENSION ANS(5)
    REAL X, Span, Yzero, K1X, K2X2, T, RT
    REAL Ybar, FX
*
    DATA R /.001987/
*
```

```
      T=273.15 + ANS(1)
      RT=R*T
      K1X  = exp(-Ans(2)/RT)*X       !k1*X
      K2X2  = exp(-Ans(3)/RT)*X*X       !k2*X
      Ybar = ((K1X + 2.*K2X2)/(1. + K1X + K2X2))/2.
      FX= Ybar * Ans(4) + Ans(5)
*
      RETURN
      END



      SUBROUTINE START(NAME,MAXP,DNAME,MAXD,MAXV)
C
C       THIS ROUTINE IS USED TO SET THE VARIABLE NAMES FOR C          THE
PARAMETERS. THESE NAMES MUST CORRESPOND TO THE
C       VARIABLES USED IN THE FX ROUTINE.
c
      CHARACTER*8 NAME(5),NAMES(5)
      CHARACTER*8 DNAME(3),DNAMES(3)
      DATA NAMES/'Temp','dG1 ','dG2 ','Span','Yzero'/
      DATA DNAMES/'dG12est', 'EndLowX', 'EndHighX'/
C
      MAXV=1
C     maxv is the # of independent variables for the fit.
C          This is usually set to 1.  However, to fit multiple
C          set of data it could be set to 2.  The second vector
C          of X values can then be used to specify which
C     data set is actually being fit. If this is greater
C          than 1 then X in the
C     FX routine must be dimensioned appropriately.
C
      MAXP=5
C          MAXP is the # of parameters in model being fit by
C          these routines.
      DO 10 I=1,MAXP
   10  NAME(I)=NAMES(I)
C          NAME is the names of the actual fitting parameters.

      MAXD=3
C MAXD specifies the number of derived parameters.  A
C derived parameter is simply a quantity that you wish
C evaluated from the fitting answers after the fit is
C finished.  By using this feature the program will
C complete the actual error propagation for the derived
C parameters.  In the current
```

```
C example, we calculate the area under the exponential
C decay.
C
      DO 110 I=1,MAXD
  110  DNAME(I)=DNAMES(I)
C DNAME is the names of the derived parameters.

      RETURN
      END


      subroutine derive(old,new)
C     This routine is used to map the OLD (fitted)
C          parameters into the
C          desired derived (NEW) parameters.
C
       real old(5),new(1)
      DATA R /.001987/
        T=273.15 + old(1)
       RT = R * T
*  Calculate estimate of dG cooperativity for equal
*  intrinsic affinities
       new(1) = -RT*ALOG(4.) + old(3) - 2. * old(2)
*  Calculated endpoint at low [X]
       new(2) = 1. * old(5)
*  Calculated endpoint at high [X]
       new(3) = old(4) + old(5)
       return
       end
```

APPENDIX C

NMR ASSIGNMENTS OF APO $PCAM_{76-148}$

Amide Assignments of Apo $PCaM_{76-148}$

Below are apo PCaM amide assignments determined in 10 mM D_4-imidazole, 100 mM KCl, 50 μM D_{16}-EDTA, 0.01% NaN_3, pH 6.5, 298.15 K

M76 N-H	128.582	8.462	N111 N-H	119.645	7.672
K77 N-H	123.092	8.519	L112 N-H	119.617	7.748
E78 N-H	122.549	8.597	G113 N-H	107.639	8.107
Q79 N-H	120.502	8.385	E114 N-H	119.557	8.048
D80 N-H	121.813	8.432	K115 N-H	121.092	8.432
S81 N-H	116.038	8.367	L116 N-H	121.217	7.731
E82 N-H	122.846	8.743	T117 N-H	114.079	9.052
E83 N-H	118.113	8.406	D118 N-H	121.178	8.786
E84 N-H	118.816	7.986	D119 N-H	117.112	8.278
L85 N-H	121.173	7.940	E120 N-H	120.834	7.729
I86 N-H	117.864	8.277	V121 N-H	120.580	8.232
E87 N-H	116.921	7.909	D122 N-H	119.401	8.403
A88 N-H	120.969	7.529	E123 N-H	119.626	7.775
F89 N-H	114.879	7.698	M124 N-H	119.043	7.876
K90 N-H	118.026	8.235	I125 N-H	119.076	8.579
V91 N-H	116.669	6.904	R126 N-H	117.879	7.731
F92 N-H	116.018	7.402	E127 N-H	116.569	7.755
D93 N-H	121.526	7.719	A128 N-H	120.458	7.777
R94 N-H	124.448	8.264	I130 N-H	123.259	8.378
D95 N-H	116.327	8.667	G132 N-H	109.669	8.165
G96 N-H	110.529	7.958	D133 N-H	120.198	8.420
N97 N-H	117.934	8.84	H135 N-H	119.500	8.038
G98 N-H	110.966	9.823	I136 N-H	122.114	9.138
L99 N-H	119.423	7.568	N137 N-H	125.122	8.639
I100 N-H	114.759	8.669	Y138 N-H	124.926	7.481
S101 N-H	119.045	8.797	E139 N-H	125.473	8.337
A102 N-H	124.274	8.505	E140 N-H	119.621	7.759
A103 N-H	118.398	8.295	F141 N-H	120.484	8.045
E104 N-H	119.537	7.616	V142 N-H	118.556	8.484
L105 N-H	121.404	8.16	R143 N-H	118.629	7.754
R106 N-H	117.768	8.266	M144 N-H	117.439	7.805
H107 N-H	118.521	7.682	M145 N-H	119.581	8.026
V108 N-H	120.27	7.97	V146 N-H	113.034	7.991
M109 N-H	115.629	8.129	S147 N-H	116.521	7.595
T110 N-H	113.005	7.959	K148 N-H	127.771	7.448

Carbonyl Assignments of apo $PCaM_{76-148}$

Listed below are carbonyl assignments of apo $PCaM_{76-148}$ determined in 10 mM D_4-imidazole, 100 mM KCl, 50 μM D_{16}-EDTA, 0.01% NaN_3, pH 6.5, 298.15 K

M76	175.843	T110	175.878
K77	176.488	N111	175.917
E78	176.426	L112	177.649
Q79	175.63	G113	174.786
D80	176.171	E114	176.405
S81	175.194	L116	177.529
E82	177.36	T117	175.34
E83	178.637	D118	178.109
E84	179.258	D119	178.825
L85	178.069	E120	179.412
I86	178.056	V121	177.593
E87	178.416	D122	179.17
A88	179.78	E123	178.217
F89	177.731	M124	178.732
K90	178.492	I125	177.245
V91	176.721	R126	179.317
F92	174.797	E127	177.072
D93	176.498	D129	177.253
R94	177.988	D131	177.201
D95	176.708	G132	174.328
G96	175.011	H135	172.347
N97	176.285	I136	175.07
G98	173.144	N137	175.495
L99	176.371	Y138	176.306
I100	174.419	E139	179.147
S101	175.432	E140	178.477
A102	178.856	F141	176.892
A103	181.134	V142	177.214
E104	177.798	R143	179.209
L105	179.066	M144	178.158
R106	178.531	M145	178.128
H107	177.462	V146	176.561
V108	178.552	S147	173.501
M109	178.812		

Methine, Methylene, and Methyl Assignments of apo $PCaM_{76-148}$

Listed below are methane, methylene and methyl assignments of apo $PCaM_{76-148}$ determined in 10 mM D_4-imidazole, 100 mM KCl, 50 μM D_{16}-EDTA, 0.01% NaN_3, pH 6.5, 298.15 K

M76 CA-HA 54.026 4.539
M76 CB-HB2 33.188 2.094
M76 CB-HB3 33.188 2.002
M76 CE-HE 17.939 1.867
M76 CG-HG2 31.831 2.592
M76 CG-HG3 31.827 2.548
K77 CA-HA 56.106 4.349
K77 CE-CE## 41.814 2.997
E78 CA-HA 56.633 4.264
D80 CA-HA 54.415 4.661
D80 CB-HB## 41.129 2.718
D80 CB-HB2 41.081 2.729
D80 CB-HB3 41.038 2.687
S81 CA-HA 58.65 4.474
S81 CB-HB2 63.989 4.06
S81 CB-HB3 63.79 3.94
E82 CA-HA 59.02 4.018
E82 CB-HB2 29.297 2.097
E82 CB-HB3 29.306 2.07
E82 CG-HG2 36.412 2.365
E82 CG-HG3 36.417 2.266
E83 CA-HA 59.49 3.977
L85 CA-HA 57.789 3.97
L85 CB-HB2 42.573 2.001
L85 CB-HB3 42.557 1.56
L85 CD1-HD1 24.388 0.89
L85 CD2-HD2 23.75 0.869
L85 CG-HG2 27.42 1.76
I86 CA-HA 65.493 3.866
I86 CB-HB 37.149 2.211
I86 CD-HD 12.688 1.069
I86 CG1-HG12 30.141 2.024
I86 CG1-HG13 30.088 1.401
I86 CG2-HG2 17.763 1.156
A88 CA-HA 54.926 4.145
A88 CB-HB 18.011 1.32
F89 CA-HA 59.763 4.324
F89 CB-HB2 39.428 2.611
F89 CB-HB3 39.409 2.226
K90 CA-HA 59.18 3.7
K90 CB-HB2 32.741 1.991
K90 CB-HB3 32.64 1.877
K90 CD-HD## 29.628 1.765
K90 CG-HG2 25.265 1.764
K90 CG-HG3 25.206 1.682
V91 CA-HA 64.844 3.574
V91 CB-HB 31.772 1.726
V91 CG1-HG1 21.408 0.801
V91 CG2-HG2 20.515 0.421
F92 CA-HA 58.724 4.438
F92 CB-HB2 39.368 3.514
F92 CB-HB3 39.468 2.767
F92 CD1-HD1 131.629 7.274
F92 CE1-HE1 131.976 7.401
D93 CA-HA 52.139 5.085
D93 CB-HB2 39.778 3.332
D93 CB-HB3 39.772 2.559
R94 CA-HA 57.935 4.101

R94 CD-HD## 42.91 3.274
D95 CA-HA 54.224 4.757
D95 CB-HB2 41.174 2.742
D95 CB-HB3 41.201 2.687
G96 CA-HA2 46.848 3.932
G96 CA-HA3 46.851 3.838
N97 CA-HA 52.129 4.832
N97 CB-HB2 38.905 3.073
N97 CB-HB3 38.939 2.672
G98 CA-HA3 45.381 3.74
G98 CA-HA3 45.865 3.292
L99 CA-HA 52.973 5.5
L99 CB-HB2 44.812 1.797
L99 CB-HB3 44.812 1.046
L99 CD1-HD1 25.469 0.738
L99 CD2-HD2 22.826 0.708
L99 CG-HG2 26.267 1.384
I100 CA-HA 59.281 5.016
I100 CB-HB 41.977 2.204
I100 CD-HD 14.411 0.71
I100 CG1-HG12 25.584 1.52
I100 CG1-HG13 25.578 1.272
I100 CG2-HG2 17.996 0.903
S101 CA-HA 57.526 4.922
S101 CB-HB2 65.023 4.322
S101 CB-HB3 65.02 3.988
A102 CA-HA 55.483 3.788
A102 CB-HB 18.068 1.344
A103 CA-HA 54.944 3.992
A103 CB-HB 18.187 1.337
E104 CA-HA 58.641 3.63
E104 CB-HB2 28.52 2.134
E104 CB-HB3 28.522 1.225
E104 CG-HG2 37.255 2.04
E104 CG-HG3 37.25 1.827
L105 CA-HA 59.169 3.779
L105 CB-HB2 41.77 1.696
L105 CB-HB3 41.75 1.359
L105 CD1-HD1 25.349
L105 CD2-HD2 24.757 0.167
L105 CG-HG 27.002 1.222
H106 CE-H32HE 137.655 8.193
R106 CA-HA 60.12 3.663
R106 CB-HB3 29.621 1.482
R106 CD-HD2 42.986 3.19
R106 CD-HD3 42.922 3.033
R106 CG-HG3 29.144 1.484
R106 CG-HG2? 29.207 1.713
H107 CA-HA 59.181 4.275
H107 CB-HB2 28.864 3.328
H107 CB-HB3 28.858 3.14
V108 CA-HA 66.35 3.505
V108 CB-HB 31.708 2.093
V108 CG1-HG1 23.532 1.011
V108 CG2-HG2 21.402 0.263
M109 CA-HA 56.961 4.329
M109 CB-HB2 31.296 2.258
M109 CB-HB3 31.296 2.135
M109 CE-HE 17.374 2.202
M109 CG-HG2 32.859 2.753
M109 CG-HG3 32.852 2.673
T110 CA-HA 65.115 4.164
T110 CB-HB 69.058 4.266
T110 CG2-HG2 21.528 1.283
N111 CA-HA 54.286 4.701
N111 CB-HB2 39.08 2.821
N111 CB-HB3 39.125 2.726
L112 CA-HA 55.384 4.345
L112 CB-HB2 42.892 1.783
L112 CB-HB3 42.887 1.651
L112 CD1-HD1 25.69 0.816
L112 CD2-HD2 22.89 0.769

L112 CG-HG2 26.687 1.777
G113 CA-HA2 46.011 3.933
G113 CA-HA3 46.026 3.511
L116 CA-HA 53.963 4.692
L116 CB-HB2 44.579 1.615
L116 CB-HB3 44.593 1.551
L116 CD1-HD1 26.492 0.888
L116 CD2-HD2 23.75 0.869
L116 CG-HG 27.617 1.628
T117 CA-HA 60.856 4.442
T117 CB-HB 70.757 4.674
T117 CG2-HG2 21.727 1.341
D119 CA-HA 57.074 4.39
D119 CB-HB2 40.334 2.671
D119 CB-HB3 40.285 2.536
E120 CB-HB2 30.254 2.41
E120 CB-HB3 30.261 1.937
E120 CG-HG2 37.509 2.354
E120 CG-HG3 37.477 2.271
V121 CA-HA 67.25 3.683
V121 CB-HB 31.578 2.247
V121 CG1-HG1 24.35 1.079
V121 CG2-HG2 21.775 1.003
D122 CA-HA 57.763 4.369
D122 CB-HB2 40.291 2.853
D122 CB-HB3 40.26 2.613
M124 CB-HB2 34.41 2.335
M124 CB-HG3 34.428 2.016
M124 CE-HE 17.303 1.99
M124 CG-HG2 32.631 2.788
M124 CG-HG2 32.635 2.753
M124 CG-HG3 32.546 2.439
M124 CG-HG3 32.852 2.673
I125 CA-HA 66.329 3.574
I125 CB-HB 37.556 2.005
I125 CD-HD 14.197 0.779
I125 CG2-HG2 17.145 0.845
L125 CG1-HG12 30.479 1.979
L125 CG1-HG13 30.447 0.774
R126 CD-HD## 43.294 3.247
A128 CA-HA 52.147 4.421
A128 CB-HB 19.429 1.562
D129 CB-HB2 39.988 2.982
D129 CB-HB2 40.049 2.809
D129 CB-HB3 40.049 2.74
I130 CA-HA 62.644 4.161
I130 CB-HB 38.806 1.945
I130 CD-HD 13.725 0.9
I130 CG1-HG12 27.454 1.521
I130 CG1-HG13 27.475 1.324
I130 CG2-HG2 17.999 1.035
D131 CA-HA 53.318 4.81
D131 CB-HB2 41.357 2.985
D131 CB-HB3 41.243 2.718
G132 CA-HA2 46.496 4.034
G132 CA-HA3 46.496 3.768
D133 CB-HB2 41.497 2.608
D133 CB-HB3 41.529 2.517
G134 CA-HA2 45.308 4.249
H135 ?-? 119.032 7.047
H135 CA-HA 54.94 4.977
H135 CB-HB2 29.543 3.401
H135 CB-HB3 29.557 2.89
H135 CE-HE 135.857 8.536
I136 CA-HA 59.509 4.269
I136 CB-HB 39.203 1.737
I136 CD-HD 12.541 0.652
I136 CG1-HG12 27.97 1.287
I136 CG1-HG13 27.977 1.161
I136 CG2-HG2 18.174 0.605
N137 CA-HA 52.269 5.155
N137 CB-HB2 37.68 3.097

N137 CB-HB3 37.655 2.531
Y138 CA-HA 59.34 4.092
Y138 CB-HB1 36.826 2.65
Y138 CB-HB2 36.775 2.302
Y138 CD1-HD1 133.869 6.819
Y138 CE-HE1 117.708 6.768
E139 CA-HA 60.649 3.953
E139 CB-HB2 28.668 2.209
E139 CB-HB3 28.738 2.005
E139 CG-HG3 37.118 2.093
F141 CA-HA 61.997 4.011
F141 CB-HB2 39.654 3.1
F141 CB-HB3 39.623 2.761
F141 CD1-HD1 131.395 6.872
V142 CA-HA 67.249 3.516
V142 CB-HB 31.689 2.332
V142 CG1-HG1 25.319 1.382
V142 CG2-HG2 22.474 1.141
R143 CA-HA 59.535 3.949
M144 CA-HA 58.32 4.033
M144 CB-HB2 32.76 2.113
M144 CB-HB3 32.76 1.955
M144 CE-HE 17.482 2.078
M144 CG-HG2 32.178 2.661
M144 CG-HG3 32.21 2.447
M145 CA-HA 58.762 3.875
M145 CB-HB2 33.11 2.071
M145 CB-HB3 33.035 1.943
M145 CE-HE 17.199 1.77
M145 CG-HG2 32.139 2.355
M145 CG-HG3 32.132 2.26
V146 CA-HA 62.89 4.209
V146 CB-HB 31.951 2.345
V146 CG1-HG1 21.183 0.965
V146 CG2-HG2 19.884 1
S147 CA-HA 58.65 4.474
S147 CB-HB2 63.989 4.06
S147 CB-HB3 63.79 3.94

APPENDIX D

NMR ASSIGNMENTS OF APO $PCAM_{76\_148}$ WHEN BOUND TO TFP

Amide Assignments of Apo $PCaM_{76-148}$ When Bound to TFP

Listed below are amide assignments of apo $PCaM_{76-148}$ when bound to TFP determined in 10 mM D_4-imidazole, 100 mM KCl, 50 μM D_{16}-EDTA, 0.01% NaN_3, pH 6.5, 298.15 K

M76 N-H	128.617	8.46
K77 N-H	123.08	8.523
E78 N-H	122.524	8.6
Q79 N-H	120.58	8.384
D80 N-H	121.804	8.423
S81 N-H	116.048	8.339
E82 N-H	122.868	8.775
E83 N-H	118.333	8.377
E84 N-H	118.836	8.012
L85 N-H	121.134	7.896
I86 N-H	117.981	8.245
E87 N-H	117.153	7.94
A88 N-H	121.063	7.539
F89 N-H	114.914	7.692
K90 N-H	118.058	8.189
V91 N-H	116.699	6.947
F92 N-H	116.092	7.403
D93 N-H	121.481	7.731
R94 N-H	124.216	8.25
D95 N-H	116.274	8.652
G96 N-H	110.401	7.919
N97 N-H	118.007	8.802
G98 N-H	110.98	9.824
L99 N-H	119.42	7.623
I100 N-H	114.468	8.639
S101 N-H	118.991	8.887
A102 N-H	124.244	8.499
A103 N-H	118.712	8.283
E104 N-H	119.823	7.641
L105 N-H	121.203	8.158
R106 N-H	117.825	8.227
H107 N-H	118.841	7.713
V108 N-H	119.781	7.988
M109 N-H	115.373	8.136
T110 N-H	111.38	7.961
N111 N-H	119.721	7.628
L112 N-H	119.595	7.708
G113 N-H	107.539	8.163
E114 N-H	119.757	7.972
K115 N-H	120.826	8.405
L116 N-H	122.02	7.793
T117 N-H	114.12	9.055
D118 N-H	121.143	8.775
D119 N-H	117.067	8.255
E120 N-H	120.779	7.737
V121 N-H	120.522	8.167
D122 N-H	119.364	8.365
E123 N-H	119.488	7.811
M124 N-H	118.796	7.843
I125 N-H	118.633	8.442
R126 N-H	118.474	7.792
E127 N-H	116.551	7.724
A128 N-H	120.665	7.718
I130 N-H	123.24	8.181
G132 N-H	108.708	8.232
D133 N-H	119.653	8.362
H135 N-H	119.098	8.204
I136 N-H	121.575	9.187
N137 N-H	125.286	8.753
Y138 N-H	124.855	7.475
E139 N-H	125.223	8.318
E140 N-H	119.211	7.772
F141 N-H	120.623	8.086
V142 N-H	118.542	8.421
R143 N-H	117.988	7.77
M144 N-H	117.637	7.859

M145 N-H	118.995	7.964	S147 N-H	116.306	7.575
V146 N-H	113.306	7.992	K148 N-H	127.771	7.457

Carbonyl Assignments of apo $PCaM_{76-148}$ when Bound to TFP

Listed below carbonyl assignments of apo $PCaM_{76-148}$ when bound to TFP determined in 10 mM D_4-imidazole, 100 mM KCl, 50 μM D_{16}-EDTA, 0.01% NaN_3, pH 6.5, 298.15 K

M76	175.841	N111	175.673
K77	176.502	L112	177.628
E78	176.447	G113	174.646
Q79	175.639	E114	176.201
D80	176.227	K115	176.116
S81	175.209	L116	177.555
E82	177.4	T117	175.351
E83	178.681	D118	178.095
E84	179.204	D119	178.791
I86	178.026	E120	179.414
I86	178.099	V121	177.565
E87	178.458	D122	179.156
A88	179.766	E123	178.276
F89	177.72	M124	178.657
K90	178.513	I125	177.484
V91	176.734	R126	179.07
F92	174.885	E127	176.963
D93	176.538	D129	176.605
R94	177.91	D131	177.524
D95	176.782	G132	174.441
G96	175.014	G134	174.328
N97	176.314	H135	172.82
G98	173.079	I136	174.796
L99	176.477	N137	175.551
I100	174.584	Y138	176.227
A102	175.372	E139	179.025
A102	178.988	E140	178.621
A103	181.046	F141	176.843
E104	177.788	V142	177.269
L105	178.818	R143	179.099
R106	178.429	M144	179.156
H107	177.489	M144	178.197
V108	178.669	M145	178.188
M109	178.45	V146	176.502
T110	175.745	S147	173.534

Methine, Methylene, and Methyl Assignments of apo $PCaM_{76\text{-}148}$ When Bound to TFP

Below are listed methine, methylene, and methyl assignments of apo $PCaM_{76\text{-}148}$ when bound to TFP determined in 10 mM D_4-imidazole, 100 mM KCl, 50 μM D_{16}-EDTA, 0.01% NaN_3, pH 6.5, 298.15 K

M76 CA-HA 54.05 4.527
M76 CB-HB2 33.221 2.084
M76 CB-HB3 33.148 1.996
M76 CE-HE 17.427 1.948
M76 CG-HG2 31.829 2.579
M76 CG-HG3 31.832 2.536
K77 CA-HA 56.219 4.348
K77 CB-HB2 33.165 1.84
K77 CB-HB3 33.179 1.77
K77 CD-HD## 28.884 1.685
K77 CE-K3HE## 41.838 2.989
K77 CG-HG## 24.428 1.441
E78 CA-HA 56.727 4.246
E78 CB-HB2 29.859 2.066
E78 CB-HB3 30.061 1.948
E78 CG-HG2 36.213 2.434
E78 CG-HG3 36.188 2.289
Q79 CA-HA 56.075 4.318
Q79 CB-HB## 29.478 2.031
Q79 CG-HG2 33.766 2.366
Q79 CG-HG3 33.699 2.106
D80 CA-HA 54.432 4.644
D80 CB-HB## 41.178 2.696
S81 CA-HA 58.741 4.469
S81 CB-HB2 63.949 4.032
S81 CB-HB3 63.982 3.938
E82 CA-HA 59.273 4.028
E82 CB-HB2 29.626 2.097
E82 CG-HG2 36.45 2.368
E82 CG-HG3 36.416 2.259
E83 CA-HA 59.162 4.054
L85 CA-HA 57.85 3.962
L85 CB-HB2 42.323 1.9
L85 CB-HB3 42.302 1.556
L85 CD1-HD1 25.277 0.72
L85 CD2-HD2 24.399 0.769
L85 CG-HG2 27.012 1.634
I86 CA-HA 65.55 3.854
I86 CB-HB 37.352 2.164
I86 CD-HD 12.766 1.049
I86 CG1-HG12 30.024 2.01
I86 CG1-HG13 30.169 1.361
I86 CG2-HG2 17.798 1.152
E87 CA-HA 59.08 3.924
E87 CB-HB## 29.131 2.085
E87 CG-HG## 36.242 2.382
A88 CA-HA 54.524 4.097
A88 CB-HB 17.96 1.33
F89 CA-HA 59.668 4.319
F89 CB-HB2 39.348 2.63
F89 CB-HB3 39.323 2.208
F89 CD1-HD1 131.406 7.132
F89 CD2-HD2 60.378 7.094
F89 CE##-HE## 129.423 7.132
F89 CE##-HE## 60.096 7.199
K90 CA-HA 59.193 3.726
K90 CB-HB2 32.643 1.989
K90 CB-HB3 32.724 1.9
K90 CD-HD## 29.595 1.768
K90 CE-HE2 41.75 3.047
K90 CE-HE3 41.719 3
K90 CG-HG2 25.299 1.77
K90 CG-HG3 25.286 1.68
V91 CA-HA 64.841 3.581
V91 CB-HB 31.777 1.743
V91 CG1-HG1 21.423 0.802
V91 CG2-HG2 20.51 0.427
F92 CA-HA 58.753 4.401
F92 CB-HB2 39.405 3.5
F92 CB-HB2 39.426 2.779
F92 CD##-HD## 131.635 7.269
F92 CE##-HE## 131.681 7.335

D93 CA-HA 52.144 5.071
D93 CB-HB2 39.786 3.319
D93 CB-HB3 39.818 2.561
R94 CA-HA 57.972 4.102
R94 CB-HB## 30.156 1.907
R94 CD-HD## 42.932 3.27
R94 CG-HG2 27.207 1.775
R94 CG-HG3 27.205 1.707
D95 CA-HA 54.148 4.759
D95 CB-HB2 41.045 3.017
D95 CB-HB3 41.118 2.737
G96 CA-HA2 46.798 3.93
G96 CA-HA3 46.816 3.834
N97 CA-HA 52.183 4.824
N97 CB-HB2 38.929 3.065
N97 CB-HB3 38.906 2.675
G98 CA-HA2 45.866 3.927
G98 CA-HA3 45.827 3.29
S98 CA-HA 57.537 4.879
L99 CA-HA 53.013 5.469
L99 CB-HB2 44.722 1.77
L99 CB-HB3 44.724 1.031
L99 CD1-HD1 25.402 0.732
L99 CD2-HD2 22.79 0.701
L99 CG-HG2 26.291 1.378
I100 CA-HA 59.292 5.008
I100 CB-HB 41.967 2.213
I100 CD-HD 14.397 0.707
I100 CG1-HG12 25.629 1.523
I100 CG1-HG13 25.549 1.263
I100 CG2-HG2 17.982 0.908
S101 CB-HB2 65 4.31
S101 CB-HB3 64.995 3.97
A102 CA-HA 55.478 3.802
A102 CB-HB 17.787 1.355
A103 CA-HA 54.927 3.999
A103 CB-HB 18.033 1.36
E104 CA-HA 58.644 3.656
E104 CB-HB2 28.574 2.152
E104 CB-HB3 28.498 1.27
E104 CB-HB3 28.15 1.167
E104 CG-HG2 37.234 2.064
E104 CG-HG3 37.239 1.843
L105 CA-HA 59.033 3.806
L105 CB-HB2 41.681 1.737
L105 CB-HB3 41.734 1.346
L105 CD1-HD1 25.113 0.221
L105 CD2-HD2 25.124 0.041
L105 CG-HG2 26.886 1.27
R106 CA-HA 60.055 3.666
R106 CB-HB2 29.963 1.786
R106 CD-HD2 42.894 3.203
R106 CD-HD3 42.919 3.033
R106 CG-CG3 28.816 1.51
R106 CG-HG2 28.807 1.615
H107 CA-HA 59.23 4.242
H107 CB-HB2 29.084 3.314
H107 CB-HB3 29.09 3.127
H107 CD2-HD2 119.691 6.954
H108 CE1-HE1 137.785 8.139
V108 CA-HA 66.38 3.498
V108 CB-HB 31.774 2.083
V108 CG1-HG1 23.456 1.003
V108 CG2-HG2 21.278 0.27
M109 CB-HB2 31.774 2.229
M109 CB-HB3 31.764 2.128
M109 CE-HE 17.355 2.137
M109 CG-HG## 32.845 2.707
T110 CA-HA 64.705 4.192
T110 CB-HB 69.159 4.303
T110 CG2-HG2 21.588 1.283
N111 CA-HA 54.298 4.751
N111 CB-HB1 39.202 2.812
N111 CB-HB2 39.109 2.675
L112 CA-HA 55.354 4.349
L112 CB-HB2 42.857 1.798
L112 CB-HB3 42.84 1.639
L112 CD1-HD1 25.721 0.803
L112 CD2-HD2 22.901 0.742
L112 CG-HG2 26.631 1.801
G113 CA-HA1 45.664 3.896
K115 CA-HA 56.504 4.247
K115 CB-HB2 32.153 1.858
K115 CB-HB3 32.105 1.778
K115 CD-HD## 28.873 1.669
K115 CE-HE2 41.838 2.989
K115 CE-HE3 41.833 2.949
K115 CG-HG2 24.671 1.44
K115 CG-HG3 24.735 1.378
L116 CA-HA 53.885 4.687
L116 CB-HB2 44.468 1.582
L116 CB-HB3 44.481 1.535

L116 CD1-HD1 26.391 0.841
L116 CD2-HD2 23.841 0.819
L116 CG-HG2 27.508 1.605
T117 CA-HA 60.749 4.454
T117 CB-HB 70.798 4.674
T117 CG2-HG2 21.722 1.33
D118 CA-HA 57.565 4.261
D118 CB-HB2 39.918 2.732
D118 CB-HB3 39.97 2.604
D119 CA-HA 57.077 4.388
D119 CB-HB2 40.284 2.843
D119 CB-HB2 40.328 2.668
D119 CB-HB3 40.136 2.609
E120 CA-HA 58.935 4.061
E120 CB-HB2 30.186 2.402
E120 CB-HB3 30.188 1.918
E120 CG-HG2 37.51 2.349
E120 CG-HG3 37.443 2.272
V121 CA-HA 67.13 3.657
V121 CB-HB 31.704 2.213
V121 CG1-HG1 24.239 1.046
V121 CG2-HG2 21.912 0.982
D122 CA-HA 57.741 4.36
D122 CB-HB2 40.106 2.857
D122 CB-HB3 40.136 2.609
M124 CA-HA 59.365 4.099
M124 CB-HB2 34.19 2.352
M124 CB-HB3 34.195 2.046
M124 CE-HE 17.178 1.989
M124 CG-HG2 32.69 2.783
M124 CG-HG3 32.694 2.454
I125 CA-HA 65.855 3.586
I125 CB-HB 37.491 1.983
I125 CD-HD 13.894 0.764
I125 CG1-HG12 30.15 1.898
I125 CG2-HG2 17.166 0.839
L125 CG1-HG13 30.109 0.836
R126 CA-HA 59.194 4.081
R126 CB-HB## 30.074 1.948
R126 CD-HD## 43.305 3.238
R126 CG-HG2 27.782 1.8
R126 CG-HG3 27.801 1.629
A128 CA-HA 52.218 4.38
A128 CB-HB 19.468 1.504
D129 CB-HB2 40.003 2.938
D129 CB-HB3 40.01 2.583
I130 CA-HA 62.093 4.185
I130 CB-HB 38.854 1.879
I130 CD-HD 13.611 0.876
I130 CG1-HG12 27.506 1.512
I130 CG1-HG13 27.509 1.208
I130 CG2-HG2 17.76 1.003
D131 CA-HA 53.083 4.817
D131 CB-HB2 41.471 2.6
D131 CB-HB3 41.559 2.535
G132 CA-HA2 45.958 3.927
G132 CA-HA3 46.512 3.807
G134 CA-HA2 45.958 3.971
G134 CA-HA3 45.93 3.539
H135 CA-HA 54.892 5.046
H135 CB-HB2 30.039 3.439
H135 CB-HB3 30.044 2.895
H135 CD2-HD2 48.029 6.972
H135 CE-HE 136.126 8.512
I136 CA-HA 59.621 4.29
I136 CB-HB 40.137 1.653
I136 CD-HD 13.201 0.635
I136 CG1-HG13 28.187 1.231
I136 CG2-HG2 17.917 0.601
N137 CA-HA 52.235 5.168
N137 CB-HB2 37.643 3.069
N137 CB-HB3 37.608 2.53
Y138 CA-HA 59.328 4.09
Y138 CB-HB1 36.888 2.621
Y138 CD1-HD1 133.914 6.811
Y138 CE##-HE## 117.731 6.757
E139 CA-HA 60.62 3.94
E139 CB-HB## 28.807 1.993
E139 CG-HG2 37.123 2.221
E139 CG-HG3 37.112 2.094
E140 CA-HA 58.264 4.051
E140 CB-HB2 29.27 2.157
E140 CB-HB3 29.27 2.113
E140 CG-HG2 35.675 2.306
E140 CG-HG3 35.675 2.252
F141 CA-HA 61.791 4.085
F141 CB-HB1 39.512 3.077
F141 CB-HB2 39.655 2.876
F141 CD##-HD## 131.425 6.935
E142 CG-HG 36.238 2.317
V142 CA-HA 67.25 3.456
V142 CB-HB 31.77 2.306

V142 CG1-HG1 24.997 1.342
V142 CG2-HG2 22.313 1.091
R143 CA-HA 59.459 3.938
R143 CB-HB## 29.468 1.909
R143 CD-HD## 43.046 3.19
R143 CG-HG1 27.782 1.8
R143 CG-HG2 27.618 1.766
R143 CG-HG3 27.624 1.609
M144 CE-HE 16.911 2.076
M145 CA-HA 58.264 4.051
M145 CA-HA 58.156 4.048
M145 CB-HB2 32.523 2.122
M145 CB-HB3 32.523 2.008
M145 CE-HE 17.37 1.796
M145 CG-HG2 31.941 2.647
M145 CG-HG3 31.949 2.436
V146 CA-HA 62.975 4.176
V146 CB-HB 31.77 2.306
V146 CG1-HG1 21.169 0.94
V146 CG2-HG2 20.073 0.979
S147 CA-HA 58.637 4.474
S147 CB-HB2 63.801 4.03
S147 CB-HB3 63.816 3.938

APPENDIX E

NMR ASSIGNMENTS OF APO $PCAM_{76-148}$ WHEN BOUND TO $NA_V1.2_{IQP}$

Amide Assignments of apo $PCaM_{76-148}$ When Bound to $Na_v1.2_{IQp}$

Below are amide assignments of apo $PCaM_{76-148}$ when bound to $Na_v1.2_{IQP}$ determined in 10 mM D_4-imidazole, 100 mM KCl, 50 μM D_{16}-EDTA, 0.01% NaN_3, pH 6.5, 298.15 K

K 77 N-H 123.132 8.744
E 78 N-H 121.824 8.518
Q 79 N-H 120.369 8.377
D 80 N-H 121.445 8.438
S 81 N-H 115.689 8.449
E 82 N-H 123.796 8.922
E 83 N-H 117.756 8.642
E 84 N-H 118.775 7.975
L 85 N-H 120.846 7.926
I 86 N-H 120.37 8.675
E 87 N-H 117.231 8.024
A 88 N-H 121.043 7.674
F 89 N-H 114.809 7.994
K 90 N-H 117.643 8.254
V 91 N-H 118.519 6.948
F 92 N-H 116.264 7.434
D 93 N-H 120.522 7.526
R 94 N-H 124.435 8.342
D 95 N-H 116.533 8.676
G 96 N-H 110.326 8.187
N 97 N-H 117.559 8.694
G 98 N-H 110.822 9.773
L 99 N-H 119.499 7.808
I 100 N-H 116.548 8.705
S 101 N-H 121.978 9.084
A 102 N-H 129.122 8.793
A 103 N-H 119.588 8.441
E 104 N-H 120.377 7.773
L 105 N-H 119.693 8.467
R 106 N-H 117.512 8.445
H 107 N-H 118.473 7.72
V 108 N-H 117.819 8.588
M 109 N-H 112.375 8.307
T 110 N-H 103.758 7.448
N 111 N-H 116.488 7.438
L 112 N-H 119.883 7.745
G 113 N-H 106.167 9.078
E 114 N-H 129.78 9.331
K 115 N-H 115.77 6.844
L 116 N-H 122.432 8.509
T 117 N-H 112.002 9.347
D 118 N-H 120.312 8.719
D 119 N-H 116.357 8.197
E 120 N-H 119.881 7.804
V 121 N-H 118.933 8.731
D 122 N-H 123.075 8.332
E 123 N-H 120.621 7.397
M 124 N-H 121.983 7.993
I 125 N-H 115.727 8.297
R 126 N-H 119.297 7.785
E 127 N-H 115.314 7.869
A 128 N-H 119.463 7.973
D 129 N-H 119.037 8.36
I 130 N-H 122.603 7.831
D 131 N-H 119.049 8.341
I 136 N-H 121.347 9.048
N 137 N-H 127.016 9.152
Y 138 N-H 123.19 7.193
E 139 N-H 125.718 8.437
E 140 N-H 117.759 7.417
V 142 N-H 118.912 8.578
R 143 N-H 117.124 7.715
M 144 N-H 119.249 7.771
M 145 N-H 117.727 7.857
V 146 N-H 111.161 7.993
S 147 N-H 116.623 7.633
K 148 N-H 128.318 7.839

Carbonyl Assignments of apo $CaM_{76\text{-}148}$ When Bound to $Na_v1.2_{IQp}$

Carbonyl assignments of apo $CaM_{76\text{-}148}$ when bound to $Na_v1.2_{IQp}$ determined in 10 mM D_4-imidazole, 100 mM KCl, 50 μM D_{16}-EDTA, 0.01% NaN_3, pH 6.5, 298.15 K

K77	176.74	M109	178.198
E78	176.252	T110	174.894
Q79	175.402	N111	173.557
D80	175.692	L112	176.581
S81	175.062	G113	175.888
E82	177.566	E114	175.378
E83	178.959	K115	177.848
E84	179.375	L116	177.488
L85	178.762	T117	175.363
I86	177.765	D118	177.668
E87	178.713	D119	179.624
A88	178.924	E120	178.985
F89	178.68	V121	176.25
K90	179.155	D122	179.494
V91	176.29	E123	177.482
F92	174.239	M124	177.552
D93	176.327	I125	177.429
R94	178.028	R126	178.819
D95	176.859	E127	177.069
G96	174.912	D129	176.551
N97	176.096	H135	172.991
G98	172.933	I136	175.003
L99	176.203	N137	175.653
I100	174.971	Y138	176.121
S101	175.564	E139	178.662
A102	178.755	F141	177.211
A103	180.892	V142	177.111
E104	178.533	R143	178.945
L105	177.97	M144	178.357
R106	178.451	M145	178.73
H107	177.808	V146	176.602
V108	177.786	S147	173.944

Methine, Methyline, and Methyl Assignments of apo $PCaM_{76-148}$ When Bound to $Na_v1.2_{IQp}$

Methine, methyline, and methyl assignments of apo $PCaM_{76-148}$ when bound to $Na_v1.2_{IQp}$ determined in 10 mM D_4-imidazole, 100 mM KCl, 50 μM D_{16}-EDTA, 0.01% NaN_3, pH 6.5, 298.15 K

M 76 CE-HE 16.854 2.102
K 77 CA-HA 56.437 4.347
K 77 CB-CB## 32.946 1.793
K 77 CD-HD## 29.12 1.734
K 77 CE-HE## 41.915 3.008
K 77 CG-HG## 24.663 1.438
E 78 CA-HA 56.894 4.249
E 78 CB-HB2 29.972 2.064
E 78 CB-HB3 30.005 1.938
E 78 CG-HG## 36.455 2.296
Q 79 CA-HA 56.126 4.356
Q 79 CB-HB2 29.972 2.064
Q 79 CB-HB3 30.025 1.989
Q 79 CG-HG## 33.793 2.345
D 80 CA-HA 54.443 4.651
D 80 CB-HB## 41.665 2.651
S 81 CA-HA 58.02 4.525
S 81 CB-HB2 64.513 4.125
S 81 CB-HB3 64.523 3.935
E 82 CB-HB## 29.848 2.085
E 83 CA-HA 60.255 3.991
E 83 CB-HB## 29.327 2.103
E 83 CG-HG## 36.512 2.357
E 84 CA-HA 58.896 4.018
E 84 CB-HB## 29.791 2.1
E 84 CG-HG## 36.93 2.281
L 85 CA-HA 57.737 4.097
L 85 CB-HB2 43.154 2.059
L 85 CB-HB3 43.151 1.612
L 85 CD1-HD1 25.76 0.873
L 85 CD2-HD2 25.097 0.864
L 85 CG-HG2 27.23 1.845
I 86 CA-HA 66.046 3.877
I 86 CB-HB 37.174 2.177
I 86 CD-HD 12.797 1.003
I 86 CG1-HG12 30.389 2.047
I 86 CG1-HG13 30.461 1.27
I 86 CG2-HG2 17.788 1.131
E 87 CA-HA 59.354 3.902
A 88 CA-HA 54.888 4.136
A 88 CB-HB 18.184 1.55
F 89 CA-HA 62.843 3.921
F 89 CB-HB2 40.359 2.647
F 89 CB-HB3 40.343 1.773
F 89 CD##-HD## 61.177 7.182
F 89 CE##-HE## 59.427 7.07
K 90 CA-HA 59.354 3.902
K 90 CA-HA 59.16 3.893
K 90 CB-HB2 32.611 2.006
K 90 CB-HB3 32.606 1.876
K 90 CD-HD## 29.567 1.741
K 90 CE-HE2 41.858 3.033
K 90 CE-HE3 41.859 2.97
K 90 CG-HG2 25.976 1.848
K 90 CG-HG3 25.987 1.706
V 91 CA-HA 65.174 3.458
V 91 CB-HB 31.377 1.693
V 91 CG2-HG1 22.725 0.789
V 91 CG3-HG3 20.718 0.162
F 92 CA-HA 57.585 4.539
F 92 CB-HB2 39.169 3.512
F 92 CB-HB3 39.219 2.774
F 92 CD##-HD## 59.97 6.91
F 92 CE##-HE 58.473 7.353
D 93 CA-HA 52.167 4.97
D 93 CB-HB2 40.159 3.411
D 93 CB-HB3 40.139 2.546
R 94 CA-HA 58.078 4.109
R 94 CB-HB## 30.031 1.942
R 94 CD-HD## 42.962 3.252
R 94 CG-HG## 27.016 1.831
D 95 CA-HA 54.664 4.793
D 95 CB-HB## 41.447 2.741
G 96 CA-HA2 46.658 3.956

G 96 CA-HA3 46.768 3.758
N 97 CA-HA 52.256 4.886
N 97 CB-HB2 39.263 2.983
N 97 CB-HB3 39.285 2.702
G 98 CA-HA2 45.652 3.957
G 98 CA-HA3 45.685 3.228
L 99 CA-HA 52.704 5.505
L 99 CB-HB2 45.339 1.725
L 99 CB-HB3 45.336 1.047
L 99 CD1-HD1 22.895 0.683
L 99 CD2-HD2 25.365 0.646
L 99 CG-HG2 26.453 1.334
I 100 CA-HA 59.239 4.786
I 100 CB-HB 42.667 1.788
I 100 CD-HD 15.572 0.92
I 100 CG2-HG2 17.409 1.075
S 101 CA-HA 57.719 4.697
S 101 CB-HB2 63.587 4.262
S 101 CB-HB3 63.625 4.008
A 102 CA-HA 55.492 3.843
A 102 CB-HB 18.18 1.328
A 103 CA-HA 55.114 4.039
A 103 CB-HB 18.146 1.382
E 104 CA-HA 59.076 4.179
E 104 CB-HB## 29.503 2.144
E 104 CG-HG## 36.222 2.349
L 105 CA-HA 57.623 3.823
L 105 CB-HB2 41.213 1.816
L 105 CB-HB3 41.228 1.334
L 105 CD1-HD1 22.555 0.806
L 105 CD2-HD2 25.839 0.712
L 105 CG2-HG2 26.702 1.375
R 106 CA-HA 59.785 3.606
R 106 CB-HB## 29.986 1.826
R 106 CD-HD2 42.751 3.31
R 106 CD-HD3 42.751 3.029
R 106 CG-HG2 28.302 1.556
H 107 CA-HA 60.58 4.017
H 107 CB-HB2 30.409 3.361
H 107 CB-HB3 30.398 3.132
H 107 CD2-HD2 48.793 6.917
H 107 CE-HE1 67.426 7.724
V 108 CA-HA 66.455 3.494
V 108 CB-HB 31.887 1.754
V 108 CG2-HG2 20.947 0.711
V 108 CG3-HG3 21.421 0.575
M 109 CA-HA 56.224 4.312
M 109 CB-HB2 36.698 2.334
M 109 CB-HB3 36.752 1.628
M 109 CE-HE 20.615 1.84
M 109 CG-HG2 33.867 2.749
M 109 CG-HG3 33.86 2.443
T 110 CA-HA 61.828 4.563
T 110 CB-HB 70.765 4.349
T 110 CG-HG2 21.743 1.207
N 111 CA-HA 54.695 4.881
N 111 CB-HB2 41.136 2.393
N 111 CB-HB3 41.13 2.267
L 112 CA-HA 53.388 4.775
L 112 CB-HB2 45.617 1.861
L 112 CB-HB3 45.614 1.272
L 112 CD##-HD## 23.544 0.911
L 112 CG-HG2 27.676 1.622
G 113 CA-HA2 46.878 3.863
G 113 CA-HA3 46.986 3.771
E 114 CA-HA 54.797 4.299
E 114 CB-HB2 26.529 1.799
E 114 CB-HB3 26.453 1.741
E 114 CG-HG## 35.975 2.223
K 115 CA-HA 57.701 3.87
K 115 CB-HB## 33.649 1.485
K 115 CD-HD2 29.053 1.699
K 115 CD-HD3 29.248 1.547
K 115 CE-HE2 41.715 2.91
K 115 CE-HE3 41.693 2.861
K 115 CG-HG2 24.579 1.1
K 115 CG-HG3 24.449 0.871
L 116 CA-HA 54.279 4.627
L 116 CB-HB2 41.983 1.81
L 116 CB-HB3 42.084 1.354
L 116 CD1-HD1 21.997 1.014
L 116 CD2-HD2 27.256 0.856
L 116 CG-HG2 27.686 1.975
T 117 CA-HA 60.687 4.362
T 117 CB-HB 70.956 4.725
T 117 CG-HG2 21.772 1.328
D 118 CA-HA 57.84 4.305
D 118 CB-HB2 40.455 2.67
D 118 CB-HB3 40.335 2.538
D 119 CA-HA 57.282 4.408
D 119 CB-HB2 40.455 2.67
D 119 CB-HB3 40.481 2.531

E 120 CB-HB2 32.048 2.611
E 120 CB-HB3 32.073 1.924
V 121 CA-HA 64.698 3.836
V 121 CB-HB 31.288 1.87
V 121 CG2-HG2 21.027 1.052
V 121 CG3-HG3 24.696 1.003
D 122 CA-HA 57.282 4.408
D 122 CB-HB2 39.829 2.915
D 122 CB-HB3 40.005 2.592
E 123 CA-HA 63.329 4.182
E 123 CB-HB2 28.887 2.377
E 123 CB-HB3 28.893 2.205
E 123 CG-HG## 35.453 2.509
M 124 CA-HA 59.792 3.825
M 124 CB-HB2 33.536 1.925
M 124 CB-HB3 33.692 1.668
M 124 CE-HE 18.39 1.742
M 124 CG-HG2 32.28 1.844
M 124 CG-HG3 32.317 1.627
I 125 CA-HA 63.412 3.383
I 125 CB-HB 36.287 1.99
I 125 CD-HD 11.069 0.658
I 125 CG1-HG1## 28.79 1.423
I 125 CG2-HG2 18.1 0.869
R 126 CA-HA 59.299 4.009
R 126 CD-HD2 43.24 3.21
R 126 CD-HD3 43.248 3.117
E 127 CA-HA 58.126 4.176
E 127 CB-HB2 30.883 2.332
E 127 CB-HB3 30.852 2.232
E 127 CG-HG2 37.772 2.698
E 127 CG-HG3 37.758 2.334
A 128 CA-HA 53.076 3.968
A 128 CB-HB 18.732 0.593
D 129 CA-HA 52.572 4.757
D 129 CB-HB2 39.339 2.919
D 129 CB-HB3 39.412 2.234
I 130 CA-HA 62.973 3.967
I 130 CB-HB 38.73 1.81
I 130 CD-HD 13.605 0.906
I 130 CG1-HG12 27.904 1.562
I 130 CG1-HG13 27.796 1.137
I 130 CG2-HG2 17.571 0.953
D 133 CB-HB2 41.681 2.741
D 133 CB-HB3 41.764 2.586
G 134 CA-HA2 45.769 4.075
G 134 CA-HA3 45.766 3.499
H 135 CA-HA 54.87 5.06
H 135 CB-HB2 31.026 3.41
H 135 CB-HB3 31.125 2.853
H 135 CD2-HD2 49.618 6.895
H 135 CE-HE1 66.418 8.216
I 136 CA-HA 60.468 4.136
I 136 CB-HB 40.203 1.873
I 136 CD-HD 14.375 0.569
I 136 CG1-HG12 28.119 1.331
I 136 CG1-HG13 28.143 0.848
I 136 CG2-HG2 16.174 0.508
N 137 CA-HA 52.167 4.97
N 137 CB-HB2 36.93 3.131
N 137 CB-HB3 36.932 2.591
Y 138 CA-HA 59.116 4.014
Y 138 CB-HB2 36.825 2.179
Y 138 CB-HB3 37.076 2.021
Y 138 CD##-HD## 62.918 6.645
Y 138 CE##-HE## 46.864 6.749
E 139 CA-HA 60.879 3.82
E 139 CB-HB## 28.866 1.953
E 139 CG-HG## 36.825 2.179
F 141 CA-HA 59.991 4.585
F 141 CB-HB2 39.273 3.317
F 141 CB-HB3 39.097 2.767
F 141 CD##-HD## 59.734 7.13
F 141 CE##-HE## 57.622 7.053
V 142 CA-HA 67.664 3.262
V 142 CB-HB 31.555 2.278
V 142 CG2-HG2 25.806 1.168
V 142 CG3-HG3 22.962 1.101
R 143 CA-HA 57.999 4.162
R 143 CA-HA 60.068 4.16
R 143 CD-HD## 41.915 3.01
R 143 CG-HG## 25.226 1.528
M 144 CA-HA 58.905 4.018
M 144 CB-HB2 31.693 2.375
M 144 CB-HB3 31.665 2.176
M 144 CE-HE 16.9 1.929
M 144 CG-HG2 31.514 2.76
M 144 CG-HG3 31.665 2.176
M 145 CA-HA 59.428 3.71
M 145 CB-HB2 34.527 1.931
M 145 CB-HB3 34.549 1.652
M 145 CE-HE 16.694 1.713

M 145 CG-HG2 31.426 1.802
M 145 CG-HG3 31.432 1.363
V 146 CA-HA 62.485 4.296
V 146 CB-HB 31.693 2.375
V 146 CG2-HG2 19.812 0.953
V 146 CG3-HG3 21.369 0.902
S 147 CA-HA 59.314 4.462
S 147 CB-HB2 64.113 4.019
S 147 CB-HB3 63.903 3.849

Intramolecular NOE Assignments of $Na_v1.2_{IQp}$

Intramolecular NOE assignments of $Na_v1.2_{IQp}$ determined in 10 mM D_4-imidazole, 100 mM KCl, 50 μM D_{16}-EDTA, 0.01% NaN_3, pH 6.5, 298.15 K

Q1904HA-Q1904HB# 4.06 2.108
Q1904HA-E1905HN 4.06 8.783
Q1904HA-Q1904HN 4.06 8.387
Q1904HA-V1907HN 4.063 7.776
Q1904HA-Q1904HG# 4.061 2.315
Q1904HA-Q1904HG# 4.057 2.044
Q1904HA-Q1904HB# 4.062 1.932
Q1904HA-V1907HG## 4.063 1.064
Q1904HA-V1907HG## 4.073 0.966
Q1904HB#-Q1904HN 1.935 8.395
Q1904HB#-Q1904HN 2.099 8.369
Q1904HB#-Q1904HA 2.108 4.055
Q1904HB#-Q1904HA 1.93 4.061
Q1904HB#-Q1904HE2# 1.938 6.824
Q1904HB#-Q1904HE2# 1.939 6.932
Q1904HB#-Q1904HG# 2.109 2.312
Q1904HB#-Q1904HG# 2.109 2.048
Q1904HB#-Q1904HG# 1.932 2.313
Q1904HB#-Q1904HG# 1.932 2.048
Q1904HE2#-Q1904HB# 6.825 1.942
Q1904HE2#-Q1904HE2# 7.364 7.156
Q1904HE2#-Q1904HG# 6.827 2.031
Q1904HG#-Q1904HN 2.315 8.381
Q1904HG#-Q1904HA 2.324 4.066
Q1904HG#-Q1904HA 2.053 4.066
Q1904HG#-Q1904HN 2.058 8.377
Q1904HG#-Q1904HB# 2.049 2.108
Q1904HG#-Q1904HB# 2.314 2.108
Q1904HG#-Q1904HB# 2.048 1.935
Q1904HG#-Q1904HB# 2.322 1.933
Q1904HG#-Q1904HE2# 2.019 6.937
Q1904HG#-Q1904HE2# 2.031 6.824
Q1904HN-Q1904HB# 8.381 1.934
Q1904HN-Q1904HG# 8.38 2.314
Q1904HN-Q1904HG# 8.371 2.058
Q1904HN-E1905HN 8.382 8.785
Q1904HN-Q1904HB# 8.372 2.098
E1905HA-A1909HN 3.713 8.36
E1905HA-E1906HN 3.714 7.905
E1905HA-S1908HN 3.713 8.087
E1905HA-E1905HG# 3.713 2.227
E1905HA-E1905HN 3.713 8.782
E1905HA-E1905HG# 3.715 2.294
E1905HA-E1905HB# 3.714 2.054
E1905HB#-E1905HA 2.055 3.712
E1905HB#-E1905HN 2.056 8.783
E1905HB#-E1905HG# 2.058 2.285
E1905HB#-E1905HG# 2.058 2.219
E1905HG#-E1905HA 2.213 3.709
E1905HG#-E1905HA 2.284 3.713
E1905HG#-E1906HA 2.27 3.954
E1905HG#-E1905HN 2.232 8.782
E1905HG#-E1905HN 2.271 8.784
E1905HG#-E1905HB# 2.222 2.055
E1905HG#-E1905HB# 2.274 2.053
E1905HN-Q1904HN 8.782 8.387
E1905HN-E1905HA 8.784 3.712
E1905HN-E1905HG# 8.783 2.213
E1905HN-E1905HG# 8.785 2.29
E1905HN-E1906HN 8.784 7.903
E1905HN-E1905HB# 8.784 2.058
E1906HA-E1906HN 3.955 7.897
E1906HB#-V1907HN 2.269 7.79
E1906HB#-E1906HN 2.212 7.904
E1906HB#-E1906HN 2.284 7.901
E1906HB#-E1906HG# 2.279 2.332
E1906HB#-E1906HG# 2.218 2.331
E1906HG#-E1906HA 2.338 3.964
E1906HG#-E1906HN 2.342 7.913
E1906HG#-E1906HA 2.214 3.951

E1906HG#-E1906HB# 2.335 2.216
E1906HG#-E1906HB# 2.336 2.281
E1906HN-E1906HA 7.914 3.943
E1906HN-E1906HG# 7.905 2.33
E1906HN-E1905HN 7.903 8.783
E1906HN-E1906HB# 7.905 2.211
E1906HN-E1906HB# 7.904 2.277
V1907HA-I1910HB 3.638 2.134
V1907HA-V1907HN 3.629 7.79
V1907HA-V1907HG1# 3.641 1.061
V1907HA-V1907HG2# 3.631 0.973
V1907HB-V1907HA 2.145 3.627
V1907HB-V1907HN 2.157 7.792
V1907HB-V1907HG1# 2.152 1.054
V1907HB-V1907HG2# 2.154 0.973
V1907HG##-Q1904HA 1.027 4.023
V1907HG1#-V1907HA 1.07 3.629
V1907HG1#-V1907HB 1.065 2.145
V1907HG1#-V1907HG2# 1.062 0.969
V1907HG1#-V1907HN 1.063 7.791
V1907HG1#-S1908HN 1.067 8.076
V1907HG2#-V1907HA 0.965 3.628
V1907HG2#-V1907HB 0.97 2.147
V1907HG2#-V1907HG1# 0.969 1.063
V1907HG2#-V1907HN 0.979 7.792
V1907HG2#-S1908HN 0.971 8.076
V1907HN-V1907HA 7.791 3.628
V1907HN-S1908HN 7.792 8.076
V1907HN-V1907HB 7.777 2.144
V1907HN-V1907HG1# 7.791 1.063
V1907HN-V1907HG2# 7.799 0.974
S1908HA-A1909HN 4.111 8.356
S1908HA-V1911HB 4.103 2.237
S1908HA-S1908HN 4.115 8.077
S1908HA-S1908HB# 4.107 3.856
S1908HA-S1908HB# 4.105 3.997
S1908HA-V1911HG## 4.107 1.123
S1908HB#-A1909HN 4.001 8.359
S1908HB#-A1909HN 3.849 8.357
S1908HB#-S1908HA 3.853 4.108
S1908HB#-S1908HN 4.004 8.081
S1908HB#-S1908HN 3.855 8.077
S1908HB#-S1908HA 4.009 4.107
S1908HB#-Q1904HE2# 4.021 6.819
S1908HN-S1908HB# 8.08 3.997
S1908HN-A1909HB# 8.065 1.308
S1908HN-S1908HA 8.081 4.109
S1908HN-A1909HA 8.08 3.626
S1908HN-S1908HB# 8.08 3.856
S1908HN-V1907HN 8.074 7.789
S1908HN-A1909HN 8.073 8.351
A1909HA-Q1913HN 3.609 9.177
A1909HA-S1908HN 3.619 8.07
A1909HA-I1912HN 3.619 7.459
V1909HA-I1912HB 3.632 1.582
A1909HA-A1909HN 3.619 8.357
A1909HA-A1909HB# 3.621 1.305
V1909HA-I1912HD1# 3.616 0.207
V1909HA-I1912HG## 3.622 0.651
A1909HB#-Q1913HN 1.308 9.178
A1909HB#-I1912HN 1.307 7.461
A1909HB#-S1908HN 1.305 8.075
A1909HB#-E1906HA 1.306 3.956
A1909HB#-I1910HN 1.305 7.657
A1909HB#-A1909HA 1.306 3.618
A1909HB#-A1909HN 1.306 8.357
A1909HB#-E1906HB# 1.304 2.278
A1909HB#-Q1913HB# 1.305 1.925
A1909HB#-Q1913HE2# 1.306 7.713
A1909HB#-Q1913HE2# 1.303 6.275
A1909HN-S1908HB# 8.36 3.991
A1909HN-E1905HA 8.355 3.711
A1909HN-S1908HB# 8.359 3.857
A1909HN-A1909HA 8.357 3.618
A1909HN-I1910HN 8.357 7.658
A1909HN-S1908HN 8.351 8.074
A1909HN-A1909HB# 8.357 1.305
I1910HA-Q1913HB# 3.624 1.94
I1910HA-Q1913HN 3.624 9.176
I1910HA-I1910HN 3.624 7.656
I1910HA-I1910HB 3.634 2.152
I1910HA-I1910HG1# 3.636 1.062
I1910HA-I1910HG1# 3.621 1.092
I1910HB-I1910HN 2.159 7.665
I1910HB-I1910HA 2.146 3.626
I1910HB-I1910HG1# 2.151 1.058
I1910HB-I1910HG1# 2.149 1.085
I1910HG1#-I1910HA 1.089 3.615
I1910HG1#-I1910HA 1.053 3.622
I1910HG1#-I1910HB 1.062 2.154
I1910HG1#-I1910HB 1.085 2.154
I1910HN-I1910HB 7.656 2.154

I1910HN-I1910HA 7.646 3.622
I1910HN-A1909HB# 7.659 1.304
I1910HN-V1911HN 7.65 7.596
V1911HA-I1912HN 3.542 7.46
V1911HA-R1914HN 3.543 8.965
V1911HA-R1914HB# 3.562 1.939
V1911HA-V1911HB 3.545 2.231
V1911HA-V1911HN 3.547 7.597
V1911HA-V1911HG1# 3.544 1.122
V1911HA-V1911HG2# 3.545 0.867
V1911HB-V1911HA 2.239 3.549
V1911HB-I1912HN 2.24 7.461
V1911HB-V1911HN 2.238 7.596
V1911HB-V1911HG1# 2.239 1.123
V1911HB-V1911HG2# 2.252 0.879
V1911HG##-S1908HA 1.121 4.107
V1911HG1#-V1911HA 1.123 3.544
V1911HG1#-V1911HB 1.122 2.235
V1911HG1#-V1911HG2# 1.122 0.872
V1911HG1#-V1911HN 1.123 7.597
V1911HG1#-Q1913HN 1.126 9.181
V1911HG2#-V1911HA 0.871 3.546
V1911HG2#-V1911HB 0.875 2.238
V1911HG2#-V1911HG1# 0.874 1.123
V1911HG2#-V1911HN 0.879 7.606
V1911HG2#-I1912HA 0.873 3.36
V1911HG2#-Q1913HN 0.867 9.176
V1911HN-S1908HA 7.593 4.105
V1911HN-I1912HN 7.593 7.462
V1911HN-V1911HA 7.594 3.547
V1911HN-V1911HB 7.598 2.238
V1911HN-I1910HN 7.597 7.655
V1911HN-V1911HG1# 7.597 1.123
V1911HN-V1911HG2# 7.593 0.876
I1912HA-Y1916HN 3.355 9.454
I1912HA-Q1913HN 3.366 9.177
I1912HA-A1915HN 3.357 7.89
I1912HA-I1912HD# 3.36 0.2
I1912HA-I1912HN 3.361 7.46
I1912HA-I1912HB 3.359 1.594
I1912HA-V1911HG2# 3.362 0.871
I1912HA-I1912HG1# 3.362 0.653
I1912HA-I1912HG1# 3.364 1.499
I1912HA-I1912HG2# 3.361 0.113
I1912HB-V1909HA 1.589 3.617
I1912HB-Q1913HN 1.586 9.176
I1912HB-I1912HN 1.586 7.462
I1912HB-I1912HD# 1.585 0.201
I1912HB-I1912HG1# 1.587 0.652
I1912HB-I1912HG1# 1.585 1.512
I1912HB-I1912HG2# 1.576 0.12
I1912HD1#-A1909HA 0.201 3.617
I1912HD1#-A1909HB# 0.202 1.304
I1912HD1#-I1912HA 0.2 3.36
I1912HD1#-I1912HB 0.199 1.586
I1912HD1#-I1912HG1# 0.199 1.503
I1912HD1#-I1912HG1# 0.2 0.653
I1912HD1#-I1912HG2# 0.2 0.109
I1912HD1#-I1912HN 0.2 7.46
I1912HD1#-Q1913HN 0.2 9.177
I1912HG1#-I1912HA 0.654 3.36
I1912HG1#-I1912HA 1.506 3.36
I1912HG1#-I1912HB 1.501 1.584
I1912HG1#-I1912HB 0.654 1.591
I1912HG1#-I1912HD# 1.503 0.201
I1912HG1#-I1912HD# 0.654 0.201
I1912HG1#-I1912HG2# 1.503 0.111
I1912HG1#-I1912HG2# 0.654 0.113
I1912HG1#-I1912HN 1.503 7.46
I1912HG1#-I1912HN 0.654 7.461
I1912HG1#-Q1913HA 0.653 3.794
I1912HG1#-Q1913HN 0.654 9.175
I1912HG1#-Y1916HN 0.653 9.45
I1912HG2#-I1912HA 0.111 3.36
I1912HG2#-I1912HB 0.114 1.583
I1912HG2#-I1912HD# 0.107 0.203
I1912HG2#-I1912HG1# 0.111 1.503
I1912HG2#-I1912HG1# 0.11 0.653
I1912HG2#-I1912HN 0.113 7.461
I1912HN-A1909HA 7.457 3.614
I1912HN-I1912HD# 7.46 0.202
I1912HN-I1912HA 7.46 3.36
I1912HN-Q1913HN 7.461 9.175
I1912HN-I1912HB 7.461 1.584
I1912HN-V1911HN 7.464 7.596
I1912HN-I1912HG1# 7.461 1.505
I1912HN-I1912HG1# 7.46 0.652
I1912HN-I1912HG2# 7.459 0.111
Q1913HA-Y1916HN 3.797 9.454
Q1913HA-Q1913HB# 3.782 2.664
Q1913HA-R1914HN 3.792 8.965
Q1913HA-Y1916HB# 3.79 2.969

Q1913HA-Q1913HG# 3.784 2.503
Q1913HA-Q1913HG# 3.78 2.327
Q1913HA-Q1913HB# 3.794 1.932
Q1913HA-Q1913HN 3.792 9.176
Q1913HA-I1912HG1# 3.789 0.655
Q1913HB#-Q1913HA 2.657 3.785
Q1913HB#-Q1913HA 1.942 3.789
Q1913HB#-R1914HN 2.659 8.966
Q1913HB#-Q1913HN 1.93 9.176
Q1913HB#-Q1913HN 2.658 9.176
Q1913HB#-Q1913HE2# 2.677 6.274
Q1913HB#-Q1913HE2# 1.946 7.726
Q1913HB#-Q1913HG# 1.946 2.504
Q1913HB#-Q1913HG# 2.657 2.322
Q1913HB#-Q1913HG# 2.657 2.508
Q1913HB#-Y1916HE# 1.935 7.061
Q1913HE2#-A1909HB# 7.728 1.304
Q1913HE2#-A1909HB# 6.273 1.304
Q1913HE2#-Q1913HB# 7.718 1.939
Q1913HE2#-Q1913HG# 6.274 2.504
Q1913HE2#-Q1913HG# 6.275 2.325
Q1913HE2#-Q1913HG# 7.714 2.324
Q1913HG#-Q1913HA 2.328 3.791
Q1913HG#-Q1913HA 2.504 3.791
Q1913HG#-Q1913HN 2.33 9.176
Q1913HG#-Q1913HN 2.506 9.176
Q1913HG#-Q1913HB# 2.503 2.662
Q1913HG#-Q1913HB# 2.503 1.93
Q1913HG#-Q1913HB# 2.322 1.933
Q1913HG#-Q1913HB# 2.323 2.655
Q1913HG#-Q1913HE2# 2.324 7.716
Q1913HG#-Q1913HE2# 2.503 6.274
Q1913HG#-Q1913HE2# 2.33 6.274
Q1913HG#-Q1913HE2# 2.502 7.713
Q1913HN-I1912HA 9.177 3.359
Q1913HN-Q1913HG# 9.176 2.324
Q1913HN-R1914HN 0.86 8.967
Q1913HN-Q1913HB# 9.175 1.931
Q1913HN-Q1913HA 9.175 3.789
Q1913HN-Q1913HB# 9.175 2.659
Q1913HN-Q1913HG# 9.175 2.503
Q1913HN-I1912HB 9.176 1.585
Q1913HN-R1914HN 9.175 8.968
Q1913HN-I1912HN 9.175 7.461
Q1913HN-I1912HG1# 9.176 0.653
R1914HA-R1914HD# 4.064 2.998
R1914HA-R1917HN 4.075 8.575
R1914HA-R1917HB# 4.071 1.551
R1914HA-R1914HN 4.072 8.967
R1914HA-R1914HG# 4.074 1.71
R1914HA-R1914HB# 4.072 2.151
R1914HA-R1914HG# 4.071 1.828
R1914HA-R1914HB# 4.071 1.944
R1914HA-V1911HG2# 4.066 0.885
R1914HB#-Q1913HN 2.16 9.178
R1914HB#-R1914HN 2.155 8.967
R1914HB#-R1914HN 1.944 8.967
R1914HB#-R1914HA 2.134 4.065
R1914HB#-R1914HA 1.946 4.069
R1914HB#-R1914HD# 1.951 3.168
R1914HB#-R1914HD# 2.154 3.174
R1914HB#-R1914HD# 1.949 2.998
R1914HB#-R1914HG# 1.949 1.71
R1914HB#-R1914HG# 1.949 1.828
R1914HB#-R1914HG# 2.151 1.706
R1914HB#-R1914HG# 2.149 1.828
R1914HD#-R1914HN 3.155 8.966
R1914HD#-R1914HN 3.003 8.966
R1914HD#-R1914HB# 3.003 1.944
R1914HD#-R1914HB# 3.003 2.151
R1914HD#-R1914HB# 3.154 1.944
R1914HD#-R1914HB# 3.158 2.15
R1914HD#-R1914HG# 3.172 1.719
R1914HD#-R1914HG# 3.154 1.828
R1914HD#-R1914HG# 3.003 1.828
R1914HG#-R1914HN 1.719 8.964
R1914HG#-R1914HN 1.832 8.966
R1914HG#-R1914HA 1.821 4.062
R1914HG#-R1914HB# 1.716 2.153
R1914HG#-R1914HB# 1.713 1.942
R1914HG#-R1914HB# 1.823 2.151
R1914HG#-R1914HB# 1.823 1.944
R1914HG#-R1914HD# 1.83 3.168
R1914HG#-R1914HD# 1.719 3.164
R1914HG#-R1914HD# 1.823 2.998
R1914HG#-R1917HD# 1.707 3.243
R1914HN-R1914HD# 8.969 2.991
R1914HN-R1914HA 8.966 4.072
R1914HN-Q1913HB# 8.969 2.661
R1914HN-R1914HG# 8.965 1.713
R1914HN-R1914HG# 8.969 1.827
R1914HN-R1914HB# 8.969 2.155

R1914HN-Q1913HN 8.969 9.176
R1914HN-R1914HB# 8.97 1.943
R1914HN-Q1913HB# 8.967 1.937
R1914HN-A1915HN 8.969 7.897
A1915HA-R1917HN 4.214 8.573
A1915HA-Y1916HN 4.209 9.453
A1915HA-R1918HB# 4.214 1.551
A1915HA-R1918HB# 4.215 1.55
A1915HA-R1918H 4.212 7.849
A1915HA-Y1919HN 4.208 8.032
A1915HA-A1915HN 4.214 7.904
A1915HA-A1915HB# 4.211 1.623
A1915HA-I1912HG## 4.212 1.513
A1915HB#-R1914HN 1.619 8.965
A1915HB#-A1915HA 1.634 4.214
A1915HB#-Y1916HN 1.623 9.45
A1915HB#-I1912HA 1.586 3.358
A1915HB#-A1915HN 1.624 7.896
A1915HB##-I1912HA 1.627 3.357
A1915HB##-R1918HN 1.628 7.844
A1915HN-A1915HA 7.903 4.211
A1915HN-Y1916HN 7.896 9.451
A1915HN-R1914HN 7.897 8.967
A1915HN-A1915HB# 7.897 1.623
Y1916HA-R1917HN 4.542 8.566
Y1916HA-Y1916HD# 4.545 6.968
Y1916HA-Y1919HN 4.544 8.025
Y1916HA-Y1919HB# 4.527 3.34
Y1916HA-Y1916HN 4.545 9.452
Y1916HA-Y1916HB# 4.529 2.967
Y1916HA-Y1919HB# 4.53 3.2
Y1916HA-Y1916HE# 4.543 7.082
Y1916HB#-R1917HN 2.97 8.578
Y1916HB#-Y1916HN 2.97 9.452
Y1916HB#-Y1916HD# 2.964 6.966
Y1916HB#-Y1916HE# 2.982 7.083
Y1916HD#-Y1916HB# 6.959 2.979
Y1916HE#-Y1916HN 7.088 9.451
Y1916HE#-Y1916HB# 7.089 2.973
Y1916HE#-Y1916HD# 7.089 6.968
Y1916HE#-Y1916HD# 6.969 7.086
Y1916HN-Q1913HA 9.446 3.789
Y1916HN-Y1916HE# 9.451 7.092
Y1916HN-Y1916HB# 9.45 2.968
Y1916HN-R1917HN 9.451 8.579
Y1916HN-Y1919HB# 9.449 3.207
Y1916HN-A1915HN 9.449 7.897
R1917HA-L1920HD# 3.834 0.815
R1917HA-L1920HG 3.835 1.686
R1917HA-R1917HB# 3.834 2.019
R1917HA-R1917HG# 3.833 1.872
R1917HA-R1917HG# 3.833 1.822
R1917HA-L1920HB# 3.834 1.264
R1917HA-R1917HB# 3.832 1.552
R1917HA-R1917HN 3.829 8.572
R1917HA-L1920HD# 3.83 0.851
R1917HB#-R1917HN 1.552 8.569
R1917HB#-R1917HA 2.02 3.837
R1917HB#-R1914HA 1.556 4.068
R1917HB#-R1917HA 1.552 3.836
R1917HB#-R1917HN 2.011 8.577
R1917HB#-R1917HD# 1.552 3.229
R1917HB#-R1917HD# 2.02 3.06
R1917HB#-R1917HD# 2.015 3.23
R1917HB#-R1917HD# 1.551 3.051
R1917HB#-R1917HG# 2.016 1.876
R1917HB#-R1917HG# 1.552 1.825
R1917HB#-R1917HG# 2.016 1.825
R1917HB#-R1917HG# 1.552 1.876
R1917HD#-R1917HN 3.053 8.581
R1917HD#-R1917HN 3.222 8.581
R1917HD#-R1914HG# 3.232 1.827
R1917HD#-R1917HB# 3.223 2.023
R1917HD#-R1917HB# 3.052 1.546
R1917HD#-R1917HB# 3.232 1.546
R1917HD#-R1917HG# 3.232 1.872
R1917HD#-R1917HG# 3.052 1.825
R1917HD#-R1917HG# 3.052 1.876
R1917HG#-R1917HA 1.88 3.836
R1917HG#-R1917HA 1.828 3.84
R1917HG#-R1917HN 1.815 8.573
R1917HG#-R1917HN 1.876 8.579
R1917HG#-R1917HB# 1.825 1.546
R1917HG#-R1917HB# 1.825 2.015
R1917HG#-R1917HB# 1.877 2.015
R1917HG#-R1917HB# 1.877 1.546
R1917HG#-R1917HD# 1.877 3.052
R1917HG#-R1917HD# 1.825 3.229
R1917HG#-R1917HD# 1.825 3.052
R1917HG#-R1917HD# 1.877 3.229
R1917HN-R1917HB# 8.577 1.551
R1917HN-R1917HB# 8.58 2.02

R1917HN-R1917HA 8.577 3.83
R1917HN-Y1916HN 8.577 9.452
R1917HN-R1917HG# 8.576 1.821
R1917HN-R1917HG# 8.578 1.882
R1917HN-R1918HN 8.577 7.846
R1918HB#-R1918HN 1.554 7.844
R1918HB#-R1918HD# 1.554 3.046
R1918HB#-R1918HD# 1.554 3.214
R1918HB#-R1918HG# 1.554 2.08
R1918HB#-R1918HG# 1.555 2.014
R1918HD#-R1918HB# 3.223 1.559
R1918HD#-R1918HG# 3.222 2.012
R1918HD#-R1918HG# 3.228 2.079
R1918HG#-R1918HN 2.087 7.846
R1918HG#-R1918HB# 2.015 1.548
R1918HG#-R1918HB# 2.078 1.551
R1918HG#-R1918HD# 2.078 3.214
R1918HG#-R1918HD# 2.008 3.047
R1918HG#-R1918HD# 2.015 3.214
R1918HN-R1918HD# 7.843 3.214
R1918HN-R1918HG# 7.847 2.013
R1918HN-R1918HB# 7.836 1.558
R1918HN-R1918HD# 7.828 3.047
R1918HN-R1918HG# 7.85 2.082
R1918HN-R1917HN 7.848 8.577
Y1919HA-L1920HN 4.301 8.554
Y1919HA-Y1919HB# 4.302 3.339
Y1919HA-Y1919HN 4.306 8.017
Y1919HA-Y1919HB# 4.307 3.198
Y1919HA-Y1919HD# 4.303 7.066
Y1919HB#-Y1919HA 3.34 4.304
Y1919HB#-Y1919HA 3.187 4.309
Y1919HB#-L1920HN 3.344 8.559
Y1919HB#-L1920HN 3.196 8.562
Y1919HB#-Y1916HN 3.208 9.451
Y1919HB#-Y1919HN 3.344 8.025
Y1919HB#-Y1919HN 3.19 8.029
Y1919HB#-Y1919HD# 3.197 7.072
Y1919HB#-Y1919HD# 3.344 7.067
Y1919HB#-Y1919HE# 3.348 6.968
Y1919HB#-Y1919HE# 3.203 6.968
Y1919HD#-Y1919HA 7.066 4.303
Y1919HD#-Y1919HN 7.068 8.025
Y1919HD#-L1920HN 7.07 8.56
Y1919HD#-Y1919HB# 7.068 3.342
Y1919HD#-Y1919HB# 7.075 3.197
Y1919HD#-Y1919HE# 7.062 6.967
Y1919HE#-Y1919HB# 6.976 3.345
Y1919HE#-Y1919HB# 6.968 3.2
Y1919HE#-Y1919HD# 6.969 7.068
Y1919HN-Y1919HA 8.02 4.307
Y1919HN-L1920HN 8.026 8.56
Y1919HN-Y1919HB# 8.024 3.344
Y1919HN-Y1919HB# 8.028 3.189
Y1919HN-Y1919HD## 8.024 7.068
L1920HA-L1921HN 3.566 7.55
L1920HA-Y1919HD# 3.57 7.064
L1920HA-L1920HG 3.565 1.686
L1920HA-L1920HN 3.569 8.557
L1920HA-L1920HB# 3.567 1.267
L1920HA-L1920HD1# 3.581 0.856
L1920HA-L1920HD2# 3.568 0.814
L1920HB#-L1920HA 1.269 3.573
L1920HB#-L1920HG 1.267 1.69
L1920HB#-Y1919HD# 1.26 7.066
L1920HB#-Y1919HE# 1.259 6.97
L1920HB#-L1920HD1# 1.263 0.85
L1920HB#-L1920HD2# 1.263 0.816
L1920HD1#-R1917HA 0.85 3.833
L1920HD1#-L1920HA 0.856 3.577
L1920HD1#-L1920HB# 0.854 1.262
L1920HD1#-L1920HD2# 0.854 0.814
L1920HD1#-L1920HG 0.853 1.691
L1920HD2#-L1920HA 0.817 3.569
L1920HD2#-L1920HB# 0.814 1.263
L1920HD2#-L1920HD1# 0.815 0.854
L1920HD2#-L1920HG 0.815 1.69
L1920HG-R1917HA 1.688 3.838
L1920HG-L1920HA 1.688 3.571
L1920HG-L1920HB# 1.689 1.263
L1920HG-L1920HD1# 1.676 0.849
L1920HG-L1920HD2# 1.691 0.817
L1920HN-Y1919HB# 8.559 3.343
L1920HN-Y1919HB# 8.569 3.201
L1920HN-L1920HA 8.557 3.569
L1920HN-Y1919HD# 8.56 7.068
L1920HN-L1920HG 8.557 1.689
L1920HN-L1921HN 8.556 7.553
L1920HN-Y1919HN 8.558 8.025
L1920HN-L1920HB# 8.558 1.262
L1920HN-L1920HD1# 8.56 0.851
L1920HN-L1920HD2# 8.558 0.813

L1921HA-L1921HG 4.063 1.275
L1921HA-L1920HN 4.073 8.571
L1921HA-L1921HN 4.069 7.552
L1921HA-L1921HB# 4.068 1.685
L1921HA-L1921HD1# 4.07 0.842
L1921HA-L1921HD2# 4.077 0.818
L1921HB#-L1921HA 1.679 4.067
L1921HB#-L1921HN 1.683 7.552
L1921HB#-L1921HG 1.689 1.263
L1921HB#-L1921HD1# 1.698 0.859
L1921HB#-L1921HD2# 1.687 0.815
L1921HD1#-L1921HB# 0.848 1.69
L1921HD1#-L1921HD2# 0.849 0.813
L1921HD1#-L1921HG 0.848 1.264
L1921HD1#-L1921HN 0.845 7.55
L1921HD2#-L1921HB# 0.818 1.69
L1921HD2#-L1921HD1# 0.818 0.849
L1921HD2#-L1921HG 0.818 1.267
L1921HD2#-L1921HN 0.81 7.561
L1921HG-R1917HA 1.27 3.837
L1921HG-L1921HN 1.266 7.552
L1921HG-L1921HB# 1.267 1.69
L1921HG-L1921HD1# 1.264 0.85
L1921HG-L1921HD2# 1.263 0.816
L1921HN-L1921HA 7.552 4.071
L1921HN-L1921HG 7.554 1.266
L1921HN-L1920HN 7.552 8.558
L1921HN-L1921HB# 7.551 1.685
L1921HN-L1921HD1# 7.56 0.857
L1921HN-L1921HD2# 7.55 0.804
V1925HA-V1925HB 3.921 2.139
V1925HA-V1925HN 3.93 7.754
V1925HA-V1925HG1# 3.914 1.01
V1925HA-V1925HG2# 3.92 0.942
V1925HB-V1925HA 2.136 3.916
V1925HB-V1925HN 2.13 7.761
V1925HB-V1925HG1# 2.136 1.017
V1925HB-V1925HG2# 2.116 0.927
V1925HG1#-V1925HA 1.012 3.921
V1925HG1#-V1925HB 1.012 2.139
V1925HG1#-V1925HG2# 1.012 0.934
V1925HG1#-V1925HN 1.011 7.761
V1925HG2#-V1925HA 0.94 3.921
V1925HG2#-V1925HB 0.936 2.139
V1925HG2#-V1925HG1# 0.936 1.008
V1925HG2#-V1925HN 0.942 7.766
V1925HN-V1925HA 7.763 3.921
V1925HN-V1925HB 7.767 2.136
V1925HN-V1925HG1# 7.761 1.01
V1925HN-V1925HG2# 7.761 0.94

APPENDIX F

RESTRAINT FILES USED FOR APO $CAM_{76\text{-}148}$:$NA_V1.2_{IQP}$ STRUCTURE CALCULATION

Carbon NOE Restraint File

```
assign ( residue   99 and name HA   ) ( residue  137 and name HA   )  3.00  1.20  0.00
assign ( residue  116 and name HD1# ) ( residue  124 and name HE#  )  5.00  3.20  0.50
assign ( residue   93 and name HA   ) ( residue  100 and name HA   )  5.00  3.20  0.50
assign ( residue   99 and name HA   ) ( residue  100 and name HA   )  5.00  3.20  0.50
assign ( residue   89 and name HA   ) ( residue  100 and name HD#  )  5.00  3.20  0.50
assign ( residue   93 and name HA   ) ( residue  100 and name HD#  )  5.00  3.20  0.50
assign ( residue  100 and name HD#  ) ( residue  100 and name HA   )  5.00  3.20  0.50
assign ( residue  100 and name HD#  ) ( residue  105 and name HA   )  5.00  3.20  0.50
assign ( residue  104 and name HA   ) ( residue  107 and name HA   )  6.00  4.20  0.60
assign ( residue  105 and name HA   ) ( residue  106 and name HA   )  5.00  3.20  0.50
assign ( residue  105 and name HA   ) ( residue  108 and name HA   )  5.00  3.20  0.50
assign ( residue  108 and name HG## ) ( residue 1909 and name HA   )  6.00  4.20  0.60
assign ( residue  109 and name HA   ) ( residue 1909 and name HA   )  5.00  3.20  0.50
assign ( residue  109 and name HE#  ) ( residue 1909 and name HA   )  3.00  1.20  0.30
assign ( residue  109 and name HG#  ) ( residue 1909 and name HA   )  5.00  3.20  0.50
assign ( residue  105 and name HA   ) ( residue  109 and name HG#  )  6.00  4.20  0.60
assign ( residue  110 and name HA   ) ( residue  111 and name HA   )  5.00  3.20  0.50
assign ( residue  110 and name HB   ) ( residue  111 and name HA   )  5.00  3.20  0.50
assign ( residue  110 and name HB   ) ( residue  116 and name HA   )  6.00  4.20  0.50
assign ( residue  112 and name HA   ) ( residue 1906 and name HA   )  6.00  4.20  0.60
assign ( residue  112 and name HB#  ) ( residue 1906 and name HA   )  4.00  2.20  0.40
assign ( residue  112 and name HD#  ) ( residue 1906 and name HA   )  4.00  2.20  0.40
assign ( residue  113 and name HA#  ) ( residue 1906 and name HA   )  6.00  4.20  0.40
assign ( residue  113 and name HA#  ) ( residue 1909 and name HA   )  6.00  4.20  0.60
assign ( residue  112 and name HA   ) ( residue  113 and name HA#  )  5.00  3.20  0.50
assign ( residue  110 and name HA   ) ( residue  115 and name HA   )  5.00  3.20  0.50
assign ( residue  110 and name HA   ) ( residue  115 and name HD#  )  5.00  3.20  0.50
assign ( residue  116 and name HD1# ) ( residue 1913 and name HA   )  3.00  1.20  0.30
assign ( residue  116 and name HD1# ) ( residue  121 and name HA   )  5.00  3.20  0.50
assign ( residue  116 and name HD2# ) ( residue 1913 and name HA   )  5.00  3.20  0.50
assign ( residue  116 and name HG   ) ( residue 1913 and name HA   )  5.00  3.20  0.50
assign ( residue  109 and name HA   ) ( residue  116 and name HG   )  6.00  4.20  0.60
assign ( residue  117 and name HG#  ) ( residue  117 and name HA   )  3.00  1.20  0.30
assign ( residue  120 and name HB#  ) ( residue  120 and name HA   )  4.00  2.20  0.40
assign ( residue  106 and name HA   ) ( residue  121 and name HA   )  6.00  4.20  0.60
assign ( residue  123 and name HA   ) ( residue  124 and name HB#  )  5.00  3.20  0.50
assign ( residue  102 and name HA   ) ( residue  125 and name HA   )  5.00  3.20  0.50
```

```
assign ( residue  102 and name HA   ) ( residue  125 and name HD# )   4.00  2.20  0.40
assign ( residue  106 and name HA   ) ( residue  125 and name HD# )   5.00  3.20  0.50
assign ( residue  122 and name HA   ) ( residue  125 and name HD# )   5.00  3.20  0.50
assign ( residue  125 and name HD# ) ( residue  125 and name HA   )   4.00  2.20  0.40
assign ( residue  102 and name HA   ) ( residue  125 and name HG1# )  5.00  3.20  0.50
assign ( residue  121 and name HA   ) ( residue  125 and name HG1# )  5.00  3.20  0.50
assign ( residue  121 and name HA   ) ( residue  125 and name HG2# )  5.00  3.20  0.50
assign ( residue  124 and name HA   ) ( residue  127 and name HG# )   5.00  3.20  0.50
assign ( residue  125 and name HA   ) ( residue  128 and name HB# )   5.00  3.20  0.50
assign ( residue  130 and name HD# ) ( residue  130 and name HA   )   5.00  3.20  0.50
assign ( residue  133 and name HA   ) ( residue  134 and name HA# )   5.00  3.20  0.50
assign ( residue  130 and name HA   ) ( residue  136 and name HG1# )  5.00  3.20  0.50
assign ( residue   90 and name HA   ) ( residue  138 and name HD# )   5.00  3.20  0.50
assign ( residue   90 and name HA   ) ( residue  138 and name HE# )   5.00  3.20  0.50
assign ( residue   93 and name HA   ) ( residue  138 and name HE# )   5.00  3.20  0.50
assign ( residue  138 and name HA   ) ( residue  141 and name HA   )   6.00  4.20  0.60
assign ( residue  143 and name HG# ) ( residue  143 and name HA   )   4.00  2.20  0.40
assign ( residue  145 and name HA   ) ( residue 1919 and name HA   )   5.00  3.20  0.50
assign ( residue  145 and name HA   ) ( residue  146 and name HA   )   5.00  3.20  0.50
assign ( residue  145 and name HB# ) ( residue 1919 and name HA   )   5.00  3.20  0.50
assign ( residue  145 and name HE# ) ( residue 1912 and name HA   )   5.00  3.20  0.50
assign ( residue  145 and name HE# ) ( residue 1916 and name HA   )   5.00  3.20  0.50
assign ( residue  145 and name HG# ) ( residue 1919 and name HA   )   5.00  3.20  0.50
assign ( residue  145 and name HG# ) ( residue  146 and name HA   )   5.00  3.20  0.50
assign ( residue  146 and name HA   ) ( residue  147 and name HA   )   5.00  3.20  0.50
assign ( residue   82 and name HB# ) ( residue   82 and name HA   )   5.00  3.20  0.50
assign ( residue   85 and name HD## ) ( residue 1912 and name HA   )   3.00  1.20  0.30
assign ( residue   85 and name HD## ) ( residue 1915 and name HA   )   5.00  3.20  0.50
assign ( residue   83 and name HA   ) ( residue   86 and name HG1# )   5.00  3.20  0.50
assign ( residue   88 and name HB# ) ( residue 1911 and name HA   )   5.00  3.20  0.50
assign ( residue   88 and name HB# ) ( residue 1912 and name HA   )   5.00  3.20  0.50
assign ( residue   89 and name HD# ) ( residue   92 and name HA   )   6.00  4.20  0.50
assign ( residue   87 and name HA   ) ( residue   90 and name HB# )   4.00  2.20  0.40
assign ( residue   87 and name HA   ) ( residue   90 and name HD# )   4.00  2.20  0.40
assign ( residue   87 and name HA   ) ( residue   90 and name HG# )   5.00  3.20  0.50
assign ( residue   91 and name HB   ) ( residue 1905 and name HA   )   5.00  3.20  0.50
assign ( residue   88 and name HA   ) ( residue   91 and name HB   )   5.00  3.20  0.50
assign ( residue   91 and name HG## ) ( residue 1905 and name HA   )   3.00  1.20  0.30
assign ( residue   91 and name HG## ) ( residue 1908 and name HA   )   5.00  3.20  0.50
assign ( residue   92 and name HD# ) ( residue 1905 and name HA   )   5.00  3.20  0.50
assign ( residue   92 and name HD# ) ( residue 1909 and name HA   )   5.00  3.20  0.50
assign ( residue   89 and name HA   ) ( residue   92 and name HD# )   5.00  3.20  0.50
assign ( residue   92 and name HE# ) ( residue 1905 and name HA   )   4.00  2.20  0.40
assign ( residue   92 and name HE# ) ( residue 1908 and name HA   )   6.00  4.20  0.60
assign ( residue   92 and name HE# ) ( residue 1909 and name HA   )   5.00  3.20  0.50
assign ( residue   90 and name HA   ) ( residue   93 and name HA   )   5.00  3.20  0.50
```

```
assign ( residue   90 and name HA   ) ( residue   93 and name HB# )   4.00  2.20  0.40
assign ( residue   99 and name HG   ) ( residue  137 and name HA   )   5.00  3.20  0.50
assign ( residue  100 and name HA   ) ( residue  100 and name HB   )   3.00  1.20  0.30
assign ( residue  100 and name HD# ) ( residue  100 and name HB   )   3.00  1.20  0.30
assign ( residue  105 and name HA   ) ( residue  108 and name HB   )   4.00  2.20  0.40
assign ( residue  105 and name HG   ) ( residue  108 and name HB   )   5.00  3.20  0.50
assign ( residue  108 and name HA   ) ( residue  108 and name HB   )   3.00  1.20  0.30
assign ( residue  109 and name HE# ) ( residue 1912 and name HB   )   4.00  2.20  0.40
assign ( residue  110 and name HA   ) ( residue  110 and name HB   )   3.00  1.20  0.30
assign ( residue  116 and name HB# ) ( residue  121 and name HB   )   4.00  2.20  0.40
assign ( residue  117 and name HA   ) ( residue  117 and name HB   )   3.00  1.20  0.30
assign ( residue  117 and name HG# ) ( residue  117 and name HB   )   3.00  1.20  0.30
assign ( residue  118 and name HA   ) ( residue  121 and name HB   )   5.00  3.20  0.50
assign ( residue  121 and name HA   ) ( residue  121 and name HB   )   3.00  1.20  0.30
assign ( residue  122 and name HA   ) ( residue  125 and name HB   )   5.00  3.20  0.50
assign ( residue  125 and name HA   ) ( residue  125 and name HB   )   4.00  2.20  0.40
assign ( residue  125 and name HD# ) ( residue  125 and name HB   )   5.00  3.20  0.50
assign ( residue  130 and name HA   ) ( residue  130 and name HB   )   5.00  3.20  0.50
assign ( residue  130 and name HD# ) ( residue  130 and name HB   )   5.00  3.20  0.50
assign ( residue  136 and name HA   ) ( residue  136 and name HB   )   5.00  3.20  0.50
assign ( residue  136 and name HD# ) ( residue  136 and name HB   )   5.00  3.20  0.50
assign ( residue  100 and name HB   ) ( residue  138 and name HB# )   5.00  3.20  0.50
assign ( residue  139 and name HA   ) ( residue  142 and name HB   )   5.00  3.20  0.40
assign ( residue  142 and name HA   ) ( residue  142 and name HB   )   4.00  2.20  0.40
assign ( residue  146 and name HA   ) ( residue  146 and name HB   )   3.00  1.20  0.30
assign ( residue   81 and name HB# ) ( residue  142 and name HB   )   6.00  4.20  0.50
assign ( residue   86 and name HA   ) ( residue   86 and name HB   )   4.00  2.20  0.40
assign ( residue   86 and name HD# ) ( residue   86 and name HB   )   3.00  1.20  0.30
assign ( residue   88 and name HA   ) ( residue 1911 and name HB   )   6.00  4.20  0.60
assign ( residue   88 and name HB# ) ( residue 1911 and name HB   )   4.00  2.20  0.40
assign ( residue   91 and name HA   ) ( residue   91 and name HB   )   3.00  1.20  0.30
assign ( residue   92 and name HB# ) ( residue  100 and name HB   )   5.00  3.20  0.50
assign ( residue   93 and name HA   ) ( residue  100 and name HB   )   5.00  3.20  0.50
assign ( residue   92 and name HB# ) ( residue  100 and name HD# )   4.00  2.20  0.40
assign ( residue  101 and name HA   ) ( residue  101 and name HB# )   4.00  2.20  0.40
assign ( residue  101 and name HA   ) ( residue  135 and name HB# )   5.00  3.20  0.50
assign ( residue  101 and name HB# ) ( residue  102 and name HB# )   5.00  3.20  0.50
assign ( residue  101 and name HB# ) ( residue  103 and name HB# )   5.00  3.20  0.50
assign ( residue  101 and name HB# ) ( residue  104 and name HB# )   4.00  2.20  0.40
assign ( residue  101 and name HB# ) ( residue  105 and name HB# )   5.00  3.20  0.50
assign ( residue  102 and name HA   ) ( residue  102 and name HB# )   3.00  1.20  0.30
assign ( residue  102 and name HA   ) ( residue  105 and name HB# )   4.00  2.20  0.40
assign ( residue  103 and name HA   ) ( residue  103 and name HB# )   3.00  1.20  0.30
assign ( residue  104 and name HA   ) ( residue  104 and name HB# )   3.00  1.20  0.30
assign ( residue  104 and name HA   ) ( residue  107 and name HB# )   4.00  2.20  0.40
assign ( residue  103 and name HB# ) ( residue  104 and name HB# )   4.00  2.20  0.40
```

```
assign ( residue  105 and name HA   ) ( residue  105 and name HB# )   4.00  2.20  0.40
assign ( residue  106 and name HA   ) ( residue  106 and name HB# )   3.00  1.20  0.30
assign ( residue  106 and name HA   ) ( residue  109 and name HB# )   5.00  3.20  0.50
assign ( residue  106 and name HB# ) ( residue  107 and name HA   )   5.00  3.20  0.50
assign ( residue  107 and name HA   ) ( residue  107 and name HB# )   4.00  2.20  0.40
assign ( residue  104 and name HB# ) ( residue  107 and name HB# )   5.00  3.20  0.50
assign ( residue  106 and name HB# ) ( residue  107 and name HB# )   5.00  3.20  0.50
assign ( residue  108 and name HA   ) ( residue 1909 and name HB# )   5.00  3.20  0.50
assign ( residue  107 and name HB# ) ( residue  108 and name HA   )   5.00  3.20  0.50
assign ( residue  108 and name HA   ) ( residue  111 and name HB# )   5.00  3.20  0.50
assign ( residue  108 and name HA   ) ( residue  112 and name HB# )   5.00  3.20  0.50
assign ( residue  108 and name HB   ) ( residue 1909 and name HB# )   5.00  3.20  0.50
assign ( residue  108 and name HG## ) ( residue 1909 and name HB# )   5.00  3.20  0.50
assign ( residue  109 and name HA   ) ( residue 1909 and name HB# )   5.00  3.20  0.50
assign ( residue  109 and name HA   ) ( residue  109 and name HB# )   4.00  2.20  0.40
assign ( residue  109 and name HA   ) ( residue  116 and name HB# )   5.00  3.20  0.50
assign ( residue  109 and name HE# ) ( residue 1909 and name HB# )   3.00  1.20  0.30
assign ( residue  109 and name HG# ) ( residue 1909 and name HB# )   5.00  3.20  0.50
assign ( residue  110 and name HA   ) ( residue  115 and name HB# )   5.00  3.20  0.50
assign ( residue  110 and name HA   ) ( residue  116 and name HB# )   5.00  3.20  0.50
assign ( residue  110 and name HB   ) ( residue  115 and name HB# )   5.00  3.20  0.50
assign ( residue  111 and name HA   ) ( residue  111 and name HB# )   4.00  2.20  0.40
assign ( residue  111 and name HA   ) ( residue  115 and name HB# )   5.00  3.20  0.50
assign ( residue  112 and name HA   ) ( residue 1906 and name HB# )   5.00  3.20  0.50
assign ( residue  112 and name HA   ) ( residue 1909 and name HB# )   5.00  3.20  0.50
assign ( residue  112 and name HA   ) ( residue  112 and name HB# )   4.00  2.20  0.40
assign ( residue  112 and name HB# ) ( residue 1906 and name HB# )   5.00  3.20  0.50
assign ( residue  112 and name HB# ) ( residue 1909 and name HB# )   4.00  2.20  0.40
assign ( residue  112 and name HD# ) ( residue 1906 and name HB# )   5.00  3.20  0.50
assign ( residue  112 and name HG   ) ( residue 1906 and name HB# )   5.00  3.20  0.50
assign ( residue  113 and name HA# ) ( residue 1906 and name HB# )   5.00  3.20  0.50
assign ( residue  113 and name HA# ) ( residue 1909 and name HB# )   5.00  3.20  0.50
assign ( residue  114 and name HA   ) ( residue  114 and name HB# )   4.00  2.20  0.40
assign ( residue  114 and name HA   ) ( residue  115 and name HB# )   5.00  3.20  0.50
assign ( residue  114 and name HB# ) ( residue 1913 and name HB# )   6.00  4.20  0.50
assign ( residue  115 and name HA   ) ( residue  115 and name HB# )   3.00  1.20  0.30
assign ( residue  116 and name HA   ) ( residue 1913 and name HB# )   6.00  4.20  0.50
assign ( residue  116 and name HA   ) ( residue  116 and name HB# )   4.00  2.20  0.40
assign ( residue  116 and name HA   ) ( residue  120 and name HB# )   5.00  3.20  0.50
assign ( residue  116 and name HB# ) ( residue 1913 and name HB# )   5.00  3.20  0.50
assign ( residue  109 and name HB# ) ( residue  116 and name HB# )   5.00  3.20  0.50
assign ( residue  116 and name HD1# ) ( residue 1913 and name HB# )   5.00  3.20  0.50
assign ( residue  116 and name HD2# ) ( residue 1913 and name HB# )   5.00  3.20  0.50
assign ( residue  116 and name HD2# ) ( residue  120 and name HB# )   5.00  3.20  0.50
assign ( residue  109 and name HB# ) ( residue  116 and name HG   )   4.00  2.20  0.40
assign ( residue  117 and name HB   ) ( residue  119 and name HB# )   5.00  3.20  0.50
```

```
assign ( residue  118 and name HA   ) ( residue  118 and name HB# )   3.00  1.20  0.30
assign ( residue  119 and name HA   ) ( residue  119 and name HB# )   3.00  1.20  0.30
assign ( residue  116 and name HB#  ) ( residue  120 and name HB# )   5.00  3.20  0.50
assign ( residue  117 and name HB#  ) ( residue  120 and name HB# )   5.00  3.20  0.50
assign ( residue  121 and name HA   ) ( residue  124 and name HB# )   4.00  2.20  0.40
assign ( residue  122 and name HA   ) ( residue  122 and name HB# )   3.00  1.20  0.30
assign ( residue  123 and name HA   ) ( residue  123 and name HB# )   3.00  1.20  0.30
assign ( residue  123 and name HG#  ) ( residue 1920 and name HB# )   6.00  4.20  0.60
assign ( residue  124 and name HA   ) ( residue  124 and name HB# )   3.00  1.20  0.30
assign ( residue  124 and name HE#  ) ( residue 1916 and name HB# )   5.00  3.20  0.50
assign ( residue  102 and name HB#  ) ( residue  125 and name HA   )   5.00  3.20  0.50
assign ( residue  105 and name HB#  ) ( residue  125 and name HA   )   6.00  4.20  0.50
assign ( residue  102 and name HB#  ) ( residue  125 and name HB   )   5.00  3.20  0.50
assign ( residue  105 and name HB#  ) ( residue  125 and name HB   )   5.00  3.20  0.50
assign ( residue  102 and name HB#  ) ( residue  125 and name HD# )   3.00  1.20  0.30
assign ( residue  105 and name HB#  ) ( residue  125 and name HD# )   4.00  2.20  0.40
assign ( residue  106 and name HB#  ) ( residue  125 and name HD# )   4.00  2.20  0.40
assign ( residue  102 and name HB#  ) ( residue  125 and name HG1# )   3.00  1.20  0.30
assign ( residue  105 and name HB#  ) ( residue  125 and name HG2# )   3.00  1.20  0.30
assign ( residue  122 and name HB#  ) ( residue  125 and name HG2# )   5.00  3.20  0.50
assign ( residue  126 and name HA   ) ( residue  126 and name HB# )   3.00  1.20  0.30
assign ( residue  127 and name HA   ) ( residue  127 and name HB# )   4.00  2.20  0.40
assign ( residue  124 and name HB#  ) ( residue  128 and name HA   )   6.00  4.20  0.60
assign ( residue  127 and name HB#  ) ( residue  128 and name HA   )   5.00  3.20  0.50
assign ( residue  128 and name HA   ) ( residue  128 and name HB# )   4.00  2.20  0.40
assign ( residue  128 and name HA   ) ( residue  141 and name HB# )   5.00  3.20  0.50
assign ( residue  129 and name HA   ) ( residue  129 and name HB# )   4.00  2.20  0.40
assign ( residue  133 and name HA   ) ( residue  133 and name HB# )   4.00  2.20  0.40
assign ( residue   99 and name HB#  ) ( residue  135 and name HA   )   5.00  3.20  0.50
assign ( residue  101 and name HB#  ) ( residue  135 and name HA   )   5.00  3.20  0.50
assign ( residue  135 and name HA   ) ( residue  135 and name HB# )   5.00  3.20  0.50
assign ( residue  105 and name HB#  ) ( residue  136 and name HD# )   5.00  3.20  0.50
assign ( residue  136 and name HG2# ) ( residue  138 and name HB# )   5.00  3.20  0.50
assign ( residue   99 and name HB#  ) ( residue  137 and name HA   )   5.00  3.20  0.50
assign ( residue  137 and name HA   ) ( residue  137 and name HB# )   4.00  2.20  0.40
assign ( residue  138 and name HA   ) ( residue  138 and name HB# )   3.00  1.20  0.30
assign ( residue  138 and name HA   ) ( residue  141 and name HB# )   6.00  4.20  0.60
assign ( residue   93 and name HB#  ) ( residue  138 and name HD# )   5.00  3.20  0.50
assign ( residue  138 and name HB#  ) ( residue  139 and name HA   )   4.00  2.20  0.40
assign ( residue  139 and name HA   ) ( residue  139 and name HB# )   3.00  1.20  0.30
assign ( residue  141 and name HA   ) ( residue  141 and name HB# )   4.00  2.20  0.40
assign ( residue  141 and name HA   ) ( residue  144 and name HB# )   5.00  3.20  0.50
assign ( residue  142 and name HA   ) ( residue  145 and name HB# )   5.00  3.20  0.50
assign ( residue  144 and name HA   ) ( residue  144 and name HB# )   3.00  1.20  0.30
assign ( residue  145 and name HA   ) ( residue 1919 and name HB# )   5.00  3.20  0.50
assign ( residue  145 and name HA   ) ( residue  145 and name HB# )   4.00  2.20  0.40
```

```
assign ( residue  145 and name HB#  ) ( residue 1919 and name HB#  )   5.00  3.20  0.50
assign ( residue  145 and name HE#  ) ( residue 1919 and name HB#  )   5.00  3.20  0.50
assign ( residue  145 and name HG#  ) ( residue 1919 and name HB#  )   5.00  3.20  0.50
assign ( residue  145 and name HB#  ) ( residue  146 and name HA   )   5.00  3.20  0.50
assign ( residue  146 and name HB   ) ( residue  147 and name HB#  )   5.00  3.20  0.50
assign ( residue  147 and name HA   ) ( residue  147 and name HB#  )   3.00  1.20  0.30
assign ( residue   77 and name HA   ) ( residue   77 and name HB#  )   4.00  2.20  0.40
assign ( residue   77 and name HE#  ) ( residue   77 and name HB#  )   5.00  3.20  0.50
assign ( residue   78 and name HA   ) ( residue   78 and name HB#  )   4.00  2.20  0.40
assign ( residue   78 and name HA   ) ( residue   79 and name HB#  )   4.00  2.20  0.40
assign ( residue   78 and name HB#  ) ( residue   79 and name HB#  )   5.00  3.20  0.40
assign ( residue   79 and name HA   ) ( residue   79 and name HB#  )   4.00  2.20  0.40
assign ( residue   78 and name HB#  ) ( residue   79 and name HG#  )   5.00  3.20  0.40
assign ( residue   80 and name HA   ) ( residue   80 and name HB#  )   4.00  2.20  0.30
assign ( residue   81 and name HA   ) ( residue   81 and name HB#  )   3.00  1.20  0.30
assign ( residue   81 and name HB#  ) ( residue   85 and name HB#  )   5.00  3.20  0.50
assign ( residue   83 and name HA   ) ( residue   83 and name HB#  )   3.00  1.20  0.30
assign ( residue   84 and name HA   ) ( residue   84 and name HB#  )   3.00  1.20  0.30
assign ( residue   85 and name HA   ) ( residue 1915 and name HB#  )   4.00  2.20  0.40
assign ( residue   85 and name HA   ) ( residue   85 and name HB#  )   4.00  2.20  0.40
assign ( residue   85 and name HB#  ) ( residue 1915 and name HB#  )   3.00  1.20  0.30
assign ( residue   85 and name HD## ) ( residue 1915 and name HB#  )   3.00  1.20  0.30
assign ( residue   86 and name HA   ) ( residue   89 and name HB#  )   5.00  3.20  0.50
assign ( residue   86 and name HD#  ) ( residue  139 and name HB#  )   5.00  3.20  0.50
assign ( residue   87 and name HA   ) ( residue   87 and name HB#  )   3.00  1.20  0.30
assign ( residue   88 and name HA   ) ( residue 1908 and name HB#  )   4.00  2.20  0.40
assign ( residue   88 and name HA   ) ( residue   88 and name HB#  )   3.00  1.20  0.30
assign ( residue   88 and name HB#  ) ( residue 1908 and name HB#  )   4.00  2.20  0.40
assign ( residue   88 and name HB#  ) ( residue   89 and name HA   )   5.00  3.20  0.50
assign ( residue   89 and name HA   ) ( residue   89 and name HB#  )   4.00  2.20  0.40
assign ( residue   89 and name HA   ) ( residue   92 and name HB#  )   5.00  3.20  0.50
assign ( residue   90 and name HA   ) ( residue   90 and name HB#  )   4.00  2.20  0.40
assign ( residue   91 and name HB   ) ( residue 1908 and name HB#  )   5.00  3.20  0.50
assign ( residue   91 and name HG## ) ( residue 1908 and name HB#  )   4.00  2.20  0.40
assign ( residue   92 and name HA   ) ( residue   92 and name HB#  )   4.00  2.20  0.40
assign ( residue   92 and name HD#  ) ( residue 1905 and name HB#  )   5.00  3.20  0.40
assign ( residue   92 and name HD#  ) ( residue 1908 and name HB#  )   5.00  3.20  0.50
assign ( residue   92 and name HD#  ) ( residue 1909 and name HB#  )   5.00  3.20  0.50
assign ( residue   88 and name HB#  ) ( residue   92 and name HD#  )   5.00  3.20  0.50
assign ( residue   92 and name HD#  ) ( residue   92 and name HB#  )   5.00  3.20  0.50
assign ( residue   92 and name HE#  ) ( residue 1905 and name HB#  )   5.00  3.20  0.50
assign ( residue   92 and name HE#  ) ( residue 1905 and name HG#  )   5.00  3.20  0.50
assign ( residue   92 and name HE#  ) ( residue 1908 and name HB#  )   5.00  3.20  0.50
assign ( residue   92 and name HE#  ) ( residue 1909 and name HB#  )   4.00  2.20  0.40
assign ( residue   93 and name HA   ) ( residue   93 and name HB#  )   4.00  2.20  0.40
assign ( residue   90 and name HB#  ) ( residue   93 and name HB#  )   5.00  3.20  0.50
```

```
assign ( residue   94 and name HA   ) ( residue   94 and name HB# )   3.00  1.20  0.30
assign ( residue   94 and name HG# ) ( residue   94 and name HB# )   3.00  1.20  0.30
assign ( residue   95 and name HA   ) ( residue   95 and name HB# )   3.00  1.20  0.30
assign ( residue   97 and name HA   ) ( residue   97 and name HB# )   3.00  1.20  0.30
assign ( residue   99 and name HA   ) ( residue   99 and name HB# )   4.00  2.20  0.40
assign ( residue   99 and name HA   ) ( residue  135 and name HB# )   5.00  3.20  0.50
assign ( residue   99 and name HA   ) ( residue  137 and name HB# )   5.00  3.20  0.50
assign ( residue   99 and name HB# ) ( residue  135 and name HB# )   5.00  3.20  0.50
assign ( residue  100 and name HA   ) ( residue  138 and name HD# )   6.00  4.20  0.50
assign ( residue   89 and name HD# ) ( residue  100 and name HB   )   5.00  3.20  0.50
assign ( residue  100 and name HB   ) ( residue  138 and name HD# )   5.00  3.20  0.50
assign ( residue   89 and name HD# ) ( residue  100 and name HD# )   3.00  1.20  0.30
assign ( residue  100 and name HD# ) ( residue  138 and name HD# )   5.00  3.20  0.50
assign ( residue   89 and name HD# ) ( residue  100 and name HG1# )   5.00  3.20  0.50
assign ( residue  103 and name HA   ) ( residue  106 and name HD# )   5.00  3.20  0.50
assign ( residue   89 and name HD# ) ( residue  105 and name HD1# )   5.00  3.20  0.50
assign ( residue   89 and name HD# ) ( residue  105 and name HD2# )   5.00  3.20  0.50
assign ( residue  106 and name HA   ) ( residue  106 and name HD# )   5.00  3.20  0.50
assign ( residue  106 and name HB# ) ( residue  106 and name HD# )   4.00  2.20  0.40
assign ( residue  109 and name HE# ) ( residue  112 and name HD# )   5.00  3.20  0.50
assign ( residue  111 and name HA   ) ( residue  115 and name HD# )   5.00  3.20  0.50
assign ( residue  111 and name HB# ) ( residue  112 and name HD# )   5.00  3.20  0.50
assign ( residue  111 and name HB# ) ( residue  115 and name HD# )   5.00  3.20  0.50
assign ( residue  112 and name HA   ) ( residue  112 and name HD# )   3.00  1.20  0.30
assign ( residue  112 and name HB# ) ( residue  112 and name HD# )   3.00  1.20  0.30
assign ( residue  112 and name HD# ) ( residue  113 and name HA# )   4.00  2.20  0.40
assign ( residue  114 and name HA   ) ( residue  115 and name HD# )   5.00  3.20  0.50
assign ( residue  115 and name HA   ) ( residue  115 and name HD# )   5.00  3.20  0.50
assign ( residue  115 and name HB# ) ( residue  115 and name HD# )   5.00  3.20  0.50
assign ( residue  116 and name HD1# ) ( residue 1916 and name HD# )   5.00  3.20  0.50
assign ( residue  116 and name HD2# ) ( residue 1916 and name HD# )   5.00  3.20  0.50
assign ( residue  121 and name HA   ) ( residue 1916 and name HD# )   5.00  3.20  0.50
assign ( residue  124 and name HA   ) ( residue 1916 and name HD# )   5.00  3.20  0.50
assign ( residue  124 and name HA   ) ( residue  141 and name HD# )   5.00  3.20  0.50
assign ( residue  124 and name HB# ) ( residue 1916 and name HD# )   5.00  3.20  0.50
assign ( residue  124 and name HB# ) ( residue 1919 and name HD# )   4.00  2.20  0.40
assign ( residue  124 and name HB# ) ( residue  141 and name HD# )   5.00  3.20  0.50
assign ( residue  124 and name HG# ) ( residue 1916 and name HD# )   5.00  3.20  0.50
assign ( residue  126 and name HA   ) ( residue  126 and name HD# )   5.00  3.20  0.50
assign ( residue  126 and name HB# ) ( residue  126 and name HD# )   4.00  2.20  0.40
assign ( residue  127 and name HB# ) ( residue  141 and name HD# )   5.00  3.20  0.50
assign ( residue  127 and name HG# ) ( residue 1919 and name HD# )   5.00  3.20  0.50
assign ( residue  128 and name HA   ) ( residue  141 and name HD# )   5.00  3.20  0.50
assign ( residue  128 and name HB# ) ( residue  141 and name HD# )   5.00  3.20  0.50
assign ( residue  136 and name HG2# ) ( residue  141 and name HD# )   5.00  3.20  0.50
assign ( residue  137 and name HA   ) ( residue  138 and name HD# )   5.00  3.20  0.50
```

```
assign ( residue  138 and name HA   ) ( residue  138 and name HD# )   5.00  3.20  0.50
assign ( residue  138 and name HA   ) ( residue  141 and name HD# )   5.00  3.20  0.50
assign ( residue   89 and name HD# ) ( residue  138 and name HB# )   5.00  3.20  0.50
assign ( residue  138 and name HB# ) ( residue  138 and name HD# )   5.00  3.20  0.50
assign ( residue  138 and name HB# ) ( residue  141 and name HD# )   5.00  3.20  0.50
assign ( residue   89 and name HD# ) ( residue  138 and name HD# )   5.00  3.20  0.50
assign ( residue   89 and name HD# ) ( residue  138 and name HE# )   5.00  3.20  0.50
assign ( residue  138 and name HD# ) ( residue  139 and name HA   )   5.00  3.20  0.50
assign ( residue  138 and name HD# ) ( residue  139 and name HB# )   5.00  3.20  0.50
assign ( residue  141 and name HA   ) ( residue  141 and name HD# )   4.00  2.20  0.40
assign ( residue  141 and name HB# ) ( residue  141 and name HD# )   5.00  3.20  0.50
assign ( residue   89 and name HD# ) ( residue  142 and name HA   )   6.00  4.20  0.60
assign ( residue  141 and name HD# ) ( residue  142 and name HA   )   5.00  3.20  0.50
assign ( residue  141 and name HD# ) ( residue  142 and name HB   )   5.00  3.20  0.50
assign ( residue  144 and name HB# ) ( residue 1919 and name HD# )   6.00  4.20  0.60
assign ( residue  144 and name HE# ) ( residue 1919 and name HD# )   5.00  3.20  0.50
assign ( residue  145 and name HA   ) ( residue 1919 and name HD# )   3.00  1.20  0.30
assign ( residue  145 and name HB# ) ( residue 1919 and name HD# )   5.00  3.20  0.50
assign ( residue  141 and name HD# ) ( residue  145 and name HB# )   5.00  3.20  0.50
assign ( residue  145 and name HG# ) ( residue 1919 and name HD# )   5.00  3.20  0.50
assign ( residue  141 and name HD# ) ( residue  145 and name HG# )   5.00  3.20  0.50
assign ( residue  146 and name HA   ) ( residue 1919 and name HD# )   5.00  3.20  0.50
assign ( residue   77 and name HA   ) ( residue   77 and name HD# )   5.00  3.20  0.50
assign ( residue   77 and name HB# ) ( residue   77 and name HD# )   4.00  2.20  0.30
assign ( residue   85 and name HB# ) ( residue   89 and name HD# )   5.00  3.20  0.50
assign ( residue   86 and name HA   ) ( residue   89 and name HD# )   5.00  3.20  0.50
assign ( residue   86 and name HA   ) ( residue  138 and name HD# )   5.00  3.20  0.50
assign ( residue   86 and name HD# ) ( residue  138 and name HD# )   5.00  3.20  0.50
assign ( residue   86 and name HG1# ) ( residue  138 and name HD# )   5.00  3.20  0.50
assign ( residue   88 and name HB# ) ( residue   89 and name HD# )   5.00  3.20  0.50
assign ( residue   89 and name HA   ) ( residue   89 and name HD# )   3.00  1.20  0.30
assign ( residue   89 and name HB# ) ( residue   89 and name HD# )   4.00  2.20  0.40
assign ( residue   89 and name HB# ) ( residue  138 and name HD# )   5.00  3.20  0.50
assign ( residue   90 and name HA   ) ( residue   90 and name HD# )   4.00  2.20  0.40
assign ( residue   90 and name HB# ) ( residue   90 and name HD# )   3.00  1.20  0.30
assign ( residue   92 and name HA   ) ( residue   92 and name HD# )   5.00  3.20  0.50
assign ( residue   89 and name HD# ) ( residue   92 and name HB# )   5.00  3.20  0.40
assign ( residue   89 and name HD# ) ( residue   92 and name HD# )   3.00  1.20  0.30
assign ( residue   94 and name HA   ) ( residue   94 and name HD# )   3.00  1.20  0.30
assign ( residue   94 and name HB# ) ( residue   94 and name HD# )   3.00  1.20  0.30
assign ( residue   99 and name HA   ) ( residue  138 and name HD# )   5.00  3.20  0.50
assign ( residue  100 and name HA   ) ( residue  100 and name HD1# )   4.00  2.20  0.40
assign ( residue  100 and name HA   ) ( residue  136 and name HD1# )   5.00  3.20  0.50
assign ( residue  100 and name HB   ) ( residue  100 and name HD1# )   3.00  1.20  0.30
assign ( residue  100 and name HB   ) ( residue  136 and name HD1# )   5.00  3.20  0.50
assign ( residue  100 and name HD1# ) ( residue 1912 and name HD1# )   5.00  3.20  0.50
```

```
assign ( residue  100 and name HD1# ) ( residue  105 and name HD1# )   4.00  2.20  0.40
assign ( residue  100 and name HD#  ) ( residue  136 and name HD1# )   5.00  3.20  0.40
assign ( residue  100 and name HG1# ) ( residue  100 and name HD1# )   3.00  1.20  0.30
assign ( residue  100 and name HG1# ) ( residue  136 and name HD1# )   5.00  3.20  0.50
assign ( residue  100 and name HG2# ) ( residue  136 and name HD1# )   3.00  1.20  0.30
assign ( residue  100 and name HD1# ) ( residue  102 and name HA   )   5.00  3.20  0.50
assign ( residue  102 and name HA   ) ( residue  105 and name HD1# )   5.00  3.20  0.50
assign ( residue  102 and name HA   ) ( residue  125 and name HD1# )   5.00  3.20  0.50
assign ( residue  102 and name HA   ) ( residue  136 and name HD1# )   3.00  1.20  0.30
assign ( residue  102 and name HB#  ) ( residue  125 and name HD1# )   3.00  1.20  0.30
assign ( residue  102 and name HB#  ) ( residue  136 and name HD1# )   3.00  1.20  0.30
assign ( residue  100 and name HD1# ) ( residue  105 and name HA   )   5.00  3.20  0.50
assign ( residue  105 and name HA   ) ( residue  105 and name HD1# )   3.00  1.20  0.30
assign ( residue  100 and name HD1# ) ( residue  105 and name HB#  )   5.00  3.20  0.50
assign ( residue  105 and name HB#  ) ( residue  105 and name HD1# )   4.00  2.20  0.40
assign ( residue  105 and name HB#  ) ( residue  136 and name HD1# )   4.00  2.20  0.40
assign ( residue  105 and name HD1# ) ( residue 1912 and name HD1# )   4.00  2.20  0.40
assign ( residue  105 and name HD1# ) ( residue  136 and name HD1# )   5.00  3.20  0.50
assign ( residue  105 and name HD2# ) ( residue  136 and name HD1# )   3.00  1.20  0.30
assign ( residue  100 and name HD1# ) ( residue  105 and name HG   )   5.00  3.20  0.50
assign ( residue  105 and name HG   ) ( residue  136 and name HD1# )   5.00  3.20  0.50
assign ( residue  106 and name HA   ) ( residue  125 and name HD1# )   5.00  3.20  0.50
assign ( residue  106 and name HB#  ) ( residue  125 and name HD1# )   4.00  2.20  0.40
assign ( residue  106 and name HD#  ) ( residue  125 and name HD1# )   5.00  3.20  0.50
assign ( residue  100 and name HD1# ) ( residue  108 and name HG## )   4.00  2.20  0.30
assign ( residue  109 and name HB#  ) ( residue  116 and name HD1# )   4.00  2.20  0.40
assign ( residue  109 and name HE#  ) ( residue 1912 and name HD1# )   3.00  1.20  0.30
assign ( residue  109 and name HE#  ) ( residue  116 and name HD1# )   5.00  3.20  0.50
assign ( residue  105 and name HD1# ) ( residue  109 and name HG#  )   4.00  2.20  0.40
assign ( residue  109 and name HG#  ) ( residue  116 and name HD1# )   5.00  3.20  0.50
assign ( residue  110 and name HA   ) ( residue  116 and name HD1# )   5.00  3.20  0.50
assign ( residue  110 and name HB   ) ( residue  116 and name HD1# )   5.00  3.20  0.50
assign ( residue  110 and name HG2# ) ( residue  116 and name HD1# )   3.00  1.20  0.30
assign ( residue  116 and name HA   ) ( residue  116 and name HD1# )   4.00  2.20  0.40
assign ( residue  116 and name HB#  ) ( residue  116 and name HD1# )   4.00  2.20  0.40
assign ( residue  116 and name HD1# ) ( residue  120 and name HB#  )   5.00  3.20  0.50
assign ( residue  122 and name HA   ) ( residue  125 and name HD1# )   5.00  3.20  0.50
assign ( residue  124 and name HB#  ) ( residue 1920 and name HD## )   5.00  3.20  0.50
assign ( residue  116 and name HD1# ) ( residue  124 and name HB#  )   5.00  3.20  0.50
assign ( residue  124 and name HE#  ) ( residue 1912 and name HD1# )   5.00  3.20  0.50
assign ( residue  105 and name HD1# ) ( residue  124 and name HE#  )   4.00  2.20  0.40
assign ( residue  124 and name HG#  ) ( residue 1920 and name HD## )   5.00  3.20  0.50
assign ( residue  116 and name HD1# ) ( residue  124 and name HG#  )   5.00  3.20  0.50
assign ( residue  125 and name HA   ) ( residue  125 and name HD1# )   4.00  2.20  0.40
assign ( residue  125 and name HA   ) ( residue  136 and name HD1# )   4.00  2.20  0.40
assign ( residue  125 and name HB   ) ( residue  125 and name HD1# )   4.00  2.20  0.40
```

```
assign ( residue  125 and name HB   ) ( residue  136 and name HD1# )   5.00  3.20  0.50
assign ( residue  125 and name HG1# ) ( residue  125 and name HD1# )   3.00  1.20  0.30
assign ( residue  125 and name HG1# ) ( residue  136 and name HD1# )   4.00  2.20  0.40
assign ( residue  125 and name HG2# ) ( residue  125 and name HD1# )   3.00  1.20  0.30
assign ( residue  125 and name HG2# ) ( residue  136 and name HD1# )   4.00  2.20  0.40
assign ( residue  129 and name HA   ) ( residue  136 and name HD1# )   6.00  4.20  0.60
assign ( residue  129 and name HB#  ) ( residue  136 and name HD1# )   5.00  3.20  0.50
assign ( residue  130 and name HA   ) ( residue  130 and name HD1# )   5.00  3.20  0.50
assign ( residue  130 and name HB   ) ( residue  130 and name HD1# )   3.00  1.20  0.30
assign ( residue  130 and name HB   ) ( residue  136 and name HD1# )   5.00  3.20  0.50
assign ( residue  130 and name HG1# ) ( residue  130 and name HD1# )   4.00  2.20  0.40
assign ( residue  130 and name HG1# ) ( residue  136 and name HD1# )   5.00  3.20  0.50
assign ( residue  130 and name HG2# ) ( residue  130 and name HD1# )   3.00  1.20  0.30
assign ( residue  130 and name HD1# ) ( residue  134 and name HA#  )   5.00  3.20  0.50
assign ( residue  135 and name HA   ) ( residue  136 and name HD1# )   5.00  3.20  0.50
assign ( residue   99 and name HD## ) ( residue  136 and name HA   )   5.00  3.20  0.50
assign ( residue  136 and name HA   ) ( residue  136 and name HD1# )   5.00  3.20  0.50
assign ( residue  136 and name HB   ) ( residue  136 and name HD1# )   5.00  3.20  0.50
assign ( residue  136 and name HG1# ) ( residue  136 and name HD1# )   3.00  1.20  0.30
assign ( residue  136 and name HG2# ) ( residue  136 and name HD1# )   3.00  1.20  0.30
assign ( residue   99 and name HD## ) ( residue  137 and name HA   )   3.00  1.20  0.30
assign ( residue   99 and name HD## ) ( residue  137 and name HB#  )   5.00  3.20  0.50
assign ( residue   86 and name HD1# ) ( residue  138 and name HB#  )   6.00  4.20  0.50
assign ( residue  100 and name HD1# ) ( residue  138 and name HB#  )   5.00  3.20  0.50
assign ( residue   86 and name HD1# ) ( residue  138 and name HD#  )   5.00  3.20  0.50
assign ( residue   99 and name HD## ) ( residue  138 and name HD#  )   5.00  3.20  0.50
assign ( residue  100 and name HD1# ) ( residue  138 and name HD#  )   5.00  3.20  0.50
assign ( residue   86 and name HD1# ) ( residue  138 and name HE#  )   5.00  3.20  0.50
assign ( residue  100 and name HD1# ) ( residue  138 and name HE#  )   6.00  4.20  0.60
assign ( residue   86 and name HD1# ) ( residue  139 and name HA   )   5.00  3.20  0.40
assign ( residue   86 and name HD1# ) ( residue  139 and name HB#  )   5.00  3.20  0.50
assign ( residue  141 and name HE#  ) ( residue 1912 and name HD1# )   5.00  3.20  0.50
assign ( residue   86 and name HD1# ) ( residue  142 and name HA   )   6.00  4.20  0.60
assign ( residue   86 and name HD1# ) ( residue  142 and name HB   )   5.00  3.20  0.50
assign ( residue   86 and name HD1# ) ( residue  142 and name HG## )   3.00  1.20  0.30
assign ( residue  145 and name HE#  ) ( residue 1912 and name HD1# )   6.00  4.20  0.60
assign ( residue   83 and name HA   ) ( residue   86 and name HD1# )   4.00  2.20  0.40
assign ( residue   83 and name HB#  ) ( residue   86 and name HD1# )   5.00  3.20  0.50
assign ( residue   83 and name HG#  ) ( residue   86 and name HD1# )   4.00  2.20  0.40
assign ( residue   85 and name HA   ) ( residue 1912 and name HD1# )   5.00  3.20  0.50
assign ( residue   85 and name HB#  ) ( residue 1912 and name HD1# )   5.00  3.20  0.50
assign ( residue   85 and name HD## ) ( residue 1912 and name HD1# )   4.00  2.20  0.40
assign ( residue   86 and name HA   ) ( residue   86 and name HD1# )   4.00  2.20  0.40
assign ( residue   86 and name HG1# ) ( residue   86 and name HD1# )   3.00  1.20  0.30
assign ( residue   86 and name HG2# ) ( residue   86 and name HD1# )   3.00  1.20  0.30
assign ( residue   86 and name HD1# ) ( residue   87 and name HB#  )   5.00  3.20  0.50
```

```
assign ( residue   88 and name HA   ) ( residue 1912 and name HD1# )   5.00  3.20  0.50
assign ( residue   88 and name HB#  ) ( residue 1912 and name HD1# )   3.00  1.20  0.30
assign ( residue   89 and name HA   ) ( residue 1912 and name HD1# )   3.00  1.20  0.30
assign ( residue   89 and name HA   ) ( residue  100 and name HD1# )   5.00  3.20  0.50
assign ( residue   89 and name HB#  ) ( residue 1912 and name HD1# )   5.00  3.20  0.50
assign ( residue   89 and name HB#  ) ( residue  100 and name HD1# )   5.00  3.20  0.50
assign ( residue   89 and name HD#  ) ( residue 1912 and name HD1# )   4.00  2.20  0.40
assign ( residue   89 and name HD#  ) ( residue  100 and name HD1# )   4.00  2.20  0.40
assign ( residue   89 and name HE#  ) ( residue 1912 and name HD1# )   5.00  3.20  0.50
assign ( residue   89 and name HE#  ) ( residue  100 and name HD1# )   5.00  3.20  0.50
assign ( residue   91 and name HB   ) ( residue 1912 and name HD1# )   6.00  4.20  0.60
assign ( residue   92 and name HA   ) ( residue  100 and name HD1# )   5.00  3.20  0.50
assign ( residue   92 and name HB#  ) ( residue  100 and name HD1# )   4.00  2.20  0.40
assign ( residue   92 and name HD#  ) ( residue 1912 and name HD1# )   4.00  2.20  0.40
assign ( residue   92 and name HD#  ) ( residue  100 and name HD1# )   5.00  3.20  0.50
assign ( residue   92 and name HE#  ) ( residue 1912 and name HD1# )   5.00  3.20  0.50
assign ( residue   92 and name HE#  ) ( residue  100 and name HD1# )   5.00  3.20  0.50
assign ( residue   93 and name HA   ) ( residue  100 and name HD1# )   5.00  3.20  0.50
assign ( residue   98 and name HA#  ) ( residue   99 and name HD## )   5.00  3.20  0.50
assign ( residue  100 and name HA   ) ( residue  135 and name HD2  )   5.00  3.20  0.50
assign ( residue  101 and name HA   ) ( residue  135 and name HD2  )   5.00  3.20  0.50
assign ( residue  101 and name HB#  ) ( residue  135 and name HD2  )   5.00  3.20  0.50
assign ( residue  107 and name HA   ) ( residue  107 and name HD2  )   5.00  3.20  0.50
assign ( residue  107 and name HB#  ) ( residue  107 and name HD2  )   5.00  3.20  0.50
assign ( residue  107 and name HD2  ) ( residue  108 and name HA   )   4.00  2.20  0.40
assign ( residue  107 and name HD2  ) ( residue  108 and name HB   )   5.00  3.20  0.50
assign ( residue  135 and name HA   ) ( residue  135 and name HD2  )   5.00  3.20  0.50
assign ( residue  135 and name HB#  ) ( residue  135 and name HD2  )   5.00  3.20  0.50
assign ( residue   99 and name HB#  ) ( residue  135 and name HD2  )   5.00  3.20  0.50
assign ( residue  100 and name HB   ) ( residue  105 and name HD2# )   5.00  3.20  0.50
assign ( residue  100 and name HD#  ) ( residue  105 and name HD2# )   3.00  1.20  0.30
assign ( residue  102 and name HA   ) ( residue  105 and name HD2# )   4.00  2.20  0.40
assign ( residue  105 and name HA   ) ( residue  105 and name HD2# )   4.00  2.20  0.40
assign ( residue  105 and name HB#  ) ( residue  105 and name HD2# )   3.00  1.20  0.30
assign ( residue  105 and name HD1# ) ( residue  105 and name HD2# )   3.00  1.20  0.30
assign ( residue  105 and name HD2# ) ( residue  106 and name HA   )   5.00  3.20  0.50
assign ( residue  109 and name HA   ) ( residue  116 and name HD2# )   6.00  4.20  0.60
assign ( residue  109 and name HB#  ) ( residue  116 and name HD2# )   4.00  2.20  0.40
assign ( residue  109 and name HE#  ) ( residue  116 and name HD2# )   6.00  4.20  0.60
assign ( residue  105 and name HD2# ) ( residue  109 and name HG#  )   5.00  3.20  0.50
assign ( residue  110 and name HA   ) ( residue  116 and name HD2# )   5.00  3.20  0.50
assign ( residue  110 and name HB   ) ( residue  116 and name HD2# )   5.00  3.20  0.50
assign ( residue  110 and name HG2# ) ( residue  116 and name HD2# )   3.00  1.20  0.30
assign ( residue  114 and name HG#  ) ( residue  116 and name HD2# )   5.00  3.20  0.50
assign ( residue  116 and name HA   ) ( residue  116 and name HD2# )   4.00  2.20  0.40
assign ( residue  116 and name HB#  ) ( residue  116 and name HD2# )   4.00  2.20  0.40
```

```
assign ( residue  116 and name HD1# ) ( residue  116 and name HD2# )   3.00  1.20  0.30
assign ( residue  120 and name HB#  ) ( residue 1920 and name HD## )   5.00  3.20  0.50
assign ( residue  116 and name HD2# ) ( residue  121 and name HB   )   4.00  2.20  0.40
assign ( residue  116 and name HD2# ) ( residue  121 and name HG## )   3.00  1.20  0.30
assign ( residue  123 and name HA   ) ( residue 1920 and name HD## )   5.00  3.20  0.50
assign ( residue  123 and name HB#  ) ( residue 1920 and name HD## )   5.00  3.20  0.50
assign ( residue  123 and name HG#  ) ( residue 1920 and name HD## )   4.00  2.20  0.40
assign ( residue  116 and name HD2# ) ( residue  124 and name HB#  )   5.00  3.20  0.50
assign ( residue  105 and name HD2# ) ( residue  125 and name HA   )   5.00  3.20  0.50
assign ( residue  105 and name HD2# ) ( residue  125 and name HB   )   5.00  3.20  0.50
assign ( residue  105 and name HD2# ) ( residue  125 and name HG1# )   5.00  3.20  0.50
assign ( residue  105 and name HD2# ) ( residue  125 and name HG2# )   3.00  1.20  0.30
assign ( residue  127 and name HG#  ) ( residue 1920 and name HD## )   6.00  4.20  0.60
assign ( residue   99 and name HD## ) ( residue  135 and name HA   )   5.00  3.20  0.50
assign ( residue   99 and name HD## ) ( residue  135 and name HB#  )   5.00  3.20  0.50
assign ( residue   99 and name HD## ) ( residue  135 and name HD2  )   5.00  3.20  0.50
assign ( residue  105 and name HD2# ) ( residue  136 and name HB   )   5.00  3.20  0.50
assign ( residue  105 and name HD2# ) ( residue  136 and name HG1# )   5.00  3.20  0.50
assign ( residue   85 and name HD## ) ( residue  142 and name HA   )   5.00  3.20  0.50
assign ( residue   85 and name HD## ) ( residue  142 and name HG## )   4.50  2.70  0.40
assign ( residue   81 and name HA   ) ( residue   85 and name HD## )   5.00  3.20  0.50
assign ( residue   85 and name HA   ) ( residue   85 and name HD## )   3.00  1.20  0.30
assign ( residue   85 and name HB#  ) ( residue   85 and name HD## )   3.00  1.20  0.30
assign ( residue   85 and name HD## ) ( residue   86 and name HA   )   5.00  3.20  0.50
assign ( residue   85 and name HD## ) ( residue   86 and name HG1# )   5.00  3.20  0.50
assign ( residue   85 and name HD## ) ( residue   89 and name HB#  )   5.00  3.20  0.50
assign ( residue   85 and name HD## ) ( residue   89 and name HD#  )   5.00  3.20  0.50
assign ( residue   97 and name HB#  ) ( residue   99 and name HD## )   5.00  3.20  0.50
assign ( residue   99 and name HA   ) ( residue   99 and name HD## )   4.00  2.20  0.40
assign ( residue   99 and name HB#  ) ( residue   99 and name HD## )   3.00  1.20  0.30
assign ( residue  100 and name HA   ) ( residue  138 and name HE#  )   6.00  4.20  0.60
assign ( residue  100 and name HB   ) ( residue  138 and name HE#  )   5.00  3.20  0.50
assign ( residue   89 and name HE#  ) ( residue  100 and name HD#  )   5.00  3.20  0.50
assign ( residue  100 and name HD#  ) ( residue  138 and name HE#  )   5.00  3.20  0.50
assign ( residue   89 and name HE#  ) ( residue  100 and name HG1# )   5.00  3.20  0.50
assign ( residue  105 and name HD1# ) ( residue 1916 and name HE#  )   4.00  2.20  0.40
assign ( residue   89 and name HE#  ) ( residue  105 and name HD1# )   4.00  2.20  0.40
assign ( residue   89 and name HE#  ) ( residue  105 and name HD2# )   5.00  3.20  0.50
assign ( residue  105 and name HD2# ) ( residue  124 and name HE#  )   4.00  2.20  0.40
assign ( residue  108 and name HA   ) ( residue  109 and name HE#  )   5.00  3.20  0.50
assign ( residue  109 and name HA   ) ( residue  109 and name HE#  )   4.00  2.20  0.40
assign ( residue  109 and name HB#  ) ( residue  109 and name HE#  )   5.00  3.20  0.50
assign ( residue  109 and name HG#  ) ( residue  124 and name HE#  )   5.00  3.20  0.50
assign ( residue  111 and name HA   ) ( residue  115 and name HE#  )   5.00  3.20  0.50
assign ( residue  115 and name HB#  ) ( residue  115 and name HE#  )   5.00  3.20  0.50
assign ( residue  115 and name HD#  ) ( residue  115 and name HE#  )   5.00  3.20  0.50
```

```
assign ( residue  116 and name HD1# ) ( residue 1916 and name HE#  )   4.00  2.20  0.40
assign ( residue  116 and name HD2# ) ( residue 1916 and name HE#  )   4.00  2.20  0.40
assign ( residue  116 and name HD2# ) ( residue  124 and name HE#  )   5.00  3.20  0.50
assign ( residue  120 and name HB#  ) ( residue 1916 and name HD#  )   5.00  3.20  0.50
assign ( residue  121 and name HA   ) ( residue  124 and name HE#  )   5.00  3.20  0.50
assign ( residue  123 and name HA   ) ( residue 1919 and name HE#  )   6.00  4.20  0.50
assign ( residue  123 and name HB#  ) ( residue 1919 and name HE#  )   5.00  3.20  0.50
assign ( residue  123 and name HG#  ) ( residue 1919 and name HE#  )   5.00  3.20  0.50
assign ( residue  124 and name HA   ) ( residue 1916 and name HE#  )   5.00  3.20  0.50
assign ( residue  124 and name HA   ) ( residue 1919 and name HE#  )   4.00  2.20  0.40
assign ( residue  124 and name HA   ) ( residue  124 and name HE#  )   5.00  3.20  0.50
assign ( residue  124 and name HB#  ) ( residue 1916 and name HE#  )   5.00  3.20  0.50
assign ( residue  124 and name HB#  ) ( residue 1919 and name HE#  )   5.00  3.20  0.50
assign ( residue   89 and name HE#  ) ( residue  124 and name HB#  )   5.00  3.20  0.50
assign ( residue  124 and name HB#  ) ( residue  124 and name HE#  )   5.00  3.20  0.50
assign ( residue  124 and name HE#  ) ( residue 1916 and name HE#  )   3.00  1.20  0.30
assign ( residue  124 and name HG#  ) ( residue 1916 and name HE#  )   5.00  3.20  0.50
assign ( residue  124 and name HG#  ) ( residue 1919 and name HE#  )   5.00  3.20  0.50
assign ( residue  124 and name HG#  ) ( residue  124 and name HE#  )   4.00  2.20  0.40
assign ( residue  137 and name HA   ) ( residue  138 and name HE#  )   5.00  3.20  0.50
assign ( residue  138 and name HA   ) ( residue  138 and name HE#  )   6.00  4.20  0.50
assign ( residue  138 and name HB#  ) ( residue  138 and name HE#  )   5.00  3.20  0.50
assign ( residue  138 and name HD#  ) ( residue  138 and name HE#  )   3.00  1.20  0.30
assign ( residue  138 and name HE#  ) ( residue  139 and name HA   )   5.00  3.20  0.50
assign ( residue  138 and name HE#  ) ( residue  139 and name HB#  )   5.00  3.20  0.50
assign ( residue  141 and name HA   ) ( residue  144 and name HE#  )   5.00  3.20  0.50
assign ( residue  141 and name HB#  ) ( residue  144 and name HE#  )   5.00  3.20  0.50
assign ( residue  141 and name HB#  ) ( residue  145 and name HE#  )   5.00  3.20  0.50
assign ( residue  124 and name HE#  ) ( residue  141 and name HD#  )   5.00  3.20  0.50
assign ( residue  141 and name HD#  ) ( residue  141 and name HE#  )   3.00  1.20  0.30
assign ( residue  141 and name HD#  ) ( residue  144 and name HE#  )   5.00  3.20  0.50
assign ( residue  141 and name HD#  ) ( residue  145 and name HE#  )   5.00  3.20  0.50
assign ( residue  124 and name HE#  ) ( residue  141 and name HE#  )   5.00  3.20  0.50
assign ( residue  141 and name HE#  ) ( residue  145 and name HE#  )   5.00  3.20  0.50
assign ( residue   89 and name HE#  ) ( residue  142 and name HA   )   6.00  4.20  0.60
assign ( residue  142 and name HA   ) ( residue  145 and name HE#  )   3.00  1.20  0.30
assign ( residue  144 and name HA   ) ( residue  144 and name HE#  )   4.00  2.20  0.40
assign ( residue  144 and name HB#  ) ( residue  144 and name HE#  )   5.00  3.20  0.50
assign ( residue  145 and name HA   ) ( residue  145 and name HE#  )   5.00  3.20  0.50
assign ( residue  145 and name HB#  ) ( residue  145 and name HE#  )   4.00  2.20  0.40
assign ( residue  145 and name HE#  ) ( residue 1916 and name HE#  )   4.00  2.20  0.40
assign ( residue   77 and name HD#  ) ( residue   77 and name HE#  )   4.00  2.20  0.40
assign ( residue   85 and name HB#  ) ( residue   89 and name HE#  )   5.00  3.20  0.50
assign ( residue   85 and name HD## ) ( residue   89 and name HE#  )   5.00  3.20  0.50
assign ( residue   86 and name HA   ) ( residue  138 and name HE#  )   5.00  3.20  0.50
assign ( residue   86 and name HD#  ) ( residue  138 and name HE#  )   5.00  3.20  0.50
```

```
assign ( residue   86 and name HG1# ) ( residue  138 and name HE#  )   5.00  3.20  0.50
assign ( residue   89 and name HA   ) ( residue   89 and name HE#  )   5.00  3.20  0.50
assign ( residue   89 and name HB#  ) ( residue   89 and name HE#  )   5.00  3.20  0.50
assign ( residue   89 and name HB#  ) ( residue  138 and name HE#  )   5.00  3.20  0.50
assign ( residue   89 and name HD#  ) ( residue   89 and name HE#  )   3.00  1.20  0.30
assign ( residue   90 and name HA   ) ( residue   90 and name HE#  )   5.00  3.20  0.50
assign ( residue   90 and name HB#  ) ( residue   90 and name HE#  )   5.00  3.20  0.50
assign ( residue   90 and name HB#  ) ( residue  138 and name HE#  )   5.00  3.20  0.50
assign ( residue   90 and name HD#  ) ( residue   90 and name HE#  )   4.00  2.20  0.40
assign ( residue   90 and name HD#  ) ( residue  138 and name HE#  )   5.00  3.20  0.50
assign ( residue   92 and name HD#  ) ( residue   92 and name HE#  )   4.00  2.20  0.40
assign ( residue   92 and name HD#  ) ( residue  109 and name HE#  )   5.00  3.20  0.50
assign ( residue   92 and name HE#  ) ( residue  109 and name HE#  )   5.00  3.20  0.50
assign ( residue   93 and name HB#  ) ( residue  138 and name HE#  )   4.00  2.20  0.40
assign ( residue   98 and name HA#  ) ( residue  138 and name HE#  )   5.00  3.20  0.50
assign ( residue   99 and name HA   ) ( residue  138 and name HE#  )   5.00  3.20  0.50
assign ( residue  105 and name HA   ) ( residue  105 and name HG   )   4.00  2.20  0.40
assign ( residue  105 and name HB#  ) ( residue  105 and name HG   )   3.00  1.20  0.30
assign ( residue  105 and name HD1# ) ( residue  105 and name HG   )   4.00  2.20  0.40
assign ( residue  105 and name HD2# ) ( residue  105 and name HG   )   3.00  1.20  0.30
assign ( residue  108 and name HA   ) ( residue  112 and name HG   )   5.00  3.20  0.50
assign ( residue  105 and name HG   ) ( residue  109 and name HE#  )   4.00  2.20  0.40
assign ( residue  111 and name HB#  ) ( residue  112 and name HG   )   5.00  3.20  0.50
assign ( residue  112 and name HA   ) ( residue  112 and name HG   )   4.00  2.20  0.40
assign ( residue  112 and name HB#  ) ( residue  112 and name HG   )   4.00  2.20  0.40
assign ( residue  112 and name HD#  ) ( residue  112 and name HG   )   3.00  1.20  0.30
assign ( residue  116 and name HA   ) ( residue  116 and name HG   )   5.00  3.20  0.50
assign ( residue  116 and name HB#  ) ( residue  116 and name HG   )   4.00  2.20  0.40
assign ( residue  116 and name HD1# ) ( residue  116 and name HG   )   3.00  1.20  0.30
assign ( residue  116 and name HD2# ) ( residue  116 and name HG   )   3.00  1.20  0.30
assign ( residue  123 and name HG#  ) ( residue 1920 and name HG   )   5.00  3.20  0.50
assign ( residue   85 and name HG   ) ( residue  142 and name HA   )   4.00  2.20  0.40
assign ( residue   85 and name HA   ) ( residue   85 and name HG   )   4.00  2.20  0.40
assign ( residue   85 and name HB#  ) ( residue   85 and name HG   )   4.00  2.20  0.40
assign ( residue   85 and name HD## ) ( residue   85 and name HG   )   3.00  1.20  0.30
assign ( residue   85 and name HG   ) ( residue   86 and name HA   )   5.00  3.20  0.50
assign ( residue   85 and name HG   ) ( residue   89 and name HD#  )   5.00  3.20  0.50
assign ( residue   85 and name HG   ) ( residue   89 and name HE#  )   5.00  3.20  0.50
assign ( residue   99 and name HA   ) ( residue   99 and name HG   )   4.00  2.20  0.40
assign ( residue   99 and name HB#  ) ( residue   99 and name HG   )   4.00  2.20  0.40
assign ( residue   99 and name HD## ) ( residue   99 and name HG   )   3.00  1.20  0.30
assign ( residue  101 and name HB#  ) ( residue  104 and name HG#  )   5.00  3.20  0.50
assign ( residue  104 and name HA   ) ( residue  104 and name HG#  )   3.00  1.20  0.30
assign ( residue  104 and name HB#  ) ( residue  104 and name HG#  )   3.00  1.20  0.30
assign ( residue  105 and name HG   ) ( residue  109 and name HG#  )   5.00  3.20  0.50
assign ( residue  106 and name HA   ) ( residue  106 and name HG#  )   4.00  2.20  0.40
```

```
assign ( residue  106 and name HA   ) ( residue  109 and name HG# )   6.00  4.20  0.60
assign ( residue  106 and name HB# ) ( residue  106 and name HG# )   3.00  1.20  0.30
assign ( residue  106 and name HD# ) ( residue  106 and name HG# )   4.00  2.20  0.40
assign ( residue  106 and name HG# ) ( residue  107 and name HA   )   5.00  3.20  0.50
assign ( residue  104 and name HG# ) ( residue  107 and name HB# )   5.00  3.20  0.50
assign ( residue  109 and name HA   ) ( residue  109 and name HG# )   5.00  3.20  0.50
assign ( residue  109 and name HB# ) ( residue  109 and name HG# )   5.00  3.20  0.50
assign ( residue  109 and name HE# ) ( residue 1913 and name HG# )   5.00  3.20  0.50
assign ( residue  109 and name HE# ) ( residue  109 and name HG# )   5.00  3.20  0.50
assign ( residue  106 and name HG# ) ( residue  110 and name HB   )   5.00  3.20  0.50
assign ( residue  111 and name HA   ) ( residue  115 and name HG# )   5.00  3.20  0.50
assign ( residue  113 and name HA# ) ( residue 1913 and name HG# )   5.00  3.20  0.50
assign ( residue  114 and name HA   ) ( residue  114 and name HG# )   3.00  1.20  0.30
assign ( residue  114 and name HA   ) ( residue  115 and name HG# )   5.00  3.20  0.50
assign ( residue  114 and name HB# ) ( residue  114 and name HG# )   4.00  2.20  0.40
assign ( residue  115 and name HA   ) ( residue  115 and name HG# )   4.00  2.20  0.40
assign ( residue  115 and name HB# ) ( residue  115 and name HG# )   3.00  1.20  0.30
assign ( residue  115 and name HD# ) ( residue  115 and name HG# )   4.00  2.20  0.40
assign ( residue  115 and name HE# ) ( residue  115 and name HG# )   4.00  2.20  0.40
assign ( residue  116 and name HA   ) ( residue 1913 and name HG# )   5.00  3.20  0.50
assign ( residue  116 and name HB# ) ( residue 1913 and name HG# )   5.00  3.20  0.50
assign ( residue  116 and name HD1# ) ( residue 1913 and name HG# )   4.00  2.20  0.40
assign ( residue  116 and name HD2# ) ( residue 1913 and name HG# )   5.00  3.20  0.50
assign ( residue  109 and name HG# ) ( residue  116 and name HD2# )   5.00  3.20  0.50
assign ( residue  116 and name HG   ) ( residue 1913 and name HG# )   5.00  3.20  0.50
assign ( residue  120 and name HB# ) ( residue  120 and name HG# )   4.00  2.20  0.40
assign ( residue  123 and name HA   ) ( residue  123 and name HG# )   4.00  2.20  0.40
assign ( residue  123 and name HB# ) ( residue  123 and name HG# )   3.00  1.20  0.30
assign ( residue  124 and name HA   ) ( residue  124 and name HG# )   3.00  1.20  0.30
assign ( residue  124 and name HB# ) ( residue  124 and name HG# )   4.00  2.20  0.40
assign ( residue  126 and name HA   ) ( residue  126 and name HG# )   4.00  2.20  0.40
assign ( residue  126 and name HB# ) ( residue  126 and name HG# )   3.00  1.20  0.30
assign ( residue  126 and name HD# ) ( residue  126 and name HG# )   5.00  3.20  0.50
assign ( residue  127 and name HA   ) ( residue  127 and name HG# )   5.00  3.20  0.50
assign ( residue  127 and name HB# ) ( residue  127 and name HG# )   4.00  2.20  0.40
assign ( residue   90 and name HG# ) ( residue  138 and name HE# )   5.00  3.20  0.50
assign ( residue  139 and name HA   ) ( residue  139 and name HG# )   4.00  2.20  0.40
assign ( residue  139 and name HB# ) ( residue  139 and name HG# )   3.00  1.20  0.30
assign ( residue  127 and name HG# ) ( residue  141 and name HA   )   5.00  3.20  0.50
assign ( residue  141 and name HA   ) ( residue  144 and name HG# )   5.00  3.20  0.50
assign ( residue  124 and name HG# ) ( residue  141 and name HD# )   6.00  4.20  0.50
assign ( residue  127 and name HG# ) ( residue  141 and name HD# )   5.00  3.20  0.50
assign ( residue  124 and name HG# ) ( residue  141 and name HE# )   5.00  3.20  0.50
assign ( residue  142 and name HA   ) ( residue  144 and name HG# )   5.00  3.20  0.50
assign ( residue  142 and name HA   ) ( residue  145 and name HG# )   5.00  3.20  0.50
assign ( residue  139 and name HG# ) ( residue  142 and name HG## )   4.00  2.20  0.40
```

```
assign ( residue  143 and name HD#  ) ( residue  143 and name HG#  )   4.00  2.20  0.40
assign ( residue  144 and name HA   ) ( residue  144 and name HG#  )   4.00  2.20  0.40
assign ( residue  144 and name HB#  ) ( residue  144 and name HG#  )   4.00  2.20  0.40
assign ( residue  144 and name HE#  ) ( residue  144 and name HG#  )   5.00  3.20  0.50
assign ( residue  145 and name HA   ) ( residue  145 and name HG#  )   5.00  3.20  0.50
assign ( residue  145 and name HB#  ) ( residue  145 and name HG#  )   5.00  3.20  0.50
assign ( residue  145 and name HE#  ) ( residue  145 and name HG#  )   3.00  1.20  0.30
assign ( residue   85 and name HB#  ) ( residue  146 and name HG## )   6.00  4.20  0.60
assign ( residue  144 and name HG#  ) ( residue  146 and name HG## )   5.00  3.20  0.50
assign ( residue   77 and name HA   ) ( residue   77 and name HG#  )   4.00  2.20  0.40
assign ( residue   77 and name HB#  ) ( residue   77 and name HG#  )   4.00  2.20  0.30
assign ( residue   77 and name HD#  ) ( residue   77 and name HG#  )   4.00  2.20  0.30
assign ( residue   77 and name HE#  ) ( residue   77 and name HG#  )   4.00  2.20  0.40
assign ( residue   78 and name HA   ) ( residue   78 and name HG#  )   4.00  2.20  0.40
assign ( residue   78 and name HB#  ) ( residue   78 and name HG#  )   3.00  1.20  0.30
assign ( residue   79 and name HA   ) ( residue   79 and name HG#  )   4.00  2.20  0.30
assign ( residue   79 and name HB#  ) ( residue   79 and name HG#  )   4.00  2.20  0.40
assign ( residue   80 and name HB#  ) ( residue 1914 and name HG#  )   6.00  4.20  0.60
assign ( residue   83 and name HA   ) ( residue   83 and name HG#  )   3.00  1.20  0.30
assign ( residue   83 and name HB#  ) ( residue   83 and name HG#  )   3.00  1.20  0.30
assign ( residue   83 and name HG#  ) ( residue   84 and name HA   )   4.00  2.20  0.40
assign ( residue   84 and name HA   ) ( residue   84 and name HG#  )   3.00  1.20  0.30
assign ( residue   84 and name HB#  ) ( residue   84 and name HG#  )   3.00  1.20  0.30
assign ( residue   90 and name HA   ) ( residue   90 and name HG#  )   4.00  2.20  0.40
assign ( residue   90 and name HB#  ) ( residue   90 and name HG#  )   3.00  1.20  0.30
assign ( residue   90 and name HD#  ) ( residue   90 and name HG#  )   3.00  1.20  0.30
assign ( residue   90 and name HE#  ) ( residue   90 and name HG#  )   4.00  2.20  0.40
assign ( residue   91 and name HA   ) ( residue 1905 and name HG#  )   6.00  4.20  0.50
assign ( residue   91 and name HB   ) ( residue 1905 and name HG#  )   5.00  3.20  0.50
assign ( residue   91 and name HG## ) ( residue 1905 and name HG#  )   3.00  1.20  0.30
assign ( residue   92 and name HD#  ) ( residue 1905 and name HG#  )   5.00  3.20  0.50
assign ( residue   90 and name HG#  ) ( residue   93 and name HB#  )   5.00  3.20  0.50
assign ( residue   94 and name HA   ) ( residue   94 and name HG#  )   4.00  2.20  0.40
assign ( residue   94 and name HD#  ) ( residue   94 and name HG#  )   3.00  1.20  0.30
assign ( residue  100 and name HA   ) ( residue  100 and name HG1# )   4.00  2.20  0.40
assign ( residue  100 and name HB   ) ( residue  100 and name HG1# )   3.00  1.20  0.30
assign ( residue  100 and name HD#  ) ( residue  100 and name HG1# )   3.00  1.20  0.30
assign ( residue   91 and name HG## ) ( residue  109 and name HE#  )   5.00  3.20  0.40
assign ( residue  117 and name HA   ) ( residue  121 and name HG## )   5.00  3.20  0.50
assign ( residue  118 and name HA   ) ( residue  121 and name HG## )   3.00  1.20  0.30
assign ( residue  118 and name HB#  ) ( residue  121 and name HG## )   5.00  3.20  0.50
assign ( residue  121 and name HG## ) ( residue  122 and name HA   )   5.00  3.20  0.50
assign ( residue  122 and name HA   ) ( residue  125 and name HG1# )   5.00  3.20  0.50
assign ( residue  121 and name HG## ) ( residue  122 and name HB#  )   5.00  3.20  0.50
assign ( residue  125 and name HA   ) ( residue  125 and name HG1# )   4.00  2.20  0.40
assign ( residue  125 and name HB   ) ( residue  125 and name HG1# )   3.00  1.20  0.30
```

```
assign ( residue  125 and name HD#  ) ( residue  125 and name HG1# )   3.00  1.20  0.30
assign ( residue  129 and name HA   ) ( residue  136 and name HG1# )   5.00  3.20  0.50
assign ( residue  129 and name HB#  ) ( residue  136 and name HG1# )   5.00  3.20  0.50
assign ( residue  130 and name HA   ) ( residue  130 and name HG1# )   5.00  3.20  0.50
assign ( residue  130 and name HB   ) ( residue  130 and name HG1# )   5.00  3.20  0.50
assign ( residue  130 and name HB   ) ( residue  136 and name HG1# )   5.00  3.20  0.50
assign ( residue  130 and name HD#  ) ( residue  130 and name HG1# )   4.00  2.20  0.40
assign ( residue  134 and name HA#  ) ( residue  136 and name HG1# )   4.00  2.20  0.40
assign ( residue  135 and name HA   ) ( residue  136 and name HG1# )   5.00  3.20  0.50
assign ( residue  135 and name HB#  ) ( residue  136 and name HG1# )   5.00  3.20  0.50
assign ( residue  136 and name HA   ) ( residue  136 and name HG1# )   4.00  2.20  0.40
assign ( residue  136 and name HB   ) ( residue  136 and name HG1# )   5.00  3.20  0.50
assign ( residue  136 and name HD#  ) ( residue  136 and name HG1# )   5.00  3.20  0.50
assign ( residue   86 and name HG1# ) ( residue  138 and name HB#  )   5.00  3.20  0.50
assign ( residue  138 and name HB#  ) ( residue  142 and name HG## )   5.00  3.20  0.50
assign ( residue  100 and name HG1# ) ( residue  138 and name HD#  )   5.00  3.20  0.50
assign ( residue  138 and name HD#  ) ( residue  142 and name HG## )   5.00  3.20  0.50
assign ( residue  100 and name HG1# ) ( residue  138 and name HE#  )   6.00  4.20  0.60
assign ( residue   86 and name HG1# ) ( residue  139 and name HA   )   5.00  3.20  0.50
assign ( residue   86 and name HG1# ) ( residue  139 and name HB#  )   5.00  3.20  0.50
assign ( residue  141 and name HB#  ) ( residue  142 and name HG## )   5.00  3.20  0.50
assign ( residue  141 and name HD#  ) ( residue  142 and name HG## )   5.00  3.20  0.50
assign ( residue  141 and name HE#  ) ( residue  142 and name HG## )   5.00  3.20  0.50
assign ( residue   86 and name HG1# ) ( residue  142 and name HA   )   6.00  4.20  0.60
assign ( residue  142 and name HA   ) ( residue  146 and name HG## )   5.00  3.20  0.50
assign ( residue   86 and name HG1# ) ( residue  142 and name HB   )   4.00  2.20  0.40
assign ( residue  142 and name HG## ) ( residue  146 and name HG## )   3.00  1.20  0.30
assign ( residue   81 and name HB#  ) ( residue  146 and name HG## )   5.00  3.20  0.50
assign ( residue   84 and name HA   ) ( residue 1911 and name HG## )   5.00  3.20  0.50
assign ( residue   84 and name HB#  ) ( residue 1911 and name HG## )   4.00  2.20  0.40
assign ( residue   84 and name HG#  ) ( residue 1911 and name HG## )   4.00  2.20  0.40
assign ( residue   86 and name HA   ) ( residue   86 and name HG1# )   4.00  2.20  0.40
assign ( residue   86 and name HB   ) ( residue   86 and name HG1# )   3.00  1.20  0.30
assign ( residue   86 and name HD#  ) ( residue   86 and name HG1# )   3.00  1.20  0.30
assign ( residue   87 and name HA   ) ( residue   91 and name HG## )   6.00  4.20  0.60
assign ( residue   88 and name HB#  ) ( residue 1911 and name HG## )   3.00  1.20  0.30
assign ( residue   88 and name HB#  ) ( residue   91 and name HG## )   4.00  2.20  0.40
assign ( residue   89 and name HA   ) ( residue   91 and name HG## )   5.00  3.20  0.50
assign ( residue   89 and name HB#  ) ( residue  142 and name HG## )   5.00  3.20  0.50
assign ( residue   89 and name HD#  ) ( residue  142 and name HG## )   4.00  2.20  0.40
assign ( residue   92 and name HA   ) ( residue  100 and name HG1# )   5.00  3.20  0.50
assign ( residue   92 and name HA   ) ( residue  108 and name HG## )   5.00  3.20  0.50
assign ( residue   92 and name HB#  ) ( residue  100 and name HG1# )   5.00  3.20  0.50
assign ( residue   93 and name HA   ) ( residue  100 and name HG1# )   5.00  3.20  0.50
assign ( residue  100 and name HA   ) ( residue  100 and name HG2# )   3.00  1.20  0.30
assign ( residue  100 and name HA   ) ( residue  136 and name HG2# )   6.00  4.20  0.60
```

```
assign ( residue  100 and name HB   ) ( residue  100 and name HG2# )   3.00  1.20  0.30
assign ( residue  100 and name HB   ) ( residue  136 and name HG2# )   5.00  3.20  0.50
assign ( residue  100 and name HD1# ) ( residue  100 and name HG2# )   4.00  2.20  0.40
assign ( residue  100 and name HD1# ) ( residue  136 and name HG2# )   5.00  3.20  0.50
assign ( residue  100 and name HG1# ) ( residue  100 and name HG2# )   3.00  1.20  0.30
assign ( residue  100 and name HG1# ) ( residue  136 and name HG2# )   5.00  3.20  0.50
assign ( residue  100 and name HG2# ) ( residue  136 and name HG2# )   3.00  1.20  0.30
assign ( residue  100 and name HG2# ) ( residue  102 and name HA    )   5.00  3.20  0.50
assign ( residue  102 and name HA   ) ( residue  125 and name HG2# )   5.00  3.20  0.50
assign ( residue  102 and name HB#  ) ( residue  125 and name HG2# )   4.00  2.20  0.40
assign ( residue  104 and name HA   ) ( residue  108 and name HG## )   6.00  4.20  0.60
assign ( residue  105 and name HA   ) ( residue  108 and name HG## )   4.00  2.20  0.40
assign ( residue  100 and name HG2# ) ( residue  105 and name HB#  )   5.00  3.20  0.50
assign ( residue  105 and name HB#  ) ( residue  108 and name HG## )   4.00  2.20  0.40
assign ( residue  105 and name HB#  ) ( residue  121 and name HG## )   5.00  3.20  0.50
assign ( residue  105 and name HB#  ) ( residue  136 and name HG2# )   5.00  3.20  0.50
assign ( residue  105 and name HD1# ) ( residue  108 and name HG## )   3.00  1.20  0.30
assign ( residue  105 and name HD2# ) ( residue  108 and name HG## )   5.00  3.20  0.50
assign ( residue  105 and name HG   ) ( residue  121 and name HG## )   5.00  3.20  0.50
assign ( residue  106 and name HA   ) ( residue  110 and name HG2# )   5.00  3.20  0.50
assign ( residue  106 and name HA   ) ( residue  121 and name HG## )   3.00  1.20  0.30
assign ( residue  106 and name HA   ) ( residue  125 and name HG2# )   5.00  3.20  0.50
assign ( residue  106 and name HB#  ) ( residue  110 and name HG2# )   5.00  3.20  0.50
assign ( residue  106 and name HB#  ) ( residue  121 and name HG## )   4.00  2.20  0.40
assign ( residue  106 and name HD#  ) ( residue  110 and name HG2# )   5.00  3.20  0.50
assign ( residue  106 and name HD#  ) ( residue  121 and name HG## )   5.00  3.20  0.50
assign ( residue  106 and name HD#  ) ( residue  125 and name HG2# )   5.00  3.20  0.50
assign ( residue  106 and name HG#  ) ( residue  110 and name HG2# )   5.00  3.20  0.50
assign ( residue  106 and name HG#  ) ( residue  121 and name HG## )   4.00  2.20  0.40
assign ( residue  107 and name HB#  ) ( residue  108 and name HG## )   5.00  3.20  0.50
assign ( residue  107 and name HD2  ) ( residue  108 and name HG## )   5.00  3.20  0.50
assign ( residue  108 and name HA   ) ( residue  108 and name HG## )   3.00  1.20  0.30
assign ( residue  108 and name HB   ) ( residue  108 and name HG## )   3.00  1.20  0.30
assign ( residue  108 and name HG## ) ( residue  109 and name HA    )   5.00  3.20  0.50
assign ( residue  109 and name HA   ) ( residue  110 and name HG2# )   5.00  3.20  0.50
assign ( residue  109 and name HA   ) ( residue  121 and name HG## )   5.00  3.20  0.50
assign ( residue  108 and name HG## ) ( residue  109 and name HB#  )   5.00  3.20  0.50
assign ( residue  109 and name HB#  ) ( residue  110 and name HG2# )   5.00  3.20  0.50
assign ( residue  109 and name HB#  ) ( residue  121 and name HG## )   4.00  2.20  0.40
assign ( residue  108 and name HG## ) ( residue  109 and name HE#  )   3.00  1.20  0.30
assign ( residue  109 and name HE#  ) ( residue  121 and name HG## )   5.00  3.20  0.50
assign ( residue  108 and name HG## ) ( residue  109 and name HG#  )   5.00  3.20  0.50
assign ( residue  109 and name HG#  ) ( residue  110 and name HG2# )   5.00  3.20  0.50
assign ( residue  109 and name HG#  ) ( residue  121 and name HG## )   5.00  3.20  0.50
assign ( residue  110 and name HA   ) ( residue  110 and name HG2# )   3.00  1.20  0.30
assign ( residue  110 and name HA   ) ( residue  121 and name HG## )   5.00  3.20  0.50
```

```
assign ( residue  110 and name HB   ) ( residue  110 and name HG2# )   3.00  1.20  0.30
assign ( residue  110 and name HB   ) ( residue  121 and name HG## )   5.00  3.20  0.50
assign ( residue  108 and name HG## ) ( residue  111 and name HB#  )   5.00  3.20  0.50
assign ( residue  108 and name HG## ) ( residue  112 and name HB#  )   5.00  3.20  0.50
assign ( residue  108 and name HG## ) ( residue  112 and name HD## )   5.00  3.20  0.50
assign ( residue  110 and name HG2# ) ( residue  115 and name HA   )   5.00  3.20  0.50
assign ( residue  110 and name HG2# ) ( residue  115 and name HB#  )   6.00  4.20  0.60
assign ( residue  110 and name HG2# ) ( residue  116 and name HA   )   5.00  3.20  0.50
assign ( residue  110 and name HG2# ) ( residue  116 and name HB#  )   5.00  3.20  0.50
assign ( residue  110 and name HG2# ) ( residue  116 and name HG   )   5.00  3.20  0.50
assign ( residue  110 and name HG2# ) ( residue  117 and name HA   )   5.00  3.20  0.50
assign ( residue  117 and name HA   ) ( residue  117 and name HG2# )   3.00  1.20  0.30
assign ( residue  110 and name HG2# ) ( residue  117 and name HB   )   5.00  3.20  0.50
assign ( residue  117 and name HB   ) ( residue  117 and name HG2# )   3.00  1.20  0.30
assign ( residue  110 and name HG2# ) ( residue  118 and name HA   )   4.00  2.20  0.40
assign ( residue  117 and name HG2# ) ( residue  118 and name HB#  )   5.00  3.20  0.50
assign ( residue  110 and name HG2# ) ( residue  120 and name HB#  )   5.00  3.20  0.50
assign ( residue  110 and name HG2# ) ( residue  121 and name HA   )   5.00  3.20  0.50
assign ( residue  121 and name HA   ) ( residue  121 and name HG## )   3.00  1.20  0.30
assign ( residue  110 and name HG2# ) ( residue  121 and name HB   )   4.00  2.20  0.40
assign ( residue  121 and name HB   ) ( residue  121 and name HG## )   3.00  1.20  0.30
assign ( residue  110 and name HG2# ) ( residue  121 and name HG## )   4.00  2.20  0.40
assign ( residue  122 and name HA   ) ( residue  125 and name HG2# )   5.00  3.20  0.50
assign ( residue  121 and name HG## ) ( residue  124 and name HB#  )   5.00  3.20  0.50
assign ( residue  121 and name HG## ) ( residue  124 and name HE#  )   4.00  2.20  0.40
assign ( residue  121 and name HG## ) ( residue  124 and name HG#  )   5.00  3.20  0.50
assign ( residue  125 and name HA   ) ( residue  125 and name HG2# )   3.00  1.20  0.30
assign ( residue  125 and name HA   ) ( residue  136 and name HG2# )   5.00  3.20  0.50
assign ( residue  125 and name HB   ) ( residue  125 and name HG2# )   3.00  1.20  0.30
assign ( residue  125 and name HB   ) ( residue  136 and name HG2# )   5.00  3.20  0.50
assign ( residue  125 and name HD#  ) ( residue  125 and name HG2# )   3.00  1.20  0.30
assign ( residue  125 and name HG1# ) ( residue  125 and name HG2# )   3.00  1.20  0.30
assign ( residue  128 and name HA   ) ( residue  136 and name HG2# )   4.00  2.20  0.40
assign ( residue  129 and name HA   ) ( residue  136 and name HG2# )   5.00  3.20  0.50
assign ( residue  129 and name HB#  ) ( residue  136 and name HG2# )   5.00  3.20  0.50
assign ( residue  130 and name HA   ) ( residue  130 and name HG2# )   4.00  2.20  0.40
assign ( residue  130 and name HB   ) ( residue  130 and name HG2# )   3.00  1.20  0.30
assign ( residue  130 and name HB   ) ( residue  136 and name HG2# )   5.00  3.20  0.50
assign ( residue  130 and name HG1# ) ( residue  130 and name HG2# )   5.00  3.20  0.50
assign ( residue  130 and name HG1# ) ( residue  136 and name HG2# )   5.00  3.20  0.50
assign ( residue  130 and name HG2# ) ( residue  134 and name HA#  )   5.00  3.20  0.50
assign ( residue  136 and name HA   ) ( residue  136 and name HG2# )   3.00  1.20  0.30
assign ( residue  100 and name HG2# ) ( residue  136 and name HB   )   5.00  3.20  0.50
assign ( residue  136 and name HB   ) ( residue  136 and name HG2# )   4.00  2.20  0.40
assign ( residue  136 and name HD#  ) ( residue  136 and name HG2# )   3.00  1.20  0.30
assign ( residue  136 and name HG1# ) ( residue  136 and name HG2# )   3.00  1.20  0.30
```

```
assign ( residue  136 and name HG2# ) ( residue  137 and name HA   )  5.00  3.20  0.50
assign ( residue  136 and name HG2# ) ( residue  137 and name HB#  )  5.00  3.20  0.50
assign ( residue  136 and name HG2# ) ( residue  138 and name HA   )  4.00  2.20  0.40
assign ( residue   86 and name HG2# ) ( residue  138 and name HB#  )  4.00  2.20  0.40
assign ( residue  100 and name HG2# ) ( residue  138 and name HB#  )  5.00  3.20  0.50
assign ( residue   86 and name HG2# ) ( residue  138 and name HD#  )  5.00  3.20  0.50
assign ( residue  100 and name HG2# ) ( residue  138 and name HD#  )  4.00  2.20  0.40
assign ( residue   86 and name HG2# ) ( residue  138 and name HE#  )  3.00  1.20  0.30
assign ( residue  100 and name HG2# ) ( residue  138 and name HE#  )  5.00  3.20  0.50
assign ( residue   86 and name HG2# ) ( residue  139 and name HA   )  5.00  3.20  0.50
assign ( residue  139 and name HA   ) ( residue  142 and name HG## )  4.00  2.20  0.40
assign ( residue  136 and name HG2# ) ( residue  141 and name HA   )  5.00  3.20  0.50
assign ( residue  136 and name HG2# ) ( residue  141 and name HB#  )  5.00  3.20  0.50
assign ( residue  100 and name HG2# ) ( residue  141 and name HE#  )  5.00  3.20  0.50
assign ( residue  105 and name HD2# ) ( residue  141 and name HE#  )  5.00  3.20  0.50
assign ( residue  125 and name HG2# ) ( residue  141 and name HE#  )  5.00  3.20  0.50
assign ( residue  136 and name HG2# ) ( residue  141 and name HE#  )  5.00  3.20  0.50
assign ( residue  142 and name HA   ) ( residue  142 and name HG## )  3.00  1.20  0.30
assign ( residue  142 and name HB   ) ( residue  142 and name HG## )  3.00  1.20  0.30
assign ( residue  142 and name HG## ) ( residue  145 and name HB#  )  5.00  3.20  0.50
assign ( residue  145 and name HB#  ) ( residue  146 and name HG## )  5.00  3.20  0.50
assign ( residue  145 and name HE#  ) ( residue 1911 and name HG## )  6.00  4.20  0.60
assign ( residue  142 and name HG## ) ( residue  145 and name HE#  )  4.00  2.20  0.40
assign ( residue  145 and name HE#  ) ( residue  146 and name HG## )  5.00  3.20  0.50
assign ( residue  145 and name HG#  ) ( residue  146 and name HG## )  5.00  3.20  0.50
assign ( residue  146 and name HB   ) ( residue  146 and name HG## )  3.00  1.20  0.30
assign ( residue  146 and name HG## ) ( residue  147 and name HA   )  5.00  3.20  0.50
assign ( residue  146 and name HG## ) ( residue  147 and name HB#  )  5.00  3.20  0.50
assign ( residue  146 and name HA   ) ( residue  146 and name HG## )  5.00  3.20  0.50
assign ( residue   83 and name HA   ) ( residue   86 and name HG2# )  4.00  2.20  0.40
assign ( residue   85 and name HA   ) ( residue 1911 and name HG## )  4.00  2.20  0.40
assign ( residue   85 and name HA   ) ( residue  142 and name HG## )  5.00  3.20  0.50
assign ( residue   85 and name HB#  ) ( residue  142 and name HG## )  4.00  2.20  0.40
assign ( residue   85 and name HG   ) ( residue  142 and name HG## )  5.00  3.20  0.50
assign ( residue   86 and name HA   ) ( residue   86 and name HG2# )  3.00  1.20  0.30
assign ( residue   86 and name HA   ) ( residue  142 and name HG## )  5.00  3.20  0.50
assign ( residue   86 and name HB   ) ( residue   86 and name HG2# )  3.00  1.20  0.30
assign ( residue   86 and name HD#  ) ( residue   86 and name HG2# )  3.00  1.20  0.30
assign ( residue   86 and name HG1# ) ( residue   86 and name HG2# )  3.00  1.20  0.30
assign ( residue   86 and name HG1# ) ( residue  142 and name HG## )  3.00  1.20  0.30
assign ( residue   86 and name HG2# ) ( residue   87 and name HA   )  4.00  2.20  0.40
assign ( residue   88 and name HA   ) ( residue   91 and name HG## )  5.00  3.20  0.50
assign ( residue   86 and name HG2# ) ( residue   89 and name HB#  )  5.00  3.20  0.50
assign ( residue   89 and name HD#  ) ( residue   91 and name HG## )  6.00  4.20  0.60
assign ( residue   89 and name HD#  ) ( residue  100 and name HG2# )  5.00  3.20  0.50
assign ( residue   89 and name HD#  ) ( residue  108 and name HG## )  6.00  4.20  0.60
```

```
assign ( residue   89 and name HE#  ) ( residue  100 and name HG2# )   5.00  3.20  0.50
assign ( residue   89 and name HE#  ) ( residue  108 and name HG## )   5.00  3.20  0.50
assign ( residue   89 and name HE#  ) ( residue  136 and name HG2# )   5.00  3.20  0.50
assign ( residue   86 and name HG2# ) ( residue   90 and name HE#  )   4.00  2.20  0.40
assign ( residue   86 and name HG2# ) ( residue   90 and name HG#  )   4.00  2.20  0.40
assign ( residue   91 and name HA   ) ( residue   91 and name HG## )   3.00  1.20  0.30
assign ( residue   91 and name HB   ) ( residue   91 and name HG## )   3.00  1.20  0.30
assign ( residue   91 and name HG## ) ( residue   92 and name HA   )   5.00  3.20  0.50
assign ( residue   91 and name HG## ) ( residue   92 and name HB#  )   5.00  3.20  0.50
assign ( residue   92 and name HB#  ) ( residue  100 and name HG2# )   5.00  3.20  0.50
assign ( residue   92 and name HB#  ) ( residue  108 and name HG## )   5.00  3.20  0.50
assign ( residue   91 and name HG## ) ( residue   92 and name HD#  )   5.00  3.20  0.50
assign ( residue   92 and name HD#  ) ( residue  108 and name HG## )   5.00  3.20  0.50
assign ( residue   91 and name HG## ) ( residue   92 and name HE#  )   5.00  3.20  0.50
assign ( residue   92 and name HE#  ) ( residue  108 and name HG## )   5.00  3.20  0.50
assign ( residue   93 and name HA   ) ( residue  100 and name HG2# )   5.00  3.20  0.50
assign ( residue  107 and name HD2  ) ( residue  111 and name HB#  )   5.00  3.20  0.50
assign ( residue  107 and name HE1  ) ( residue  111 and name HB#  )   5.00  3.20  0.50
assign ( residue  113 and name HA#  ) ( residue 1910 and name HG2# )   6.00  4.20  0.60
assign ( residue  113 and name HA#  ) ( residue 1910 and name HD#  )   4.00  2.20  0.40
assign ( residue  112 and name HG   ) ( residue 1909 and name HB#  )   4.00  2.20  0.40
assign ( residue   81 and name HA   ) ( residue   82 and name HA   )   5.00  3.20  0.50
assign ( residue   83 and name HA   ) ( residue   86 and name HB   )   3.00  3.20  0.30
assign ( residue   84 and name HA   ) ( residue   87 and name HB#  )   3.00  3.20  0.30
assign ( residue  145 and name HE#  ) ( residue 1912 and name HG1# )   4.00  2.20  0.40
assign ( residue  141 and name HE#  ) ( residue 1912 and name HG1# )   5.00  3.20  0.50
assign ( residue  124 and name HE#  ) ( residue 1912 and name HG1# )   5.00  3.20  0.50
assign ( residue  109 and name HE#  ) ( residue 1912 and name HG1# )   5.00  3.20  0.50
assign ( residue  109 and name HG#  ) ( residue 1912 and name HG1# )   6.00  4.20  0.60
assign ( residue   89 and name HD#  ) ( residue 1912 and name HG1# )   4.00  2.20  0.50
assign ( residue   89 and name HE#  ) ( residue 1912 and name HG1# )   5.00  2.20  0.50
assign ( residue   88 and name HB#  ) ( residue 1912 and name HG1# )   3.00  1.20  0.30
assign ( residue   85 and name HA   ) ( residue 1912 and name HG1# )   5.00  3.20  0.50
assign ( residue   85 and name HB#  ) ( residue 1912 and name HG1# )   5.00  3.20  0.50
assign ( residue   85 and name HD## ) ( residue 1912 and name HG1# )   4.00  2.20  0.40
assign ( residue   85 and name HA   ) ( residue 1912 and name HG2# )   5.00  3.20  0.50
assign ( residue   85 and name HB#  ) ( residue 1912 and name HG2# )   5.00  3.20  0.50
assign ( residue   85 and name HD## ) ( residue 1912 and name HG2# )   4.00  2.20  0.30
assign ( residue   88 and name HA   ) ( residue 1912 and name HG2# )   5.00  3.20  0.40
assign ( residue   88 and name HB#  ) ( residue 1912 and name HG2# )   5.00  3.20  0.40
assign ( residue   89 and name HA   ) ( residue 1912 and name HG2# )   5.00  3.20  0.50
assign ( residue   89 and name HD#  ) ( residue 1912 and name HG2# )   4.00  2.20  0.40
assign ( residue  124 and name HE#  ) ( residue 1912 and name HG2# )   5.00  3.20  0.50
assign ( residue  109 and name HG#  ) ( residue 1912 and name HG2# )   4.00  2.20  0.40
assign ( residue  109 and name HE#  ) ( residue 1912 and name HG2# )   4.00  2.20  0.40
assign ( residue  141 and name HE#  ) ( residue 1912 and name HG2# )   5.00  3.20  0.50
```

assign (residue 145 and name HE#) (residue 1912 and name HG2#) 5.00 3.20 0.40
assign (residue 101 and name HA) (residue 135 and name HA) 4.00 2.20 0.00
assign (residue 112 and name HG) (residue 1906 and name HA) 5.00 3.20 0.50
assign (residue 121 and name HA) (residue 125 and name HD#) 5.00 3.20 0.50
assign (residue 146 and name HG##) (residue 1919 and name HA) 5.00 3.20 0.50
assign (residue 105 and name HB#) (residue 108 and name HB) 5.00 3.20 0.50
assign (residue 114 and name HG#) (residue 1913 and name HB#) 4.00 2.20 0.40
assign (residue 91 and name HG##) (residue 1905 and name HB#) 4.00 2.20 0.40
assign (residue 89 and name HD#) (residue 141 and name HE#) 4.00 2.20 0.40
assign (residue 116 and name HD2#) (residue 121 and name HA) 4.00 2.20 0.40
assign (residue 124 and name HE#) (residue 1916 and name HD#) 4.00 2.20 0.40
assign (residue 106 and name HG#) (residue 110 and name HA) 5.00 3.20 0.50
assign (residue 110 and name HA) (residue 115 and name HG#) 6.00 4.20 0.60
assign (residue 146 and name HG##) (residue 1918 and name HG#) 5.00 3.20 0.50
assign (residue 89 and name HE#) (residue 142 and name HG##) 5.00 3.20 0.50
assign (residue 105 and name HD2#) (residue 136 and name HG2#) 4.00 2.20 0.40
assign (residue 86 and name HG2#) (residue 139 and name HB#) 5.00 3.20 0.50
assign (residue 83 and name HG#) (residue 86 and name HG2#) 5.00 2.20 0.50
assign (residue 85 and name HB#) (residue 1911 and name HG##) 4.00 2.20 0.40
assign (residue 86 and name HG2#) (residue 90 and name HD#) 4.00 2.20 0.40

Nitrogen NOE Restraint File

assign (residue 146 and name HN) (residue 1919 and name HD#) 5.00 3.20 0.50
assign (residue 109 and name HN) (residue 1913 and name HE2#) 5.00 3.20 0.50
assign (residue 110 and name HN) (residue 1913 and name HE2#) 5.00 3.20 0.50
assign (residue 113 and name HN) (residue 1913 and name HE2#) 5.00 3.20 0.50
assign (residue 114 and name HN) (residue 1913 and name HE2#) 5.00 3.20 0.50
assign (residue 114 and name HN) (residue 1913 and name HB#) 5.00 3.20 0.50
assign (residue 88 and name HN) (residue 1912 and name HD1#) 5.00 3.20 0.50
assign (residue 89 and name HN) (residue 1912 and name HD1#) 5.00 3.20 0.50
assign (residue 89 and name HN) (residue 1911 and name HG##) 5.00 3.20 0.50
assign (residue 86 and name HG#) (residue 90 and name HN) 5.00 3.20 0.50
assign (residue 88 and name HN) (residue 1911 and name HG##) 5.00 3.20 0.50
assign (residue 91 and name HN) (residue 1908 and name HB#) 5.00 3.20 0.50
assign (residue 146 and name HG##) (residue 148 and name HN) 5.00 3.20 0.50
assign (residue 147 and name HB#) (residue 148 and name HN) 4.00 2.20 0.40
assign (residue 147 and name HA) (residue 148 and name HN) 4.00 3.20 0.30
assign (residue 145 and name HA) (residue 147 and name HN) 5.00 3.20 0.50
assign (residue 145 and name HB#) (residue 147 and name HN) 5.00 3.20 0.50
assign (residue 147 and name HB#) (residue 147 and name HN) 5.00 3.20 0.50
assign (residue 146 and name HA) (residue 147 and name HN) 4.00 2.20 0.40
assign (residue 146 and name HB) (residue 147 and name HN) 4.00 2.20 0.40
assign (residue 146 and name HG##) (residue 147 and name HN) 4.00 2.20 0.40
assign (residue 147 and name HA) (residue 147 and name HN) 3.00 1.20 0.30

assign (residue 147 and name HN) (residue 148 and name HN) 3.00 1.20 0.30
assign (residue 142 and name HA) (residue 146 and name HN) 5.00 3.20 0.50
assign (residue 144 and name HB#) (residue 146 and name HN) 6.00 4.20 0.60
assign (residue 144 and name HG#) (residue 146 and name HN) 6.00 4.20 0.60
assign (residue 145 and name HA) (residue 146 and name HN) 5.00 3.20 0.50
assign (residue 145 and name HG#) (residue 146 and name HN) 5.00 3.20 0.50
assign (residue 146 and name HN) (residue 147 and name HB#) 5.00 3.20 0.50
assign (residue 145 and name HB#) (residue 146 and name HN) 4.00 2.20 0.40
assign (residue 146 and name HB) (residue 146 and name HN) 4.00 2.20 0.40
assign (residue 146 and name HA) (residue 146 and name HN) 3.00 1.20 0.30
assign (residue 146 and name HG##) (residue 146 and name HN) 3.00 1.20 0.30
assign (residue 146 and name HN) (residue 147 and name HN) 3.00 1.20 0.30
assign (residue 146 and name HN) (residue 148 and name HN) 4.00 2.20 0.40
assign (residue 141 and name HD#) (residue 145 and name HN) 5.00 3.20 0.50
assign (residue 142 and name HN) (residue 145 and name HN) 5.00 3.20 0.50
assign (residue 144 and name HG#) (residue 145 and name HN) 5.00 3.20 0.50
assign (residue 145 and name HG#) (residue 145 and name HN) 5.00 3.20 0.50
assign (residue 145 and name HN) (residue 146 and name HG##) 5.00 3.20 0.50
assign (residue 145 and name HN) (residue 147 and name HB#) 5.00 3.20 0.50
assign (residue 142 and name HA) (residue 145 and name HN) 4.00 2.20 0.40
assign (residue 144 and name HB#) (residue 145 and name HN) 4.00 2.20 0.40
assign (residue 145 and name HA) (residue 145 and name HN) 4.00 2.20 0.40
assign (residue 145 and name HB#) (residue 145 and name HN) 4.00 2.20 0.40
assign (residue 145 and name HE#) (residue 145 and name HN) 4.00 2.20 0.40
assign (residue 145 and name HN) (residue 146 and name HN) 3.00 1.20 0.30
assign (residue 142 and name HA) (residue 144 and name HN) 5.00 3.20 0.50
assign (residue 142 and name HG##) (residue 144 and name HN) 5.00 3.20 0.50
assign (residue 142 and name HN) (residue 144 and name HN) 5.00 3.20 0.50
assign (residue 144 and name HG#) (residue 144 and name HN) 4.00 2.20 0.40
assign (residue 144 and name HN) (residue 146 and name HG##) 4.00 2.20 0.40
assign (residue 144 and name HA) (residue 144 and name HN) 3.00 1.20 0.30
assign (residue 144 and name HB#) (residue 144 and name HN) 3.00 1.20 0.30
assign (residue 144 and name HE#) (residue 144 and name HN) 4.00 2.20 0.40
assign (residue 144 and name HN) (residue 145 and name HN) 3.00 1.20 0.30
assign (residue 142 and name HA) (residue 143 and name HN) 5.00 3.20 0.50
assign (residue 143 and name HA) (residue 143 and name HN) 5.00 3.20 0.50
assign (residue 143 and name HD#) (residue 143 and name HN) 5.00 3.20 0.50
assign (residue 143 and name HG#) (residue 143 and name HN) 5.00 3.20 0.50
assign (residue 143 and name HN) (residue 146 and name HG##) 5.00 3.20 0.50
assign (residue 142 and name HB) (residue 143 and name HN) 4.00 2.20 0.40
assign (residue 142 and name HG##) (residue 143 and name HN) 4.00 2.20 0.40
assign (residue 143 and name HN) (residue 145 and name HN) 4.00 2.20 0.40
assign (residue 143 and name HN) (residue 147 and name HB#) 5.00 3.20 0.50
assign (residue 143 and name HB#) (residue 143 and name HN) 3.00 1.20 0.30
assign (residue 138 and name HA) (residue 142 and name HN) 5.00 3.20 0.50
assign (residue 138 and name HD#) (residue 142 and name HN) 6.00 4.20 0.60

assign (residue 141 and name HA) (residue 142 and name HN) 5.00 3.20 0.50
assign (residue 141 and name HD#) (residue 142 and name HN) 5.00 3.20 0.50
assign (residue 141 and name HE#) (residue 142 and name HN) 5.00 3.20 0.50
assign (residue 89 and name HD#) (residue 142 and name HN) 5.00 3.20 0.50
assign (residue 89 and name HE#) (residue 142 and name HN) 5.00 3.20 0.50
assign (residue 139 and name HA) (residue 142 and name HN) 4.00 2.20 0.40
assign (residue 141 and name HB#) (residue 142 and name HN) 4.00 2.20 0.40
assign (residue 142 and name HG##) (residue 142 and name HN) 4.00 2.20 0.40
assign (residue 142 and name HA) (residue 142 and name HN) 3.00 1.20 0.30
assign (residue 142 and name HB) (residue 142 and name HN) 3.00 1.20 0.30
assign (residue 142 and name HN) (residue 143 and name HN) 3.00 1.20 0.30
assign (residue 136 and name HG2#) (residue 140 and name HN) 5.00 3.20 0.50
assign (residue 137 and name HA) (residue 140 and name HN) 5.00 3.20 0.50
assign (residue 137 and name HB#) (residue 140 and name HN) 5.00 3.20 0.50
assign (residue 137 and name HN) (residue 140 and name HN) 5.00 3.20 0.50
assign (residue 138 and name HD#) (residue 140 and name HN) 5.00 3.20 0.50
assign (residue 139 and name HA) (residue 140 and name HN) 5.00 3.20 0.50
assign (residue 140 and name HN) (residue 142 and name HN) 5.00 3.20 0.50
assign (residue 139 and name HG#) (residue 140 and name HN) 4.00 2.20 0.40
assign (residue 140 and name HN) (residue 143 and name HN) 4.00 2.20 0.40
assign (residue 139 and name HB#) (residue 140 and name HN) 5.00 3.20 0.50
assign (residue 136 and name HG2#) (residue 139 and name HN) 6.00 4.20 0.60
assign (residue 137 and name HA) (residue 139 and name HN) 5.00 3.20 0.50
assign (residue 137 and name HB#) (residue 139 and name HN) 5.00 3.20 0.50
assign (residue 139 and name HN) (residue 142 and name HG##) 6.00 4.20 0.60
assign (residue 139 and name HN) (residue 143 and name HN) 5.00 3.20 0.50
assign (residue 99 and name HD##) (residue 139 and name HN) 5.00 3.20 0.50
assign (residue 138 and name HA) (residue 139 and name HN) 4.00 2.20 0.40
assign (residue 138 and name HD#) (residue 139 and name HN) 4.00 2.20 0.40
assign (residue 139 and name HA) (residue 139 and name HN) 4.00 2.20 0.40
assign (residue 139 and name HG#) (residue 139 and name HN) 4.00 2.20 0.40
assign (residue 139 and name HB#) (residue 139 and name HN) 3.00 1.20 0.30
assign (residue 139 and name HN) (residue 140 and name HN) 3.00 1.20 0.30
assign (residue 100 and name HB) (residue 138 and name HN) 5.00 3.20 0.50
assign (residue 99 and name HG) (residue 138 and name HN) 5.00 3.20 0.50
assign (residue 89 and name HB#) (residue 138 and name HN) 5.00 3.20 0.50
assign (residue 100 and name HG2#) (residue 138 and name HN) 5.00 3.20 0.50
assign (residue 100 and name HN) (residue 138 and name HN) 5.00 3.20 0.50
assign (residue 136 and name HG2#) (residue 138 and name HN) 5.00 3.20 0.50
assign (residue 137 and name HB#) (residue 138 and name HN) 5.00 3.20 0.50
assign (residue 138 and name HB#) (residue 138 and name HN) 5.00 3.20 0.50
assign (residue 138 and name HN) (residue 140 and name HN) 5.00 3.20 0.50
assign (residue 99 and name HA) (residue 138 and name HN) 5.00 3.20 0.50
assign (residue 99 and name HD##) (residue 138 and name HN) 5.00 3.20 0.50
assign (residue 138 and name HA) (residue 138 and name HN) 4.00 2.20 0.40
assign (residue 138 and name HN) (residue 139 and name HN) 4.00 2.20 0.40

assign (residue 137 and name HA) (residue 138 and name HN) 3.00 1.20 0.30
assign (residue 138 and name HD#) (residue 138 and name HN) 3.00 1.20 0.30
assign (residue 100 and name HG2#) (residue 137 and name HN) 5.00 3.20 0.50
assign (residue 136 and name HB) (residue 137 and name HN) 5.00 3.20 0.50
assign (residue 136 and name HG1#) (residue 137 and name HN) 5.00 3.20 0.50
assign (residue 137 and name HN) (residue 138 and name HN) 5.00 3.20 0.50
assign (residue 99 and name HD##) (residue 137 and name HN) 5.00 3.20 0.50
assign (residue 136 and name HG2#) (residue 137 and name HN) 4.00 2.20 0.40
assign (residue 137 and name HA) (residue 137 and name HN) 4.00 2.20 0.40
assign (residue 137 and name HB#) (residue 137 and name HN) 4.00 2.20 0.40
assign (residue 136 and name HA) (residue 137 and name HN) 3.00 1.20 0.30
assign (residue 100 and name HG2#) (residue 136 and name HN) 5.00 3.20 0.50
assign (residue 100 and name HN) (residue 136 and name HN) 5.00 3.20 0.50
assign (residue 135 and name HB#) (residue 136 and name HN) 5.00 3.20 0.50
assign (residue 136 and name HA) (residue 136 and name HN) 5.00 3.20 0.50
assign (residue 136 and name HD1#) (residue 136 and name HN) 5.00 3.20 0.50
assign (residue 136 and name HG1#) (residue 136 and name HN) 5.00 3.20 0.50
assign (residue 136 and name HG2#) (residue 136 and name HN) 5.00 3.20 0.50
assign (residue 135 and name HA) (residue 136 and name HN) 4.00 2.20 0.40
assign (residue 136 and name HB) (residue 136 and name HN) 4.00 2.20 0.40
assign (residue 130 and name HG2#) (residue 131 and name HN) 5.00 3.20 0.50
assign (residue 131 and name HN) (residue 136 and name HG1#) 5.00 3.20 0.50
assign (residue 100 and name HN) (residue 130 and name HN) 6.00 4.20 0.60
assign (residue 129 and name HB#) (residue 130 and name HN) 5.00 3.20 0.50
assign (residue 130 and name HA) (residue 130 and name HN) 5.00 3.20 0.50
assign (residue 130 and name HB) (residue 130 and name HN) 5.00 3.20 0.50
assign (residue 130 and name HD1#) (residue 130 and name HN) 5.00 3.20 0.50
assign (residue 130 and name HG1#) (residue 130 and name HN) 5.00 3.20 0.50
assign (residue 130 and name HG2#) (residue 130 and name HN) 5.00 3.20 0.50
assign (residue 130 and name HN) (residue 131 and name HN) 5.00 3.20 0.50
assign (residue 129 and name HA) (residue 130 and name HN) 4.00 2.20 0.40
assign (residue 128 and name HB#) (residue 129 and name HN) 5.00 3.20 0.50
assign (residue 129 and name HN) (residue 130 and name HG1#) 5.00 3.20 0.50
assign (residue 129 and name HN) (residue 130 and name HN) 5.00 3.20 0.50
assign (residue 129 and name HN) (residue 141 and name HB#) 5.00 3.20 0.50
assign (residue 129 and name HN) (residue 141 and name HD#) 5.00 3.20 0.50
assign (residue 129 and name HB#) (residue 129 and name HN) 4.00 2.20 0.40
assign (residue 129 and name HN) (residue 130 and name HA) 5.00 3.20 0.40
assign (residue 129 and name HA) (residue 129 and name HN) 3.00 1.20 0.30
assign (residue 127 and name HA) (residue 128 and name HN) 5.00 3.20 0.50
assign (residue 127 and name HN) (residue 128 and name HN) 5.00 3.20 0.50
assign (residue 128 and name HA) (residue 128 and name HN) 5.00 3.20 0.50
assign (residue 128 and name HB#) (residue 128 and name HN) 5.00 3.20 0.50
assign (residue 128 and name HN) (residue 129 and name HN) 5.00 3.20 0.50
assign (residue 124 and name HA) (residue 127 and name HN) 5.00 3.20 0.50
assign (residue 125 and name HG2#) (residue 127 and name HN) 5.00 3.20 0.50

```
assign ( residue  126 and name HA   ) ( residue  127 and name HN   )  5.00  3.20  0.50
assign ( residue  126 and name HG#  ) ( residue  127 and name HN   )  5.00  3.20  0.50
assign ( residue  127 and name HN   ) ( residue  128 and name HA   )  5.00  3.20  0.50
assign ( residue  127 and name HN   ) ( residue  128 and name HB#  )  5.00  3.20  0.50
assign ( residue  127 and name HN   ) ( residue  129 and name HN   )  5.00  3.20  0.50
assign ( residue  127 and name HN   ) ( residue  141 and name HD#  )  5.00  3.20  0.50
assign ( residue  127 and name HA   ) ( residue  127 and name HN   )  4.00  2.20  0.40
assign ( residue  127 and name HB#  ) ( residue  127 and name HN   )  4.00  2.20  0.40
assign ( residue  127 and name HG#  ) ( residue  127 and name HN   )  4.00  2.20  0.40
assign ( residue  124 and name HA   ) ( residue  126 and name HN   )  5.00  3.20  0.50
assign ( residue  125 and name HA   ) ( residue  126 and name HN   )  5.00  3.20  0.50
assign ( residue  125 and name HD1# ) ( residue  126 and name HN   )  5.00  3.20  0.50
assign ( residue  126 and name HD#  ) ( residue  126 and name HN   )  5.00  3.20  0.50
assign ( residue  126 and name HG#  ) ( residue  126 and name HN   )  5.00  3.20  0.50
assign ( residue  126 and name HN   ) ( residue  141 and name HD#  )  6.00  4.20  0.60
assign ( residue  125 and name HG2# ) ( residue  126 and name HN   )  4.00  2.20  0.40
assign ( residue  126 and name HN   ) ( residue  127 and name HA   )  5.00  3.20  0.50
assign ( residue  125 and name HB   ) ( residue  126 and name HN   )  4.00  2.20  0.40
assign ( residue  126 and name HA   ) ( residue  126 and name HN   )  3.00  1.20  0.30
assign ( residue  121 and name HG## ) ( residue  125 and name HN   )  5.00  3.20  0.50
assign ( residue  122 and name HA   ) ( residue  125 and name HN   )  5.00  3.20  0.50
assign ( residue  123 and name HA   ) ( residue  125 and name HN   )  5.00  3.20  0.50
assign ( residue  123 and name HB#  ) ( residue  125 and name HN   )  5.00  3.20  0.50
assign ( residue  123 and name HN   ) ( residue  125 and name HN   )  5.00  3.20  0.50
assign ( residue  124 and name HA   ) ( residue  125 and name HN   )  5.00  3.20  0.50
assign ( residue  124 and name HE#  ) ( residue  125 and name HN   )  5.00  3.20  0.50
assign ( residue  124 and name HG#  ) ( residue  125 and name HN   )  5.00  3.20  0.50
assign ( residue  125 and name HA   ) ( residue  125 and name HN   )  5.00  3.20  0.50
assign ( residue  125 and name HD1# ) ( residue  125 and name HN   )  5.00  3.20  0.50
assign ( residue  125 and name HG2# ) ( residue  125 and name HN   )  5.00  3.20  0.50
assign ( residue  125 and name HN   ) ( residue  126 and name HN   )  4.00  2.20  0.40
assign ( residue  125 and name HB   ) ( residue  125 and name HN   )  4.00  2.20  0.40
assign ( residue  125 and name HG1# ) ( residue  125 and name HN   )  3.00  1.20  0.30
assign ( residue  121 and name HG## ) ( residue  124 and name HN   )  5.00  3.20  0.50
assign ( residue  121 and name HN   ) ( residue  124 and name HN   )  5.00  3.20  0.50
assign ( residue  122 and name HA   ) ( residue  124 and name HN   )  5.00  3.20  0.50
assign ( residue  122 and name HN   ) ( residue  124 and name HN   )  5.00  3.20  0.50
assign ( residue  123 and name HA   ) ( residue  124 and name HN   )  5.00  3.20  0.50
assign ( residue  123 and name HB#  ) ( residue  124 and name HN   )  5.00  3.20  0.50
assign ( residue  124 and name HE#  ) ( residue  124 and name HN   )  5.00  3.20  0.50
assign ( residue  124 and name HN   ) ( residue  125 and name HD1# )  5.00  3.20  0.50
assign ( residue  124 and name HN   ) ( residue  125 and name HG1# )  5.00  3.20  0.50
assign ( residue  124 and name HN   ) ( residue  125 and name HG2# )  5.00  3.20  0.50
assign ( residue  124 and name HN   ) ( residue  126 and name HN   )  5.00  3.20  0.50
assign ( residue  124 and name HA   ) ( residue  124 and name HN   )  4.00  2.20  0.40
assign ( residue  124 and name HB#  ) ( residue  124 and name HN   )  4.00  2.20  0.40
```

```
assign ( residue  124 and name HG#  ) ( residue  124 and name HN   )  4.00  2.20  0.40
assign ( residue  124 and name HN   ) ( residue  125 and name HN   )  4.00  2.20  0.40
assign ( residue  121 and name HA   ) ( residue  123 and name HN   )  5.00  3.20  0.50
assign ( residue  121 and name HG## ) ( residue  123 and name HN   )  5.00  3.20  0.50
assign ( residue  123 and name HB#  ) ( residue  123 and name HN   )  5.00  3.20  0.50
assign ( residue  123 and name HN   ) ( residue  125 and name HD1# )  5.00  3.20  0.50
assign ( residue  123 and name HN   ) ( residue  125 and name HG1# )  5.00  3.20  0.50
assign ( residue  123 and name HN   ) ( residue  125 and name HG2# )  5.00  3.20  0.50
assign ( residue  123 and name HN   ) ( residue  126 and name HN   )  5.00  3.20  0.50
assign ( residue  122 and name HA   ) ( residue  123 and name HN   )  4.00  2.20  0.40
assign ( residue  122 and name HB#  ) ( residue  123 and name HN   )  4.00  2.20  0.40
assign ( residue  123 and name HA   ) ( residue  123 and name HN   )  3.00  1.20  0.30
assign ( residue  123 and name HN   ) ( residue  124 and name HN   )  3.00  1.20  0.30
assign ( residue  121 and name HA   ) ( residue  122 and name HN   )  5.00  3.20  0.50
assign ( residue  122 and name HN   ) ( residue  123 and name HA   )  5.00  3.20  0.50
assign ( residue  122 and name HN   ) ( residue  123 and name HB#  )  5.00  3.20  0.50
assign ( residue  122 and name HN   ) ( residue  125 and name HD1# )  5.00  3.20  0.50
assign ( residue  122 and name HN   ) ( residue  125 and name HG1# )  5.00  3.20  0.50
assign ( residue  122 and name HN   ) ( residue  125 and name HG2# )  5.00  3.20  0.50
assign ( residue  122 and name HN   ) ( residue  126 and name HN   )  6.00  4.20  0.60
assign ( residue  121 and name HB   ) ( residue  122 and name HN   )  4.00  2.20  0.40
assign ( residue  121 and name HG## ) ( residue  122 and name HN   )  3.00  1.20  0.30
assign ( residue  122 and name HA   ) ( residue  122 and name HN   )  3.00  1.20  0.30
assign ( residue  122 and name HB#  ) ( residue  122 and name HN   )  3.00  1.20  0.30
assign ( residue  122 and name HN   ) ( residue  123 and name HN   )  3.00  1.20  0.30
assign ( residue  117 and name HA   ) ( residue  121 and name HN   )  5.00  3.20  0.50
assign ( residue  120 and name HA   ) ( residue  121 and name HN   )  5.00  3.20  0.50
assign ( residue  121 and name HN   ) ( residue  122 and name HB#  )  5.00  3.20  0.50
assign ( residue  121 and name HN   ) ( residue  123 and name HN   )  5.00  3.20  0.50
assign ( residue  121 and name HN   ) ( residue  125 and name HD1# )  5.00  3.20  0.50
assign ( residue  121 and name HN   ) ( residue  125 and name HG2# )  5.00  3.20  0.50
assign ( residue  121 and name HA   ) ( residue  121 and name HN   )  4.00  2.20  0.40
assign ( residue  121 and name HG## ) ( residue  121 and name HN   )  4.00  2.20  0.40
assign ( residue  121 and name HN   ) ( residue  122 and name HN   )  4.00  2.20  0.40
assign ( residue  121 and name HB   ) ( residue  121 and name HN   )  3.00  1.20  0.30
assign ( residue  120 and name HN   ) ( residue  121 and name HG## )  5.00  3.20  0.50
assign ( residue  120 and name HN   ) ( residue  123 and name HN   )  5.00  3.20  0.50
assign ( residue  117 and name HB   ) ( residue  120 and name HN   )  4.00  2.20  0.40
assign ( residue  117 and name HG2# ) ( residue  120 and name HN   )  4.00  2.20  0.40
assign ( residue  119 and name HA   ) ( residue  120 and name HN   )  4.00  2.20  0.40
assign ( residue  120 and name HA   ) ( residue  120 and name HN   )  4.00  2.20  0.40
assign ( residue  120 and name HB#  ) ( residue  120 and name HN   )  4.00  2.20  0.40
assign ( residue  120 and name HN   ) ( residue  121 and name HN   )  3.00  1.20  0.30
assign ( residue  117 and name HG2# ) ( residue  119 and name HN   )  5.00  3.20  0.50
assign ( residue  119 and name HN   ) ( residue  121 and name HB   )  6.00  4.20  0.60
assign ( residue  119 and name HN   ) ( residue  121 and name HG## )  5.00  3.20  0.50
```

```
assign ( residue  119 and name HN   ) ( residue  122 and name HB# )   5.00  3.20  0.50
assign ( residue  117 and name HB   ) ( residue  119 and name HN   )   3.00  1.20  0.30
assign ( residue  119 and name HA   ) ( residue  119 and name HN   )   3.00  1.20  0.30
assign ( residue  119 and name HB# ) ( residue  119 and name HN   )   3.00  1.20  0.30
assign ( residue  119 and name HN   ) ( residue  120 and name HN   )   3.00  1.20  0.30
assign ( residue  119 and name HN   ) ( residue  121 and name HN   )   4.00  2.20  0.40
assign ( residue  117 and name HN   ) ( residue  118 and name HN   )   5.00  3.20  0.50
assign ( residue  118 and name HN   ) ( residue  120 and name HN   )   5.00  3.20  0.50
assign ( residue  117 and name HG2# ) ( residue  118 and name HN   )   4.00  2.20  0.40
assign ( residue  118 and name HB# ) ( residue  118 and name HN   )   4.00  2.20  0.40
assign ( residue  118 and name HN   ) ( residue  119 and name HN   )   4.00  2.20  0.40
assign ( residue  117 and name HA   ) ( residue  118 and name HN   )   3.00  1.20  0.30
assign ( residue  117 and name HB   ) ( residue  118 and name HN   )   3.00  1.20  0.30
assign ( residue  118 and name HA   ) ( residue  118 and name HN   )   3.00  1.20  0.30
assign ( residue  116 and name HD1# ) ( residue  117 and name HN   )   5.00  3.20  0.50
assign ( residue  116 and name HD2# ) ( residue  117 and name HN   )   5.00  3.20  0.50
assign ( residue  117 and name HA   ) ( residue  117 and name HN   )   5.00  3.20  0.50
assign ( residue  117 and name HB   ) ( residue  117 and name HN   )   5.00  3.20  0.50
assign ( residue  117 and name HN   ) ( residue  119 and name HN   )   5.00  3.20  0.50
assign ( residue  117 and name HN   ) ( residue  120 and name HN   )   5.00  3.20  0.50
assign ( residue  117 and name HN   ) ( residue  121 and name HN   )   5.00  3.20  0.50
assign ( residue  117 and name HN   ) ( residue  120 and name HB# )   4.00  2.20  0.40
assign ( residue  116 and name HA   ) ( residue  117 and name HN   )   3.00  1.20  0.30
assign ( residue  117 and name HG2# ) ( residue  117 and name HN   )   3.00  1.20  0.30
assign ( residue  111 and name HN   ) ( residue  116 and name HN   )   5.00  3.20  0.50
assign ( residue  114 and name HN   ) ( residue  116 and name HN   )   5.00  3.20  0.50
assign ( residue  116 and name HN   ) ( residue  117 and name HN   )   5.00  3.20  0.50
assign ( residue  116 and name HA   ) ( residue  116 and name HN   )   4.00  2.20  0.40
assign ( residue  116 and name HB# ) ( residue  116 and name HN   )   4.00  2.20  0.40
assign ( residue  116 and name HD1# ) ( residue  116 and name HN   )   4.00  2.20  0.40
assign ( residue  116 and name HD2# ) ( residue  116 and name HN   )   4.00  2.20  0.40
assign ( residue  116 and name HG   ) ( residue  116 and name HN   )   4.00  2.20  0.40
assign ( residue  115 and name HA   ) ( residue  116 and name HN   )   3.00  1.20  0.30
assign ( residue  113 and name HN   ) ( residue  115 and name HN   )   5.00  3.20  0.50
assign ( residue  115 and name HE# ) ( residue  115 and name HN   )   5.00  3.20  0.50
assign ( residue  115 and name HN   ) ( residue  116 and name HN   )   5.00  3.20  0.50
assign ( residue  114 and name HB# ) ( residue  115 and name HN   )   4.00  2.20  0.40
assign ( residue  115 and name HD# ) ( residue  115 and name HN   )   4.00  2.20  0.40
assign ( residue  114 and name HA   ) ( residue  115 and name HN   )   3.00  1.20  0.30
assign ( residue  115 and name HA   ) ( residue  115 and name HN   )   3.00  1.20  0.30
assign ( residue  115 and name HB# ) ( residue  115 and name HN   )   3.00  1.20  0.30
assign ( residue  115 and name HG# ) ( residue  115 and name HN   )   3.00  1.20  0.30
assign ( residue  114 and name HB# ) ( residue  114 and name HN   )   5.00  3.20  0.50
assign ( residue  114 and name HN   ) ( residue  115 and name HN   )   5.00  3.20  0.50
assign ( residue  113 and name HA# ) ( residue  114 and name HN   )   4.00  2.20  0.40
assign ( residue  114 and name HA   ) ( residue  114 and name HN   )   4.00  2.20  0.40
```

```
assign ( residue  114 and name HG#  ) ( residue  114 and name HN   )  4.00  2.20  0.40
assign ( residue  112 and name HD#  ) ( residue  114 and name HN   )  4.00  2.20  0.40
assign ( residue  112 and name HG   ) ( residue  113 and name HN   )  5.00  3.20  0.50
assign ( residue  113 and name HN   ) ( residue  114 and name HN   )  5.00  3.20  0.50
assign ( residue  112 and name HB#  ) ( residue  113 and name HN   )  4.00  2.20  0.40
assign ( residue  113 and name HA#  ) ( residue  113 and name HN   )  4.00  2.20  0.40
assign ( residue  112 and name HA   ) ( residue  113 and name HN   )  3.00  1.20  0.30
assign ( residue  112 and name HD#  ) ( residue  113 and name HN   )  3.00  1.20  0.30
assign ( residue  110 and name HA   ) ( residue  112 and name HN   )  5.00  3.20  0.50
assign ( residue  110 and name HB   ) ( residue  112 and name HN   )  5.00  3.20  0.50
assign ( residue  112 and name HN   ) ( residue  113 and name HA#  )  5.00  3.20  0.50
assign ( residue  112 and name HN   ) ( residue  113 and name HN   )  5.00  3.20  0.50
assign ( residue  111 and name HB#  ) ( residue  112 and name HN   )  4.00  2.20  0.40
assign ( residue  112 and name HA   ) ( residue  112 and name HN   )  4.00  2.20  0.40
assign ( residue  112 and name HB#  ) ( residue  112 and name HN   )  4.00  2.20  0.40
assign ( residue  112 and name HD#  ) ( residue  112 and name HN   )  3.00  1.20  0.30
assign ( residue  112 and name HG   ) ( residue  112 and name HN   )  3.00  1.20  0.30
assign ( residue  109 and name HN   ) ( residue  111 and name HN   )  5.00  3.20  0.50
assign ( residue  111 and name HN   ) ( residue  112 and name HD#  )  5.00  3.20  0.50
assign ( residue  111 and name HA   ) ( residue  111 and name HN   )  4.00  2.20  0.40
assign ( residue  111 and name HB#  ) ( residue  111 and name HN   )  4.00  2.20  0.40
assign ( residue  111 and name HN   ) ( residue  112 and name HN   )  3.00  1.20  0.30
assign ( residue  109 and name HG#  ) ( residue  110 and name HN   )  5.00  3.20  0.50
assign ( residue  110 and name HN   ) ( residue  112 and name HG   )  5.00  3.20  0.50
assign ( residue  110 and name HN   ) ( residue  116 and name HN   )  5.00  3.20  0.50
assign ( residue  110 and name HN   ) ( residue  121 and name HG## )  5.00  3.20  0.50
assign ( residue  110 and name HA   ) ( residue  110 and name HN   )  4.00  2.20  0.40
assign ( residue  110 and name HB   ) ( residue  110 and name HN   )  4.00  2.20  0.40
assign ( residue  110 and name HG2# ) ( residue  110 and name HN   )  3.00  1.20  0.30
assign ( residue  105 and name HA   ) ( residue  109 and name HN   )  5.00  3.20  0.50
assign ( residue  106 and name HA   ) ( residue  109 and name HN   )  5.00  3.20  0.50
assign ( residue  107 and name HN   ) ( residue  109 and name HN   )  5.00  3.20  0.50
assign ( residue  108 and name HA   ) ( residue  109 and name HN   )  4.00  2.20  0.40
assign ( residue  108 and name HG## ) ( residue  109 and name HN   )  5.00  3.20  0.50
assign ( residue  109 and name HN   ) ( residue  112 and name HN   )  5.00  3.20  0.50
assign ( residue  109 and name HA   ) ( residue  109 and name HN   )  4.00  2.20  0.40
assign ( residue  109 and name HB#  ) ( residue  109 and name HN   )  4.00  2.20  0.40
assign ( residue  109 and name HE#  ) ( residue  109 and name HN   )  4.00  2.20  0.40
assign ( residue  109 and name HG#  ) ( residue  109 and name HN   )  4.00  2.20  0.40
assign ( residue  109 and name HN   ) ( residue  110 and name HN   )  4.00  2.20  0.40
assign ( residue  105 and name HA   ) ( residue  108 and name HN   )  5.00  3.20  0.50
assign ( residue  107 and name HA   ) ( residue  108 and name HN   )  5.00  3.20  0.50
assign ( residue  107 and name HB#  ) ( residue  108 and name HN   )  5.00  3.20  0.50
assign ( residue  107 and name HD#  ) ( residue  108 and name HN   )  5.00  3.20  0.50
assign ( residue  108 and name HN   ) ( residue  112 and name HD#  )  5.00  3.20  0.50
assign ( residue  108 and name HA   ) ( residue  108 and name HN   )  4.00  2.20  0.40
```

assign (residue 108 and name HB) (residue 108 and name HN) 4.00 2.20 0.40
assign (residue 108 and name HG##) (residue 108 and name HN) 4.00 2.20 0.40
assign (residue 108 and name HN) (residue 109 and name HN) 4.00 2.20 0.40
assign (residue 104 and name HB#) (residue 107 and name HN) 5.00 3.20 0.50
assign (residue 104 and name HG#) (residue 107 and name HN) 5.00 3.20 0.50
assign (residue 105 and name HA) (residue 107 and name HN) 5.00 3.20 0.50
assign (residue 106 and name HG#) (residue 107 and name HN) 5.00 3.20 0.50
assign (residue 107 and name HN) (residue 108 and name HG##) 5.00 3.20 0.50
assign (residue 107 and name HA) (residue 107 and name HN) 4.00 2.20 0.40
assign (residue 107 and name HN) (residue 108 and name HN) 4.00 2.20 0.40
assign (residue 106 and name HB#) (residue 107 and name HN) 3.00 1.20 0.30
assign (residue 107 and name HB#) (residue 107 and name HN) 3.00 1.20 0.30
assign (residue 103 and name HA) (residue 106 and name HN) 5.00 3.20 0.50
assign (residue 105 and name HA) (residue 106 and name HN) 5.00 3.20 0.50
assign (residue 106 and name HD#) (residue 106 and name HN) 5.00 3.20 0.50
assign (residue 106 and name HG#) (residue 106 and name HN) 5.00 3.20 0.50
assign (residue 106 and name HN) (residue 107 and name HB#) 5.00 3.20 0.50
assign (residue 106 and name HN) (residue 125 and name HD1#) 5.00 3.20 0.50
assign (residue 105 and name HB#) (residue 106 and name HN) 4.00 2.20 0.40
assign (residue 106 and name HA) (residue 106 and name HN) 4.00 2.20 0.40
assign (residue 106 and name HN) (residue 107 and name HN) 4.00 2.20 0.40
assign (residue 106 and name HB#) (residue 106 and name HN) 3.00 1.20 0.30
assign (residue 104 and name HG#) (residue 105 and name HN) 5.00 3.20 0.50
assign (residue 105 and name HD1#) (residue 105 and name HN) 5.00 3.20 0.50
assign (residue 105 and name HD2#) (residue 105 and name HN) 4.00 2.20 0.40
assign (residue 104 and name HB#) (residue 105 and name HN) 3.00 1.20 0.30
assign (residue 105 and name HA) (residue 105 and name HN) 3.00 1.20 0.30
assign (residue 105 and name HB#) (residue 105 and name HN) 3.00 1.20 0.30
assign (residue 105 and name HG) (residue 105 and name HN) 5.00 3.20 0.50
assign (residue 101 and name HA) (residue 104 and name HN) 5.00 3.20 0.50
assign (residue 104 and name HN) (residue 105 and name HA) 5.00 3.20 0.50
assign (residue 103 and name HA) (residue 104 and name HN) 4.00 2.20 0.40
assign (residue 104 and name HA) (residue 104 and name HN) 4.00 2.20 0.40
assign (residue 104 and name HG#) (residue 104 and name HN) 4.00 2.20 0.40
assign (residue 103 and name HB#) (residue 104 and name HN) 3.00 1.20 0.30
assign (residue 104 and name HB#) (residue 104 and name HN) 3.00 1.20 0.30
assign (residue 104 and name HN) (residue 105 and name HN) 3.00 1.20 0.30
assign (residue 103 and name HN) (residue 104 and name HG#) 5.00 3.20 0.50
assign (residue 101 and name HB#) (residue 103 and name HN) 4.00 2.20 0.40
assign (residue 102 and name HA) (residue 103 and name HN) 4.00 2.20 0.40
assign (residue 101 and name HA) (residue 103 and name HN) 4.00 2.20 0.40
assign (residue 103 and name HA) (residue 103 and name HN) 3.00 1.20 0.30
assign (residue 103 and name HB#) (residue 103 and name HN) 3.00 1.20 0.30
assign (residue 103 and name HN) (residue 104 and name HN) 3.00 1.20 0.30
assign (residue 101 and name HB#) (residue 102 and name HN) 5.00 3.20 0.50
assign (residue 102 and name HN) (residue 103 and name HA) 5.00 3.20 0.50

```
assign ( residue  102 and name HN   ) ( residue  104 and name HN   )  5.00  3.20  0.50
assign ( residue  102 and name HN   ) ( residue  125 and name HG2# )  5.00  3.20  0.50
assign ( residue  102 and name HN   ) ( residue  135 and name HA   )  5.00  3.20  0.50
assign ( residue  102 and name HN   ) ( residue  136 and name HD1# )  5.00  3.20  0.50
assign ( residue  102 and name HA   ) ( residue  102 and name HN   )  4.00  2.20  0.40
assign ( residue  102 and name HN   ) ( residue  103 and name HN   )  4.00  2.20  0.40
assign ( residue  102 and name HN   ) ( residue  136 and name HG1# )  3.00  1.20  0.30
assign ( residue  100 and name HD1# ) ( residue  101 and name HN   )  5.00  3.20  0.50
assign ( residue  100 and name HG1# ) ( residue  101 and name HN   )  5.00  3.20  0.50
assign ( residue  100 and name HG2# ) ( residue  101 and name HN   )  5.00  3.20  0.50
assign ( residue  101 and name HB#  ) ( residue  101 and name HN   )  5.00  3.20  0.50
assign ( residue  101 and name HN   ) ( residue  102 and name HN   )  5.00  3.20  0.50
assign ( residue  101 and name HN   ) ( residue  104 and name HB#  )  5.00  3.20  0.50
assign ( residue  101 and name HN   ) ( residue  104 and name HG#  )  5.00  3.20  0.50
assign ( residue  101 and name HN   ) ( residue  104 and name HN   )  5.00  3.20  0.50
assign ( residue  100 and name HB   ) ( residue  101 and name HN   )  4.00  2.20  0.40
assign ( residue  101 and name HA   ) ( residue  101 and name HN   )  3.00  1.20  0.30
assign ( residue  100 and name HD1# ) ( residue  100 and name HN   )  5.00  3.20  0.50
assign ( residue  100 and name HG1# ) ( residue  100 and name HN   )  5.00  3.20  0.50
assign ( residue  100 and name HN   ) ( residue  101 and name HN   )  5.00  3.20  0.50
assign ( residue  100 and name HN   ) ( residue  136 and name HG2# )  5.00  3.20  0.50
assign ( residue  100 and name HN   ) ( residue  138 and name HD#  )  5.00  3.20  0.50
assign ( residue   99 and name HD## ) ( residue  100 and name HN   )  5.00  3.20  0.50
assign ( residue   99 and name HN   ) ( residue  100 and name HN   )  5.00  3.20  0.50
assign ( residue  100 and name HA   ) ( residue  100 and name HN   )  4.00  2.20  0.40
assign ( residue  100 and name HB   ) ( residue  100 and name HN   )  4.00  2.20  0.40
assign ( residue  100 and name HG2# ) ( residue  100 and name HN   )  4.00  2.20  0.40
assign ( residue   99 and name HN   ) ( residue  137 and name HA   )  5.00  3.20  0.50
assign ( residue   98 and name HA#  ) ( residue   99 and name HN   )  5.00  3.20  0.50
assign ( residue   99 and name HA   ) ( residue   99 and name HN   )  4.00  2.20  0.40
assign ( residue   99 and name HB#  ) ( residue   99 and name HN   )  4.00  2.20  0.40
assign ( residue   99 and name HD## ) ( residue   99 and name HN   )  4.00  2.20  0.40
assign ( residue   99 and name HG   ) ( residue   99 and name HN   )  4.00  2.20  0.40
assign ( residue   98 and name HN   ) ( residue  138 and name HE#  )  5.00  3.20  0.50
assign ( residue   96 and name HA#  ) ( residue   98 and name HN   )  5.00  3.20  0.50
assign ( residue   97 and name HA   ) ( residue   98 and name HN   )  5.00  3.20  0.50
assign ( residue   97 and name HB#  ) ( residue   98 and name HN   )  5.00  3.20  0.50
assign ( residue   98 and name HN   ) ( residue   99 and name HA   )  5.00  3.20  0.50
assign ( residue   98 and name HN   ) ( residue   99 and name HB#  )  5.00  3.20  0.50
assign ( residue   98 and name HN   ) ( residue   99 and name HD## )  5.00  3.20  0.50
assign ( residue   98 and name HA#  ) ( residue   98 and name HN   )  4.00  2.20  0.40
assign ( residue   98 and name HN   ) ( residue   99 and name HN   )  3.00  1.20  0.30
assign ( residue   97 and name HN   ) ( residue   98 and name HA#  )  5.00  3.20  0.50
assign ( residue   97 and name HN   ) ( residue   99 and name HN   )  5.00  3.20  0.50
assign ( residue   96 and name HA#  ) ( residue   97 and name HN   )  4.00  2.20  0.40
assign ( residue   97 and name HA   ) ( residue   97 and name HN   )  4.00  2.20  0.40
```

```
assign ( residue   97 and name HB#  ) ( residue   97 and name HN   )   4.00  2.20  0.40
assign ( residue   97 and name HN   ) ( residue   98 and name HN   )   3.00  1.20  0.30
assign ( residue   93 and name HA   ) ( residue   96 and name HN   )   5.00  3.20  0.50
assign ( residue   93 and name HB#  ) ( residue   96 and name HN   )   5.00  3.20  0.50
assign ( residue   94 and name HB#  ) ( residue   96 and name HN   )   5.00  3.20  0.50
assign ( residue   94 and name HG#  ) ( residue   96 and name HN   )   5.00  3.20  0.50
assign ( residue   96 and name HN   ) ( residue   97 and name HB#  )   5.00  3.20  0.50
assign ( residue   96 and name HN   ) ( residue   98 and name HA#  )   5.00  3.20  0.50
assign ( residue   96 and name HN   ) ( residue   98 and name HN   )   5.00  3.20  0.50
assign ( residue   95 and name HA   ) ( residue   96 and name HN   )   4.00  2.20  0.40
assign ( residue   96 and name HA#  ) ( residue   96 and name HN   )   3.00  1.20  0.30
assign ( residue   96 and name HN   ) ( residue   97 and name HN   )   3.00  1.20  0.30
assign ( residue   93 and name HA   ) ( residue   95 and name HN   )   5.00  3.20  0.50
assign ( residue   94 and name HA   ) ( residue   95 and name HN   )   5.00  3.20  0.50
assign ( residue   94 and name HG#  ) ( residue   95 and name HN   )   5.00  3.20  0.50
assign ( residue   95 and name HN   ) ( residue   96 and name HA#  )   5.00  3.20  0.50
assign ( residue   95 and name HN   ) ( residue   98 and name HA#  )   5.00  3.20  0.50
assign ( residue   95 and name HN   ) ( residue   98 and name HN   )   5.00  3.20  0.50
assign ( residue   94 and name HB#  ) ( residue   95 and name HN   )   4.00  2.20  0.40
assign ( residue   95 and name HA   ) ( residue   95 and name HN   )   3.00  1.20  0.30
assign ( residue   95 and name HB#  ) ( residue   95 and name HN   )   3.00  1.20  0.30
assign ( residue   95 and name HN   ) ( residue   96 and name HN   )   3.00  1.20  0.30
assign ( residue   95 and name HN   ) ( residue   99 and name HA   )   5.00  3.20  0.50
assign ( residue   93 and name HB#  ) ( residue   94 and name HN   )   5.00  3.20  0.50
assign ( residue   94 and name HD#  ) ( residue   94 and name HN   )   5.00  3.20  0.50
assign ( residue   94 and name HN   ) ( residue   95 and name HA   )   5.00  3.20  0.50
assign ( residue   94 and name HN   ) ( residue   95 and name HB#  )   5.00  3.20  0.50
assign ( residue   94 and name HN   ) ( residue   98 and name HA#  )   5.00  3.20  0.50
assign ( residue   93 and name HA   ) ( residue   94 and name HN   )   3.00  1.20  0.30
assign ( residue   94 and name HA   ) ( residue   94 and name HN   )   3.00  1.20  0.30
assign ( residue   94 and name HB#  ) ( residue   94 and name HN   )   3.00  1.20  0.30
assign ( residue   94 and name HG#  ) ( residue   94 and name HN   )   3.00  1.20  0.30
assign ( residue   94 and name HN   ) ( residue   95 and name HN   )   3.00  1.20  0.30
assign ( residue   91 and name HB   ) ( residue   93 and name HN   )   5.00  3.20  0.50
assign ( residue   91 and name HG## ) ( residue   93 and name HN   )   5.00  3.20  0.50
assign ( residue   92 and name HB#  ) ( residue   93 and name HN   )   5.00  3.20  0.50
assign ( residue   92 and name HD#  ) ( residue   93 and name HN   )   5.00  3.20  0.50
assign ( residue   93 and name HN   ) ( residue   94 and name HA   )   5.00  3.20  0.50
assign ( residue   93 and name HN   ) ( residue   94 and name HG#  )   5.00  3.20  0.50
assign ( residue   93 and name HN   ) ( residue   94 and name HN   )   5.00  3.20  0.50
assign ( residue   90 and name HA   ) ( residue   93 and name HN   )   4.00  2.20  0.40
assign ( residue   92 and name HA   ) ( residue   93 and name HN   )   4.00  2.20  0.40
assign ( residue   93 and name HA   ) ( residue   93 and name HN   )   4.00  2.20  0.40
assign ( residue   93 and name HB#  ) ( residue   93 and name HN   )   3.00  1.20  0.30
assign ( residue   92 and name HN   ) ( residue  138 and name HE#  )   5.00  3.20  0.50
assign ( residue   91 and name HB   ) ( residue   92 and name HN   )   5.00  3.20  0.50
```

```
assign ( residue   91 and name HG## ) ( residue   92 and name HN   )   5.00  3.20  0.50
assign ( residue   89 and name HD#  ) ( residue   92 and name HN   )   4.00  2.20  0.40
assign ( residue   92 and name HB#  ) ( residue   92 and name HN   )   4.00  2.20  0.40
assign ( residue   92 and name HA   ) ( residue   92 and name HN   )   3.00  1.20  0.30
assign ( residue   92 and name HD#  ) ( residue   92 and name HN   )   3.00  1.20  0.30
assign ( residue   92 and name HE#  ) ( residue   92 and name HN   )   5.00  3.20  0.50
assign ( residue   92 and name HN   ) ( residue   93 and name HN   )   3.00  1.20  0.30
assign ( residue   88 and name HA   ) ( residue   91 and name HN   )   5.00  3.20  0.50
assign ( residue   90 and name HB#  ) ( residue   91 and name HN   )   4.00  2.20  0.40
assign ( residue   90 and name HG#  ) ( residue   91 and name HN   )   4.00  2.20  0.40
assign ( residue   91 and name HA   ) ( residue   91 and name HN   )   3.00  1.20  0.30
assign ( residue   91 and name HB   ) ( residue   91 and name HN   )   3.00  1.20  0.30
assign ( residue   91 and name HG## ) ( residue   91 and name HN   )   4.00  2.20  0.40
assign ( residue   91 and name HN   ) ( residue   92 and name HN   )   3.00  1.20  0.30
assign ( residue   90 and name HN   ) ( residue  138 and name HE#  )   5.00  3.20  0.50
assign ( residue   88 and name HA   ) ( residue   90 and name HN   )   5.00  3.20  0.50
assign ( residue   88 and name HN   ) ( residue   90 and name HN   )   5.00  3.20  0.50
assign ( residue   89 and name HD#  ) ( residue   90 and name HN   )   5.00  3.20  0.50
assign ( residue   90 and name HE#  ) ( residue   90 and name HN   )   5.00  3.20  0.50
assign ( residue   90 and name HN   ) ( residue   91 and name HA   )   5.00  3.20  0.50
assign ( residue   90 and name HN   ) ( residue   91 and name HG## )   4.00  2.20  0.40
assign ( residue   90 and name HN   ) ( residue   92 and name HN   )   5.00  3.20  0.50
assign ( residue   89 and name HB#  ) ( residue   90 and name HN   )   4.00  2.20  0.40
assign ( residue   90 and name HG#  ) ( residue   90 and name HN   )   4.00  2.20  0.40
assign ( residue   90 and name HN   ) ( residue   91 and name HB   )   5.00  3.20  0.50
assign ( residue   89 and name HA   ) ( residue   90 and name HN   )   4.00  2.20  0.30
assign ( residue   90 and name HA   ) ( residue   90 and name HN   )   3.00  1.20  0.30
assign ( residue   90 and name HB#  ) ( residue   90 and name HN   )   3.00  1.20  0.30
assign ( residue   90 and name HN   ) ( residue   91 and name HN   )   3.00  1.20  0.30
assign ( residue   89 and name HN   ) ( residue  138 and name HD#  )   5.00  3.20  0.50
assign ( residue   86 and name HN   ) ( residue   89 and name HN   )   5.00  3.20  0.50
assign ( residue   89 and name HN   ) ( residue   91 and name HG## )   6.00  4.20  0.60
assign ( residue   89 and name HN   ) ( residue   91 and name HN   )   5.00  3.20  0.50
assign ( residue   89 and name HN   ) ( residue   92 and name HN   )   5.00  3.20  0.50
assign ( residue   88 and name HA   ) ( residue   89 and name HN   )   4.00  2.20  0.40
assign ( residue   88 and name HB#  ) ( residue   89 and name HN   )   3.00  1.20  0.30
assign ( residue   89 and name HA   ) ( residue   89 and name HN   )   3.00  1.20  0.30
assign ( residue   89 and name HB#  ) ( residue   89 and name HN   )   3.00  1.20  0.30
assign ( residue   89 and name HD#  ) ( residue   89 and name HN   )   4.00  2.20  0.40
assign ( residue   89 and name HN   ) ( residue   90 and name HN   )   3.00  1.20  0.30
assign ( residue   85 and name HD## ) ( residue   88 and name HN   )   5.00  3.20  0.50
assign ( residue   87 and name HA   ) ( residue   88 and name HN   )   4.00  2.20  0.40
assign ( residue   88 and name HA   ) ( residue   88 and name HN   )   3.00  1.20  0.30
assign ( residue   88 and name HB#  ) ( residue   88 and name HN   )   3.00  1.20  0.30
assign ( residue   88 and name HN   ) ( residue   89 and name HN   )   3.00  1.20  0.30
assign ( residue   87 and name HN   ) ( residue   88 and name HA   )   5.00  3.20  0.50
```

```
assign ( residue   87 and name HN   ) ( residue   88 and name HB#  )   5.00  3.20  0.50
assign ( residue   85 and name HA   ) ( residue   87 and name HN   )   4.00  2.20  0.40
assign ( residue   86 and name HG2# ) ( residue   87 and name HN   )   4.00  2.20  0.40
assign ( residue   83 and name HB## ) ( residue   87 and name HN   )   5.00  3.20  0.50
assign ( residue   83 and name HG#  ) ( residue   87 and name HN   )   5.00  3.20  0.50
assign ( residue   87 and name HA   ) ( residue   87 and name HN   )   3.00  1.20  0.30
assign ( residue   87 and name HN   ) ( residue   88 and name HN   )   3.00  1.20  0.30
assign ( residue   83 and name HG#  ) ( residue   86 and name HN   )   5.00  3.20  0.50
assign ( residue   85 and name HA   ) ( residue   86 and name HN   )   5.00  3.20  0.50
assign ( residue   85 and name HB#  ) ( residue   86 and name HN   )   5.00  3.20  0.50
assign ( residue   85 and name HG   ) ( residue   86 and name HN   )   5.00  3.20  0.50
assign ( residue   86 and name HD1# ) ( residue   86 and name HN   )   5.00  3.20  0.50
assign ( residue   86 and name HN   ) ( residue   88 and name HN   )   5.00  3.20  0.50
assign ( residue   86 and name HN   ) ( residue   89 and name HD#  )   5.00  3.20  0.50
assign ( residue   86 and name HA   ) ( residue   86 and name HN   )   4.00  2.20  0.40
assign ( residue   86 and name HG1# ) ( residue   86 and name HN   )   4.00  2.20  0.40
assign ( residue   86 and name HG2# ) ( residue   86 and name HN   )   4.00  2.20  0.40
assign ( residue   86 and name HN   ) ( residue   87 and name HN   )   4.00  2.20  0.40
assign ( residue   86 and name HB   ) ( residue   86 and name HN   )   3.00  1.20  0.30
assign ( residue   85 and name HN   ) ( residue  142 and name HG## )   5.00  3.20  0.50
assign ( residue   84 and name HG#  ) ( residue   85 and name HN   )   4.00  2.20  0.40
assign ( residue   85 and name HA   ) ( residue   85 and name HN   )   3.00  1.20  0.30
assign ( residue   85 and name HB#  ) ( residue   85 and name HN   )   3.00  1.20  0.30
assign ( residue   85 and name HD## ) ( residue   85 and name HN   )   5.00  3.20  0.50
assign ( residue   85 and name HG   ) ( residue   85 and name HN   )   4.00  2.20  0.40
assign ( residue   85 and name HN   ) ( residue   86 and name HN   )   3.00  1.20  0.30
assign ( residue   82 and name HA   ) ( residue   84 and name HN   )   5.00  3.20  0.50
assign ( residue   84 and name HN   ) ( residue   85 and name HB#  )   5.00  3.20  0.50
assign ( residue   84 and name HN   ) ( residue   85 and name HD## )   5.00  3.20  0.50
assign ( residue   84 and name HA   ) ( residue   84 and name HN   )   3.00  1.20  0.30
assign ( residue   84 and name HB#  ) ( residue   84 and name HN   )   3.00  1.20  0.30
assign ( residue   84 and name HG#  ) ( residue   84 and name HN   )   3.00  1.20  0.30
assign ( residue   82 and name HA   ) ( residue   83 and name HN   )   5.00  3.20  0.50
assign ( residue   83 and name HG#  ) ( residue   83 and name HN   )   4.00  2.20  0.40
assign ( residue   83 and name HN   ) ( residue   84 and name HN   )   4.00  2.20  0.40
assign ( residue   83 and name HA   ) ( residue   83 and name HN   )   3.00  1.20  0.30
assign ( residue   83 and name HB#  ) ( residue   83 and name HN   )   3.00  1.20  0.30
assign ( residue   82 and name HN   ) ( residue  142 and name HG## )   5.00  3.20  0.50
assign ( residue   80 and name HB#  ) ( residue   82 and name HN   )   5.00  3.20  0.50
assign ( residue   81 and name HB#  ) ( residue   82 and name HN   )   5.00  3.20  0.50
assign ( residue   82 and name HN   ) ( residue  146 and name HB   )   5.00  3.20  0.50
assign ( residue   82 and name HN   ) ( residue   84 and name HN   )   5.00  3.20  0.50
assign ( residue   82 and name HN   ) ( residue   83 and name HN   )   4.00  2.20  0.40
assign ( residue   82 and name HA   ) ( residue   82 and name HN   )   3.00  1.20  0.30
assign ( residue   82 and name HN   ) ( residue   83 and name HB#  )   5.00  3.20  0.50
assign ( residue   81 and name HA   ) ( residue   81 and name HN   )   4.00  2.20  0.40
```

assign (residue 81 and name HN) (residue 82 and name HN) 4.00 2.20 0.40
assign (residue 81 and name HN) (residue 83 and name HB#) 6.00 4.20 0.60
assign (residue 80 and name HB#) (residue 81 and name HN) 3.00 1.20 0.30
assign (residue 81 and name HB#) (residue 81 and name HN) 3.00 1.20 0.30
assign (residue 80 and name HA) (residue 80 and name HN) 4.00 2.20 0.40
assign (residue 79 and name HA) (residue 80 and name HN) 3.00 1.20 0.30
assign (residue 80 and name HB#) (residue 80 and name HN) 3.00 1.20 0.30
assign (residue 79 and name HA) (residue 79 and name HN) 4.00 2.20 0.40
assign (residue 79 and name HB#) (residue 79 and name HN) 4.00 2.20 0.40
assign (residue 79 and name HG#) (residue 79 and name HN) 5.00 3.20 0.40
assign (residue 78 and name HA) (residue 79 and name HN) 3.00 1.20 0.30
assign (residue 77 and name HN) (residue 78 and name HN) 5.00 3.20 0.50
assign (residue 78 and name HA) (residue 78 and name HN) 5.00 3.20 0.50
assign (residue 78 and name HN) (residue 79 and name HG#) 5.00 3.20 0.50
assign (residue 77 and name HN) (residue 78 and name HA) 4.00 2.20 0.40
assign (residue 78 and name HB#) (residue 81 and name HN) 5.00 3.20 0.50
assign (residue 82 and name HA) (residue 85 and name HN) 5.00 3.20 0.50
assign (residue 84 and name HA) (residue 87 and name HN) 4.00 2.20 0.40
assign (residue 146 and name HB) (residue 148 and name HN) 5.00 3.20 0.40
assign (residue 140 and name HN) (residue 142 and name HB) 6.00 4.20 0.60
assign (residue 81 and name HN) (residue 84 and name HN) 5.00 3.20 0.50
assign (residue 81 and name HN) (residue 84 and name HG#) 5.00 3.20 0.50
assign (residue 82 and name HN) (residue 85 and name HN) 5.00 3.20 0.50

Hydrogen Bonding Restraint File

Hydrogen bonding restraint file derived from amide exchange data
assign (residue 114 and name N) (residue 1913 and name OE1) 2.90 0.20 0.40
assign (residue 114 and name HN) (residue 1913 and name OE1) 1.80 0.00 0.60
assign (residue 83 and name HN) (residue 79 and name O) 1.80 0.00 0.60
assign (residue 86 and name HN) (residue 82 and name O) 1.80 0.00 0.60
assign (residue 87 and name HN) (residue 83 and name O) 1.80 0.00 0.60
assign (residue 88 and name HN) (residue 84 and name O) 1.80 0.00 0.60
assign (residue 89 and name HN) (residue 85 and name O) 1.80 0.00 0.60
assign (residue 90 and name HN) (residue 86 and name O) 1.80 0.00 0.60
assign (residue 91 and name HN) (residue 87 and name O) 1.80 0.00 0.60
assign (residue 105 and name HN) (residue 101 and name O) 1.80 0.00 0.60
assign (residue 106 and name HN) (residue 102 and name O) 1.80 0.00 0.60
assign (residue 108 and name HN) (residue 104 and name O) 1.80 0.00 0.60
assign (residue 109 and name HN) (residue 105 and name O) 1.80 0.00 0.60
assign (residue 110 and name HN) (residue 106 and name O) 1.80 0.00 0.60
assign (residue 111 and name HN) (residue 107 and name O) 1.80 0.00 0.60
assign (residue 112 and name HN) (residue 108 and name O) 1.80 0.00 0.60
assign (residue 116 and name HN) (residue 112 and name O) 1.80 0.00 0.60
assign (residue 121 and name HN) (residue 117 and name O) 1.80 0.00 0.60
assign (residue 122 and name HN) (residue 118 and name O) 1.80 0.00 0.60

assign (residue 123 and name HN) (residue 119 and name O) 1.80 0.00 0.60
assign (residue 124 and name HN) (residue 120 and name O) 1.80 0.00 0.60
assign (residue 125 and name HN) (residue 121 and name O) 1.80 0.00 0.60
assign (residue 126 and name HN) (residue 122 and name O) 1.80 0.00 0.60
assign (residue 128 and name HN) (residue 124 and name O) 1.80 0.00 0.60
assign (residue 138 and name HN) (residue 98 and name O) 1.80 0.00 0.60
assign (residue 142 and name HN) (residue 138 and name O) 1.80 0.00 0.60
assign (residue 143 and name HN) (residue 139 and name O) 1.80 0.00 0.60
assign (residue 144 and name HN) (residue 140 and name O) 1.80 0.00 0.60
assign (residue 145 and name HN) (residue 141 and name O) 1.80 0.00 0.60
assign (residue 146 and name HN) (residue 142 and name O) 1.80 0.00 0.60
assign (residue 100 and name HN) (residue 136 and name O) 1.80 0.00 0.60
assign (residue 136 and name HN) (residue 100 and name O) 1.80 0.00 0.60
assign (residue 1913 and name HE2#) (residue 112 and name O) 1.80 0.00 0.60
assign (residue 114 and name HN) (residue 1913 and name OE1) 1.80 0.00 0.60
assign (residue 83 and name N) (residue 79 and name O) 2.90 0.20 0.40
assign (residue 86 and name N) (residue 82 and name O) 2.90 0.20 0.40
assign (residue 87 and name N) (residue 83 and name O) 2.90 0.20 0.40
assign (residue 88 and name N) (residue 84 and name O) 2.90 0.20 0.40
assign (residue 89 and name N) (residue 85 and name O) 2.90 0.20 0.40
assign (residue 90 and name N) (residue 86 and name O) 2.90 0.20 0.40
assign (residue 91 and name N) (residue 87 and name O) 2.90 0.20 0.40
assign (residue 105 and name N) (residue 101 and name O) 2.90 0.20 0.40
assign (residue 106 and name N) (residue 102 and name O) 2.90 0.20 0.40
assign (residue 108 and name N) (residue 104 and name O) 2.90 0.20 0.40
assign (residue 109 and name N) (residue 105 and name O) 2.90 0.20 0.40
assign (residue 110 and name N) (residue 106 and name O) 2.90 0.20 0.40
assign (residue 111 and name N) (residue 107 and name O) 2.90 0.20 0.40
assign (residue 112 and name N) (residue 108 and name O) 2.90 0.20 0.40
assign (residue 116 and name N) (residue 112 and name O) 2.90 0.20 0.60
assign (residue 121 and name N) (residue 117 and name O) 2.90 0.20 0.40
assign (residue 122 and name N) (residue 118 and name O) 2.90 0.20 0.40
assign (residue 123 and name N) (residue 119 and name O) 2.90 0.20 0.40
assign (residue 124 and name N) (residue 120 and name O) 2.90 0.20 0.40
assign (residue 125 and name N) (residue 121 and name O) 2.90 0.20 0.40
assign (residue 126 and name N) (residue 122 and name O) 2.90 0.20 0.40
assign (residue 128 and name N) (residue 124 and name O) 2.90 0.20 0.40
assign (residue 142 and name N) (residue 138 and name O) 2.90 0.20 0.40
assign (residue 143 and name N) (residue 139 and name O) 2.90 0.20 0.40
assign (residue 144 and name N) (residue 140 and name O) 2.90 0.20 0.40
assign (residue 145 and name N) (residue 141 and name O) 2.90 0.20 0.40
assign (residue 146 and name N) (residue 142 and name O) 2.90 0.20 0.40
assign (residue 100 and name N) (residue 136 and name O) 2.90 0.20 0.40
assign (residue 136 and name N) (residue 100 and name O) 2.90 0.20 0.40
assign (residue 1913 and name NE2) (residue 112 and name O) 2.90 0.20 0.40
assign (residue 114 and name N) (residue 1913 and name OE1) 2.90 0.20 0.40

```
assign ( residue 1908 and name HN )  ( residue 1904 and name O )  1.80 0.00 0.60
assign ( residue 1909 and name HN )  ( residue 1905 and name O )  1.80 0.00 0.60
assign ( residue 1910 and name HN )  ( residue 1906 and name O )  1.80 0.00 0.60
assign ( residue 1911 and name HN )  ( residue 1907 and name O )  1.80 0.00 0.60
assign ( residue 1912 and name HN )  ( residue 1908 and name O )  1.80 0.00 0.60
assign ( residue 1913 and name HN )  ( residue 1909 and name O )  1.80 0.00 0.60
assign ( residue 1914 and name HN )  ( residue 1910 and name O )  1.80 0.00 0.60
assign ( residue 1915 and name HN )  ( residue 1911 and name O )  1.80 0.00 0.60
assign ( residue 1916 and name HN )  ( residue 1912 and name O )  1.80 0.00 0.60
assign ( residue 1917 and name HN )  ( residue 1913 and name O )  1.80 0.00 0.60
assign ( residue 1918 and name HN )  ( residue 1914 and name O )  1.80 0.00 0.60
assign ( residue 1919 and name HN )  ( residue 1915 and name O )  1.80 0.00 0.60
assign ( residue 1920 and name HN )  ( residue 1916 and name O )  1.80 0.00 0.60
assign ( residue 1921 and name HN )  ( residue 1917 and name O )  1.80 0.00 0.60
assign ( residue 1908 and name N )  ( residue 1904 and name O )  2.90 0.20 0.40
assign ( residue 1909 and name N )  ( residue 1905 and name O )  2.90 0.20 0.40
assign ( residue 1910 and name N )  ( residue 1906 and name O )  2.90 0.20 0.40
assign ( residue 1911 and name N )  ( residue 1907 and name O )  2.90 0.20 0.40
assign ( residue 1912 and name N )  ( residue 1908 and name O )  2.90 0.20 0.40
assign ( residue 1913 and name N )  ( residue 1909 and name O )  2.90 0.20 0.40
assign ( residue 1914 and name N )  ( residue 1910 and name O )  2.90 0.20 0.40
assign ( residue 1915 and name N )  ( residue 1911 and name O )  2.90 0.20 0.40
assign ( residue 1916 and name N )  ( residue 1912 and name O )  2.90 0.20 0.40
assign ( residue 1917 and name N )  ( residue 1913 and name O )  2.90 0.20 0.40
assign ( residue 1918 and name N )  ( residue 1914 and name O )  2.90 0.20 0.40
assign ( residue 1919 and name N )  ( residue 1915 and name O )  2.90 0.20 0.40
assign ( residue 1920 and name N )  ( residue 1916 and name O )  2.90 0.20 0.40
assign ( residue 1921 and name N )  ( residue 1917 and name O )  2.90 0.20 0.40
```

$Na_v1.2_{IQp}$ Intramolecular Restraint File

```
assign ( residue 1904 and name HA   ) ( residue 1904 and name HN   )   5.00  3.20  0.50
assign ( residue 1904 and name HA   ) ( residue 1905 and name HN   )   5.00  3.20  0.50
assign ( residue 1904 and name HA   ) ( residue 1907 and name HN   )   4.00  2.20  0.40
assign ( residue 1904 and name HB#  ) ( residue 1904 and name HA   )   4.00  2.20  0.40
assign ( residue 1904 and name HE2# ) ( residue 1904 and name HB#  )   5.00  3.20  0.50
assign ( residue 1904 and name HG#  ) ( residue 1904 and name HA   )   5.00  3.20  0.50
assign ( residue 1904 and name HG#  ) ( residue 1904 and name HB#  )   4.00  2.20  0.40
assign ( residue 1904 and name HG#  ) ( residue 1904 and name HE2# )   5.00  3.20  0.50
assign ( residue 1904 and name HN   ) ( residue 1904 and name HB#  )   5.00  3.20  0.50
assign ( residue 1904 and name HN   ) ( residue 1904 and name HG#  )   5.00  3.20  0.50
assign ( residue 1905 and name HA   ) ( residue 1906 and name HN   )   5.00  3.20  0.50
assign ( residue 1905 and name HA   ) ( residue 1908 and name HN   )   5.00  3.20  0.50
assign ( residue 1905 and name HB#  ) ( residue 1905 and name HA   )   4.00  2.20  0.40
assign ( residue 1905 and name HG#  ) ( residue 1905 and name HA   )   5.00  3.20  0.50
assign ( residue 1905 and name HG#  ) ( residue 1905 and name HB#  )   3.00  1.20  0.30
assign ( residue 1904 and name HN   ) ( residue 1905 and name HN   )   5.00  3.20  0.50
```

assign (residue 1905 and name HN) (residue 1905 and name HA) 5.00 3.20 0.50
assign (residue 1905 and name HN) (residue 1905 and name HB#) 4.00 2.20 0.40
assign (residue 1905 and name HN) (residue 1905 and name HG#) 5.00 3.20 0.50
assign (residue 1906 and name HB#) (residue 1906 and name HA) 5.00 3.20 0.50
assign (residue 1906 and name HB#) (residue 1907 and name HN) 4.00 2.20 0.40
assign (residue 1906 and name HG#) (residue 1906 and name HA) 5.00 3.20 0.50
assign (residue 1906 and name HG#) (residue 1906 and name HB#) 3.00 1.20 0.30
assign (residue 1905 and name HN) (residue 1906 and name HN) 4.00 2.20 0.40
assign (residue 1906 and name HN) (residue 1906 and name HA) 5.00 3.20 0.50
assign (residue 1906 and name HN) (residue 1906 and name HB#) 4.00 2.20 0.40
assign (residue 1906 and name HN) (residue 1906 and name HG#) 5.00 3.20 0.50
assign (residue 1907 and name HB) (residue 1907 and name HA) 4.00 2.20 0.40
assign (residue 1904 and name HA) (residue 1907 and name HG##) 5.00 3.20 0.50
assign (residue 1907 and name HG##) (residue 1907 and name HA) 3.00 1.20 0.30
assign (residue 1907 and name HG##) (residue 1907 and name HB) 3.00 1.20 0.30
assign (residue 1907 and name HG##) (residue 1908 and name HN) 4.00 2.20 0.40
assign (residue 1907 and name HN) (residue 1907 and name HA) 4.00 2.20 0.40
assign (residue 1907 and name HN) (residue 1907 and name HB) 4.00 2.20 0.40
assign (residue 1907 and name HN) (residue 1907 and name HG##) 4.00 2.20 0.40
assign (residue 1908 and name HA) (residue 1909 and name HN) 5.00 3.20 0.50
assign (residue 1904 and name HE2#) (residue 1908 and name HB#) 5.00 3.20 0.50
assign (residue 1908 and name HB#) (residue 1908 and name HA) 5.00 3.20 0.50
assign (residue 1907 and name HN) (residue 1908 and name HN) 4.00 2.20 0.40
assign (residue 1908 and name HN) (residue 1908 and name HA) 5.00 3.20 0.50
assign (residue 1908 and name HN) (residue 1908 and name HB#) 5.00 3.20 0.50
assign (residue 1908 and name HN) (residue 1909 and name HA) 5.00 3.20 0.50
assign (residue 1909 and name HA) (residue 1913 and name HN) 5.00 3.20 0.50
assign (residue 1906 and name HA) (residue 1909 and name HB#) 4.00 2.20 0.40
assign (residue 1906 and name HB#) (residue 1909 and name HB#) 5.00 3.20 0.50
assign (residue 1908 and name HN) (residue 1909 and name HB#) 5.00 3.20 0.50
assign (residue 1909 and name HB#) (residue 1909 and name HA) 3.00 1.20 0.30
assign (residue 1909 and name HB#) (residue 1912 and name HN) 5.00 3.20 0.50
assign (residue 1909 and name HB#) (residue 1913 and name HB#) 5.00 3.20 0.50
assign (residue 1909 and name HB#) (residue 1913 and name HN) 5.00 3.20 0.50
assign (residue 1905 and name HA) (residue 1909 and name HN) 5.00 3.20 0.50
assign (residue 1908 and name HB#) (residue 1909 and name HN) 5.00 3.20 0.50
assign (residue 1908 and name HN) (residue 1909 and name HN) 3.00 1.20 0.30
assign (residue 1909 and name HN) (residue 1909 and name HA) 4.00 2.20 0.40
assign (residue 1909 and name HN) (residue 1909 and name HB#) 3.00 1.20 0.30
assign (residue 1909 and name HN) (residue 1910 and name HN) 4.00 2.20 0.40
assign (residue 1910 and name HB) (residue 1910 and name HA) 4.00 2.20 0.40
assign (residue 1910 and name HG1#) (residue 1910 and name HA) 4.00 2.20 0.40
assign (residue 1910 and name HG1#) (residue 1910 and name HB) 3.00 1.20 0.30
assign (residue 1909 and name HB#) (residue 1910 and name HN) 4.00 2.20 0.40
assign (residue 1910 and name HN) (residue 1910 and name HA) 5.00 3.20 0.50
assign (residue 1910 and name HN) (residue 1910 and name HB) 5.00 3.20 0.50

assign (residue 1911 and name HA) (residue 1912 and name HN) 5.00 3.20 0.50
assign (residue 1911 and name HB) (residue 1911 and name HA) 5.00 3.20 0.50
assign (residue 1911 and name HB) (residue 1912 and name HN) 4.00 2.20 0.40
assign (residue 1908 and name HA) (residue 1911 and name HG##) 5.00 3.20 0.50
assign (residue 1911 and name HG##) (residue 1911 and name HA) 3.00 1.20 0.30
assign (residue 1911 and name HG##) (residue 1911 and name HB) 3.00 1.20 0.30
assign (residue 1911 and name HG##) (residue 1913 and name HN) 5.00 3.20 0.50
assign (residue 1910 and name HN) (residue 1911 and name HN) 3.00 1.20 0.30
assign (residue 1911 and name HN) (residue 1911 and name HA) 4.00 2.20 0.40
assign (residue 1911 and name HN) (residue 1911 and name HB) 4.00 2.20 0.40
assign (residue 1911 and name HN) (residue 1911 and name HG##) 4.00 2.20 0.40
assign (residue 1912 and name HA) (residue 1912 and name HB) 4.00 2.20 0.40
assign (residue 1912 and name HA) (residue 1912 and name HD#) 5.00 3.20 0.50
assign (residue 1912 and name HA) (residue 1916 and name HN) 5.00 3.20 0.50
assign (residue 1912 and name HB) (residue 1912 and name HD#) 4.00 2.20 0.40
assign (residue 1909 and name HA) (residue 1912 and name HD1#) 5.00 3.20 0.50
assign (residue 1909 and name HB#) (residue 1912 and name HD1#) 5.00 3.20 0.50
assign (residue 1912 and name HD1#) (residue 1912 and name HA) 5.00 3.20 0.50
assign (residue 1912 and name HD1#) (residue 1912 and name HB) 4.00 2.20 0.40
assign (residue 1912 and name HD1#) (residue 1912 and name HN) 5.00 3.20 0.50
assign (residue 1912 and name HD1#) (residue 1913 and name HN) 5.00 3.20 0.50
assign (residue 1911 and name HN) (residue 1912 and name HN) 4.00 2.20 0.40
assign (residue 1912 and name HN) (residue 1912 and name HA) 5.00 3.20 0.50
assign (residue 1912 and name HN) (residue 1912 and name HB) 4.00 2.20 0.40
assign (residue 1912 and name HN) (residue 1912 and name HD#) 5.00 3.20 0.50
assign (residue 1913 and name HA) (residue 1914 and name HN) 5.00 3.20 0.50
assign (residue 1913 and name HB#) (residue 1913 and name HA) 5.00 3.20 0.50
assign (residue 1913 and name HB#) (residue 1916 and name HE#) 5.00 3.20 0.50
assign (residue 1909 and name HB#) (residue 1913 and name HE2#) 5.00 3.20 0.50
assign (residue 1913 and name HE2#) (residue 1913 and name HB#) 4.00 2.20 0.40
assign (residue 1913 and name HG#) (residue 1913 and name HA) 5.00 3.20 0.50
assign (residue 1913 and name HG#) (residue 1913 and name HB#) 5.00 3.20 0.50
assign (residue 1913 and name HG#) (residue 1913 and name HE2#) 5.00 3.20 0.50
assign (residue 1912 and name HA) (residue 1913 and name HN) 5.00 3.20 0.50
assign (residue 1912 and name HB) (residue 1913 and name HN) 5.00 3.20 0.50
assign (residue 1912 and name HN) (residue 1913 and name HN) 5.00 3.20 0.50
assign (residue 1913 and name HN) (residue 1913 and name HA) 5.00 3.20 0.50
assign (residue 1913 and name HN) (residue 1913 and name HB#) 5.00 3.20 0.50
assign (residue 1913 and name HN) (residue 1913 and name HG#) 5.00 3.20 0.50
assign (residue 1911 and name HG##) (residue 1914 and name HA) 5.00 3.20 0.50
assign (residue 1914 and name HA) (residue 1914 and name HD#) 5.00 3.20 0.50
assign (residue 1913 and name HN) (residue 1914 and name HB#) 5.00 3.20 0.50
assign (residue 1914 and name HB#) (residue 1914 and name HA) 4.00 2.20 0.40
assign (residue 1914 and name HD#) (residue 1914 and name HB#) 5.00 3.20 0.50
assign (residue 1914 and name HG#) (residue 1914 and name HA) 4.00 2.20 0.40
assign (residue 1914 and name HG#) (residue 1914 and name HB#) 5.00 3.20 0.50

assign (residue 1914 and name HG#) (residue 1914 and name HD#) 5.00 3.20 0.50
assign (residue 1913 and name HB#) (residue 1914 and name HN) 5.00 3.20 0.50
assign (residue 1913 and name HN) (residue 1914 and name HN) 5.00 3.20 0.50
assign (residue 1914 and name HN) (residue 1914 and name HA) 5.00 3.20 0.50
assign (residue 1914 and name HN) (residue 1914 and name HB#) 5.00 3.20 0.50
assign (residue 1914 and name HN) (residue 1914 and name HD#) 5.00 3.20 0.50
assign (residue 1914 and name HN) (residue 1914 and name HG#) 5.00 3.20 0.50
assign (residue 1915 and name HA) (residue 1916 and name HN) 5.00 3.20 0.50
assign (residue 1915 and name HA) (residue 1919 and name HN) 4.00 2.20 0.40
assign (residue 1914 and name HN) (residue 1915 and name HB#) 5.00 3.20 0.50
assign (residue 1915 and name HB#) (residue 1915 and name HA) 4.00 2.20 0.40
assign (residue 1915 and name HB#) (residue 1916 and name HN) 4.00 2.20 0.40
assign (residue 1912 and name HA) (residue 1915 and name HB##) 3.00 1.20 0.30
assign (residue 1915 and name HB##) (residue 1918 and name HN) 5.00 3.20 0.50
assign (residue 1914 and name HN) (residue 1915 and name HN) 4.00 2.20 0.40
assign (residue 1915 and name HN) (residue 1915 and name HA) 5.00 3.20 0.50
assign (residue 1915 and name HN) (residue 1915 and name HB#) 3.00 1.20 0.30
assign (residue 1916 and name HA) (residue 1916 and name HB#) 5.00 3.20 0.50
assign (residue 1916 and name HA) (residue 1916 and name HD#) 5.00 3.20 0.50
assign (residue 1916 and name HA) (residue 1916 and name HE#) 4.00 2.20 0.40
assign (residue 1916 and name HA) (residue 1916 and name HN) 5.00 3.20 0.50
assign (residue 1916 and name HA) (residue 1917 and name HN) 5.00 3.20 0.50
assign (residue 1916 and name HB#) (residue 1917 and name HN) 5.00 3.20 0.50
assign (residue 1916 and name HD#) (residue 1916 and name HB#) 5.00 3.20 0.50
assign (residue 1916 and name HE#) (residue 1916 and name HB#) 4.00 2.20 0.40
assign (residue 1916 and name HE#) (residue 1916 and name HD#) 3.00 1.20 0.30
assign (residue 1915 and name HN) (residue 1916 and name HN) 4.00 2.20 0.40
assign (residue 1916 and name HN) (residue 1916 and name HB#) 5.00 3.20 0.50
assign (residue 1916 and name HN) (residue 1916 and name HE#) 5.00 3.20 0.50
assign (residue 1917 and name HA) (residue 1920 and name HD#) 5.00 3.20 0.50
assign (residue 1917 and name HB#) (residue 1917 and name HA) 5.00 3.20 0.50
assign (residue 1914 and name HG#) (residue 1917 and name HD#) 4.00 2.20 0.40
assign (residue 1917 and name HD#) (residue 1917 and name HB#) 5.00 3.20 0.50
assign (residue 1917 and name HD#) (residue 1917 and name HN) 5.00 3.20 0.50
assign (residue 1917 and name HG#) (residue 1917 and name HA) 5.00 3.20 0.50
assign (residue 1917 and name HG#) (residue 1917 and name HB#) 3.00 1.20 0.30
assign (residue 1917 and name HG#) (residue 1917 and name HD#) 5.00 3.20 0.50
assign (residue 1916 and name HN) (residue 1917 and name HN) 5.00 3.20 0.50
assign (residue 1917 and name HN) (residue 1917 and name HA) 5.00 3.20 0.50
assign (residue 1917 and name HN) (residue 1917 and name HB#) 5.00 3.20 0.50
assign (residue 1917 and name HN) (residue 1917 and name HG#) 5.00 3.20 0.50
assign (residue 1918 and name HD#) (residue 1918 and name HB#) 5.00 3.20 0.50
assign (residue 1918 and name HG#) (residue 1918 and name HB#) 5.00 3.20 0.50
assign (residue 1918 and name HG#) (residue 1918 and name HD#) 5.00 3.20 0.50
assign (residue 1917 and name HN) (residue 1918 and name HN) 4.00 2.20 0.40
assign (residue 1918 and name HN) (residue 1918 and name HB#) 5.00 3.20 0.50

assign (residue 1918 and name HN) (residue 1918 and name HD#) 5.00 3.20 0.50
assign (residue 1918 and name HN) (residue 1918 and name HG#) 5.00 3.20 0.50
assign (residue 1919 and name HA) (residue 1920 and name HN) 5.00 3.20 0.50
assign (residue 1916 and name HN) (residue 1919 and name HB#) 4.00 2.20 0.40
assign (residue 1919 and name HB#) (residue 1919 and name HA) 5.00 3.20 0.50
assign (residue 1919 and name HD#) (residue 1919 and name HA) 5.00 3.20 0.50
assign (residue 1919 and name HD#) (residue 1919 and name HB#) 4.00 2.20 0.40
assign (residue 1919 and name HD#) (residue 1919 and name HN) 5.00 3.20 0.50
assign (residue 1919 and name HE#) (residue 1919 and name HB#) 5.00 3.20 0.50
assign (residue 1919 and name HE#) (residue 1919 and name HD#) 3.00 1.20 0.30
assign (residue 1919 and name HN) (residue 1919 and name HA) 5.00 3.20 0.50
assign (residue 1919 and name HN) (residue 1919 and name HB#) 4.00 2.20 0.40
assign (residue 1919 and name HN) (residue 1919 and name HD##) 5.00 3.20 0.50
assign (residue 1919 and name HD#) (residue 1920 and name HA) 5.00 3.20 0.50
assign (residue 1920 and name HA) (residue 1921 and name HN) 5.00 3.20 0.50
assign (residue 1919 and name HD#) (residue 1920 and name HB#) 4.00 2.20 0.40
assign (residue 1919 and name HE#) (residue 1920 and name HB#) 5.00 3.20 0.50
assign (residue 1920 and name HB#) (residue 1920 and name HA) 4.00 2.20 0.40
assign (residue 1917 and name HA) (residue 1920 and name HD##) 5.00 3.20 0.50
assign (residue 1920 and name HD##) (residue 1920 and name HA) 3.00 1.20 0.30
assign (residue 1920 and name HD##) (residue 1920 and name HB#) 3.00 1.20 0.30
assign (residue 1917 and name HA) (residue 1920 and name HG) 6.00 4.20 0.50
assign (residue 1920 and name HG) (residue 1920 and name HA) 5.00 3.20 0.50
assign (residue 1920 and name HG) (residue 1920 and name HB#) 3.00 1.20 0.30
assign (residue 1920 and name HG) (residue 1920 and name HD##) 4.00 2.20 0.40
assign (residue 1919 and name HB#) (residue 1920 and name HN) 5.00 3.20 0.50
assign (residue 1919 and name HD#) (residue 1920 and name HN) 5.00 3.20 0.50
assign (residue 1919 and name HN) (residue 1920 and name HN) 4.00 2.20 0.40
assign (residue 1920 and name HN) (residue 1920 and name HA) 5.00 3.20 0.50
assign (residue 1920 and name HN) (residue 1920 and name HB#) 4.00 2.20 0.40
assign (residue 1920 and name HN) (residue 1920 and name HD##) 5.00 3.20 0.50
assign (residue 1920 and name HN) (residue 1920 and name HG) 4.00 2.20 0.40
assign (residue 1920 and name HN) (residue 1921 and name HA) 5.00 3.20 0.50
assign (residue 1921 and name HA) (residue 1921 and name HD##) 5.00 3.20 0.50
assign (residue 1921 and name HA) (residue 1921 and name HG) 5.00 3.20 0.50
assign (residue 1921 and name HB#) (residue 1921 and name HA) 4.00 2.20 0.40
assign (residue 1921 and name HD##) (residue 1921 and name HB#) 4.00 2.20 0.40
assign (residue 1917 and name HA) (residue 1921 and name HG) 5.00 3.20 0.50
assign (residue 1921 and name HG) (residue 1921 and name HB#) 3.00 1.20 0.30
assign (residue 1921 and name HG) (residue 1921 and name HD##) 3.00 1.20 0.30
assign (residue 1920 and name HN) (residue 1921 and name HN) 4.00 2.20 0.40
assign (residue 1921 and name HN) (residue 1921 and name HA) 5.00 3.20 0.50
assign (residue 1921 and name HN) (residue 1921 and name HB#) 3.00 1.20 0.30
assign (residue 1921 and name HN) (residue 1921 and name HD##) 5.00 3.20 0.50
assign (residue 1921 and name HN) (residue 1921 and name HG) 5.00 3.20 0.50
assign (residue 1925 and name HB) (residue 1925 and name HA) 4.00 2.20 0.40

assign (residue 1925 and name HG##) (residue 1925 and name HA) 4.00 2.20 0.40
assign (residue 1925 and name HG##) (residue 1925 and name HB) 3.00 1.20 0.30
assign (residue 1925 and name HN) (residue 1925 and name HA) 5.00 3.20 0.50
assign (residue 1925 and name HN) (residue 1925 and name HB) 4.00 2.20 0.30
assign (residue 1925 and name HN) (residue 1925 and name HG##) 5.00 3.20 0.50
assign (residue 1907 and name HA) (residue 1910 and name HB) 4.00 2.20 0.00
assign (residue 1908 and name HA) (residue 1911 and name HB) 5.00 3.20 0.00
assign (residue 1909 and name HA) (residue 1912 and name HB) 4.00 2.20 0.00
assign (residue 1912 and name HA) (residue 1915 and name HB#) 4.00 2.20 0.00
assign (residue 1914 and name HA) (residue 1917 and name HB#) 4.00 2.20 0.00
assign (residue 1915 and name HA) (residue 1918 and name HB#) 4.00 2.20 0.00
assign (residue 1916 and name HA) (residue 1919 and name HB#) 4.00 2.20 0.00
assign (residue 1917 and name HA) (residue 1920 and name HB#) 4.00 2.20 0.00
assign (residue 1910 and name HA) (residue 1913 and name HB#) 4.00 2.20 0.00
assign (residue 1911 and name HA) (residue 1914 and name HB#) 4.00 2.20 0.00
assign (residue 1913 and name HA) (residue 1916 and name HB#) 4.00 2.20 0.00
assign (residue 1918 and name HA) (residue 1921 and name HB#) 4.00 2.20 0.00
assign (residue 1908 and name HA) (residue 1911 and name HN) 4.00 2.20 0.00
assign (residue 1909 and name HA) (residue 1912 and name HN) 4.00 2.20 0.00
assign (residue 1911 and name HA) (residue 1914 and name HN) 4.00 2.20 0.00
assign (residue 1912 and name HA) (residue 1915 and name HN) 4.00 2.20 0.00
assign (residue 1913 and name HA) (residue 1916 and name HN) 4.00 2.20 0.00
assign (residue 1916 and name HA) (residue 1919 and name HN) 4.00 2.20 0.00
assign (residue 1917 and name HA) (residue 1920 and name HN) 4.00 2.20 0.00
assign (residue 1907 and name HA) (residue 1910 and name HN) 4.00 2.20 0.00
assign (residue 1910 and name HA) (residue 1913 and name HN) 4.00 2.20 0.00
assign (residue 1914 and name HA) (residue 1917 and name HN) 4.00 2.20 0.00
assign (residue 1915 and name HA) (residue 1918 and name HN) 4.00 2.20 0.00
assign (residue 1918 and name HA) (residue 1921 and name HN) 4.00 2.20 0.00
assign (residue 1912 and name HD1#) (residue 1912 and name HG2#) 4.00 2.20 0.40
assign (residue 1912 and name HN) (residue 1912 and name HG2#) 5.00 3.20 0.50
assign (residue 1912 and name HD1#) (residue 1912 and name HG1#) 4.00 2.20 0.40
assign (residue 1912 and name HN) (residue 1912 and name HG1#) 5.00 3.20 0.50
assign (residue 1911 and name HG##) (residue 1912 and name HA) 5.00 3.20 0.50
assign (residue 1912 and name HG##) (residue 1915 and name HA) 5.00 3.20 0.50
assign (residue 1912 and name HG2#) (residue 1912 and name HA) 5.00 3.20 0.50
assign (residue 1912 and name HG2#) (residue 1912 and name HB) 3.00 1.20 0.30
assign (residue 1912 and name HG2#) (residue 1912 and name HD#) 3.00 1.20 0.30
assign (residue 1912 and name HG2#) (residue 1916 and name HN) 5.00 3.20 0.50
assign (residue 1912 and name HG2#) (residue 1913 and name HA) 5.00 3.20 0.50
assign (residue 1912 and name HG2#) (residue 1913 and name HN) 5.00 3.20 0.50
assign (residue 1912 and name HG1#) (residue 1912 and name HA) 5.00 3.20 0.50
assign (residue 1912 and name HG1#) (residue 1912 and name HB) 5.00 3.20 0.50
assign (residue 1912 and name HG1#) (residue 1912 and name HD#) 3.00 1.20 0.30
assign (residue 1912 and name HG1#) (residue 1912 and name HG2#) 4.00 2.20 0.40

TALOS Dihedral Angle Restraint File

Values derived using chemical shift index

```
assign (resid 81 and name C  )
      (resid 82   and name N  )
      (resid 82   and name CA )
      (resid 82   and name C  )
      1.0   -59.000 14 2

assign (resid 82 and name N  )
      (resid 82   and name CA  )
      (resid 82   and name C )
      (resid 83   and name N  )
      1.0   -39.000 18 2

assign (resid 82 and name C  )
      (resid 83   and name N  )
      (resid 83   and name CA )
      (resid 83   and name C  )
      1.0   -61.000 10 2

assign (resid 83 and name N  )
      (resid 83   and name CA  )
      (resid 83   and name C )
      (resid 84   and name N  )
      1.0   -42.000 12 2

assign (resid 83 and name C  )
      (resid 84   and name N  )
      (resid 84   and name CA )
      (resid 84   and name C  )
      1.0   -64.000 12 2

assign (resid 84 and name N  )
      (resid 84   and name CA  )
      (resid 84   and name C )
      (resid 85   and name N  )
      1.0   -42.000 8 2

assign (resid 84 and name C  )
      (resid 85   and name N  )
      (resid 85   and name CA )
      (resid 85   and name C  )
      1.0   -63.000 12 2

assign (resid 85 and name N  )
```

```
      (resid 85   and name CA  )
      (resid 85   and name C )
      (resid 86   and name N  )
      1.0   -45.000 12 2

assign (resid 85 and name C  )
      (resid 86   and name N  )
      (resid 86   and name CA )
      (resid 86   and name C  )
      1.0   -61.000 8 2

assign (resid 86 and name N  )
      (resid 86   and name CA  )
      (resid 86   and name C )
      (resid 87   and name N  )
      1.0   -44.000 14 2

assign (resid 86 and name C  )
      (resid 87   and name N  )
      (resid 87   and name CA )
      (resid 87   and name C  )
      1.0   -61.000 12 2

assign (resid 87 and name N  )
      (resid 87   and name CA  )
      (resid 87   and name C )
      (resid 88   and name N  )
      1.0   -43.000 12 2

assign (resid 87 and name C  )
      (resid 88   and name N  )
      (resid 88   and name CA )
      (resid 88   and name C  )
      1.0   -67.000 6 2

assign (resid 88 and name N  )
      (resid 88   and name CA  )
      (resid 88   and name C )
      (resid 89   and name N  )
      1.0   -41.000 18 2

assign (resid 88 and name C  )
      (resid 89   and name N  )
      (resid 89   and name CA )
      (resid 89   and name C  )
      1.0   -65.000 8 2
```

```
assign (resid 89 and name N  )
      (resid 89   and name CA  )
      (resid 89   and name C )
      (resid 90   and name N  )
      1.0   -43.000 6 2

assign (resid 89 and name C  )
      (resid 90   and name N  )
      (resid 90   and name CA )
      (resid 90   and name C  )
      1.0   -64.000 14 2

assign (resid 90 and name N  )
      (resid 90   and name CA  )
      (resid 90   and name C )
      (resid 91   and name N  )
      1.0   -39.000 16 2

assign (resid 90 and name C  )
      (resid 91   and name N  )
      (resid 91   and name CA )
      (resid 91   and name C  )
      1.0   -70.000 18 2

assign (resid 91 and name N  )
      (resid 91   and name CA  )
      (resid 91   and name C )
      (resid 92   and name N  )
      1.0   -32.000 22 2

assign (resid 91 and name C  )
      (resid 92   and name N  )
      (resid 92   and name CA )
      (resid 92   and name C  )
      1.0   -103.000 24 2

assign (resid 92 and name N  )
      (resid 92   and name CA  )
      (resid 92   and name C )
      (resid 93   and name N  )
      1.0   5.000 24 2

assign (resid 98 and name C  )
      (resid 99   and name N  )
      (resid 99   and name CA )
```

```
      (resid 99   and name C  )
      1.0   -127.000 34 2

assign (resid 99 and name N  )
      (resid 99   and name CA  )
      (resid 99   and name C )
      (resid 100   and name N  )
      1.0   153.000 20 2

assign (resid 99 and name C  )
      (resid 100   and name N  )
      (resid 100   and name CA )
      (resid 100   and name C  )
      1.0   -132.000 22 2

assign (resid 100 and name N  )
      (resid 100   and name CA  )
      (resid 100   and name C )
      (resid 101   and name N  )
      1.0   142.000 30 2

assign (resid 100 and name C  )
      (resid 101   and name N  )
      (resid 101   and name CA )
      (resid 101   and name C  )
      1.0   -95.000 60 2

assign (resid 101 and name N  )
      (resid 101   and name CA  )
      (resid 101   and name C )
      (resid 102   and name N  )
      1.0   123.000 44 2

assign (resid 101 and name C  )
      (resid 102   and name N  )
      (resid 102   and name CA )
      (resid 102   and name C  )
      1.0   -59.000 12 2

assign (resid 102 and name N  )
      (resid 102   and name CA  )
      (resid 102   and name C )
      (resid 103   and name N  )
      1.0   -40.000 24 2

assign (resid 102 and name C  )
```

```
      (resid 103   and name N  )
      (resid 103   and name CA )
      (resid 103   and name C  )
      1.0   -64.000 12 2

assign (resid 103 and name N  )
      (resid 103   and name CA  )
      (resid 103   and name C )
      (resid 104   and name N  )
      1.0   -43.000 10 2

assign (resid 103 and name C  )
      (resid 104   and name N  )
      (resid 104   and name CA )
      (resid 104   and name C  )
      1.0   -66.000 12 2

assign (resid 104 and name N  )
      (resid 104   and name CA  )
      (resid 104   and name C )
      (resid 105   and name N  )
      1.0   -43.000 12 2

assign (resid 104 and name C  )
      (resid 105   and name N  )
      (resid 105   and name CA )
      (resid 105   and name C  )
      1.0   -65.000 12 2

assign (resid 105 and name N  )
      (resid 105   and name CA  )
      (resid 105   and name C )
      (resid 106   and name N  )
      1.0   -40.000 16 2

assign (resid 105 and name C  )
      (resid 106   and name N  )
      (resid 106   and name CA )
      (resid 106   and name C  )
      1.0   -64.000 12 2

assign (resid 106 and name N  )
      (resid 106   and name CA  )
      (resid 106   and name C )
      (resid 107   and name N  )
      1.0   -41.000 10 2
```

```
assign (resid 106 and name C  )
      (resid 107   and name N  )
      (resid 107   and name CA )
      (resid 107   and name C  )
      1.0   -63.000 6 2

assign (resid 107 and name N  )
      (resid 107   and name CA  )
      (resid 107   and name C )
      (resid 108   and name N  )
      1.0   -47.000 10 2

assign (resid 107 and name C  )
      (resid 108   and name N  )
      (resid 108   and name CA )
      (resid 108   and name C  )
      1.0   -64.000 22 2

assign (resid 108 and name N  )
      (resid 108   and name CA  )
      (resid 108   and name C )
      (resid 109   and name N  )
      1.0   -40.000 28 2

assign (resid 108 and name C  )
      (resid 109   and name N  )
      (resid 109   and name CA )
      (resid 109   and name C  )
      1.0   -83.000 22 2

assign (resid 109 and name N  )
      (resid 109   and name CA  )
      (resid 109   and name C )
      (resid 110   and name N  )
      1.0   -30.000 18 2

assign (resid 117 and name C  )
      (resid 118   and name N  )
      (resid 118   and name CA )
      (resid 118   and name C  )
      1.0   -59.000 10 2

assign (resid 118 and name N  )
      (resid 118   and name CA  )
      (resid 118   and name C )
```

```
      (resid 119   and name N  )
      1.0   -39.000 14 2

assign (resid 118 and name C  )
      (resid 119   and name N  )
      (resid 119   and name CA )
      (resid 119   and name C  )
      1.0   -65.000 10 2

assign (resid 119 and name N  )
      (resid 119   and name CA  )
      (resid 119   and name C )
      (resid 120   and name N  )
      1.0   -41.000 8 2

assign (resid 119 and name C  )
      (resid 120   and name N  )
      (resid 120   and name CA )
      (resid 120   and name C  )
      1.0   -68.000 8 2

assign (resid 120 and name N  )
      (resid 120   and name CA  )
      (resid 120   and name C )
      (resid 121   and name N  )
      1.0   -41.000 14 2

assign (resid 120 and name C  )
      (resid 121   and name N  )
      (resid 121   and name CA )
      (resid 121   and name C  )
      1.0   -64.000 20 2

assign (resid 121 and name N  )
      (resid 121   and name CA  )
      (resid 121   and name C )
      (resid 122   and name N  )
      1.0   -41.000 8 2

assign (resid 121 and name C  )
      (resid 122   and name N  )
      (resid 122   and name CA )
      (resid 122   and name C  )
      1.0   -62.000 10 2

assign (resid 122 and name N  )
```

```
      (resid 122   and name CA  )
      (resid 122   and name C )
      (resid 123   and name N  )
      1.0   -40.000 18 2

assign (resid 122 and name C  )
      (resid 123   and name N  )
      (resid 123   and name CA )
      (resid 123   and name C  )
      1.0   -69.000 14 2

assign (resid 123 and name N  )
      (resid 123   and name CA  )
      (resid 123   and name C )
      (resid 124   and name N  )
      1.0   -38.000 14 2

assign (resid 123 and name C  )
      (resid 124   and name N  )
      (resid 124   and name CA )
      (resid 124   and name C  )
      1.0   -63.000 12 2

assign (resid 124 and name N  )
      (resid 124   and name CA  )
      (resid 124   and name C )
      (resid 125   and name N  )
      1.0   -44.000 10 2

assign (resid 124 and name C  )
      (resid 125   and name N  )
      (resid 125   and name CA )
      (resid 125   and name C  )
      1.0   -64.000 10 2

assign (resid 125 and name N  )
      (resid 125   and name CA  )
      (resid 125   and name C )
      (resid 126   and name N  )
      1.0   -44.000 16 2

assign (resid 125 and name C  )
      (resid 126   and name N  )
      (resid 126   and name CA )
      (resid 126   and name C  )
      1.0   -61.000 14 2
```

```
assign (resid 126 and name N  )
      (resid 126   and name CA  )
      (resid 126   and name C )
      (resid 127   and name N  )
      1.0   -42.000 14 2

assign (resid 126 and name C  )
      (resid 127   and name N  )
      (resid 127   and name CA )
      (resid 127   and name C  )
      1.0   -75.000 24 2

assign (resid 127 and name N  )
      (resid 127   and name CA  )
      (resid 127   and name C )
      (resid 128   and name N  )
      1.0   -29.000 24 2

assign (resid 127 and name C  )
      (resid 128   and name N  )
      (resid 128   and name CA )
      (resid 128   and name C  )
      1.0   -84.000 28 2

assign (resid 128 and name N  )
      (resid 128   and name CA  )
      (resid 128   and name C )
      (resid 129   and name N  )
      1.0   -16.000 34 2

assign (resid 134 and name C  )
      (resid 135   and name N  )
      (resid 135   and name CA )
      (resid 135   and name C  )
      1.0   -117.000 54 2

assign (resid 135 and name N  )
      (resid 135   and name CA  )
      (resid 135   and name C )
      (resid 136   and name N  )
      1.0   136.000 54 2

assign (resid 135 and name C  )
      (resid 136   and name N  )
      (resid 136   and name CA )
```

```
      (resid 136   and name C  )
      1.0   -110.000 64 2

assign (resid 136 and name N  )
      (resid 136   and name CA  )
      (resid 136   and name C )
      (resid 137   and name N  )
      1.0   127.000 42 2

assign (resid 136 and name C  )
      (resid 137   and name N  )
      (resid 137   and name CA )
      (resid 137   and name C  )
      1.0   -86.000 28 2

assign (resid 137 and name N  )
      (resid 137   and name CA  )
      (resid 137   and name C )
      (resid 138   and name N  )
      1.0   110.000 36 2

assign (resid 138 and name C  )
      (resid 139   and name N  )
      (resid 139   and name CA )
      (resid 139   and name C  )
      1.0   -67.000 22 2

assign (resid 139 and name N  )
      (resid 139   and name CA  )
      (resid 139   and name C )
      (resid 140   and name N  )
      1.0   -33.000 24 2

assign (resid 139 and name C  )
      (resid 140   and name N  )
      (resid 140   and name CA )
      (resid 140   and name C  )
      1.0   -60.000 16 2

assign (resid 140 and name N  )
      (resid 140   and name CA  )
      (resid 140   and name C )
      (resid 141   and name N  )
      1.0   -39.000 16 2

assign (resid 140 and name C  )
```

```
      (resid 141   and name N  )
      (resid 141   and name CA )
      (resid 141   and name C  )
      1.0   -60.000 16 2

assign (resid 141 and name N  )
      (resid 141   and name CA  )
      (resid 141   and name C )
      (resid 142   and name N  )
      1.0   -39.000 16 2

assign (resid 141 and name C  )
      (resid 142   and name N  )
      (resid 142   and name CA )
      (resid 142   and name C  )
      1.0   -62.000 6 2

assign (resid 142 and name N  )
      (resid 142   and name CA  )
      (resid 142   and name C )
      (resid 143   and name N  )
      1.0   -44.000 14 2

assign (resid 142 and name C  )
      (resid 143   and name N  )
      (resid 143   and name CA )
      (resid 143   and name C  )
      1.0   -62.000 12 2

assign (resid 143 and name N  )
      (resid 143   and name CA  )
      (resid 143   and name C )
      (resid 144   and name N  )
      1.0   -41.000 12 2

assign (resid 143 and name C  )
      (resid 144   and name N  )
      (resid 144   and name CA )
      (resid 144   and name C  )
      1.0   -63.000 8 2

assign (resid 144 and name N  )
      (resid 144   and name CA  )
      (resid 144   and name C )
      (resid 145   and name N  )
      1.0   -40.000 8 2
```

```
assign (resid 144 and name C  )
      (resid 145   and name N  )
      (resid 145   and name CA )
      (resid 145   and name C  )
      1.0   -71.000 22 2

assign (resid 145 and name N  )
      (resid 145   and name CA  )
      (resid 145   and name C )
      (resid 146   and name N  )
      1.0   -37.000 24 2

assign (resid 145 and name C  )
      (resid 146   and name N  )
      (resid 146   and name CA )
      (resid 146   and name C  )
      1.0   -89.000 50 2

assign (resid 146 and name N  )
      (resid 146   and name CA  )
      (resid 146   and name C )
      (resid 147   and name N  )
      1.0   -17.000 38 2

assign
(residue 1903 and name C )
(residue 1904 and name N )
(residue 1904 and name CA )
(residue 1904 and name C )
 1.00   -65.00   20.00  2

assign
(residue 1904 and name C )
(residue 1905 and name N )
(residue 1905 and name CA )
(residue 1905 and name C )
 1.00   -65.00   20.00  2

assign
(residue 1905 and name C )
(residue 1906 and name N )
(residue 1906 and name CA )
(residue 1906 and name C )
 1.00   -65.00   20.00  2
```

```
assign
(residue 1906 and name C )
(residue 1907 and name N )
(residue 1907 and name CA )
(residue 1907 and name C )
 1.00   -65.00   20.00  2

assign
(residue 1907 and name C )
(residue 1908 and name N )
(residue 1908 and name CA )
(residue 1908 and name C )
 1.00   -65.00   20.00  2

assign
(residue 1908 and name C )
(residue 1909 and name N )
(residue 1909 and name CA )
(residue 1909 and name C )
 1.00   -65.00   20.00  2

assign
(residue 1909 and name C )
(residue 1910 and name N )
(residue 1910 and name CA )
(residue 1910 and name C )
 1.00   -65.00   20.00  2

assign
(residue 1910 and name C )
(residue 1911 and name N )
(residue 1911 and name CA )
(residue 1911 and name C )
 1.00   -65.00   20.00  2

assign
(residue 1911 and name C )
(residue 1912 and name N )
(residue 1912 and name CA )
(residue 1912 and name C )
 1.00   -65.00   20.00  2

assign
(residue 1912 and name C )
(residue 1913 and name N )
(residue 1913 and name CA )
```

```
(residue 1913 and name C )
 1.00   -65.00   20.00  2

assign
(residue 1913 and name C )
(residue 1914 and name N )
(residue 1914 and name CA )
(residue 1914 and name C )
 1.00   -65.00   20.00  2

assign
(residue 1914 and name C )
(residue 1915 and name N )
(residue 1915 and name CA )
(residue 1915 and name C )
 1.00   -65.00   20.00  2

assign
(residue 1915 and name C )
(residue 1916 and name N )
(residue 1916 and name CA )
(residue 1916 and name C )
 1.00   -65.00   20.00  2

assign
(residue 1916 and name C )
(residue 1917 and name N )
(residue 1917 and name CA )
(residue 1917 and name C )
 1.00   -65.00   20.00  2

assign
(residue 1917 and name C )
(residue 1918 and name N )
(residue 1918 and name CA )
(residue 1918 and name C )
 1.00   -65.00   20.00  2

assign
(residue 1918 and name C )
(residue 1919 and name N )
(residue 1919 and name CA )
(residue 1919 and name C )
 1.00   -65.00   20.00  2

assign
```

```
(residue 1919 and name C )
(residue 1920 and name N )
(residue 1920 and name CA )
(residue 1920 and name C )
 1.00   -65.00   20.00  2

assign
(residue 1920 and name C )
(residue 1921 and name N )
(residue 1921 and name CA )
(residue 1921 and name C )
 1.00   -65.00   20.00  2
```

BIBLIOGRAPHY

Abuzzahab, F. S., 1977. The treatment of schizophrenia with long-acting oral neuroleptics: a six-month double-blind investigation of penfluridol versus trifluoperazine. Psychopharmacol Bull. 13**,** 26-7.

Ackers, G. K., 1979. Linked Functions in Allosteric Proteins: An Exact Theory for the Effect of Organic Phosphates on Oxygen Affinity of Hemoglobin. Biochemistry. 15**,** 3372-3380.

Akyol, Z., Bartos, J. A., Merrill, M. A., Faga, L. A., Jaren, O. R., Shea, M. A., Hell, J. W., 2004. Apo–Calmodulin Binds with its COOH-terminal Domain to the N-methyl-D-aspartate Receptor NR1 C0 Region. Journal of Biological Chemistry. 279**,** 2166-2175.

Allison, S. A., Bacquet, R. J., McCammon, J. A., 1988. Simulation of the diffusion-controlled reaction between superoxide and superoxide dismutase. II. Detailed models. Biopolymers. 27**,** 251-69.

André, I., Kesvatera, T., Jönsson, B., Åkerfeldt, K. S., Linse, S., 2004. The Role of Electrostatic Interactions in Calmodulin–Peptide Complex Formation. Biophysical Journal. 87**,** 1929-1938.

Andre, I., Kesvatera, T., Jonsson, B., Linse, S., 2006. Salt Enhances Calmodulin-Target Interaction. Biophysical Journal. 90**,** 2903-2910.

Antosiewicz, J., McCammon, J. A., 1995. Electrostatic and hydrodynamic orientational steering effects in enzyme-substrate association. Biophys J. 69**,** 57-65.

Arnone, A., 1972. X-ray Diffraction Study of Binding of 2,3-diphosphoglycerate to Human Deoxyhaemoglobin. Nature. 237**,** 146-149.

Ataman, Z. A., Gakhar, L., Sorensen, B. R., Hell, J. W., Shea, M. A., 2007. The NMDA Receptor NR1 C1 Region Bound to Calmodulin: Structural Insights into Functional Differences between Homologous Domains. Structure. 15**,** 1603-17.

Babu, Y. S., Bugg, C. E., Cook, W. J., 1988. Structure of calmodulin refined at 2.2 Å resolution. Journal of Molecular Biology. 204**,** 191-204.

Bahler, M., Rhoads, A., 2002. Calmodulin signaling via the IQ motif. FEBS Lett. 513**,** 107-13.

Baker, N. A., Sept, D., Joseph, S., Holst, M. J., McCammon, J. A., 2001. Electrostatics of nanosystems: Application to microtubules and the ribosome. PNAS. 98**,** 10037-10041.

Barrington, M., Majewski, H., Trifluoperazine and calmidazolium have multiple actions on the release of noradrenaline from sympathetic nerves of mouse atria. Naunyn Schmiedebergs Arch.Pharmacol., Vol. 349, 1994, pp. 133-139.

Bayley, P., Martin, S., Browne, P., Royer, C., 2003. Time-resolved flourescence anistropy studies show domain-specific interactions of calmodulin with IQ target sequences of myosin V. European Biophysical Journal. 32**,** 122-127.

Bayley, P. M., Findlay, W. A., Martin, S. R., 1996. Target recognition by calmodulin: Dissecting the kinetics and affinity of interaction using short peptide sequences. Protein Sci. 5**,** 1215-1228.

Beamer, L. J., Pabo, C. O., 1992. Refined 1.8 A crystal structure of the lambda repressor-operator complex. J Mol Biol. 227**,** 177-96.

Beaven, G. H., Holiday, E. R., 1952. Ultraviolet absorption spectra of proteins and amino acids. Advances in Protein Chemistry. 7**,** 319-386.

Benesch, R., Benesch, R. E., 1967. The effect of organic phosphates from the human erythrocyte on the allosteric properties of hemoglobin. Biochem Biophys Res Commun. 26**,** 162-7.

Black, D. J., Halling, D. B., Mandich, D. V., Pedersen, S., Altschuld, R. A., Hamilton, S. L., 2005. Calmodulin interactions with IQ peptides from voltage dependent calcium channels. Am. J. Physiol. Cell Physiol. 288**,** C669-C676.

Black, D. J., Leonard, J., Persechini, A., 2006. Biphasic Ca2+-dependent switching in a calmodulin-IQ domain complex. Biochemistry. 45**,** 6987-95.

Brooks, B. R., Bruccoleri, R. E., Olafson, B. D., States, D. J., Swaminathan, S., Karplus, M., 1983. CHARMM: a program for macromolecular energy minimization and dynamics calculations. J. Comput. Chem. 4**,** 187-217.

Brunger, A. T., Adams, P. D., Clore, G. M., DeLano, W. L., Gros, P., Grosse-Kunstleve, R. W., Jiang, J. S., Kuszewski, J., Nilges, N., Pannu, N. S., Read, R. J., Rice, L. M., Simonson, T., Warren, G. L., 1998. Crystallography & NMR system: A new software suite for macromolecular structure determination. Acta Crystallogr. D54 (Pt 5)**,** 905-921.

Burgess, J., 1988. Ion in Solution. 191.

Caetano, W., Barbosa, L. R., Itri, R., Tabak, M., 2003. Trifluoperazine effects on anionic and zwitterionic micelles: a study by small angle X-ray scattering. J Colloid Interface Sci. 260**,** 414-22.

Caetano, W., Tabak, M., 2000. Interaction of Chlorpromazine and Trifluoperazine with Anionic Sodium Dodecyl Sulfate (SDS) Micelles: Electronic Absorption and Fluorescence Studies. J Colloid Interface Sci. 225**,** 69-81.

Carscallen, H. B., Rochman, H., Lovegrove, T. D., 1968. High dosage trifluoperazine in schizophrenia. Comparison of the efficacy of high and usual doses of trifluoperazine in the treatment of chronic schizophrenics. Can Psychiatr Assoc J. 13**,** 459-61.

Catterall, A. C., 2000a. Structure and regulation of voltage-gated Ca2+-channels. Annu.Rev.Cell Dev.Biol. 16**,** 521-555.

Catterall, W. A., 2000b. From Ionic Currents to Molecular Mechanisms: The Structure and Function of Voltage-Gated Sodium Channels. Neuron. 26**,** 13-25.

Cens, T., Rousset, M., Leyris, J. P., Fesquet, P., Charnet, P., 2006. Voltage- and calcium-dependent inactivation in high voltage-gated Ca(2+) channels. Prog Biophys Mol Biol. 90**,** 104-17.

Chapman, D., 1913. A contribution to the theory of electrocapillarity. Phil. Mag. 25**,** 475-481.

Chapman, E. R., Au, D., Alexander, K. A., Nicolson, T. A., Storm, D. R., 1991. Characterization of the calmodulin binding domain of neuromodulin. Functional significance of serine 41 and phenylalanine 42. J.Biol.Chem. 266**,** 207-213.

Chattopadhyaya, R., Meador, W. E., Means, A. R., Quiocho, F. A., 1992. Calmodulin Structure Refined at 1·7 Å Resolution. Journal of Molecular Biology. 228(4), 1177-1192.

Chen, C., Feng, Y., Short, J. H., Wand, A. J., 1993. The main chain dynamics of a peptide bound to calmodulin. J.Biol.Chem. 306, 510-514.

Chen, Y., Pawar, P., Pan, G., Ma, L., Liu, H., McDonald, J. M., 2008. Calmodulin binding to the Fas-mediated death-inducing signaling complex in cholangiocarcinoma cells. J Cell Biochem. 103, 788-99.

Cheung, W. Y., 1980. Calmodulin Plays a Pivotal Role in Cellular Regulation. Science. 207, 19-27.

Chin, D., Means, A. R., 2000. Calmodulin: a prototypical calcium sensor. Trends in Cell Biology. 10, 322-328.

Clapperton, J. A., Martin, S. R., Smerdon, S. J., Gamblin, S. J., Bayley, P. M., 2002. Structure of the Complex of Calmodulin with the Target Sequences of Calmodulin-Dependent Protein Kinase I: Studies of the Kinase Activation Mechanism. Biochemistry. 41, 14669-14679.

Clore, G. M., Gronenborn, A. M., 1994. Multidimensional heteronuclear magnetic resonance of proteins. Meths. Enzymol. 239, 349-363.

Clow, A., Jenner, P., Marsden, C. D., Theodorou, A., 1980. Regional changes in brain dopamine receptor function during six months trifluoperazine administration to rats [proceedings]. Br J Pharmacol. 68, 163P-164P.

Colbran, R. J., 1992. Regulation and role of brain calcium/calmodulin-dependent protein kinase II. Neurochem.Int. 21, 469-497.

Cook, W. J., Walter, L. J., Walter, M. R., 1994. Drug Binding by Calmodulin: Crystal Structure of a Calmodulin-Trifluoperazine Complex. Biochemistry. 33, 15259-15265.

Cormier, J. W., Rivolta, I., Tateyama, M., Yang, A. S., Kass, R. S., 2002. Secondary Structure of the Human Cardiac Na^+ Channel C Terminus. Journal of Biological Chemistry. 277, 9233-9241.

Cornilescu, G., Delaglio, F., Bax, A., 1999a. Protein backbone angle restraints from searching a database for chemical shift and sequence homology. J. Biomol. NMR. 13, 289-302.

Cox, J. A., 1988. Interactive properties of calmodulin. Biochem.J. 249, 621-629.

Craven , C. J., Whitehead, B., Jones, S. K., Thulin, E., Blackburn, G. M., Waltho, J. P., 1996. Complexes formed between calmodulin and the antagonists J-8 and TFP in solution. Biochemistry. 35, 10287-10299.

Creighton, T., 1993. Proteins: Structures and Molecular Properties. WH Freeman, San Francisco, CA.

Crivici, A., Ikura, M., 1995. Molecular and Structural Basis of Target Recognition by Calmodulin. Annual Review of Biophysics and Biomolecular Structure. 24, 85-116.

Crouch, T. H., Klee, C. B., 1980. Positive Cooperative Binding of Calcium to Bovine Brain Calmodulin. Biochemistry. 19, 3692-3698.

Cui, Y., Wen, J., Sze, K. H., Man, D., Lin, D., Liu, M., Zhu, G., 2003. Interaction between calcium-free calmodulin and IQ motif of neurogranin studied by nuclear magnetic resonance spectroscopy. Analytical Biochemistry. 315**,** 175-182.

Delaglio, F., Grzesiek, S., Vuister, G. W., Zhu, G., Pfeifer, J., Bax, A., 1995a. NMRPipe: A multidimensional spectral processing system based on UNIX pipes. J. Biomol. NMR. 6**,** 277-293.

Deschênes, I., Trottier, E., Chahine, M., 2001. Implication of the C-Terminal Region of the α-Subunit of Voltage-gated Sodium Channels in Fast Inactivation. Journal of Membrane Biology. 183**,** 103-114.

Ehlers, M. D., Zhang, S., Bernhardt, J. P., Huganir, R. L., 1996. Inactivation of NMDA receptors by direct interaction of calmodulin with the NR1 subunit. Cell. 84**,** 745-755.

Ehrhardt, M. R., Urbauer, J. L., Wand, A. J., 1995. The energetics and dynamics of molecular recognition by calmodulin. Biochemistry. 34**,** 2731-2738.

Evans, T. I., Shea, M. A., 2009. Energetics of calmodulin domain interactions with the calmodulin binding domain of CaMKII. Proteins. 76**,** 47-61.

Evans, T. I. A., Shea, M. A., Domain-Specific Calmodulin Interactions with CaMKII. Biophysical Journal, Vol. 90, 2006, pp. 519a.

Fallon, J. L., Baker, M. R., Xiong, L., Loy, R. E., Yang, G., Dirksen, R. T., Hamilton, S. L., Quiocho, F. A., 2009. Crystal structure of dimeric cardiac L-type calcium channel regulatory domains bridged by Ca2+* calmodulins. Proc Natl Acad Sci U S A. 106**,** 5135-40.

Fallon, J. L., Halling, D. B., Hamilton, S. L., Quiocho, F. A., 2005. Structure of calmodulin bound to the hydrophobic IQ domain of the cardiac Cav1.2 calcium channel. Structure. 13**,** 1881-1886.

Fanger, C. M., Ghanshani, S., Logsdon, N. J., Rauer, H., Kalman, K., Zhou, J., Beckingham, K., K.G., C., Cahalan, M. D., J., A., 1999. Calmodulin mediates calcium-dependent activation of the intermediate conductance K_{Ca} channel, IKCa1. Journal of Biological Chemistry. 274**,** 5746-5754.

Fesik, S. W., Zuiderweg, E. R. P., 1988. Heteronuclear three-dimensional NMR spectroscopy. A strategy for the simplification of homonuclear two-dimensional NMR spectra. J. Magn. Reson. 78**,** 588-593.

Fraczkiewicz, R., Braun, W., 1998. Exact and Efficient Analytical Calculation of the Accessible Surface Areas and Their Gradients for Macromolecules. J. Comp. Chem. 19**,** 319-333.

Frankfurt, O. S., Sugarbaker, E. V., Robb, J. A., Villa, L., Synergistic induction of apoptosis in breast cancer cells by tamoxifen and calmodulin inhibitors. Cancer Lett., Vol. 97, 1995, pp. 149-154.

Gauron, E. F., Rowley, V. N., 1970. Chronic administration of trifluoperazine in multiple dosages and multiple durations. Eur J Pharmacol. 13**,** 35-9.

Gerendasy, D. D., Herron, S. R., Jennings, P. A., Sutcliffe, J. G., 1995. Calmodulin stabilizes an amphiphilic α-helix within RC3/neurogranin and GAP-43/neuromodulin only when Ca^{2+} is absent. J.Biol.Chem. 270**,** 6741-6750.

Gerendasy, D. D., Herron, S. R., Watson, J. B., Sutcliffe, J. G., 1994. Mutational and biophysical studies suggest RC3/neurogranin regulates calmodulin availability. J.Biol.Chem. 269**,** 22420-22426.

Gilson, M. K., Honig, B., 1988. Calculation of the Total Electrostatic Energy of a Macromolecular System: Solvation Energies, Binding Energies, and confromational Analysis. Proteins. 4**,** 7-18.

Goddard, T. D., Kneller, D. G., SPARKY. University of California, San Francisco.

Gouy, M., 1910. Sur la constitution de la charge electrique a la surface d'un electrolyte. J. Phys. 9**,** 457-468.

Guex, N., Peitsch, M. C., 1997. SWISS-MODEL and the Swiss-PdbViewer: An environment for comparative protein modeling. Electrophoresis. 18**,** 2714-2723.

Gustin, M. C., Martinac, B., Saimi, Y., Culbertson, M. R., Kung, C., 1986. Ion Channels in Yeast. Science. 233**,** 1195-1197.

Halling, D. B., Aracena-Parks, P., Hamilton, S. L., 2005. Regulation of voltage-gated Ca2+ channels by calmodulin. Sci STKE. 315**,** 1-11.

Halling, D. B., Georgiou, D. K., Black, D. J., Yang, G., Fallon, J. L., Quiocho, F. A., Pedersen, S. E., Hamilton, S. L., 2009. Determinants in CaV1 channels that regulate the Ca2+ sensitivity of bound calmodulin. J Biol Chem. 284**,** 20041-51.

Harmat, V., Bocskei, Z., Naray-Szabo, G., Bata, I., Csutor, A. S., Hermecz, I., Aranyi, P., Szabo, B., Liliom, K., Vertessy, B. G., Ovadi, J., 2000a. A new potent calmodulin antagonist with arylalkylamine structure: crystallographic, spectroscopic and functional studies. J Mol Biol. 297**,** 747-55.

Hart, R. C., Bates, M. D., Cormier, M. J., Rosen, G. M., Conn, P. M., 1983. Synthesis and Characterization of Calmodulin Antagonistic Drugs. Methods Enzymol. 102**,** 195-205.

Heidorn, D. B., Seeger, P. A., Rokop, S. E., Blumenthal, D. K., Means, A. R., Crespi, H., Trewhella, J., 1989. Changes in the Structure of Calmodulin Induced by a Peptide Based on the Calmodulin-Binding Domain of Myosin Light Chain Kinase. Biochemistry. 28**,** 6757-6764.

Hennessey, T. M., Kung, C., 1984. An anticalmodulin Drug, W-7, inhibits the voltage-dependent calcium current in *Paramecium caudatum*. Journal of Experimental Biology. 110**,** 169-181.

Herzog, R. I., Liu, C., Waxman, S. G., Cummins, T. R., 2003. Calmodulin Binds to the C Terminus of Sodium Channels $Na_v1.4$ and $Na_v1.6$ and Differentially Modulates Their Functional Properties. Journal of Neuroscience. 23**,** 8261-8270.

Hidaka, H., Ishikawa, T., 1992. Molecular pharmacology of calmodulin pathways in the cell functions. Cell Calcium. 13**,** 465-472.

Hille, B., 2001. Ion Channels of Excitable Membranes, 3rd Edition. 814.

Hodes, C. B., 1960. Low dosage Trifluoperazine (Stelazine) in General Practice. J Coll Gen Pract. 3**,** 441-444.

Hoeflich, K. P., Ikura, M., 2002. Calmodulin in Action: Diversity in Target Recognition and Activation Mechanisms. Cell. 108**,** 739-742.

Honig, B., Nicholls, A., 1995. Classical electrostatics in biology and chemistry. Science. 268**,** 1144-1149.

Horvath, I., Harmat, V., Perczel, A., Palfi, V., Nyitray, L., Nagy, A., Hlavanda, E., Naray-Szabo, G., Ovadi, J., 2005. The structure of the complex of calmodulin with KAR-2. The Journal of Biological Chemistry. 280**,** 8266-8274.

Houdusse, A., Gaucher, J. F., Krementsova, E., Mui, S., Trybus, K. M., Cohen, C., 2006. Crystal structure of apo-calmodulin bound to the first two IQ motifs of myosin V reveals essential recognition features. Proc Natl Acad Sci U S A. 103**,** 19326-31.

Ikura, M., Barbato, G., Klee, C. B., Bax, A., 1992. Solution structure of calmodulin and its complex with a myosin light chain kinase fragment. Cell Calcium. 13**,** 391-400.

Ikura, M., Bax, A., 1992. Isotope-filtered 2D NMR of a protein-peptide complex: study of a skeletal muscle myosin light chain kinase fragment bound to calmodulin. J. Am. Chem. Soc. 114**,** 2433-2440.

Jaren, O. R., Kranz, J. K., Sorensen, B. R., Wand, A. J., Shea, M. A., 2002. Calcium-Induced Conformational Switching of Paramecium Calmodulin: Changes in the Protein Backbone Observed by Heteronuclear NMR Studies. Biochemistry. 41**,** 14158-14166.

Johnson, B. A., Blevins, R. A., 1994. NMR View: A computer program for the visualization and analysis of NMR data. J. Biomol. NMR. 4**,** 603-614.

Johnson, M. L., Correia, J. J., Yphantis, D. A., Halvorson, H. R., 1981. Analysis of Data From the Analytical Ultracentrifuge by Nonlinear Least-Squares Techniques. Biophys.J. 36**,** 575-588.

Johnson, M. L., Frasier, S. G., 1985. Nonlinear least-squares analysis. Methods Enzymol. 117**,** 301-342.

Karimi-Nejad, Y., Warren, G. L., Schipper, D., Brunger, A. T., Boelens, R., 1998. NMR structure calculation methods for large proteins: Application of torsion angle dynamics and distance geometry/ simulated annealing to the 269-residue protein serine protease PB92. Mol. Phys. 95**,** 1099-1112.

Kerwin, R., Rupniak, N. M., Jenner, P., Marsden, C. D., 1984. Functional increase in striatal dopaminergic activity following continuous long-term treatment with trifluoperazine. Neurosci Lett. 45**,** 329-34.

Kim, E. Y., Rumpf, C. H., Fujiwara, Y., Cooley, E. S., Van Petegem, F., Minor, D. L., Jr., 2008. Structures of CaV2 Ca2+/CaM-IQ domain complexes reveal binding modes that underlie calcium-dependent inactivation and facilitation. Structure. 16**,** 1455-67.

Klee, C. B., Calmodulin: Structure-Function Relationships. In: W. Y. Cheung, (Ed.), Calcium and Cell Function vol.I Calmodulin. academic press, new york, 1980, pp. 59-77.

Klee, C. B., Interaction of calmodulin with Ca2+ and target proteins. In: P. Cohen, C. B. Klee, Eds.), Calmodulin. Elsevier, New York, 1988, pp. 35-56.

Klee, C. B., Haiech, J., 1980. Concerted Role of Calmodulin and Calcineurin in Calcium Regulation. Ann.N.Y.Acad.Sci., 43-54.

Kleerekoper, Q., Liu, W., Choi, D., Putkey, J. A., 1998. Identification of binding sites for bepridil and trifluoperazine on cardiac troponin C. J Biol Chem. 273, 8153-60.

Koide, H., Kinoshita, T., Tanaka, Y., Tanaka, S., Nagura, N., Meyer zu Horste, G., Miyagi, A., Ando, T., 2006. Identification of the single specific IQ motif of myosin V from which calmodulin dissociates in the presence of Ca2+. Biochemistry. 45, 11598-604.

Kovesi, I., Menyhard, D. K., Laberge, M., Fidy, J., 2008. Interaction of antagonists with calmodulin: insights from molecular dynamics simulations. J Med Chem. 51, 3081-93.

Kuboniwa, H., Tjandra, N., Grzesiek, S., Ren, H., Klee, C. B., Bax, A., 1995. Solution structure of calcium-free calmodulin. Nature Struct. Biol. 2, 768-776.

Kung, C., Preston, R. R., Maley, M. E., Ling, K.-Y., Kanabrocki, J. A., Seavey, B. R., Saimi, Y., 1992. *In vivo Paramecium* mutants show that calmodulin orchestrates membrane responses to stimuli. Cell Calcium. 13, 413-425.

Lahti, R. A., Evans, D. L., Stratman, N. C., Figur, L. M., 1993. Dopamine D4 versus D2 receptor selectivity of dopamine receptor antagonists: possible therapeutic implications. Eur J Pharmacol. 236, 483-6.

Levitan, I. B., 1999. It is calmodulin after all! Mediator of the calcium modulation of multiple ion channels. Neuron. 22, 645-648.

Ling, K.-Y., Preston, R. R., Burns, R., Kink, J. A., Saimi, Y., Kung, C., 1992. Primary Mutations in Calmodulin Prevent Activation of the Ca^{2++} -Dependent Na^{+} Channel in *Paramecium*. Proteins:Structure,Function,and Genetics. 12, 365-371.

Linse, S., Brodin, P., Johansson, C., Thulin, E., Grundstrom, T., Forsén, S., 1988. The role of protein surface charges in ion binding. Nature. 335, 651-652.

Linse, S., Chazin, W. J., Quantitative measurements of the cooperativity in an EF-hand protein with sequential calcium binding. Protein Sci., Vol. 4, 1995, pp. 1038-1044.

Linse, S., Johansson, C., Brodin, P., Grundström, T., Drakenberg, T., Forsén, S., 1991. Electrostatic Contributions to the Binding of Ca^{2+} in Calbindin D_{9k}. Biochemistry. 30, 154-162.

Liu, Y., Buck, D. C., Macey, T. A., Lan, H., Neve, K. A., 2007. Evidence that calmodulin binding to the dopamine D2 receptor enhances receptor signaling. J Recept Signal Transduct Res. 27, 47-65.

Liu, Y., Storm, D. R., 1990. Regulation of free calmodulin levels by neuromodulin: Neuron growth and regeneration. TIPS. 11, 107-111.

Lydan, O'Day, 1988. Different Developmental Functions for Calmodulin in Dictyostelium: Trifluoperazine and R24571 Both Inhibit Cell and Pronuclear Fucion but Enhance Gamete Formation. Exp.Cell Res. 178**,** 51-63.

Mantegazza, M., Yu, F. H., Catterall, W. A., Scheuer, T., 2001. Role of the C-terminal domain in inactivation of brain and cardiac sodium channel. Proceedings of the National Academy of Science. 98**,** 15348-15353.

Martin, L. G., Connors, J. M., McGrath, J. J., Freeman, J., 1975. Altitude-induced erythrocytic 2,3-DPG and hemoglobin changes in rats of various ages. J Appl Physiol. 39**,** 258-61.

Martin, S. R., Andersson-Teleman, A., Bayley, P. M., Drakenberg, T., Forsén, S., 1985. Kinetics of calcium dissociation from calmodulin and its tryptic fragments A stopped-flow fluorescence study using Quin 2 reveals a two-domain structure. Eur.J.Biochem. 151**,** 543-550.

Martin, S. R., Bayley, P. M., 2004. Calmodulin bridging of IQ motifs in myosin-V. FEBS Letters. 567**,** 166-170.

Martin, S. R., Linse, S., Bayley, P. M., Forsen, S., 1986. Kinetics of Cadmium and Terbium Dissociation from Calmodulin and Its Tryptic Fragments. Eur. J. Biochem. 161**,** 595-601.

Masino, L., Martin, S. R., Bayley, P. M., 2000. Ligand binding and thermodynamic stability of a multidomain protein, calmodulin. Protein Science. 9**,** 1519-1529.

Massom, L., Lee, H., Jarrett, H. W., 1990a. Trifluoperazine binding to porcine brain calmodulin and skeletal muscle troponin C. Biochemistry. 29**,** 671-81.

Massom, L. R., Lukas, T. J., Persechini, A., Kretsinger, R. H., Watterson, D. M., Jarrett, H. W., 1991. Trifluoperazine binding to mutant calmodulins. Biochemistry. 30**,** 663-667.

Matsushima, N., Hayashi, N., Jinbo, Y., Izumi, Y., 2000. Ca^{2+}-bound calmodulin forms a compact globular structure on binding four trifluoperazine molecules in solution. Biochem J. 347 Pt 1**,** 211-5.

Matsushima, N., Hayashi, N., Watanabe, N., Jinbo, Y., Izumi, Y., 2007. Binding of trifluoperazine to apocalmodulin revealed by a combination of small-angle X-ray scattering and nuclear magnetic resonance. Journal of Applied Crystallography. 40**,** S179-S183.

Meador, W. E., Means, A. R., Quiocho, F. A., 1992. Target enzyme recognition by calmodulin: 2.4 Å Structure of a calmodulin-peptide complex. Science. 257**,** 1251-1255.

Meador, W. E., Means, A. R., Quiocho, F. A., 1993. Modulation of calmodulin plasticity in molecular recognition on the basis of X-ray structures. Science. 262**,** 1718-1721.

Mori, M., Konno, T., Morii, T., Nagayama, K., Imoto, K., 2003. Regulatory interaction of sodium channel IQ-motif with calmodulin C-terminal lobe. Biochemical and Biophysical Research Communications. 307**,** 290-296.

Mori, M., Konno, T., Ozawa, T., Murata, M., Imoto, K., Nagayama, K., 2000. Novel Interaction of the Voltage-Dependent Sodium Channel (VDSC) with Calmodulin: Does VDSC Acquire Calmodulin-Mediated Ca^{2+}-Sensitivity? Biochemistry. 39**,** 1316-1323.

Mori, M. X., Erickson, M. G., Yue, D. T., 2004. Functional Stoichiometry and Local Enrichment of Calmodulin Interacting with Ca^{2+} Channels. Science. 304**,** 432-435.

Mori, M. X., Vander Kooi, C. W., Leahy, D. J., Yue, D. T., 2008. Crystal structure of the CaV2 IQ domain in complex with Ca2+/calmodulin: high-resolution mechanistic implications for channel regulation by Ca2+. Structure. 16**,** 607-20.

Murshudov, G. N., Vagin, A. A., Dodson, E. J., 1997. Refinement of macromolecular structures by the maximum-likelihood method. Acta Crystallographica Section D, Biological Crystallography. 53**,** 240-255.

Newman, R. A., Shea, M. A., Interactions of Calmodulin with Regulatory Regions of the Ryanodine Receptor Type 1: Distinct Roles of Domains in Protein Allostery. Biophysical Journal, Vol. 90, 2006, pp. 398a.

Newman, R. A., Van Scyoc, W.S., Sorensen, B.R., Jaren, O.R., and Shea, M.A., 2008. Interdomain coopertivity of calmodulin to melittin preferentially increases calcium affinity of sites I and II. Proteins: Structure, Function, and Bioinformatics. 71**,** 1792-1812.

Noguchi, M., Izumi, Y., Yoshino, H., 2004. Target recognition by calmodulin: the role of acid region contiguous to the calmodulin-binding domain of calcineurin A. FEBS Lett. 573**,** 121-6.

O'Neil, K. T., DeGrado, W. F., 1990. How calmodulin binds its targets: sequence independent recognition of amphiphilic alpha-helices. Trends Biochem. Sci. 15**,** 59-64.

O'Neil, K. T., Erickson-Viitanen, S., Wolfe, H. R., Jr., DeGrado, W. F., The Structural Basis for the Calmodulin-Amphiphilic Peptide Interaction. Biophys.J., Vol. 51, 1987, pp. 451a.

Ogawa, Y., Tanokura, M., 1984. Calcium Binding to Calmodulin: Effects of Ionic Strength, Mg^{2+}, pH and Temperature. J.Biochem. 95**,** 19-28.

Osawa, M., Swindells, M. B., Tanikawa, J., Tanaka, T., Mase, T., Furuya, T., Ikura, M., 1998. Solution structure of calmodulin-W-7 complex: the basis of diversity in molecular recognition. Journal of Molecular Biology. 276**,** 165-176.

Oybir, F., 1962. Trifluoperazine in chronic, withdrawn schizophrenics. Dis Nerv Syst. 23**,** 348-50.

Palmer, A. G., 2001. NMR PROBES OF MOLECULAR DYNAMICS: Overview and Comparison with Other Techniques. Annu. Rev. Biophys. Biomol. Struct. 30**,** 129-155.

Pedigo, S., Kephart, C. R., Shea, M. A., 1992. Cooperative Calcium Binding by Calmodulin as Probed by Endoproteinase Glu-C. Biophys.J. 61**,** A211.

Pedigo, S., Shea, M. A., 1993. Cooperative Calcium Binding by Calmodulin. Biophys.J. 64(2, part 2)**,** A168.

Pedigo, S., Shea, M. A., 1995. Quantitative endoproteinase GluC footprinting of cooperative Ca^{2+} binding to calmodulin: Proteolytic susceptibility of E31 and E87 indicates interdomain interactions. Biochemistry. 34**,** 1179-1196.

Peersen, O. B., Madsen, T. S., Falke, J. J., 1997. Intermolecular tuning of calmodulin by target peptides and proteins: differential effects on Ca2+ binding and implications for kinase activation. Protein Science. 6**,** 794-807.

Pelech, S. L., Jetha, F., Vance, D. E., 1983. Trifluoperazine and other anaesthetics inhibit rat liver CTP: phosphocholine cytidylyltransferase. FEBS Lett. 158**,** 89-92.

Pervushin, K., Billeter, M., Siegal, G., Wuthrich, K., 1996. Structural role of a buried salt bridge in the 434 repressor DNA-binding domain. J Mol Biol. 264**,** 1002-12.

Pettersen, E. F., Goddard, T. D., Huang, C. C., Couch, G. S., Greenblatt, D. M., Meng, E. C., Ferrin, T. E., 2004. UCSF Chimera--a visualization system for exploratory research and analysis. J Comput Chem. 25**,** 1605-12.

Pflugrath, J. W., 1999. The finer things in X-ray diffraction data collection. Acta Crystallographica Section D, Biological Crystallography. 55**,** 1718-1725.

Pitt, G. S., Regulation of calcium ion channels by accessory subunits. 2005.

Preston, R. R., Saimi, Y., Kung, C., 1992. Calcium current Activated upon Hyperpolarization of *Paramecium tetraurelia*. J.Gen.Physiol. 100**,** 233-251.

Prozialeck, W. C., Weiss, B., 1982. Inhibition of calmodulin by phenothiazines and related drugs: structure-activity relationships. J.Pharmacol.Exp.Ther. 222, #3**,** 509-516.

Putkey, J. A., Kleerekoper, Q., Gaertner, T. R., WAxham, M. N., 2003. A New Role for IQ Motif Proteins in Regulating Calmodulin Function. Journal of Biological Chemistry. 278**,** 49667-49670.

Putkey, J. A., Slaughter, G. R., Means, A. R., 1985. Bacterial expression and characterization of proteins derived from the chicken calmodulin cDNA and a calmodulin processed gene. Journal of Biological Chemistry. 260**,** 4704-4712.

Quintana, A. R., Wang, D., Forbes, J. E., Waxham, M. N., 2005. Kinetics of calmodulin binding to calcineurin. Biochemical and Biophysical Research Communications. 334**,** 674-680.

Rao, S. T., Wu, S., Satyshur, K. A., Ling, K.-Y., Kung, C., Sundaralingam, M., 1993. Structure of *Paramecium tetraurelia* calmodulin at 1.8Å resolution. Protein Science. 2**,** 436-447.

Roberts, D. M., Harmon, A. C., 1992. Calcium-Modulated Proteins: Targets of Intracellular Calcium Signals in Plants. Ann.Rev.Plant Physiol.Plant Mol.Biol. 43**,** 375-414.

Roudebush, R. E., Berry, P. L., Layman, N. K., Butler, L. D., Bryant, H. U., 1991. Dissociation of immunosuppression by chlorpromazine and trifluoperazine from pharmacologic activities as dopamine antagonists. Int J Immunopharmacol. 13**,** 961-8.

Saimi, Y., Kung, C., 1994. Ion Channel regulation by calmodulin binding. FEBS Lett. 350**,** 155-158.

Saimi, Y., Kung, C., 2002. Calmodulin as an Ion-Channel Subunit. Annual Review of Physiology. 64**,** 289-311.

Schaller, K. L., Caldwell, J. H., 2003. Expression and distribution of voltage-gated sodium channels in the cerebellum. Cerebellum. 2**,** 2-9.

Schumacher, M. A., Crum, M., Miller, M. C., 2004. Crystal structures of apocalmodulin and an apocalmodulin/SK potassium channel gating domain complex. Structure. 12**,** 849-860.

Schumacher, M. A., Rivard, A. F., Bachinger, H. P., Adelman, J. P., 2001. Structure of the gating domain of a Ca^{2+}-activated K^{+} channel complexed with Ca^{2+}/calmodulin. Nature. 410**,** 1120-1124.

Seamon, K. B., 1980. Calcium- and Magnesium-Dependent Conformational States of Calmodulin As Determined by Nuclear-Magnetic Resonance. Biochemistry. 19**,** 207-215.

Shah, V. N., Wingo, T. L., Weiss, K. L., Williams, C. K., Balser, J. R., Chazin, W. J., 2006. Calcium-dependent regulation of the voltage-gated sodium channel hH1: intrinsic and extrinsic sensors use a common molecular switch. Proc Natl Acad Sci U S A. 103**,** 3592-7.

Sharp, K. A., Friedman, R. A., Misra, V., Hecht, J., Honig, B., 1995. Salt effects on polyelectrolyte-ligand binding: comparison of Poisson-Boltzmann, and limiting law/counterion binding models. Biopolymers. 36**,** 245-62.

Sharp, K. A., Honig, B., 1990. Electrostatic Interactions in Macromolecules: Theory and Applications. Annu.Rev.Biophys.Biophys.Chem. 19**,** 301-309.

Sheets, P. L., Gerner, P., Wang, C. F., Wang, S. Y., Wang, G. K., Cummins, T. R., 2006. Inhibition of Nav1.7 and Nav1.4 sodium channels by trifluoperazine involves the local anesthetic receptor. J Neurophysiol. 96**,** 1848-59.

Shen, Y., Delaglio, F., Cornilescu, G., Bax, A., 2009a. TALOS+: a hybrid method for predicting protein backbone torsion angles from NMR chemical shifts. J Biomol NMR. 44**,** 213-23.

Shifman, J. M., Mayo, S. L., 2002. Modulating Calmodulin Binding Specificity through Computational Protein Design. Journal of Molecular Biology. 323**,** 417-423.

Shifman, J. M., Mayo, S. L., 2003. Exploring the origins of binding specificity through the computational redesign of calmodulin. Proceedings of the National Academy of Sciences. 100**,** 13274-13279.

Siegel, F. L., 1973. Calcium-binding proteins. Structure and Bonding. 17**,** 221-252.

Sobczak, S., Honig, A., Nicolson, N. A., Riedel, W. J., 2002. Effects of acute tryptophan depletion on mood and cortisol release in first-degree relatives of type I and type II bipolar patients and healthy matched controls. Neuropsychopharmacology. 27**,** 834-42.

Sobolev, V., Sorokine, A., Prilusky, J., Abola, E. E., Edelman, M., 1999. Automated analysis of interatomic contacts in proteins. Bioinformatics. 15**,** 327-332.

Sorensen, B. R., Coffeen, L. A., Hultman, R., Shea, M. A., Linker Residues Stabilize Calmodulin N-domain and Reduce Its Calcium Affinity. Biophysical Journal, Vol. 82, 2002a, pp. 332a.

Sorensen, B. R., Faga, L. A., Hultman, R., Shea, M. A., 2002b. Interdomain linker increases thermostability and decreases calcium affinity of calmodulin N-domain. Biochemistry. 41**,** 15-20.

Sorensen, B. R., Shea, M. A., Hydrodynamic & Proteolytic Footprinting Studies of Calcium-Induced Interdomain Interactions in Calmodulin. Biophys.J., Vol. 72, 1997, pp. A76.

Sorensen, B. R., Shea, M. A., 1998. Interactions between domains of apo calmodulin alter calcium binding and stability. Biochemistry. 37**,** 4244-4253.

Starovasnik, M. A., Su, D. R., Beckingham, K., Klevit, R. E., 1992. A series of point mutations reveal interactions between the calcium-binding sites of calmodulin. Protein Science. 1**,** 245-253.

Stein, E. G., Rice, L. M., Brünger, A. T., 1997. Torsion-Angle Molecular Dynamics as a New Efficient Tool for NMR Structure Calculation. J. Magn. Reson. 124**,** 154-164.

Strynadka, N. C. J., James, M. N. G., 1989. Crystal Structures of the Helix-Loop-Helix Calcium-Binding Proteins. Annu. Rev. Biochem. 58**,** 951-998.

Sugase, K., Dyson, H. J., Wright, P. E., 2007. Mechanism of coupled folding and binding of an intrinsically disordered protein. Nature. 447**,** 1021-5.

Suizu, T., Tsutsumi, H., Kawado, A., Suginami, K., Imayasu, S., Murata, K., Calcium ion influx during sporulation in the yeast *Saccharomyces cerevisiae*. Can.J.Microbiol., Vol. 41, 1995, pp. 1035-1037.

Swindells, M. B., Ikura, M., 1996. Pre-formation of the semi-open conformation by the apo-calmodulin C-terminal domain and implications for binding IQ-motifs. Nature Structural Biology. 3**,** 501-504.

Tang, L., Shukla, P. K., Wang, Z. J., 2006. Trifluoperazine, an orally available clinically used drug, disrupts opioid antinociceptive tolerance. Neurosci Lett. 397**,** 1-4.

Tanokura, M., Yamada, K., 1985. Effects of trifluoperazine on calcium binding by calmodulin. J. Biol. Chem. 260**,** 8680-8682.

Terrak, M., Wu, G., Stafford, W. F., Lu, R. C., Dominguez, R., 2003. Two distinct myosin light chain structures are induced by specific variations within the bound IQ motifs - functional implications. European Molecular Biology Organization Journal. 22**,** 362-371.

Theoharis, N. T., Sorensen, B. R., Theisen-Toupal, J., Shea, M. A., 2008. The Neuronal Voltage-Dependent Sodium Channel Type II IQ Motif Lowers the Calcium Affinity of the C-Domain of Calmodulin. Biochemistry. 47**,** 112-23.

Tjandra, N., Bax, A., Crivici, A., M., I., Calmodulin Structure and Target Interaction. In: E. Carafoli, C. Klee, Eds.), Calcium *as a* Cellular Regulator. Oxford University Press, Inc., New York, NY, 1999, pp. 152-170.

Trimmer, J. S., Rhodes, K. J., 2004. Localization of Voltage-Gated Ion Channels in Mammalian Brian. Annual Review of Physiology. 66**,** 477-519.

Trott, O., Olson, A. J., 2010. AutoDock Vina: Improving the speed and accuracy of docking with a new scoring function, efficient optimization, and multithreading. J Comput Chem. 31**,** 455-61.

Trybus, K. M., Gushchin, M. I., Lui, H., Hazelwood, L., Krementsova, E. B., Volkmann, N., Hanein, D., 2007. Effect of Calcium on Calmodulin Bound to the IQ Motifs of Myosin V. J Biol Chem. 282**,** 23316-25.

Tse, J. K., Giannetti, A. M., Bradshaw, J. M., 2007. Thermodynamics of calmodulin trapping by Ca2+/calmodulin-dependent protein kinase II: subpicomolar Kd determined using competition titration calorimetry. Biochemistry. 46**,** 4017-27.

van Petegem, F., Chatelain, F. C., Minor Jr., D. L., 2005. Insights into voltage-gated calcium channel regulation from the structure of the $Ca(_V)1.2$ IQ domain-Ca^{2+}/calmodulin complex. Nature Structural and Molecular Biology. 12**,** 1108-1115.

Vandonselaar, M., Hickie, R. A., Quail, J. W., Delbaere, L. T., 1994a. Trifluoperazine-induced conformational change in Ca(2+)-calmodulin. Nat Struct Biol. 1**,** 795-801.

VanScyoc, W. S., Newman, R. A., Sorensen, B. R., Shea, M. A., 2006. Calcium Binding by Calmodulin Mutants Having Domain-Specific Effects on Regulation of Ion Channels. Biochemistry. 45**,** 14311-24.

VanScyoc, W. S., Shea, M. A., 2001a. Phenylalanine fluorescence studies of calcium binding to N-Domain fragments of *Paramecium* calmodulin mutants show increased calcium affinity correlates with increased disorder. Protein Science. 10**,** 1758-1768.

VanScyoc, W. S., Sorensen, B. R., Rusinova, E., Laws, W. R., Ross, J. B., Shea, M. A., 2002. Calcium binding to calmodulin mutants monitored by domain-specific intrinsic phenylalanine and tyrosine fluorescence. Biophysical Journal. 83**,** 2767-2780.

Venter, J. C., Adams, M. D., Myers, E. W., Li, P. W., Mural, R. J., Sutton, G. G., Smith, H. O., Yandell, M., Evans, C. A., Holt, R. A., Gocayne, J. D., Amanatides, P., Ballew, R. M., Huson, D. H., Wortman, J. R., Zhang, Q., Kodira, C. D., Zheng, X. H., Chen, L., Skupski, M., Subramanian, G., Thomas, P. D., Zhang, J., Gabor Miklos, G. L., Nelson, C., Broder, S., Clark, A. G., Nadeau, J., McKusick, V. A., Zinder, N., Levine, A. J., Roberts, R. J., Simon, M., Slayman, C., Hunkapiller, M., Bolanos, R., Delcher, A., Dew, I., Fasulo, D., Flanigan, M., Florea, L., Halpern, A., Hannenhalli, S., Kravitz, S., Levy, S., Mobarry, C., Reinert, K., Remington, K., Abu-Threideh, J., Beasley, E., Biddick, K., Bonazzi, V., Brandon, R., Cargill, M., Chandramouliswaran, I., Charlab, R., Chaturvedi, K., Deng, Z., Di Francesco, V., Dunn, P., Eilbeck, K., Evangelista, C., Gabrielian, A. E., Gan, W., Ge, W., Gong, F., Gu, Z., Guan, P., Heiman, T. J., Higgins, M. E., Ji, R. R., Ke, Z., Ketchum, K. A., Lai, Z., Lei, Y., Li, Z., Li, J., Liang, Y., Lin, X., Lu, F., Merkulov, G. V., Milshina, N., Moore, H. M., Naik, A. K., Narayan, V. A., Neelam, B., Nusskern, D., Rusch, D. B., Salzberg, S., Shao, W., Shue, B., Sun, J., Wang, Z., Wang, A., Wang, X., Wang, J., Wei, M., Wides, R., Xiao, C., Yan, C., Yao, A., Ye, J., Zhan, M., Zhang, W., Zhang, H., Zhao, Q., Zheng, L., Zhong, F., Zhong, W., Zhu, S., Zhao, S., Gilbert, D., Baumhueter, S., Spier, G., Carter, C., Cravchik, A., Woodage, T., Ali, F., An, H., Awe, A., Baldwin, D., Baden, H., Barnstead, M., Barrow, I., Beeson, K., Busam, D., Carver, A., Center, A., Cheng, M. L., Curry, L., Danaher, S., Davenport, L., Desilets, R., Dietz, S., Dodson, K., Doup, L., Ferriera, S., Garg, N., Gluecksmann, A., Hart, B., Haynes, J., Haynes, C., Heiner, C., Hladun, S., Hostin, D., Houck, J., Howland, T., Ibegwam, C., Johnson, J., Kalush, F., Kline, L., Koduru, S., Love, A., Mann, F., May, D., McCawley, S., McIntosh, T., McMullen, I., Moy, M., Moy, L., Murphy, B., Nelson, K., Pfannkoch, C., Pratts, E., Puri, V., Qureshi, H., Reardon, M., Rodriguez, R., Rogers, Y. H., Romblad, D., Ruhfel, B., Scott, R., Sitter, C., Smallwood, M., Stewart, E., Strong, R., Suh, E., Thomas, R., Tint, N. N., Tse, S., Vech, C., Wang, G., Wetter, J., Williams, S., Williams, M., Windsor, S., Winn-Deen, E., Wolfe, K., Zaveri, J., Zaveri, K., Abril, J. F., Guigo, R.,

Campbell, M. J., Sjolander, K. V., Karlak, B., Kejariwal, A., Mi, H., Lazareva, B., Hatton, T., Narechania, A., Diemer, K., Muruganujan, A., Guo, N., Sato, S., Bafna, V., Istrail, S., Lippert, R., Schwartz, R., Walenz, B., Yooseph, S., Allen, D., Basu, A., Baxendale, J., Blick, L., Caminha, M., Carnes-Stine, J., Caulk, P., Chiang, Y. H., Coyne, M., Dahlke, C., Mays, A., Dombroski, M., Donnelly, M., Ely, D., Esparham, S., Fosler, C., Gire, H., Glanowski, S., Glasser, K., Glodek, A., Gorokhov, M., Graham, K., Gropman, B., Harris, M., Heil, J., Henderson, S., Hoover, J., Jennings, D., Jordan, C., Jordan, J., Kasha, J., Kagan, L., Kraft, C., Levitsky, A., Lewis, M., Liu, X., Lopez, J., Ma, D., Majoros, W., McDaniel, J., Murphy, S., Newman, M., Nguyen, T., Nguyen, N., Nodell, M., Pan, S., Peck, J., Peterson, M., Rowe, W., Sanders, R., Scott, J., Simpson, M., Smith, T., Sprague, A., Stockwell, T., Turner, R., Venter, E., Wang, M., Wen, M., Wu, D., Wu, M., Xia, A., Zandieh, A., Zhu, X., 2001. The sequence of the human genome. Science. 291**,** 1304-51.

Vertessy, B. G., Harmat, V., Bocskei, Z., Naray-Szabo, G., Orosz, F., Ovadi, J., 1998a. Simultaneous binding of drugs with different chemical structures to Ca2+-calmodulin: crystallographic and spectroscopic studies. Biochemistry. 37**,** 15300-10.

Vogel, H. J., Andersson, T., Braunlin, W. H., Drakenberg, T., Forsen, S., 1984. Trifluoperazine binding to calmodulin: a shift reagent 43CA NMR study. Biochem Biophys Res Commun. 122**,** 1350-6.

Vuister, G. W., Kim, S.-J., Wu, C., Bax, A., 1994. 2D and 3D NMR study of phenylalanine residues in proteins by reverse isotopic labeling. J. Am. Chem. Soc. 116**,** 9206-9210.

Wall, M. E., Clarage, J. B., Phillips, G. N., 1997. Motions of calmodulin characterized using both Bragg and diffuse X-ray scattering. Structure. 5**,** 1599-1612.

Wallis, G. G., 1958. Clinical trial of trifluoperazine in mental disorders. J R Nav Med Serv. 44**,** 271-4.

Wand, A. J., 2001. Dynamic activation of protein function: A view emerging from NMR spectroscopy. Nature Struct.Biol. 8**,** 926 - 931.

Wang, J. H., Sharma, R. K., 1980. On the Mechanism of Activation of Cyclic Nucleotide Phosphodiesterase by Calmodulin. Ann.N.Y.Acad.Sci. 356**,** 190-204.

Wang, J. H., Sharma, R. K., Tam, S. W., Calmodulin Binding Proteins. In: W. Y. Cheung, (Ed.), Calcium and Cell Function vol.I Calmodulin. Academic Press, New York, 1980, pp. 305-328.

Weiss, B., Wallace, T. L., Mechanisms and Pharmacological Implications of Altering Calmodulin Activity. In: W. Y. Cheung, (Ed.), Calcium and Cell Function vol.1 Calmodulin. Academic Press, London, 1980, pp. 329-379.

Weiss, L. A., Escayg, A., Kearney, J. A., Trudeau, M., MacDonald, B. T., Mori, M., Reichert, J., Buxbaum, J. D., Meisler, M. H., 2003. Sodium channels SCN1A, SCN2A and SCN3A in familial autism. Molecular Psychistry. 8**,** 186-194.

Wilson, M. A., Brunger, A. T., 2000. The 1.0 Å Crystal Structure of Ca^{2+} -bound Calmodulin: an Analysis of Disorder and Implications for Functionally Relevant Plasticity. Journal of Molecular Biology. 301**,** 1237-1256.

Woods, A. S., Marcellino, D., Jackson, S. N., Franco, R., Ferre, S., Agnati, L. F., Fuxe, K., 2008. How calmodulin interacts with the adenosine A(2A) and the dopamine D(2) receptors. J Proteome Res. 7**,** 3428-34.

Yagi, K., Yazawa, M., Ikura, M., Hikichi, K., 1990. Interaction between calmodulin and target proteins. Adv.Exp.Med.Biol. 255**,** 147-154.

Yamaotsu, N., Suga, M., Hirono, S., 2001. Molecular Dynamics Simulation of the Calmodulin-Trifluoperazine Complex in Aqueous Solution. Biopolymers. 58**,** 410-421.

Yamazaki, T., Lee, W., Arrowsmith, C. H., Muhandiram, D. R., Kay, L. E., 1994. A suite of triple-resonance NMR experiments for the backbone assignment of 15N, 13C, 2H-labeled proteins with high sensitivity. J. Am. Chem. Soc. 116**,** 11655-11666.

Yamniuk, A. P., Vogel, H. J., 2004. Calmodulin's flexibility allows for promiscuity in its interactions with target proteins and peptides. Molecular Biotechnology. 27**,** 33-57.

Yang , W., Lee, H., Hellinga, H., Yang, J. J., 2002. Structural analysis, identification, and design of calcium-binding sites in proteins. Proteins: Structure, Function, and Genetics. 47**,** 344-356.

Yap, K. L., Ames, J. B., Swindells, M. B., Ikura, M., 1999. Diversity of conformational states and changes within the EF-hand protein superfamily. Proteins. 37**,** 499-507.

Yap, K. L., Kim, J., Truong, K., Sherman, M., Yuan, T., Ikura, M., 2000. Calmodulin Target Database. Journal of Structural and Functional Genomics. 1**,** 8-14.

Yu, F. H., Catterall, W. A., 2003. Overview of the voltage-gated sodium channel family. Genome Biology. 4**,** 207.1-207.7.

Zhang, M., Tanaka, T., Ikura, M., 1995. Calcium-induced conformational transition revealed by the solution structure of apo calmodulin. Nature Struct. Biol. 2**,** 758-767.